POSITION PAPER ON THE POTENTIAL OF INADVERTENT WEATHER MODIFICATION OF THE FLORIDA PENINSULA RESULTING FROM THE STABILIZED GROUND CLOUD

Eugene Bollay
Lance Bosart
Earl Droessler
James Jiusto
G. Garland Lala
Volker Mohnen
Vincent Schaefer
Patrick Squires

Institute on Man & Science
Rensselaerville, New York 12147

NAS9-14940
000-001
August 1976
Final Report for Period March-August 1976

Prepared for
LYNDON B. JOHNSON SPACE CENTER
Houston, Texas 77058

1. Report No. 1	2. Government Accession No.	3. Recipient's Catalog No.

4. Title
Position Paper on the Potential of Inadvertent Weather Modification of the Florida Peninsula Resulting from the Stabilized Ground Cloud

5. Report Date
August 1976

6. Performing Organiz. Code

7. Author(s)
Eugene Bollay, Bollay Associates, Santa Barbara, Calif.
Lance, Bosart, Dept. of Atmospheric Science, The University at Albany, Albany, N. Y.
Earl Droessler, N. Carolina State University, Raleigh, N. C.
James Jiusto, Atmospheric Sciences Research Center, The University at Albany, Albany, N. Y.
G. Garland Lala, Atmospheric Sciences Research Center, The University at Albany, Albany, N. Y.
Volker Mohnen, Atmospheric Sciences Research Center, The University at Albany, Albany, N. Y.
Vincent Schaefer, Atmospheric Sciences Research Center, The University at Albany, Albany, N.Y.
Patrick Squires, Desert Research Institute, Reno, Nev.

8. Performing Organiz. Rep. No.

10. Work Unit No.

11. Contract or Grant No.
NAS9-14940

13. Type of Report & Period Covered
Final Report, Mar.-Aug., 1976

14. Sponsoring Agency Code

9. Performing Organization Name & Address
Institute on Man & Science
Rensselaerville, N. Y. 12147

12. Sponsoring Agency Name & Address
NASA Lyndon B. Johnson Space Center
Houston, Texas 77058

15. Supplementary Notes

16. Abstract

SEE ATTACHED

17. Key Words
Inadvertent Weather Modification
Climatology of Florida Peninsula
Cloud Physics, Light Scattering by Aerosols

18. Distribution Statement

19. Security Classification (of this report)	20. Security Classification (of this page)	21. No. of Pages	22. Price

Abstract

This position paper on Inadvertent Weather Modification is based on data characterizing the physical, chemical and dispersion state of the stabilized ground cloud within the first three hours after launch supplied by NASA-Lyndon B. Johnson Space Center. From this government-supplied information we have estimated the extent of the S.G.C. and the particle content for times three hours, one day, three days and seven days after launch. We then discussed in detail the involvement of the S.G.C. in warm and cold cloud formation processes and the interaction of the S.G.C. aerosol with solar radiation for the times after launch mentioned above. Based on the climatology of the Florida Peninsula, we assessed the risk for weather modification. Certain weather situations warrant launch rescheduling because of the risk of

- possible impact on hurricanes
- hail formation and lightning activity
- strong wind developments
- intensification of high rainfall rates

The cumulative effects of 40 launches per year on weather modification were found to be insignificant.

TABLE OF CONTENTS

Preface

We have investigated the possible impact of the stabilized space shuttle exhaust cloud ("Stabilized Ground Cloud, S.G.C.") on the "weather" of the Florida Peninsula for a time period of three hours after launch up to seven days after launch. This position paper is based on information supplied by NASA-Lyndon B. Johnson Space Center (all data on the S.G.C.) and on information extracted from pertinent literature. An assessment team was formed consisting of the following members who have complementary research experience in vital areas of inadvertent weather modification:

Dr. Volker A. Mohnen, Director Atmospheric Sciences Research Center The University at Albany	Scientific Project Director and Chairman of the Assessment Team. Principal discussant of Chapter VI entitled "Solar Attenuation Model for the Stabilized Ground Cloud."
Dr. Vincent J. Schaefer Leading Professor, Atmospheric Sciences Research Center, The University at Albany	Principal discussant of Chapter I entitled "Historical Notes."
Mr. Eugene Bollay, Former Chief, Office of Weather Modification, NOAA	Principal discussant of Chapter II entitled "Summary Review from Overt Weather Modification Efforts."
Dr. G. Garland Lala, Research Associate, Atmospheric Sciences Research Center, The University at Albany	Principal discussant of Chapter III entitled "Assumptions and Numerical Values."
Dr. Patrick Squires, Head Atmospheric Physics, Desert Research Institute, Reno, Nevada	Principal discussant of Chapter IV entitled "Warm Clouds."
Dr. James E. Jiusto, Head Atmospheric Physics, Atmospheric Sciences Research Center, The University at Albany	Principal discussant of Chapter V entitled "Cloud Physics Processes - Cold Clouds."
Dr. Lance Bosart, Associate Professor, Dept. of Atmospheric Science, The University at Albany	Principal discussant of Chapter VII entitled "Florida Synoptic Climatology."

Dr. Earl G. Droessler, Reviewer
North Carolina State University
Research Administration
Box 5356
Raleigh, North Carolina

The assessment team met twice for three days each at the Institute on Man & Science (April 1976) and at the Atmospheric Sciences Research Center's Field Station at Whiteface Mountain, New York (July 1976). In the interim period, the members of the team have been in regular contact through individual and conference calls. The problem was approached as outlined in the block diagram.

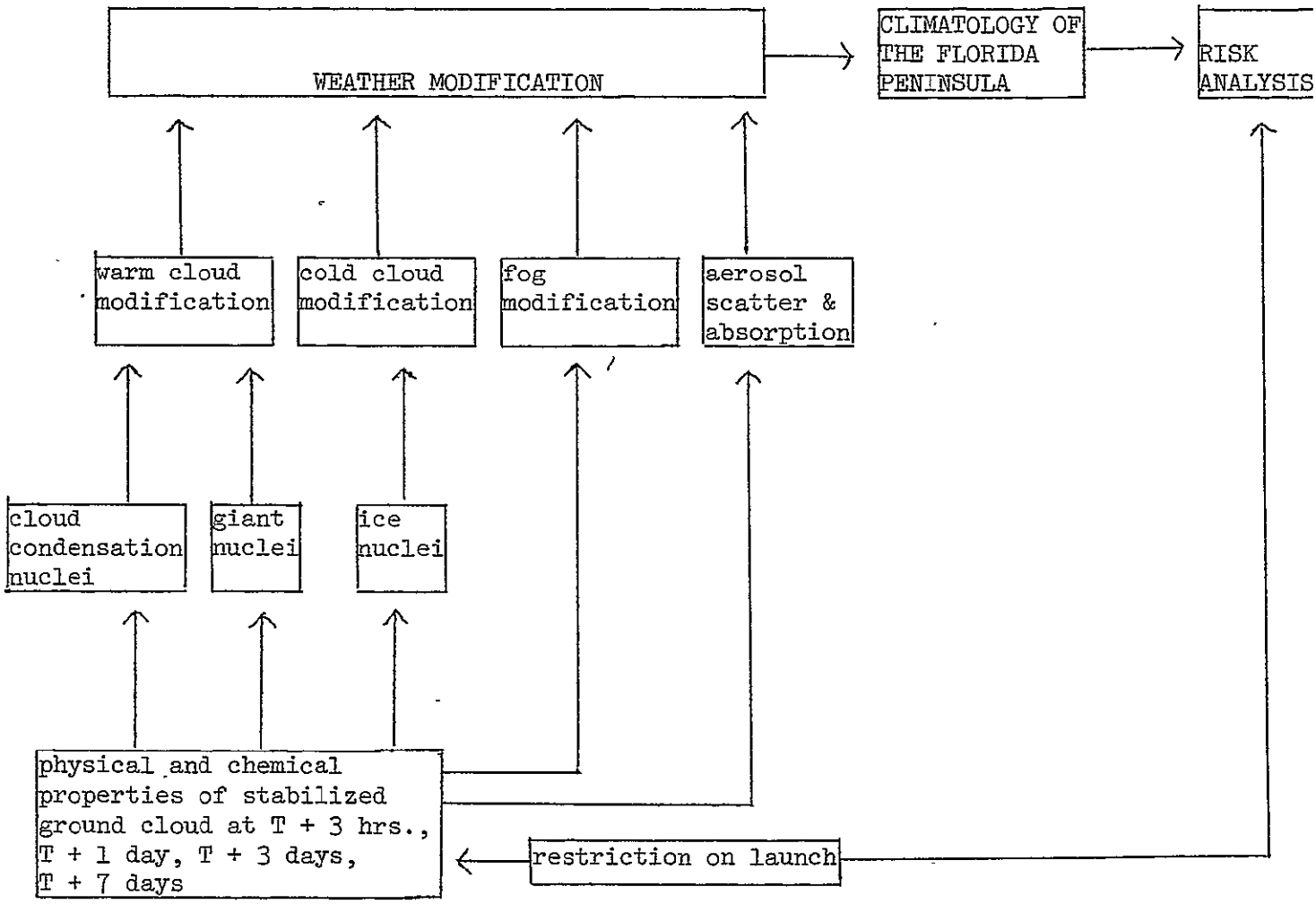

The following risk situations for inadvertent weather modification due to the space shuttle exhaust were concluded:

1. Exhaust cloud encountering active convective precipitation cells with consequent vertical transport to the upper troposphere and potential for acid rain

(a) sea breeze convergence during the warm season with attendent afternoon thunderstorms. Effects include possible localized hail and brief wind gusts in excess of 20 ms^{-1}. Affected area is less than 100 km^2 with a time scale of less than T + 1 day.

(b) frontal and prefrontal activity including squall lines with attendent thunderstorms. Effects include possible localized hail, wind gusts in excess of 30 ms^{-1} and tornadoes. Affected area is 100-500 km^2 with a time scale of less than T + 2 days.

(c) general air mass thunderstorms not associated with (a) and (b) above but responding to different summer synoptic flow patterns. Effects include possible localized hail and brief wind gusts in excess of 20 ms^{-1}. Affected area is less than 100 km^2 with a time scale of less than T + 1 day.

(d) tropical storms in the vicinity of the Florida peninsula within 24 hours of launch time. Potential effect of shuttle exhaust cloud caught up in the circulation of a tropical storm is unknown in terms of inadvertent weather modification. A subsequent change of direction of such a storm might be interpreted as <u>not</u> an "act of God" by some people with possible social and legal problem from communities in the landfall region.

2. In the months November-April, when advective and radiative fogs maximize, very significant worsening of visibility conditions in foggy situations could occur within the area affected by the dissipating S.G.C. up to T + 1 day (area affected up to 10^4 km^2) and particularly under wind flow conditions from the S-E quadrant.

3. Minor risk associated with easterly flow in lower troposphere (unless tropical disturbances are present) particularly in those situations where atmosphere is table under those conditions, clouds do not reach the level where ice phase processes are operative. However, overseeding of warm clouds with CCN could result in a very significant reduction of precipitation over the entire area affected by the dispersing cloud. Effect diminishes after T + 1 day. (Criteria: shallow warm cloud system and no ice phase.)

4. Stagnating anticyclonic conditions with reduced dispersion of S.G.C. Little cloudiness is normally associated with conditions of this type. The impact is therefore restricted only in the area of visibility deterioration and solar energy reduction. This constitutes therefore a nuisance and conceivably might violate EPA standards. On rare occasions air mass thunderstorms may develop, particularly along the sea breeze convergence zone, under stagnant anticyclonic conditions during the warm season. The risk would then be equivalent to 1(c) above.

5. Possible modification of a major hurricane located east of Florida peninsula at time of launch. Air from launch site would participate in the storm circulation and might indeed cause some modification effects producing unknown results. Any subsequent veering of such a storm would undoubtedly cause serious social and legal problems.

6. Cumulative effects: for the projected 40 launches per year assuming several days spacing between launches is considered negligible.

7. Minimal risk and impact: strong westerly winds system extending through the lower troposphere.

Certain weather situations warrant launch rescheduling because of the risk of

- possible impact on hurricanes
- hail formation and lightning activity
- strong wind developments
- intensification of high rainfall rates

The cumulative effects of 40 launches per year on weather modification were found to be insignificant.

Chapter I

HISTORICAL NOTES

The impact of modern technology on the quality and properties of the global atmosphere has been the continuing interest of investigators for more than 35 years.

Some of the first problems studied related to the role that small airborne particulates played in the formation of snow and ice crystals in the atmosphere of eastern New York (Schaefer, 1942). This expanded within a few years to the subject of the filtration of poisonous smokes (Langmuir and Blodgett, 1961) and then the utilization of large quantities of smoke to protect army troops in Europe and navy ships in the South Pacific (Langmuir, 1948).

There followed investigation of the role of airborne snow on the communication effectiveness of airborne radios on B-17 and other aircraft (Schaefer, 1947), then of the safety of aircraft flying in supercooled clouds (Langmuir, et al., 1946), along with the study of snow crystals and methods for replicating them in the free atmosphere (Schaefer, 1941) which led to the discovery of a method for the seeding of supercooled clouds in the free atmosphere (Schaefer, 1946, 1950).

During the period of 1944-45 some studies were carried out on the effectiveness of Al_2O_3 as an ice-forming nucleus, and the role played by organic and inorganic vapors on the growth habits of ice crystals (Schaefer, 1953).

The possible role that particles and gases play in local, regional and global weather patterns is a research concern of an increasing number of scientists. Some of the work was summarized in a review paper

several years ago (Schaefer, 1969). More recently it was the theme of a major conference on inadvertent weather modification (Blanchard, 1974).

Studies were conducted on the effectiveness of several different types of particles as heterogeneous ice nuclei (Schaefer, 1949; Vonnegut, 1947) which followed shortly after Schaefer's discovery that dry ice and other substances colder than -40°C(F) led to the formation of tremendous numbers of ice embryos formed through homogeneous nucleation. Shortly after these discoveries were announced and substantiated by field work (Schaefer, 1947) in supercooled clouds, Langmuir proposed that warm clouds could also be modified through the sudden injection of large water drops or hygroscopic materials that would trigger or enhance coalescence and thus initiate the precipitation process (Langmuir, 1948). At a considerably earlier time, Houghton and Radford (1938) had conducted field studies of the stability of ground fogs. Following Schaefer and Vonnegut's work with dry ice and silver iodide, Fournier d'Albe, et al. (1955) in India carried out some seeding of warm clouds using sodium chloride. Langmuir had suggested the use of ammonium sulfate for similar purposes, but the field tests we carried out were not very encouraging.

Since that time, others have attempted the modification of warm clouds by salt particle seeding (Schleusener and Kocielski, 1971; Biswas and Dennis, 1971; Simpson and Dennis, 1974). It should be noted that the utilization of hygroscopic materials to affect the precipitation process in warm clouds either overtly or inadvertently, involves an entirely different mechanism than is involved when a change of phase is involved.

The use of salt-like or watery substances involves particles that must be larger than 25 μm to be effective. Since dry ice or silver iodide seeding in supercooled clouds can be effective with particles less than 0.01 μm, this means that a difference in weight or mass of about 10 billionfold is involved in producing effective particles in the two processes if one assumes that there is a one to one relationship between nucleus and precipitation particle. Langmuir has suggested that the injection of large water droplets into an actively developing warm cloud would lead to a chain reaction (Langmuir, 1948). Thus, a relatively small amount of seeding material could dramatically accentuate the growth mechanism. More recent attempts to model such growth mechanisms suggest that this may be possible (Berry, 1967).

In any event, it is important for this report on the space shuttle program to consider both effects, i.e., whether either or both warm and cold cloud modification is possible from the residue of the ground cloud produced during launching.

The concentration of airborne particulates affecting the air quality of the global atmosphere has been a recent study of one of us (Schaefer, 1972; 1973; undated). Earlier it was pointed out evidence exists that the effluent of sugar centrales in Puerto Rico produced (Schaefer, 1949) much larger convective clouds than formed over the sea upwind of the island under tradewind cloud development. It was also suggested (Schaefer, 1958) that the massive convective clouds which formed in Africa prior to the start of the rain season showed strong evidence of being overseeded with cloud condensation nuclei produced by the burning of the bush on a massive scale. Such clouds, though forming to vertical

heights of 35-40,000 feet, produced little if any precipitation, though the tops of these clouds formed ice crystal streamers extending for hundreds of miles.

The possibility of the overseeding of clouds by the launch cloud products, which might enhance their stability and repress the precipitation-forming mechanisms in the local and downwind atmosphere, will also be considered.

Figure I-1 shows the basic relationships which exist between airborne particulates on the global scale as related to natural and anthropogenic sources. Figure I-2 then shows typical patterns found in maritime air, and Fig. I-3 in continental air. Since the air flow pattern at the lower levels of the atmosphere over the Florida peninsula are likely to consist of maritime air, its modification toward continental air properties would likely be of interest in assessing possible inadvertent effects.

Figure I-1

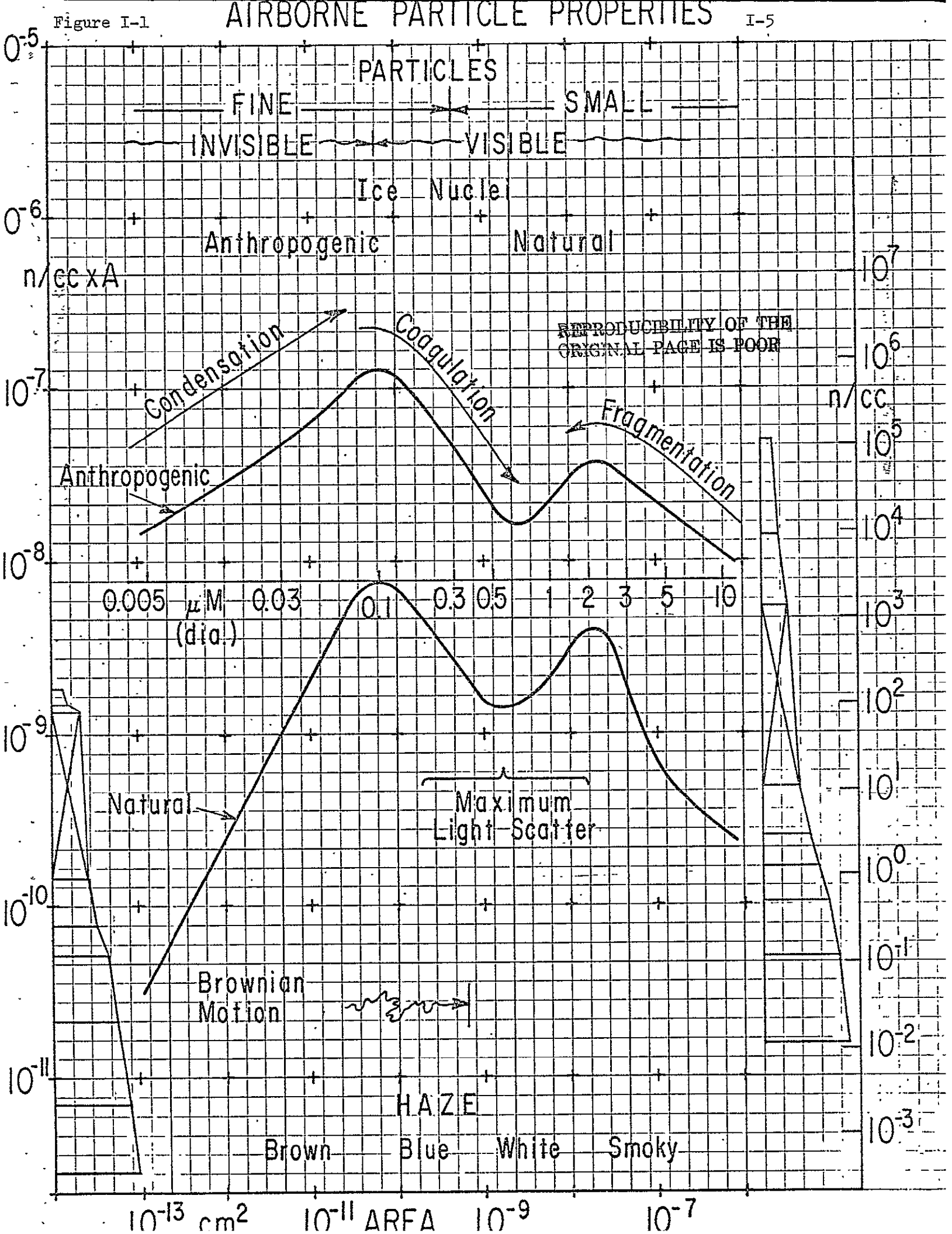

Figure I-2

Range of Airborne Particulates Global Scale

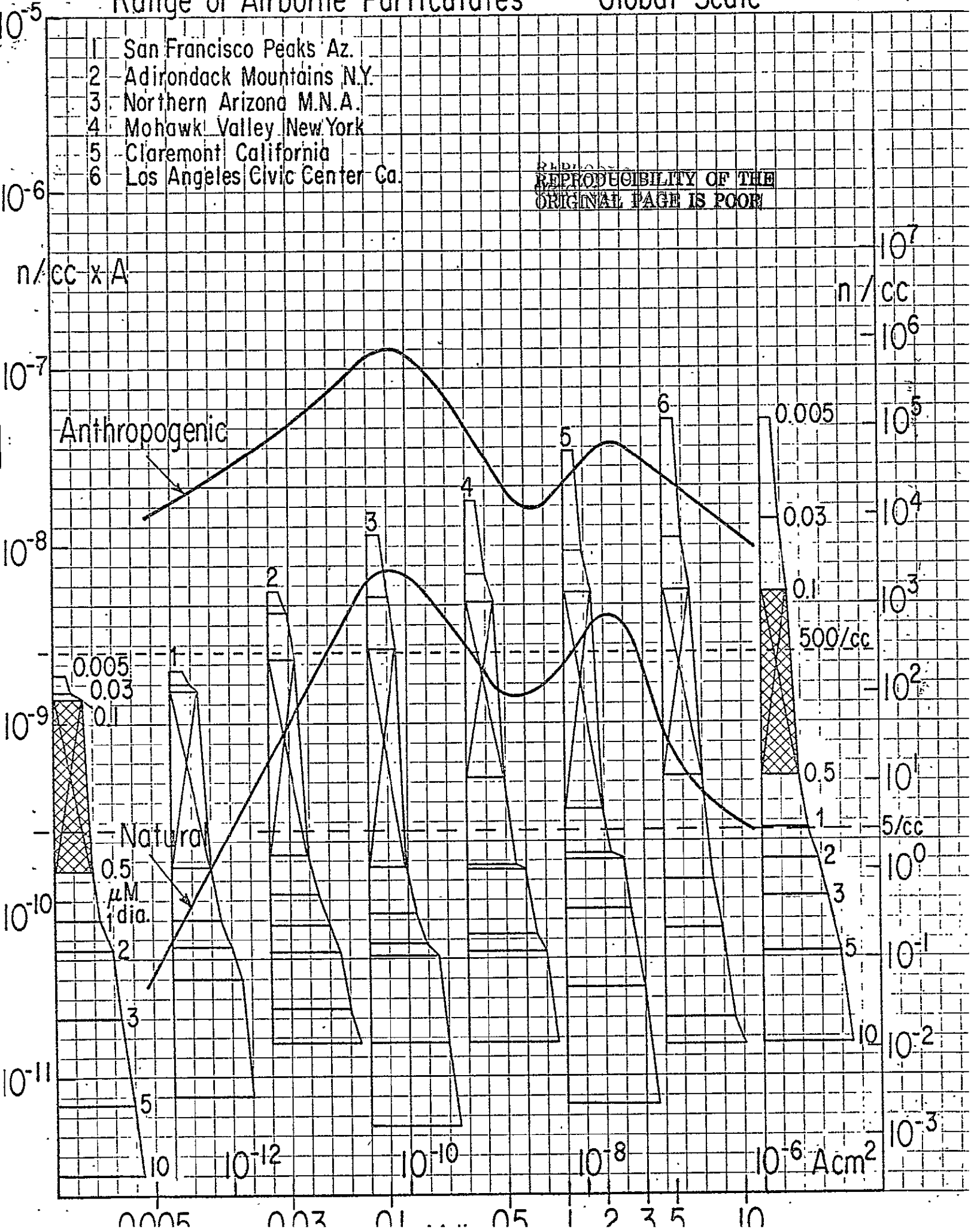

Figure I-3

ANTHROPOGENIC AND NATURAL FOGS

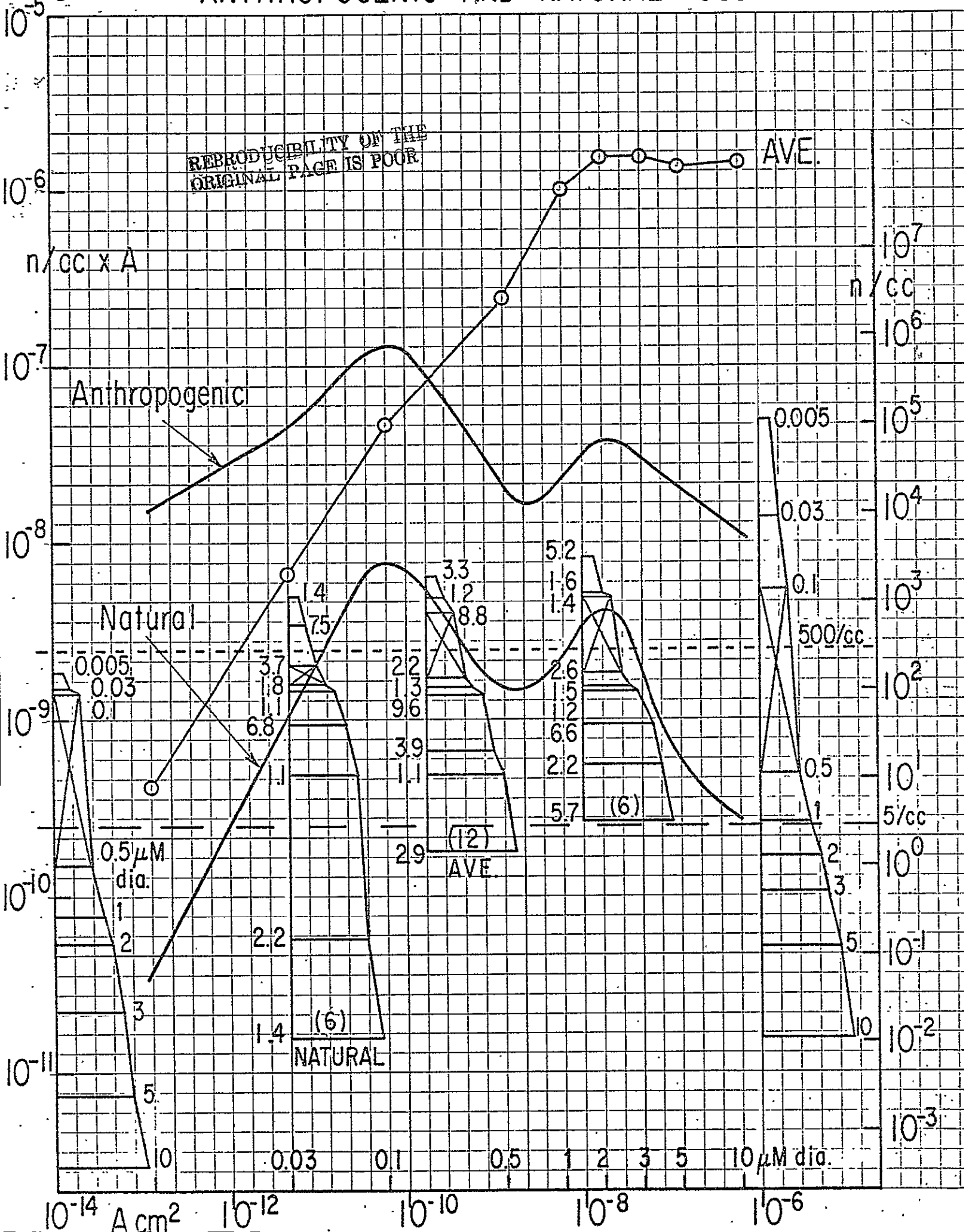

TITLES OF FIGURES

REFERENCES

1. Berry, E., 1967: "Cloud Droplet Growth by Collection", J. Atmos. Sci., 24, 688.

2. Biswas, K. and A. Dennis, 1971: "Formation of Rainshower by Salt Seeding", J. Appl. Meteor., 10, 780-784.

3. Blanchard, D.C., 1974: "Final Report on the Second Inadvertent Weather Modification Workshop", ASRC Publ. 366.

4. Dennis, A., Schleusener, R. and A. Kocielski, 1971: "Modification of Precipitation from Convective Clouds in Australia", AMS, 103-110.

5. Fournier d'Albe, A.M.A. Lateer, S.I. Rasool and I.H. Zaidi, 1955: "The Cloud-Seeding Trials in the Central Punjab, July-September, 1954", Q. J. Roy. Met. Soc., 81, 574.

6. Houghton, H. and W. Radford, 1938: "On the Local Dissipation of Natural Fog", M.I.T. Papers in Phys. Oceanog. Met., 6, No. 3.

7. Langmuir, I. and V.J. Schaefer, et al., 1946: "Basic Icing Research by General Electric Co.", Report N. 5539, AAF Tech. Report.

8. Langmuir, I., 1948: "The Growth of Particles in Smokes and Clouds and the Production of Snow from Supercooled Clouds", Proc. Amer. Phil. Soc., 92, 167.

9. Langmuir, I., 1948: "The Production of Rain by a Chain Reaction in Cumulus Clouds at Temperatures Above Freezing", J. Amer. Meteor., 5, 175.

10. Langmuir, I. and K. Blodgett, 1961: "Report on Smokes and Filters", Collected Works of Irving Langmuir, Pergamon Press, N.Y.

11. Schaefer, V.J., 1941: "Method for Making Snowflake Replicas", Sci., 93, 239.

12. Schaefer, V.J., 1942: "Use of Snowflake Replicas for Studying Winter Storms", Nature, 149, 81.

13. _____, 1946: "The Production of Ice Crystals in a Cloud of Super-Cooled Water Droplets", Science, 104, 457.

14. _____, 1947: "Properties of Particles of Snow and the Electrical Effect they Produce in Storms", Trans. Amer. Geophys. Union, 28, 587.

15. _____, 1947: "Methods of Dissipating Supercooled Clouds in the Natural Atmosphere", J. Inst. Navig., 1, 172.

16. Schaefer, V.J., 1949: "The Formation of Ice Crystals in the Laboratory and the Atmosphere", Chem. Rev., 44, 291.

17. _____, 1949: "Report on Cloud Studies in Puerto Rico", G.E. Research Lab. Report No. RL-190, Schenectady, N.Y., April, 1949.

18. _____, 1950: "The Effects Produced by Seeding Supercooled Clouds with Dry Ice and Silver Iodide", Centenary Proc. of the Royal Meteor. Soc., 42.

19. _____, 1953: "Final Report, Project Cirrus, March 1953", G.E. Research Lab., Schenectady, N.Y. Report RL-785.

20. _____, 1958: "Cloud Explorations Over Africa", Trans. N.Y. Acad. Sciences, 20, 535.

21. _____, 1969: "Inadvertent Modification of the Atmosphere by Air Pollution", Bull. Amer. Met. Soc., 50, 199.

22. _____, 1972: "Fine Particle Measurements in the Air over the North Atlantic Ocean", J. de Recherches Atmospherique, 6, 507.

23. _____, 1973: "High Concentrations of Condensation Nuclei in the Lower Stratosphere", J. de Recherches Atmospherique, 7, 161.

24. _____, (in preparation): "The Air Quality Patterns on the Global Scale", Final Report to National Science Foundation under Grant DE57100321A03.

- 1 18.

25. Simpson, J. and A. Dennis, 1974: "Cumulus Clouds and Their Modification", (in Weather and Climate Mod., W. Hess, ed.), J. Wiley & Sons, 229-282.

26. Vonnegut, B., 1947: "The Nucleation of Ice Formation by Silver Iodide", J. Appl. Phys., 18, 593.

Chapter II

SUMMARY REVIEW FROM OVERT WEATHER MODIFICATION EFFORTS

Outline

Chapter II

SUMMARY REVIEW FROM OVERT WEATHER MODIFICATION EFFORTS

A. BACKGROUND

Soon after the discovery by Langmuir, Schaefer (1946) and Vonnegut (1947) that there was a scientific basis for man to modify nature's way of producing rainfall, economic pressures and entrepreneurs were ready to put this knowledge to use. The time was 1946. Where are we now, thirty years later?

Weather modification is an all encompassing term, still way beyond man's fondest dreams. What we can do is cloud seeding. It is a reality and there is scientific theory to back it up.

The underlying physical basis for cloud seeding is the altering of the size spectrum or phase of the cloud condensate through the manipulation of the population of the condensation, freezing or sublimation nuclei. There is experimental evidence that micro physical changes and dynamic changes are brought about when nuclei are added or when naturally occurring nuclei are activated.

The internal characteristics of clouds determines the behavior of clouds, whether they grow, whether precipitation elements can develop from the cloud droplets, and the lifetime of the clouds. The nature of the aerosols and the updraft speed determines the number of cloud droplets formed with the aerosols serving as condensation nuclei. Different air masses, maritime and continental, have varying aerosol populations. Typically maritime air masses have aerosols ranging from a few tens to hundreds per cm^3, whereas continental air masses may vary from several hundred to several thousand per cm^3. The mass of average cloud droplets

is about 10^{-9} gram and the mass of an average precipitation element is about 10^{-3} gram.

There are two processes by means of which we can explain the transformation and growth of cloud particles into precipitation drops.

One process leading to the formation of precipitation elements depends on the availability of ice particles and the presence of supercooled cloud particles. Because ice has a lower vapor pressure than water there is a transfer of water vapor to the ice particles leading to the growth of precipitation size elements. This is known as the Bergeron-Findeisen process. It is believed to be the principal mechanism in causing precipitation in the middle and high latitudes.

Another process explains the formation of precipitation elements from clouds which are warmer than freezing. The process depends on the collision and coalescence of cloud droplets having different size and mass falling at different speeds through the air. In maritime air, particularly where larger cloud droplets are expected because of the presence of giant condensation nuclei, the larger cloud droplets can grow at the expense of the small droplets very quickly to reach raindrop size and fall out as precipitation. In air mass clouds of continental origin there are many more condensation nuclei and there is very active competition for available moisture amongst a large population of cloud droplets and frequently no precipitation sized particles form and, therefore, no rain falls from many such clouds.

It is believed that both processes, the Bergeron and the collision and coalescence process are active and in competition simultaneously. There are no adequate statistics that establish the percentage of the

total precipitation produced by either process or whether there is a critical time factor when one process may be the dominant one in the life cycle of a cloud.

An additional feature of the Bergeron-Findeisen process leads to an increase in temperature resulting in increased cloud buoyancy when supercooled cloud drops are converted to ice crystals and the latent heat of fusion is released.

The impact man can make in weather modification is to affect either the condensation nuclei population and the ice forming nuclei population in clouds (i.e., aerosols). Adding nuclei of one kind or another is called cloud seeding.

There is ample evidence that precipitation will decrease when there is an overabundance of nuclei, either cloud forming nuclei (CCN) or ice forming nuclei (IN) (Project White Top, Climax I, etc.). Almost all cloud seeding experiments in the past were carried out in the anticipation that htere was a shortage in natural nuclei which is not always the case. In California and Colorado where cloud seeding has been underway during many winter seasons, clouds having optimum seedability have been discovered as a function of cloud top temperature (Grant and Elliott, 1974). Whenever clouds are seeded in storms having sufficient depth to reach a cloud top temperature in the range of -5°C to -25°C, increases in precipitation occur. When colder cloud top temperatures are observed and the clouds are seeded, decreases in precipitation will follow, suggesting that there are so many natural ice nuclei that the addition of artificial nuclei will only increase the competition for the available water vapor and fewer ice crystals can grow to the size of precipitation elements. Figure II-1 illustrates

schematically the cloud top temperature window.

Figure II-1 CLOUD TOP TEMPERATURE SEEDING WINDOW

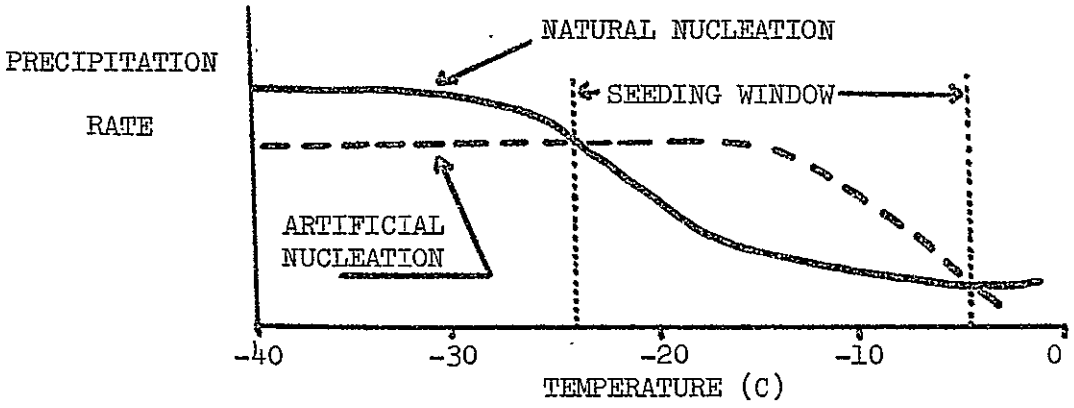

The most common nuclei used for cloud seeding are Salt and Urea for warm cloud seeding (Collision and Coalescence Process), and Silver Iodide for cold cloud seeding (Bergeron-Findeisen process).

Precipitation Modification using the warm cloud seeding process (Collision and Coalescence) has received relatively little attention in this country and in the rest of the world. There are no long time experiments that have been accepted by the scientific community as yardsticks of performance or achievement. Research experiments of short duration and operational programs have been carried out, some with encouraging results but statistically inconclusive.

One reported experiment (Biswas, et al., 1967) using salt as a warm cloud seeding agent was conducted for a total of 18 experimental seasons in three climatologically similar regions in northwest India during the years 1957-1965. In this statistically randomized experiment, a 21% increase in the total seasonal precipitation was reported.

The technical feasibility of modifying warm fog has been demonstrated in certain meteorological situations. Results have shown that the application of heat to disperse warm fog at airports appears to be a more direct and dependable technique without undesireable side effects, such as corrosion from salt.

B. WHERE DO WE STAND IN COLD CLOUD SEEDING

1. Cold Fog

Cold fog dispersal is operational at selected airports and air bases using both surface and aircraft type silver iodide dispensers.

2. Snowpack Augmentation

Snowpack can be increased and in some cases redistributed in mountainous areas of the west by seeding winter orographic clouds. One of the longest cloud seeding programs (Elliott, 1975) carried out in this country, and still ongoing, shows an 8.5% increase in annual stream flow for over a 25 year period. The seeding has been carried out largely with ground generators dispersing silver iodide particles in the size range of 0.01 to 0.1 microns diameter. During a typical operational day, covering 15 hours, about 630 gr. of silver iodide are released from a total of seven generators scattered throughout the mountains.

3. Mesoscale Modification (Winter Convective Band Modification)

A program (Brown and Elliott, 1972) indicating that mesoscale changes can be produced by seeding convective bands imbedded in winter storm clouds was carried out in Santa Barbara county during 1967-1971. Statistical evidence suggested that precipitation increases over 100% were occurring over large areas 100-150 miles downwind from the seeding source. The seeding nuclei were produced with LW-83 pyrotechnic devices (Navy) producing 400 grams of silver iodide in a three minute period. These devices were burned every 15 minutes as long as the convective band was over the seeding area. This program can be considered a forerunner to programs related to the modification of winter storm systems on the Pacific Coast. It also presents good evidence that sizeable extra-area effects are likely and possible.

4. Cumulus Modification

One of the classic experiments (Simpson and Woodley, 1971) in weather modification deals with the precipitation augmentation from carefully selected individual cumulus clouds in south Florida. Seeding effects of 200 to 300% have been demonstrated. The seeding operations were carried out from aircraft and the silver iodide nuclei were generated by pyrotechnic devices. The amount of silver iodide expended per day of experimentation typically ranged from 4 to 15 kilograms. The same program is now investigating the precipitation augmentation from multiple convective clouds and assessing the total area effect. The work is still in progress. Preliminary indications suggest much smaller increases in precipitation by seeding multiple clouds.

The study also showed that in south Florida (Holle, 1974), there are cumulus clouds favorable for seeding from mid-April through mid-September. Outside of this season seedable cumulus clouds are more rare and at least half of them are associated with cold frontal activity moving down the peninsula.

5. Hail Suppression

Commercial operations related to hail suppression activities report success but lack satisfactory evaluation systems. A major National Hail Research Experiment has been established by the National Science Foundation at the National Center for Atmospheric Research. As of this date no results can be reported. Modification of hail forming clouds is reported to be operational in the U.S.S.R. and to some extent in South Africa.

6. Hurricane Modification

The modification of hurricanes (Gentry, 1970) by expanding the eye of the storm radially outwards by cloud seeding is one of the major national goals. Experiments in hurricane Debbie in 1969 provided encouraging evidence that maximum winds can be reduced by a pattern of cloud seeding using silver iodide. Plans are now being made and the necessary equipment and instrumentation procured to carry out an important demonstration program.

7. Lightning Suppression

Lightning suppression experiments (Kasemir, 1973) using silver iodide are inconclusive. Another method of lightning suppression still in the experimental stage uses "chaff needles" to bleed off the electrical fields. This appears a promising method if operational means for delivering the chaff to the electric field forming centers in cumulo-nimbus clouds can be developed.

The modification of tornadoes or other severe storms are research interests still in the design stage. Some excellent modelling efforts are underway to determine where and when severe storm modification might be feasible.

C. REFERENCES

1. Biswas, K.R., R.K. Kapoor, K.K. Kanuga, and Bh.V. Ramanamurty, 1967: "Cloud Seeding Experiment Using Common Salt", J. Appl. Meteor., 6, 914-923.

2. Brown, K.J. and R.D. Elliott, 1972: "Mesoscale Changes in the Atmosphere Due to Convective Band Seeding", AMS Third Conference on Weather Modification, June 26-29, 1972, Rapid City, South Dakota.

3. Elliott, R.D., 1975: "The Upper San Joaquin River Basin Cloud Seeding Project", AMS Special Regional Weather Mod. Conf. Nov. 11-13, 1975, San Francisco, California.

4. Gentry, R. Cecil, 1970: "Hurricane Debbie Modification Experiments August, 1969"; Science 168, 473-475.

5. Graut, L.O. and R.D. Elliott, 1974: "The Cloud Seeding Temperature Window", J. Appl. Meteor., 13, 355-363.

6. Holle, R.L., 1974: "Populations of Parameters Related to Dynamic Cumulus Seeding Over Florida", J. Appl. Meteor., 13.

7. Kasemir, H.W., 1973: "Lightning Suppression by Chaff Seeding", NOAA Tech. Report ERL284.

8. Schaefer, V.J., 1946: "The Production of Ice Crystals in a Cloud of Supercooled Water Droplets", Science, 104, 457.

9. Simpson, J. and W.L. Woodley, 1971: "Seeding Cumulus in Florida: New 1970 Results", Science 172, 117-126.

10. Vonnegut, B., 1947: "The Nucleation of Ice Formation by Silver Iodide", J. Appl. Phys., 18, 227-228.

Chapter III

ASSUMPTIONS AND NUMERICAL VALUES

Outline

Chapter III

ASSUMPTIONS AND NUMERICAL VALUES

A. INTRODUCTION

In any attempt to assess the weather modification effect of an aerosol cloud, one of the most important aspects is the particle size distribution and number concentration. The distribution and concentration are important in determining whether entrainment of the aerosol into a cloud will inhibit or promote precipitation and will also determine the dominant precipitation mechanism. Equally important is the background aerosol character and its concentration relative to the aerosol being introduced. Knowing the distribution and concentration of the two aerosols allows one to estimate whether there will be any weather modification impact and the magnitude of the effect.

B. BACKGROUND AEROSOLS

From a warm-cloud weather modification perspective, specification of the aerosol in terms of a supersaturation spectrum is more meaningful. A supersaturation spectrum gives the total number of particles (cloud condensation nuclei) activated at a given supersaturation. Typical supersaturations used are in the range of 0.2% to 2% which covers the range of supersaturation occurring naturally in clouds and fog. Supersaturation spectra follow a power law of the form

$$N = CS^K$$

where S is the supersaturation, C is the concentration at 1% supersaturation and K is the slope of the spectrum. Measurements of the supersaturate spectra over the Florida peninsula have been carried out by Fitzgerald (1972) for aerosols of both maritime and continental origins. The results of these measurements are summarized below

Maritime aerosol $N = 2420\ S^{0.46}$

Continental aerosol $N = 5913\ S^{0.53}$

where N is the concentration of particles (cm^{-3}) activated at a supersaturation S, the latter being expressed in absolute units; for example, at $S = 10^{-2}$ (often expressed as "1%") $N = 291\ cm^{-3}$ in a maritime aerosol, or 515 cm^{-3} in a continental aerosol.

Background levels of ice nuclei for evaluating the potential weather modification impact on cold clouds are given in Chapter V (Figure V-2).

C. VOLUME OF THE SGC AND AEROSOL MASS CONCENTRATION

1. Cloud Volume as a Function of Time

The specification of the volume of the stabilized ground cloud is based on a linear extrapolation of NASA measurements of the cloud volume shortly after launch (NASA Staff-Langley Research Center). Volume estimates derived in this manner are probably conservatively small but offer a reasonable approximation considering the lack of data on the cloud volume at long times after the launch. Note that extrapolation of the growth curve plotted along with the data leads to a cloud volume of 1200 km^3 at 3 hours as opposed to the volume of 600 km^3 used in these calculations. Table III-I below gives the estimated volume of the stabilized ground cloud at various times after launch.

TABLE III-I

Estimated Cloud Volume vs. Time

Time	Volume of the Cloud
T + 3 hrs.	6×10^2 km^3
T + 1 day	5×10^3 km^3
T + 3 days	1.5×10^4 km^3
T + 7 days	3.5×10^4 km^3

2. Aerosol Mass Concentration in the Stabilized Ground Cloud

Specification of mass concentrations in the stabilized ground cloud is a difficult problem because of a lack of data on cloud volume and mass concentration at long times after the launch. The approach followed here is to start with the total emission of Al_2O_3 in the ground cloud and to assume that this mass is maintained in the cloud volume as specified in Table III-I.

The determination of the total mass of Al_2O_3 in the stabilized ground cloud was obtained from integration of the calculated emission of the space shuttle vehicle as given in NASA-JPL Tech. Memo. 33-712. Based on the information that the material emitted during the first 20 to 24 seconds (2 km altitude increment) makes up the stabilized ground cloud leads to an estimate of 10^8 grams of Al_2O_3 in the cloud. Table III-II gives the mass concentration as a function of time based on the conservation of the total mass of material in the ground cloud and the cloud volume as given in Table III-I. (A 10 percent mass loss due to surface deposition is allowed during the first 3 hours.)

TABLE III-II

Al_2O_3 Mass Concentration vs. Time

Time	Mass Concentration of Al_2O_3
T + 3 hrs.	150 $\mu g\ m^{-3}$
T + 1 day	18 $\mu g\ m^{-3}$
T + 3 days	6 $\mu g\ m^{-3}$
T + 7 days	2.6 $\mu g\ m^{-3}$

D. AEROSOL SIZE DISTRIBUTION AND NUMBER CONCENTRATION

1. Size Distribution

Aerosol size distributions for the Al_2O_3 aerosol were extracted from the data presented by Varsi (1976). This data, presented in the form of histograms, was normalized and integrated to obtain cumulative distributions of the fraction of particles larger than the indicated size (diameter) and is presented in Figures III-1 through III-6. Power law functions were fit to these distributions with the resulting values for N, the fraction greater than diameter, in terms of D, diameter in microns, indicated on the figures.

Inspection of these figures indicate that the data can be partitioned into two groups: one with a steep slope (Figures III-1, III-3, III-5) associated with early measurements and the other with a shallow slope (Figures III-2, III-4, III-6) characteristic of later measurements or long time averages. This change of slope with time reflects the effects of coagulation at high concentration resulting in fewer small particles. For the purpose of this study, which is concerned with the cloud at long times after the launch, the distributions with the shallow slopes are more appropriate.

Distributions obtained with the electrical mobility analyzer (Fig. III-3 through III-6) exhibit a shallow slope in the size region less than 0.07 μm. This is typical of size distribution at small sizes where coagulation rapidly acts to remove the very small particles. Thus, to realistically describe the characteristics of the Al_2O_3 aerosol two distributions are needed; one for the small sizes ($0.01\ \mu m \leq D \leq 0.07\ \mu m$) and a second for the large sizes ($0.07\ \mu m \leq D \leq 50\ \mu m$). The distribution at large sizes has been

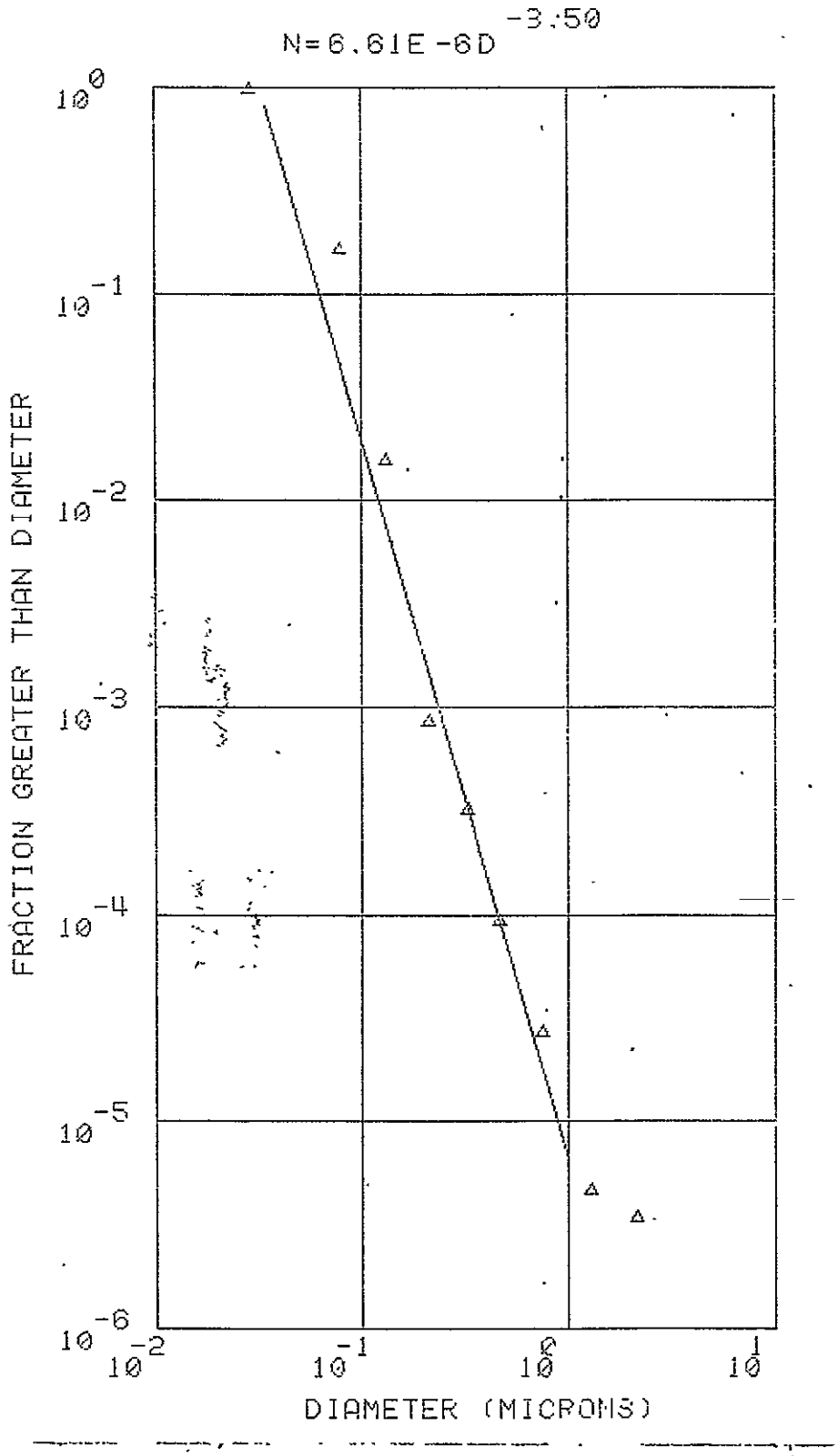

Figure III-1

Cumulative normalized data from tape impactor

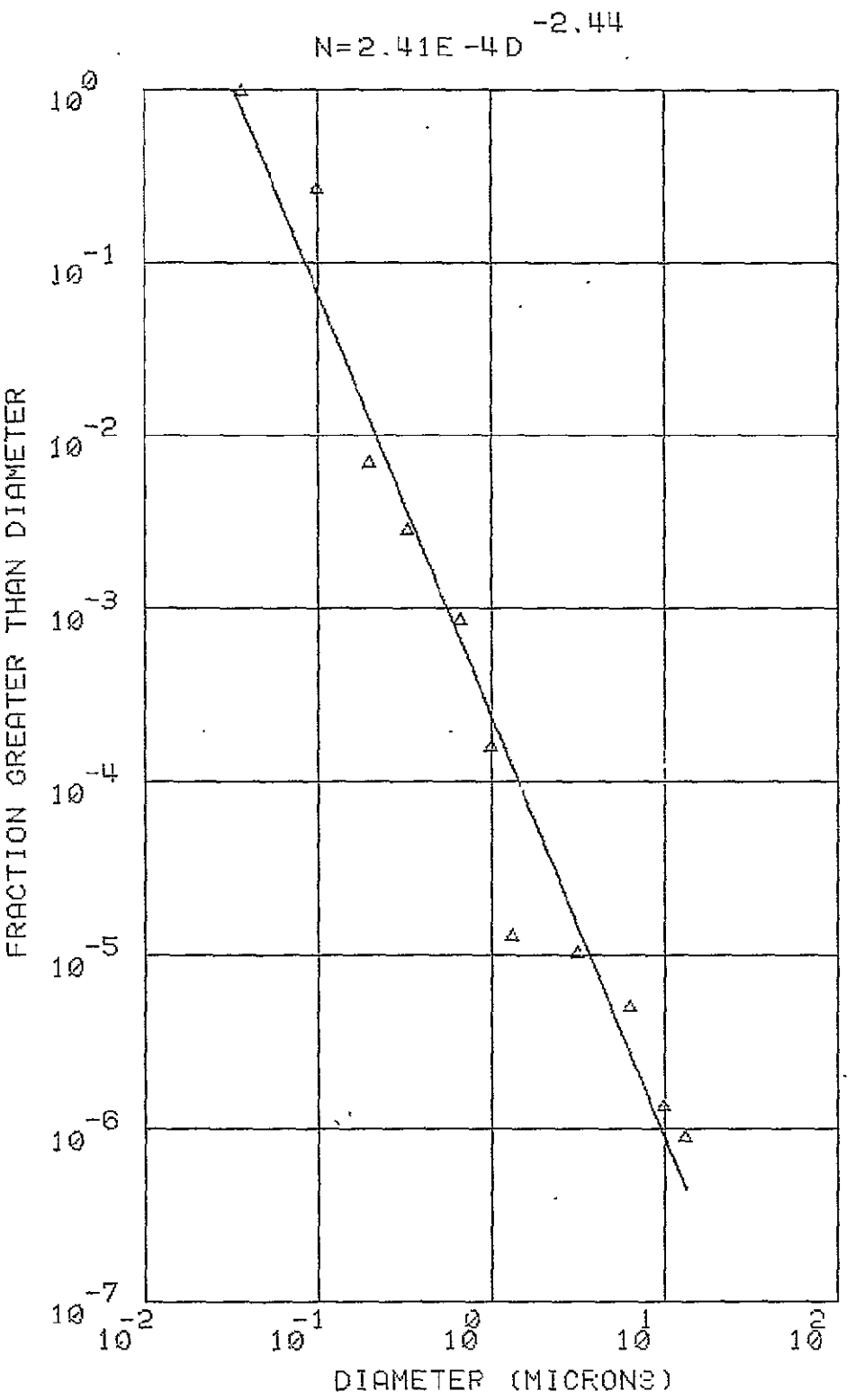

Figure III-2

Cumulative normalized data from wire impactor

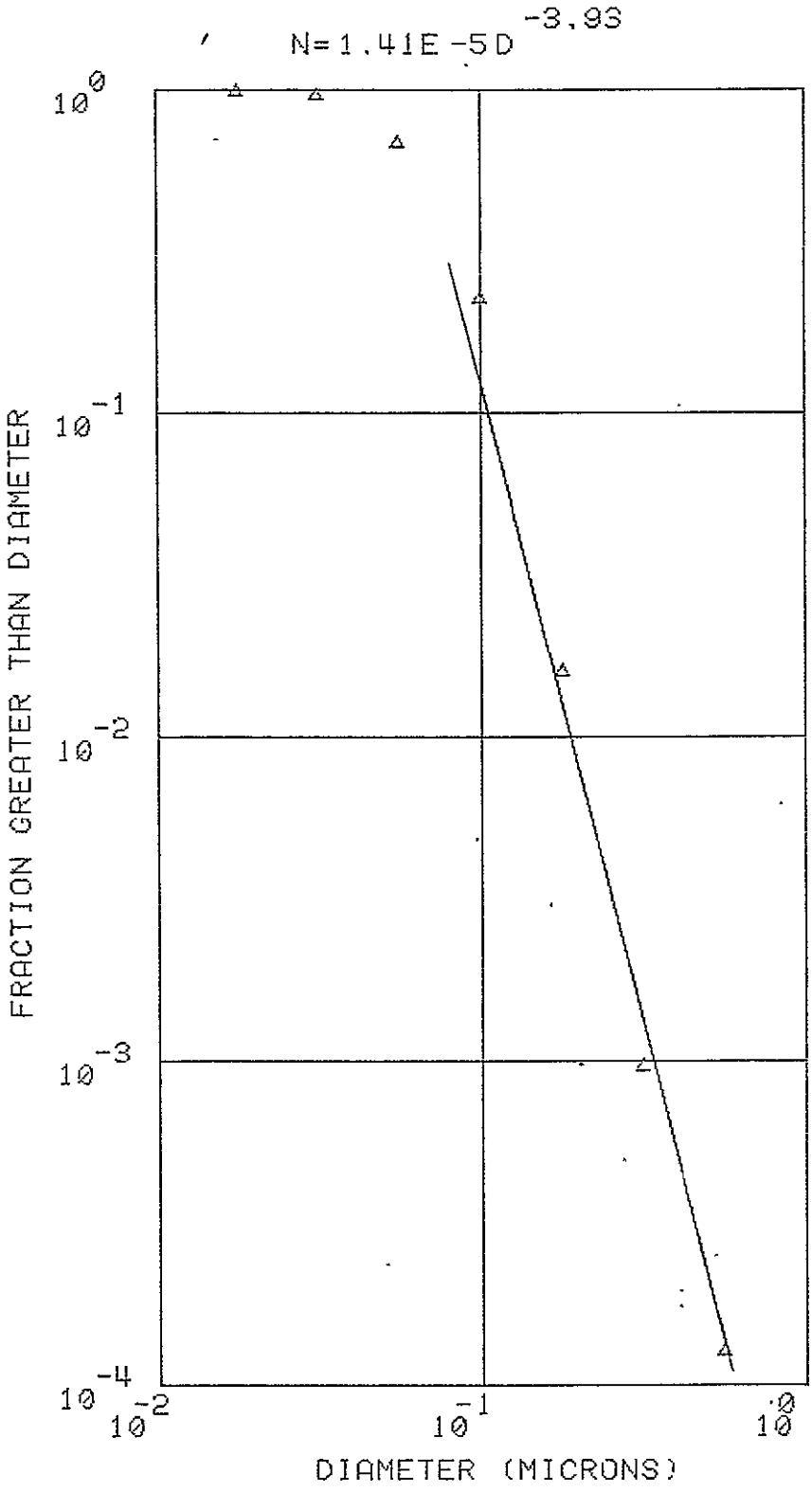

Figure III-3

Cumulative normalized data from electrical mobility analyzer (WTR- T + 6:30)

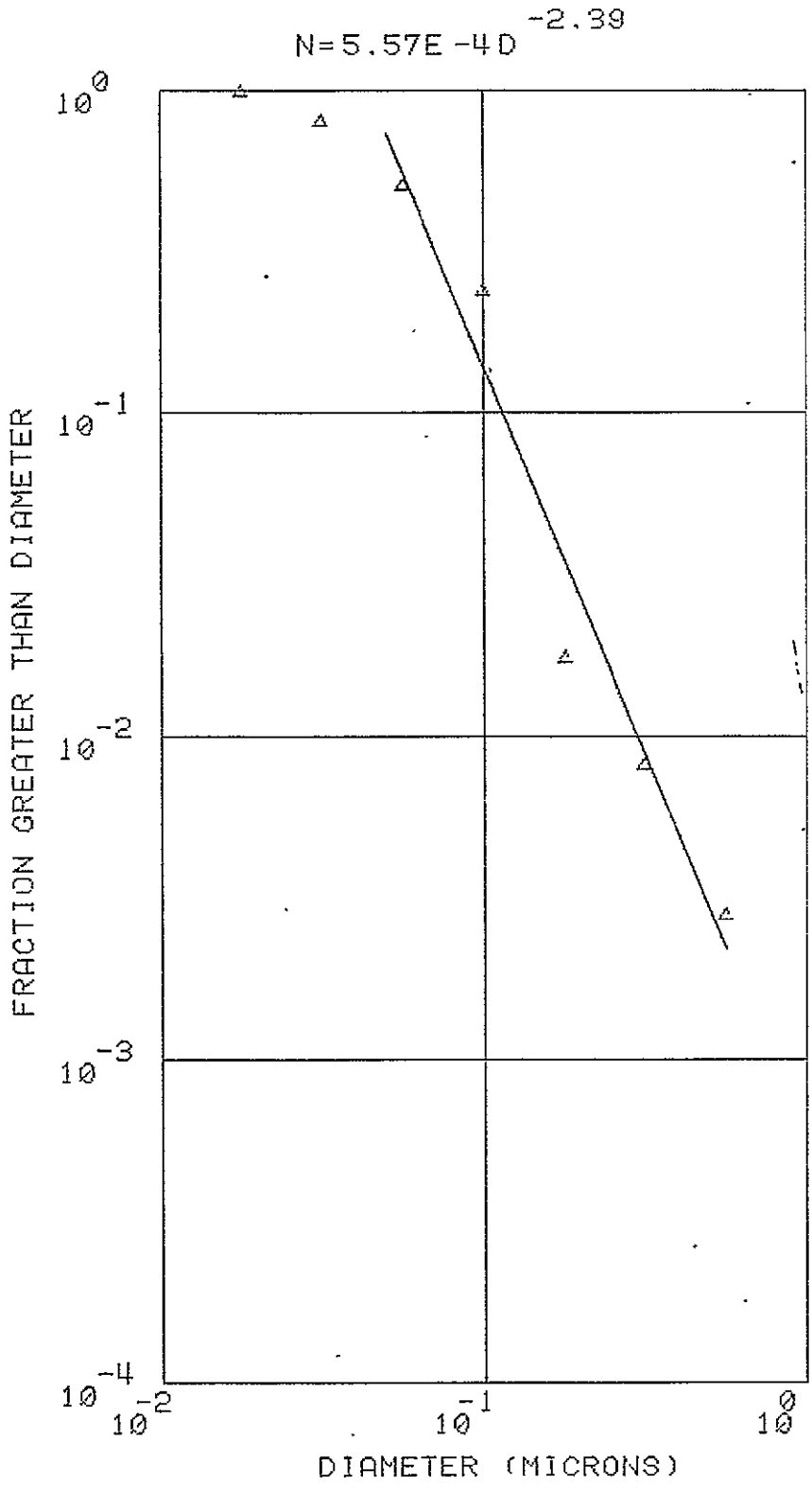

Figure III-4

Cumulative normalized data from electrical mobility analyzer (WTR- T + 13:30)

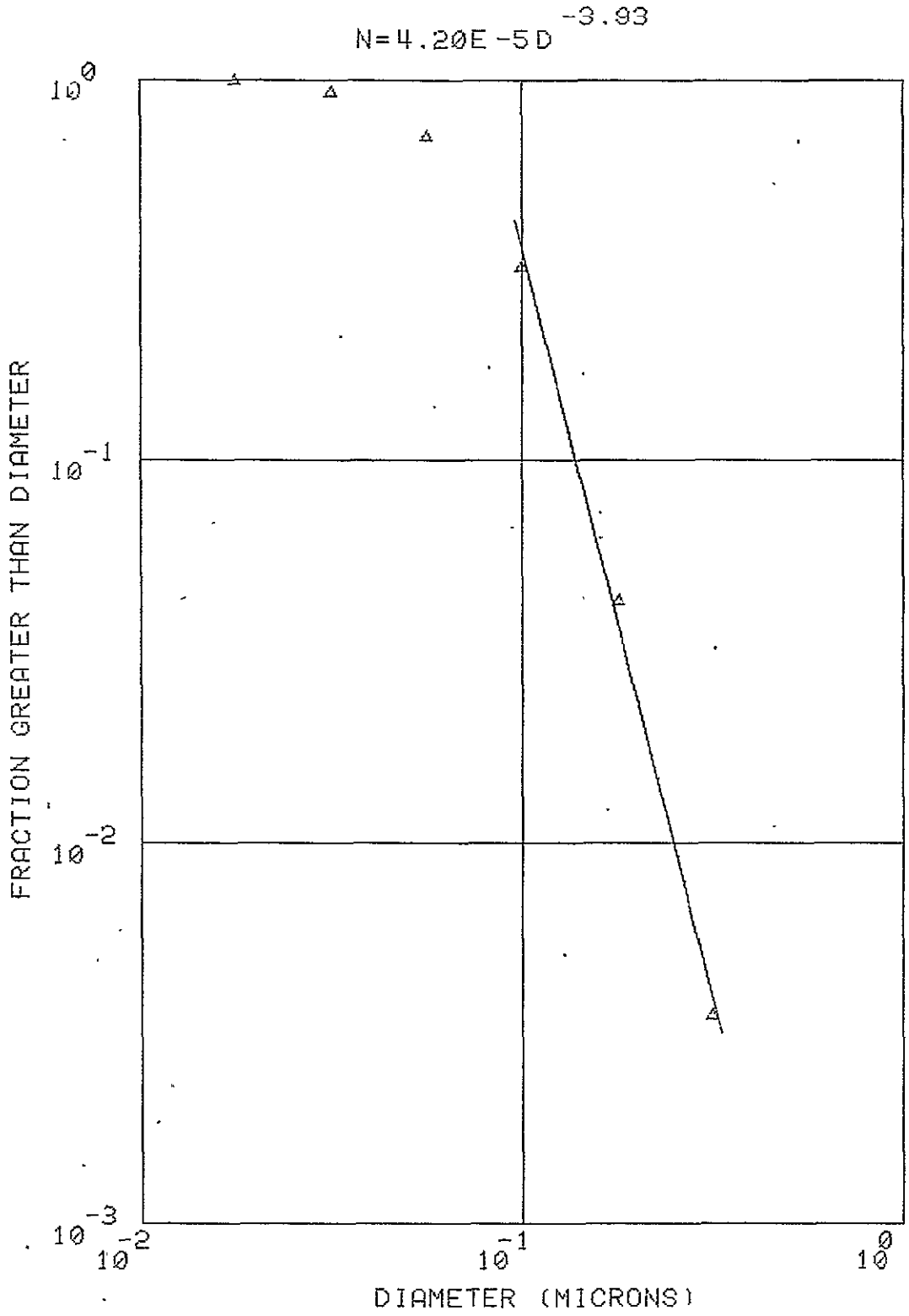

Figure III-5

Cumulative normalized data from electrical mobility analyzer (ETR- T + 7)

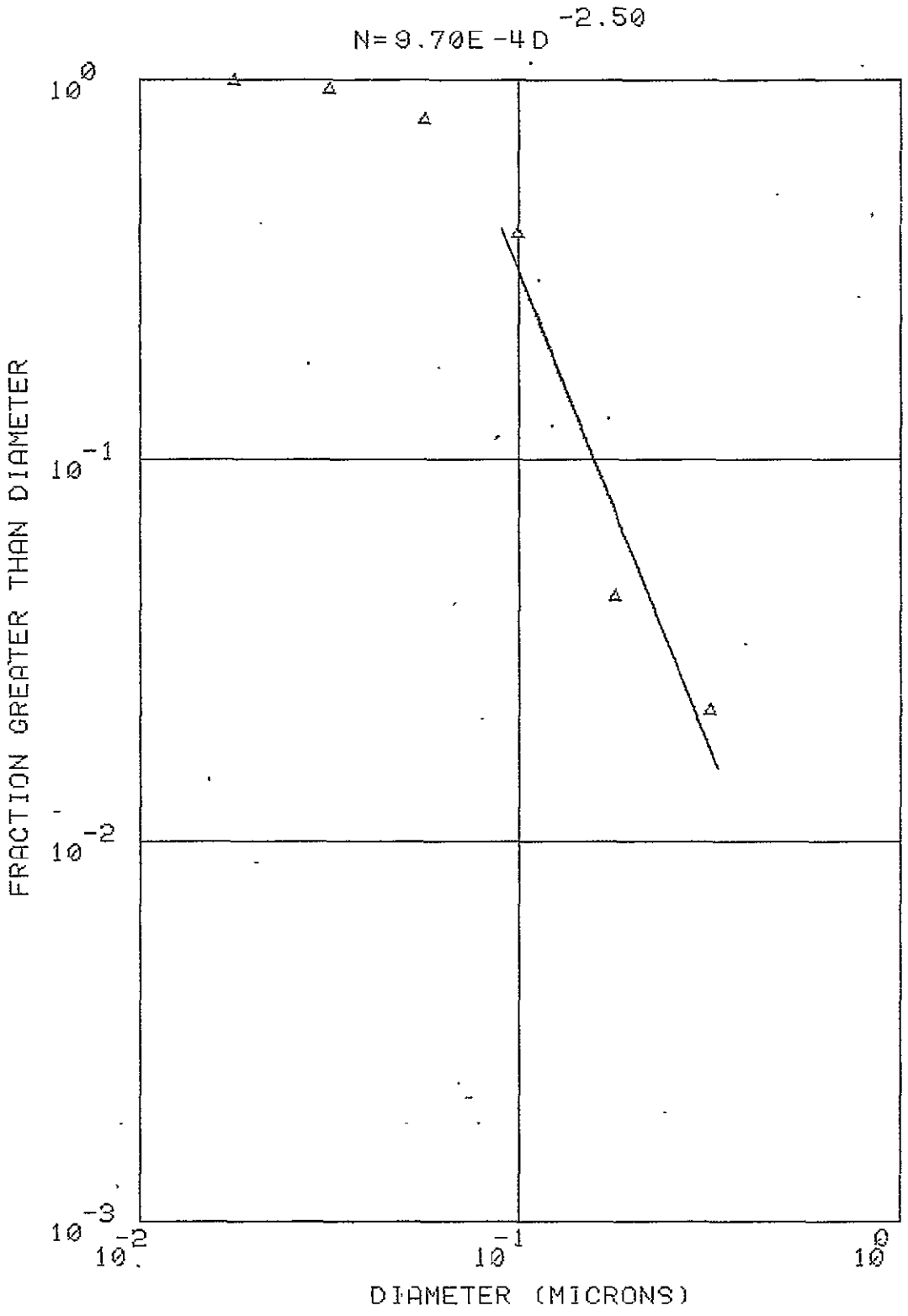

Figure III-6

Cumulative normalized data from electrical mobility analyzer (ETR- T + 13)

terminated at 50 μm because sedimentation of particles larger than this size will rapidly remove them from the cloud.

Inspection of the size distribution at longer times (Figures III-2, III-4, III-6) indicate that an average distribution of the form

$$-dN = N_1 D^{-3.5} dD \quad (0.07\ \mu m \leq D \leq 50\ \mu m)$$

is appropriate. At the smaller sizes, the data can be described by a similar function of the form

$$-dN = N_o D^{-1.75} dD \quad (0.02\ \mu m \leq D \leq 0.07\ \mu m)$$

where the slope is one half the value for the distribution at larger sizes.

2. Aerosol number concentration

Having specified the form of the size distribution, the problem of determining the number concentration remains. The determination of the number concentration is best accomplished through the requirement of mass conservation. By integration of the mass represented by the two distributions, assuming the density of an aerosol particle to be 2.5 g cm^{-3} (Varsi, 1976), and the requirement of continuity of the two cumulative distributions, the number concentration can be calculated from the mass concentration as given in Table III-II. Following this procedure, the number concentration was calculated as a function of time with the results given in Table III-III

TABLE III-III

Computed Aerosol Concentrations (0.02 μm < D < 50 μm)

Time	Aerosol Number Concentration
T + 3 hrs.	6.63×10^{9} m^{-3}
T + 1 day	7.96×10^{8} m^{-3}
T + 3 days	2.65×10^{9} m^{-3}
T + 7 days	1.14×10^{8} m^{-3}

For the purposes of this evaluation, the total mass of material in the cloud at 3 hours is assumed conserved at later times and the form of the distribution function is assumed constant with time.

E. SUMMARY AND RECOMMENDATIONS

Specification of the Al_2O_3 aerosol in the stabilized ground cloud has been accomplished in terms of cloud volume, average mass concentration, and the particle size distribution. These results have been derived from extrapolated cloud volume data, mass of Al_2O_3 in the ground cloud, and measured size distributions. Under the assumption that all mass present at three hours is present at later times and the size distribution remains constant in form, the resulting set of specifications are consistent with mass conservation.

Future measurements of the aerosol in the stabilized ground cloud should concentrate on the problem of determining the mass balance and size distribution for times extending to at least several hours after launch. It would also be of vital importance to measure total particle concentration, and particularly the spectra of cloud condensation nuclei and ice nuclei during the same period. The availability of a complete and consistent set of data on the aerosol in the stabilized ground cloud is essential to improving estimates of the inadvertent weather modification impact of shuttle exhaust products. Measurements of size distributions alone would be a quite inadequate substitute for specific measurements of those properties which are of direct cloud physical importance.

F. REFERENCES

1. Fitzgerald, J.W., 1972: "A Study of the Initial Phase of Cloud Droplet Growth by Condensation: Comparison Between Theory and Observation", University of Chicago Cloud Physics Lab., Tech. Note, 44, 144 pp.

2. NASA Staff, 1975: "Nozzle Exit Exhaust Products From Space Shuttle Boost Vehicle (November 1973 Design)", NASA-JPL Tech. Memo. 37-712.

3. NASA Staff, 1975: "Information Presented at the Atmospheric Effects Working Group Meeting, November 4-5, 1975", Langley Research Center.

4. Varsi, G., 1976: "Particulate Measurements, Presentation at Space Shuttle Environmental Assessment Workshop (Stratosphere) March, 1976.

Chapter IV

WARM CLOUDS

Outline

Chapter IV

WARM CLOUDS

A. INTRODUCTORY REMARKS

As described in Chapter III, at 3 hours from launch, the SGC has a volume of about 600 km^3, having by then mixed with many times its original volume of ambient air within the surface mixing layer. The enlarged and diluted cloud will then contain an aerosol consisting of the natural background aerosol, with the addition of particles derived from the SGC, the properties of which have been discussed in Chapter III. The 3-hour cloud will continue to be further diluted with additional volumes of ambient air during its subsequent drift downwind, and at some point in its history may become involved in upcurrents which could result in the formation of cloud and precipitation. Even while still in the surface layers, the SGC may become involved in condensation processes if fog forms.

The microphysical properties of the resulting water cloud may be modified in several ways, as a result of the presence of the artifically added aerosol. In some circumstances, such modification could have significant effects on the formation of precipitation and on the dynamical behaviour of the cloud.

With the Florida area, the enlarged and diluted SGC will usually become involved in convective (rather than stratiform) clouds. These form in updrafts caused by heating contrasts or by squall line convergence. The artificial aerosol can then influence cloud physics processes in the following ways:

(a) It may provide giant hygroscopic particles which act as the embryos for raindrop formation;

(b) It may modify the basic microstructure of the cloud, tending to convert clouds which naturally would have had a colloidally unstable maritime microstructure into colloidally stable continental type clouds, thus tending to delay rain formation;

(c) It may catalyze the formation of ice particles, so enhancing precipitation formation (discussed in Chapter V);

(d) As a result of increased ice formation, the additional latent heat released may warm the cloud sufficiently to cause it to break through a stable layer. If this occurs, the basic updraft may increase, and the cloud may become both deeper and wider than previously, with the possibility of greatly increased precipitation (Chapter V).

B. THE S.G.C. PARTICLE SIZE DISTRIBUTION AND SURFACE PROPERTIES

1. Size Distribution

As discussed in Chapter III, measurements made on the S.G.C. aerosol indicate that in the size range 0.035 μm<r<5 μm, the concentration ($N(r_p)$) of particles per cm^3 for which $r>r_p$ is given by a relation of the form

$$\ln N(r_p) = a_1 - 2.5 \ln r_p$$

It is assumed here that this same law holds for sizes up to r = 25 μm. In the region below r = 0.035 μm, it is expected that coagulation in the early SGC will have reduced the slope of the distribution, which will be approximated down to r = 0.01 μm by:

$$\ln N(r_p) = a_o - 0.75 \ln r_p$$

These relations obviously must give the same value of $N(r_p)$ when $r_p = r_1 = 0.035$ μm. Thus, the constants a_1 and a_o, which are functions of time and decrease as the cloud is mixed and diluted, are related as follows:

$$\exp a_o = r_1^{-1.75} \exp a_1$$
$$= 3.531 \times 10^9 \exp a_1 ,$$

all lengths being expressed in centimeters.

Writing A(t) for $\exp a_1$, it then results that in the range 0.035 μm<r_p<25 μm,

$$N(r_p) = A(t)\, r_p^{-2.5}$$

while in the range 0.01 μm<r_p<0.035 μm,

$$N(r_p) = 3.531 \times 10^9\, A(t)\, r_p^{-0.75}$$

Taking the density of the aerosol particles (Chapter III) as 2.5 g cm^{-3} for all sizes, and writing $M_1(r_p)$ for the mass concentration (g cm^{-3}) of the aerosol in the form of particles for which $r>r_p$, in the range 0.035 μm$<r_p<$25 μm the mass distribution is given by:

$$M_1(r_1) - M_1(r_2) = 52.36\ A(t)\ (r_2^{0.5} - r_1^{0.5})$$

In particular, the total mass of concentration (g cm^{-3}) in the whole range considered, from r = 0.035 μm to r = 25 μm, is 2.520 A(t) g cm^{-3}.

In writing similary $M_o(r_p)$ for the range below 0.035 μm,

$$M_o(r_1) - M_o(r_2) = 1.233\times10^{10}\ A(t)\ (r_2^{2.25} - r_1^{2.25})$$

and over the range 0.01 μm$<r_p<$0.035 μm, the total mass concentration is 6.143×10^{-3} A(t). Thus the total mass concentration of the aerosol in the range r_p = 0.01 μm to 25 μm is 2.526 A(t) g cm^{-3}. This expression for the total aerosol mass concentration is essentially independent of the lower limit of particle radius.

At T + 3 hours, as discussed in Chapter III, the total mass of the aerosol particles in the SGC cloud is taken to be 9×10^{7} g, the cloud volume at that time being 600 km^3, so that the mean mass concentration is 1.5×10^{-10} g cm^{-3}. Thus at T + 3 hours, A(t) = 5.938×10^{-11}. At later epochs, A(t) will be smaller, in inverse proportion to the total volume of the mixed and diluted SGC.

Thus, at T + 3 hours, in the size range 0.035 μm<r_p<25 μm,

$$N(r_p) = 5.938 \times 10^{-11} \; r_p^{-2.5},$$

and over this range, the total number concentration is 2.591×10^3 cm^{-3}.

In the range 0.01 μm<r_p<0.035 μm,

$$N(r_p) = 2.097 \times 10^{-1} \; r_p^{-0.75},$$

and over this range, the total number concentration is 4.040×10^3 cm^{-3}. Thus the total number concentration at T + 3 hours in the range 0.01 μm<r_p<25 μm is 6.631×10^3 particles per cm^3.

2. Surface Properties

It is assumed here that the surface properties of the Al_2O_3 particles have been irreversibly modified by reaction with gaseous HCl and H_2O to form a soluble surface layer. The reaction is supposed to proceed to a uniform depth x cm in every particle, irrespective of its size. It is further supposed that the reaction combines y grams of gaseous material with each gram of Al_2O_3, resulting in the formation of (1+y) grams of soluble hydrated surface chloride, which is assumed to have a constant effective molecular weight (in dilute solution) of M. Nominal values assumed are x = 10^{-8} and 10^{-7} cm, y = 1, M = 30. These values imply an areal surface density of the soluble product of 5×10^{-8} to 5×10^{-7} g cm^{-2} (0.5 to 5 mg per m^2).

C. GIANT AEROSOL PARTICLES

When a giant hygroscopic nucleus (r>1μm) is exposed to the saturated air within a cloud, it forms a droplet which outgrows its neighbors which typically contain nuclei with radii of less than 0.1 μm; this is a result of the strong depression of the equilibrium vapor pressure over the surface of the large droplet. Such fast-growing droplets can become the embryos of raindrops, since some of them can rather quickly reach sizes at which collision-coalescence growth begins. It is generally agreed that those giant soluble particles (such as sea salt particles) which have dry radii exceeding 10 μm are candidates to form precipitation embryos, and that if they occur in concentrations exceeding 10^{-3} cm^{-3}, they may well cause precipitation formation.

As discussed in paragraph B, the Al_2O_3 particles derived from the SGC are only partly soluble. Since the giant particle effect depends on the strong and persistent vapor pressure lowering by the solute (which is very large compared with the opposing Kelvin effect), the relevant factor is the mass of soluble material in the particle.

It is assumed here that an outer layer of depth x cm on each particle has combined with gases in the SGC to form a soluble material, the reaction involving y grams of gas for each gram of Al_2O_3. The resulting layer of soluble material then has a mass $4\pi\rho_p(1+y)r_p^2x$, where ρ_p is taken as 2.5 g cm^{-3} (Chapter IV).

The mass of a sea salt particle of radius 10^{-3} cm and density 1.2 g cm^{-3} is about $5x10^{-9}$ g. The modified Al_2O_3 particle which has a coating of soluble material of equal mass must have a radius of about $(5x10^{-9}/4\pi\rho_p(1+y)x)^{1/2}$. Taking ρ_p = 2.5 g cm^{-3}, and giving y the nominal value of 1, and x a maximum value of 10^{-7} cm, this is about $2.8x10^{-2}$ cm, which lies well above the assumed maximum size ($r_p = 2.5x10^{-3}$ cm) of particles in the SGC at T + 3 hours. Even if the size distribution assumed for particle radii exceeding r_p = 0.035 μm were extrapolated to $2.8x10^{-2}$ cm, the expected concentration at T + 3 hours would be only about $5x10^{-7}$ cm^{-3}, which is very small compared with the concentration of such particles necessary to initiate rain formation ($\sim 10^{-3}$ cm^{-3}).

It may be concluded that at and beyond T + 3 hours, any giant particles present would have no significant effect on rain formation.

D. CLOUD FORMATION

The most critical property of a particle with regard to cloud formation is its critical supersaturation (S_c), that is, the maximum supersaturation with which a large droplet can be in equilibrium. As discussed in paragraph B, it is assumed that the Al_2O_3 particles have been chlorinated to a depth x cm, resulting in the production of a hygroscopic water soluble material, the average molecular weight of the ions produced at complete dissociation in a dilute solution (M) being about 30. If a unit mass of Al_2O_3 combines with surrounding gas to form a mass (1+y) of the chlorinated soluble compound, after chlorination has occurred, a particle of Al_2O_3 with an original radius of r_p will contain a mass $\frac{4}{3}\pi \rho_p (r_p-x)^3$ grams of unaltered Al_2O_3, together with $\frac{4}{3}\pi \rho_p (1+y) [r_p^3 - (r_p-x)^3]$ grams of the soluble product of the chlorination reaction, ρ_p being the density of the Al_2O_3 particles. On exposure to high relative humidity, a haze droplet will be formed which will consist of a droplet of solution enclosing a particle of Al_2O_3 of radius (r_p-x).

If this haze droplet has a radius r(cm), assuming that the solution is dilute, the molar ratio of the solution (μ) will be given approximately by:

$$\mu = \frac{M_o \rho_p (1+y) [r_p^3 - (r_p-x)^3]}{M \rho_L [r^3-(r_p-x)^3]} \text{ moles per mole.}$$

where M_o is the molecular weight of water, M is the effective molecular weight of the solute (assumed to be 30), and ρ_L is the density of the solution which is taken to be equal to that of water.

As the relative humidity increases, the haze droplet radius will increase. When the air is close to saturation (either slightly supersaturated or slightly undersaturated) the equilibrium supersaturation of the haze droplet (S(r)) is given approximately (in absolute units) by:

$$S(r) = \frac{2\sigma M_o}{RT\rho_L r} - \mu(r)$$

S(r) is stationary (and a maximum) when

$$\frac{2\sigma M_o}{RT\rho_L r^2} = -\frac{\partial \mu}{\mu r}$$

$$= \frac{3 r^2 M_o \rho_p (1+y) [r_p^3 - (r_p-x)^3]}{M \rho_L [r^3-(r_p-x)^3]^2}$$

The corresponding "critical" value of $r(r_c)$ is thus found by solving the equation:

$$f(r) = r^6 - \frac{3 \rho_p(1+y) [r_p^3 - (r_p-x)^3] RT r^4}{2 M\sigma}$$

$$- 2(r_p-x)^3 r^3 + (r_p-x)^6 = 0 \qquad (1)$$

Since $f(r)$ is positive at $r=0$, and can be shown to have one and only one turning point in the region $r>0$, $f(r)=0$ has either no real roots, or two. Since at $r=(r_p-x)$, $f(r)$ is negative, there must be two real roots greater than zero, one greater and one less than (r_p-x). Only the larger root has physical meaning, since r necessarily exceeds (r_p-x).

The corresponding critical supersaturation (S_c) is then given by:

$$S_c = S(r_c) = \frac{2\sigma M_o}{RT\rho_L r_c} - \mu(r_c)$$

In view of the definition of r_c, $[r_c^3 - (r_p-x)^3]$ is proportional to r_c^2, and it results that:

$$S_c = \frac{2\sigma M_o}{RT\rho_L r_c} - \frac{1}{r_c^2}\sqrt{\frac{2\sigma\rho_p M_o^2 (1+y) [r_p^3 - (r_p-x)^3]}{3 RT M\rho_L^2}} \qquad (2)$$

Thus, in a case where the entire particle has been transformed into a soluble material ($x=r_p$), it results that:

$$S_c^2 = \frac{32 \sigma^3 M M_o^2}{27 \rho_p(1+y) \rho_L^2 R^3 T^3 r_p^3}, \qquad (3)$$

which agrees with the usual formula for the critical supersaturation of a soluble particle with a density equal to $\rho_p(1+y)$.

An evaluation of the effect of the diluted SGC in increasing the concentration of cloud condensation nuclei would therefore involve solving equation (1) to find r_c, and hence evaluatting S_c from equation (2). A much simpler approximate procedure is to compare the actual SGC aerosol with one containing the same mass of soluble material in each particle, but without the insoluble component (of radius $(r_p - x)$). It can be shown that the effect of the insoluble component in the SGC aerosol is to lower the critical supersaturation of the particle. Thus the "soluble component only" aerosol will provide a lower bound to the effect of the SGC on the S_c spectrum and hence on cloud formation.

Consider a haze droplet of radius r formed on an aerosol particle consisting of a mass m of soluble material of molecular weight M and containing an insoluble particle of radius r_i. Then the molar fraction comprised by the solute is approximately

$$\frac{3m\ M_o}{4\pi\rho_L M(r^3 - r_i^3)}$$

and hence for this composite particle,

$$S(r) = \frac{2\sigma M_o}{RT\ \rho_L r} - \frac{3m\ M_o}{4\pi\rho_L\ M(r^3 - r_i^3)} \qquad (4)$$

As before S_c $(= S(r_c))$ is found by solving $\frac{\partial S}{\partial r} = 0$ to find r_c, and substituting this value of r back in the expression for S(r).

Now, from equation (4),

$$\frac{\partial S_c}{\partial r_i} = \left(\frac{\partial S(r)}{\partial r}\right)_{r_c} \frac{\partial r_c}{\partial r_i} + \left(\frac{\partial S(r)}{\partial r_i}\right)_{r_c}$$

$$= \left(\frac{\partial S(r)}{\partial r_i}\right)_{r_c},$$

since $\left(\frac{\partial S(r)}{\partial r}\right)_{r_c} = 0$

Hence ,

$$\frac{\partial S_c}{\partial r_c} = \frac{-9m\ M_o r_i^{\,2}}{4\pi\rho_L\ M(r_c^{\,3} - r_i^{\,3})^2}$$

Similarly,

$$\left(\frac{\partial^2 S_c}{\partial r_i^{\,2}}\right)_{r_c} = \frac{\partial}{\partial r_i}\ \frac{\partial S_c}{\partial r_i}$$

$$= \frac{-18m\ M_o\ r_i}{4\pi\rho_L\ M(r_c^{\,3} - r_i^{\,3})^2} - \frac{54\ m\ M_o r_i^{\,4}}{4\pi\rho_L(r_c^{\,3} - r_i^{\,3})^3}$$

Thus, using the fact that $\left(\frac{\partial S(r)}{\partial r}\right)_{r_c}$ is zero, it can be shown that not only the first derivative of S_c with respect to r_c is negative, but all the higher derivations also. Hence, the critica supersaturation of the particles is a monotonically decreasing function of r_i.

The S_c values for the "soluble component only" aerosol may be deduced from equation (3) by substituting $3r_p^{\,2}x$ for $r_p^{\,3}$, or alternatively by differentiating equation (4) with respect to r (with $r_i = 0$), substituting this value back into (4), and finally substituting $4\pi\rho_p(1+y)\ r_p^{\,2}x$ for m.

Either of these procedures yield:

$$S_c^{\,2} = \frac{32\ M\ M_o^{\,2}\sigma^3}{81\rho_p\rho_L^{\,2}\ (1+y)R^3T^3r_p^{\,2}x}$$

so that one may write

$$S_c = \frac{b}{r_p}$$

where $b^2 = \frac{32\ M\ M_o^2 \sigma^3}{81 \rho_p \rho_L^2 (1+y)\ R^3 T^3 x}$

At 20°C, taking y = 1, for $x = 10^{-8}$ cm, $b = 4.514 \times 10^{-8}$. For $x = 10^{-7}$ cm, $b = 1.427 \times 10^{-8}$. Warm cloud effects are discussed below for the two cases.

The concentration ($N(S_c)$) of particles with critical supersaturations less than S_c is equal to that of particles exceeding $(\frac{b}{S_c})$ in radius. In the size range 0.035 μm<r_p<25 μm, th distribution is given at T + 3 hours by:

$$N(S_c) = 5.938 \times 10^{-11} \left(\frac{b}{S_c}\right)^{-2.5}$$

while in the size range 0.01 μm<r_p<0.035 μm,

$$N(S_c) = 0.2097 \left(\frac{b}{S_c}\right)^{-0.75}$$

The value of b depends on that of x.

Thus, for $x = 10^{-8}$ cm,

$$N(S_c) = 1.372 \times 10^{8}\ S_c^{2.5}$$

for values of S_c up to 1.290×10^{-2}. For greater values of S_c,

$$N(S_c) = 6.771 \times 10^{4}\ S_c^{0.75}$$

On the other hand, for $x = 10^{-7}$ cm,

$$N(S_c) = 2.441 \times 10^{9}\ S_c^{2.5}$$

for values of S_c up to 4.077×10^{-3}. For greater values of S_c,

$$N(S_c) = 1.606 \times 10^{5}\ S_c^{0.75}$$

The spectrum of the critical supersaturations (S_c) of the natural aerosol in the Florida region has been studied by Fitzgerald (1972) who found that over the ocean, the average distribution was

$$N(S_c) = 2420\ S_c^{0.46}$$

where S_c is expressed, as earlier, in absolute units (not percent and $N(S_c)$ is the concentration of particles with critical supersaturations less than S_c.

Over the land, Fitzgerald found:

$$N(S_c) = 5913\ S_c^{0.53}$$

Depending on the nature of the aerosol and the speed of updra cloud droplet formation occurs on particles with critical supersaturations typically in the range 10^{-3} to 10^{-2}.

The following Table IV-I compares the artificial CCN concentrations at T + 3 hours with the natural background concentration found by Fitzgerald (1972).

Table IV-1

Concentrations of artificial CCN activated at various supersaturations characteristic of cloud formation in the SGC cloud at T + 3 hours, and in the natural atmosphere in Florida.

S_c (absolute units)	Concentrations (cm^{-3})			
	For $x=10^{-8}$cm (artificial particles only)	For $x=10^{-7}$cm (artificial particles only)	In the Natural Atmosphere Over Ocean	In the Natural Atmosphere Over Land
10^{-3}	4.3×10^{0}	7.7×10^{1}	1.0×10^{2}	1.5×10^{2}
3×10^{-3}	5.8×10^{1}	1.2×10^{3}	1.7×10^{2}	2.7×10^{2}
6×10^{-3}	3.8×10^{2}	3.5×10^{3}	2.3×10^{2}	3.9×10^{2}
10^{-2}	1.4×10^{3}	5.1×10^{3}	2.9×10^{2}	5.2×10^{2}

The following Table IV-2 shows how many hours must elapse before the concentration of artificial CCN becomes equal to or less than that characteristic of the background aerosol over the land. When this occurs, the total concentration will be twice that of the natural atmosphere. The decrease of the artificial component has been calculated on the basis of the linear increas in cloud volume discussed in Chapter III.

Table IV-2

Time in hours beyond T + 3 hours until the SGC is diluted to the degree that the total concentration of CCN (artificial and natural) is twice that characteristic of the Florida peninsula.

S_c (Absolute units)	Time (hours) beyond T + 3 hours	
	$x = 10^{-8}$ cm	$x = 10^{-7}$ cm
10^{-3}	0	0
$3x10^{-3}$	0	10
$6x10^{-3}$	2	24
10^{-2}	11	26

E. CONCLUSIONS AND RESEARCH RECOMMENDATIONS

As discussed in paragraph C, the concentration of giant particles in the SGC is far too low to result in enhanced warm rain formation.

However, at T + 3 hours and for some hours afterwards, the SGC may contain a concentration of CCN which is large compared with that which is naturally present. Thus if chlorination penetrates to a depth of $x = 10^{-7}$ cm in the Al_2O_3 particles, the SGC will have a definite effect on cloud formation for a day or more, resulting in highly continental clouds which will be quite inefficient in forming rain by the warm rain process. In the case where $x = 10^{-8}$ cm, this effect is probably appreciable for a few hours only.

Since the effects of the SGC on cloud formation seem likely be very significant, it would appear to be important to make direct measurements of the spectrum of the critical supersaturations of SGC aerosol. This would provide in a direct manner a far more certain basis for the estimation of warm cloud effects than is presently available, or could be deduced from chemical analyses.

F. REFERENCES

1. Fitzgerald, J.W. (1972): "A Study of the Initial Phase of Cloud Droplet Growth by Condensation; Comparison Between Theory and Observation", University of Chicago, Cloud Physics Lab. Tech., Note No. 44.

Chapter V

CLOUD PHYSICS PROCESSES - COLD CLOUDS

Outline

Chapter V

CLOUD PHYSICS PROCESSES - COLD CLOUDS

A. ICE PHASE DEVELOPMENT AND PRECIPITATION IN CLOUDS

1. General

Only a small percentage of clouds reach the precipitation stage. The progression from minute cloud droplets (circa 1-25 μm radius) to falling hydrometeors, if it is to occur at all, involves three basic processes:

a. droplet collisions and coalescence

b. the ice crystal or Bergeron-Findeison process whereby ice crystals grow by diffusion of water vapor at the expense of evaporating supercooled drops and from cloud vapor generated in vertical updrafts

c. the ice crystal process augmented by collisions with droplets (riming) and/or other crystals (aggregation)

Warm rain or that due entirely to droplet coalescence dominates at tropical latitudes. It may even play a role at higher latitudes with unstable clouds not extending to or far above the freezing level. The ice crystal mechanism clearly is dominant at polar latitudes and also highly significant at mid-latitudes. In the latter zone, where the world's population and industrialized nations are concentrated, the ice phase combined with collisional mechanisms (item c) prevail. It is well recognized that the heavier mid-latitude precipitation (rain or snow) can only be explained by this combination of mechanisms (Houghton, 1950).

2. Florida Precipitation Processes

Florida, being a sub-tropical region, can experience rainfall by either mechanism (a) or (c) above. However, deep cloud systems and the

ice phase undoubtedly are instrumental in the major production of rainfall on the peninsula. As described in Chapter VII, the summer rainy season extends from roughly May to September or October. During this time, rainfall is likely every day (50% probability) vs. 1-2 days per week in winter, and half the rainfall comes from local showers and thundershowers (Bradley, 1972).

Clearly in these deep convection systems, ice nuclei and crystals are the initial building blocks for subsequent riming, snowflake aggregation, latent heat release, and heavy rainfall. The Florida Area Cumulus Experiment (FACE), conducted by NOAA since 1970, is predicated on the belief that cloud seeding with additional ice nuclei in organized convective systems will enhance rainfall. The effectiveness of FACE to date is not entirely clear; however, the recognized role of the ice phase in Florida precipitation and the comparison between ice nuclei seeding concentrations and that inadvertently released in NASA space shuttle launches are highly relevant (Section C).

Standard temperature lapse rates for summer and winter at latitude 30°N (AFCRL Handbook of Geophysics, 1965) are shown in Figure V-1. It is evident that the freezing levels during the respective warm and cold seasons average roughly 5 and 3.5 km. The -5°C levels, below which ice crystals are only rarely observed, are at approximately 6 and 4 km. As a first approximation then, cloud systems with tops below these levels will not be influenced by ice and only warm rain processes will be involved. In strong convection, particularly in summer, Florida clouds can penetrate well above 6-8 km where freezing phenomena are paramount.

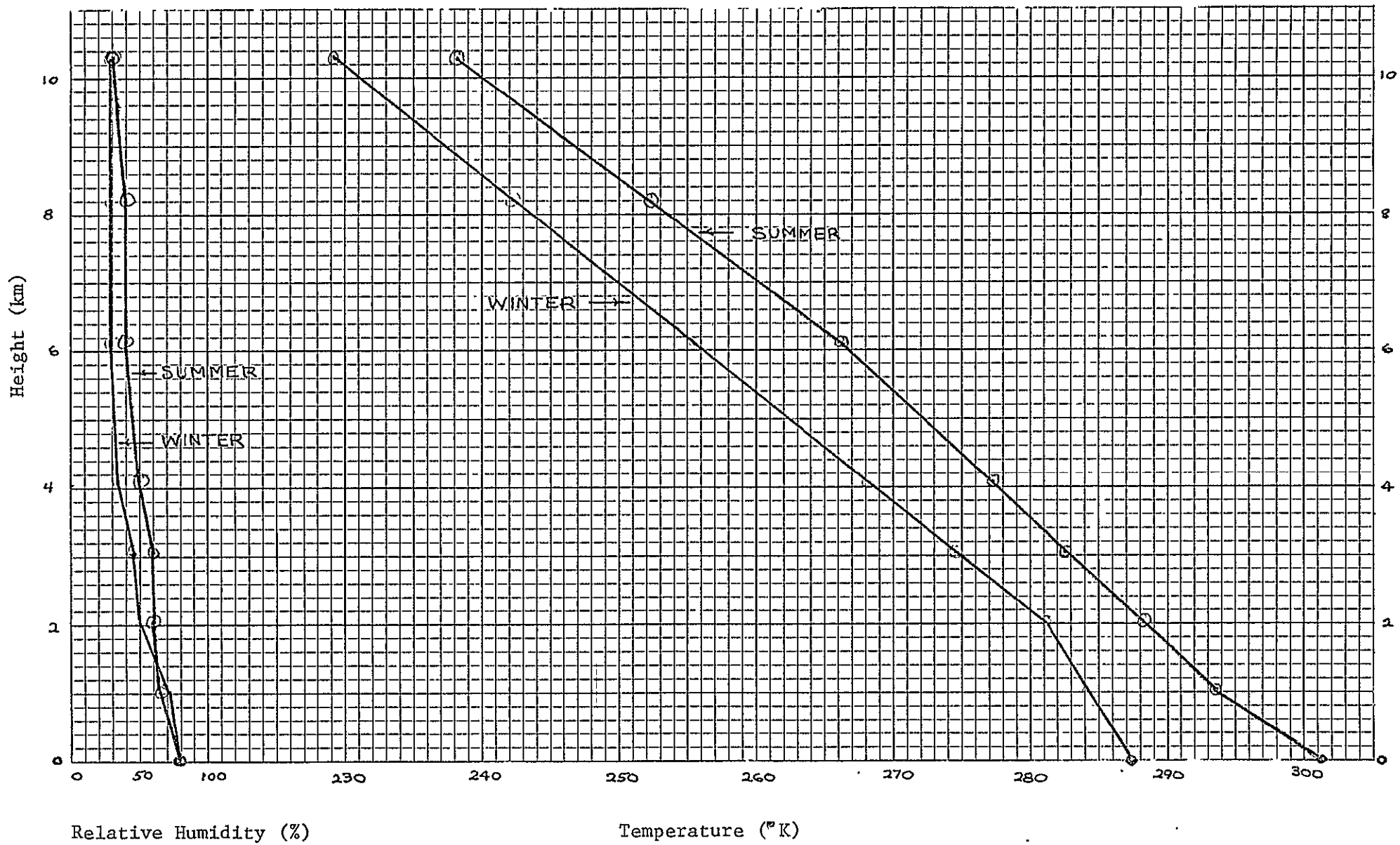

Figure V-1 Subtropical Lapse Rates (30°N)

B. ICE NUCLEATION MODES AND NATURAL ICE NUCLEI (IN) CONCENTRATIONS

1. Ice Nucleation Modes

Particles that promote the formation of ice in clouds are believed to do so via:

a. condensation-freezing

b. contact (with a supercooled drop)

c. sublimation (or direct deposition of vapor onto a solid nucleant)

While uncertainty remains, the condensation-freezing process is a principal mode of nucleation in the atmosphere. In short, mixed ice nuclei, consisting of mainly hydrophobic composition with some hygroscopic sites are effective in attracting water and then initiating freezing. Evidence suggests that this nucleus type may represent the most general type of IN. Contact nuclei, necessarily very small and hydrophobic to avoid building up a water film, appear capable of freezing contacting droplets at relatively warm temperatures. Sublimation nuclei now are considered to be comparatively rare in natural cloud processes, although artificial seeding agents such as silver iodide can act in this manner.

2. Natural IN Concentrations and Sources

While condensation nuclei are plentiful in the atmosphere, particularly over continents and at mid-latitudes, ice nuclei are scarce. The well-quoted global concentration of IN is $1\ell^{-1}$ at -20°C (some 6 orders of magnitude less plentiful than cloud condensation nuclei). For every 4°C temperature warming, there is an approximate order of magnitude decline in activated ice nuclei. Figure V-2 illustrates the

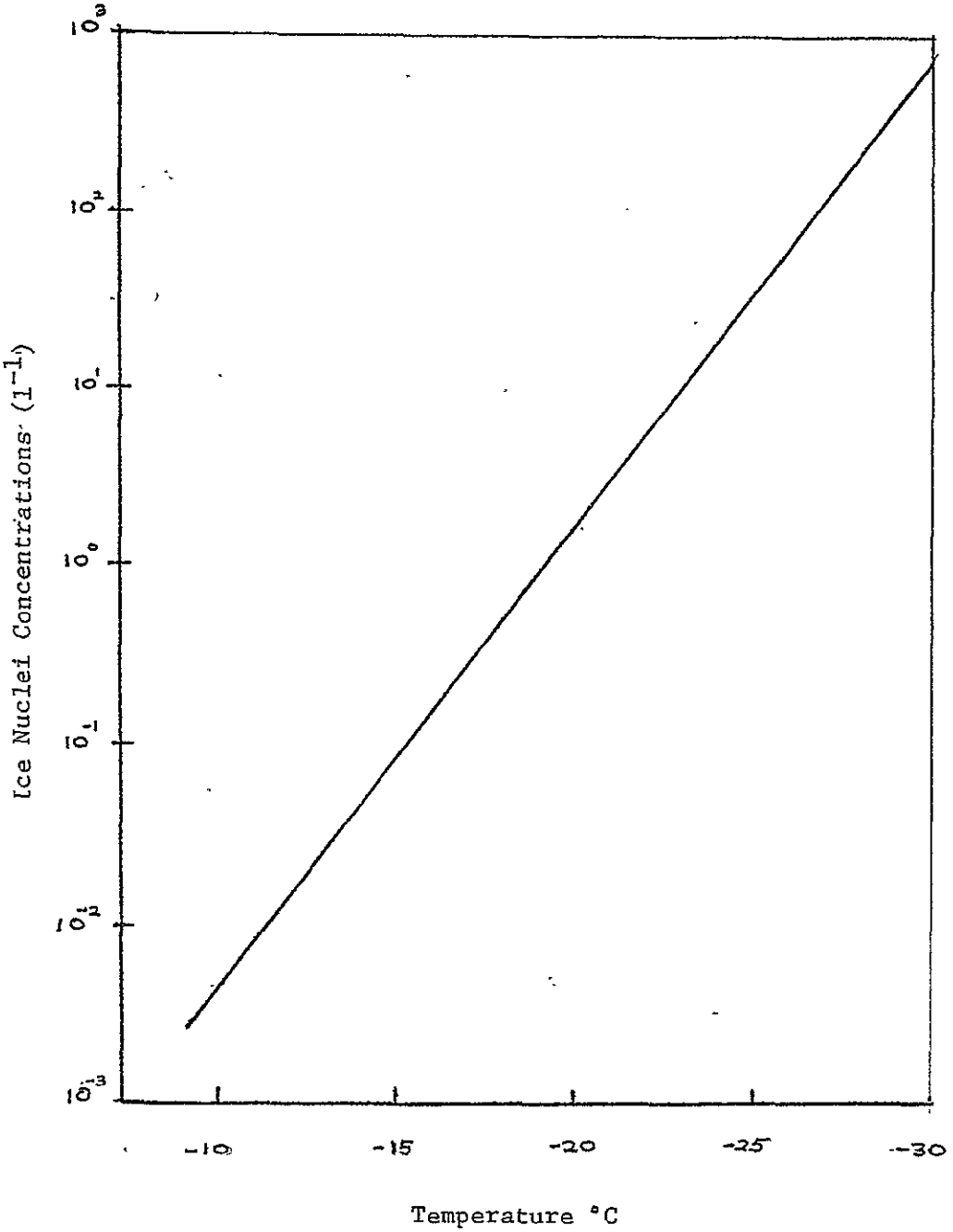

Figure V-2 Ice Nuclei Concentrations vs. Temperature

average concentration of IN as a function of temperature as obtained from the empirical function of Fletcher (1962):

$$IN\ (\ell^{-1}) = 10^{-5} \exp\ (0.6\ \Delta T)$$

where ΔT is the degree of supercooling. While order-of-magnitude departures from this curve occur, it typifies measurements of natural IN concentration made to date.

During the last 10-15 years, however, observational evidence has accumulated to the effect that ice crystal concentrations in clouds sometimes greatly exceed that expected on the basis of ice nuclei concentrations--by factors of up to 10^4. Such occurrences seem more common in aged maritime clouds containing some relatively large drops (e.g., Mossop, 1971). Recent laboratory results (Hallett and Mossop, 1974) indicate that this so-called ice-multiplication process may be at least partially resolved. Crystal enhancement apparently necessitates riming of drops larger than 25 μm dia. at selective temperatures very close to -5°C. In a summary of ice crystal (IC) measurements in clouds by several investigators, it was generalized (Hobbs, 1974) that the IC/IN ratio was on the order of 10^4 at -4°C decreasing to about 10^2 at -14°C and 10^1 at -20°C.

Thus in those selective clouds where multiplication has taken place, background levels of ice might be of order 1 ℓ^{-1} at -14°C and 10-20 ℓ^{-1} at -20°C (in contrast to Figure V-2 values). The foregoing measurements and estimates will be of relevance in estimating the importance of potential IN released in solid rocket motor (SRM) launches by NASA where maritime clouds are often prevalent.

While the sources of naturally occurring ice nuclei are also tenuous, the activity spectra of several suspected materials have been analyzed. The earth's surface, a logical source, contains clays, silicates, and minerals that can serve as active IN (Schaefer, 1949; Mason and Maybank, 1958; Mason, 1971). Clays have activity thresholds (1 active nucleus in $\sim 10^4$) at temperatures as warm as -10°C (common kaolinite at -9°C) and reach high activity levels by -24°C. A list of some of the materials examined and their ice nucleation thresholds appear in Table V-I. From collected snow crystals which were then sublimed, Kumai (1961) observed that soil particles (clays) were the commonly found central residue. Of relevance and to be discussed subsequently, the stabilized ground cloud (SGC) contains large amounts of soil material sucked up from the ground during rocket launch.

Table V-I Ice Nucleating Ability of Naturally Occuring Particles (from Mason 1971)

Substance	Chemical composition	Symmetry	Threshold temperature (° C)	References
Covellite	CuS	Hex	−5	M & M
Vaterite	$CaCO_3$	Hex	−7	M & M
β-Tridymite	SiO_2	Hex	−7	M & M
Magnetite	Fe_3O_4	Cubic	−8	M & M
			−9	I & I
Kaolinite	$Al_2(OH)_4Si_2O_5$	Triclinic	−9	M & M
			−13	I & I
Anauxite	$Al_2(OH)_4 \cdot Si_2O_5$	Monoclinic	−9	M
Illite		Monoclinic	−9	M
Metabentonite			−9	M
Microcline			−9	M & M
Hypersthene	$(Mg, Fe)_2(Si_2O_6)$	Rhombic	−10	I & I
Haematite	Fe_2O_3	Hex	−10	M & M
(Specularite)			−13	I & I
Pyrophyllite	$Al_2(OH)_2 \cdot Si_4O_{10}$	Monoclinic	−10	M
Gibbsite	$Al_2(OH)_6$		−11	M & M
Halloysite	$Al_2(OH)_4\ Si_2O_5 \cdot 2H_2O$	Monoclinic	−12	M
			−13	M & M
Dickite	$Al_2(OH)_4\ Si_2O_5$	Monoclinic	−12	M
Olivine	$(Mg, Fe)_2 \cdot SiO_4$	Rhombic	−12	P & S
			−18	I & I
Aquadag	C		−12	M & M
Dolomite	$CaMg(CO_3)_2$	Hex (Rhomb)	−14	M & M
Biotite		Monoclinic	−14	M & M
Attapulgite	$4H_2O \cdot (OH)_2Mg_5 \cdot Si_8O_{20} \cdot 4H_2O$	Monoclinic	−14	M
Muscovite		Monoclinic	−14	I & I
			< −18	M & M
Vermiculite		Monoclinic	−15	M & M
Nontronite		Monoclinic	−15	M
Montmorillonite		Monoclinic	−16	M
			< −18	M & M
Gypsum	$CaSO_4 \cdot 2H_2O$	Monoclinic	−16	M & M
Graphite	C		−16	M & M
Cinnabar	HgS	Hex	−16	M & M
Orthoclase	$KAlSi_3O_8$	Monoclinic	−17	I & I
			< −18	M & M
Anorthoclase			−17	M & M
Quartz	SiO_2	Hex	< −18	M & M
			−19	I & I
			< −20	I, K & O
Stony meteorite			−17	M & M
			−17	I & I
		(2 specimens)	< −18	M & M
		(3 specimens)	< −17	M
Volcanic ash:				
10 Japanese volcanoes			−12 to −16	I, K & O
Mt. Etna			−13	M & M
Crater Lake, Oregon			−16	S
Parieuten, Mexico			−23	S
Soils:				
American-loam, clay,			−3 to −25	S
Clay			−11	P & S
Loess, N. China			−12	I & I
			−15	I, K & O
Loess, Hanford, U.S.A.			−11	S

The following substances were found by Mason *et al.* to be inactive at temperatures above −18° C: Montmorillonite, sepiolite, albite, talc, sand, quartz, α-tridymite, and several samples of stony meteorite.

M & M = Mason and Maybank (1958), M = Mason (1960c), I & I = Isono and Ikebe (1960), I, K & O = Isono, Komabayasi, and Ono (1959), P & S = Pruppacher and Sanger (1955), S = Schaefer (1949b).

C. ICE NUCLEATION OF FLORIDA CLOUDS BY THE S.G.C.

1. Activity of Rocket Exhaust Particles - Al_2O_3

As noted in Chapter III, the stabilized ground cloud is generally confined to the first 2 km above ground. Within that altitude increment, the corresponding rocket burn yields approximately 7-10 x 10^7 g of Al_2O_3; see sample Table V-II (from NASA JPL Tech. Memo 33-712).

Some uncertainties exist as to the dominant crystalline phases and exact surface composition of the Al_2O_3 particles, particularly upon interaction with gaseous and aqueous HCl. Investigators at NASA-Langley Research Center (LaRC) (Cofer and Pellett) have suggested that a major proportion (by number and also surface area) of the alumina produced by an SRM tends to consist of submicron-size metastable alumina types. This judgment was based partly on LaRC x-ray diffraction results obtained on alumina collected by JPL from small SRM's fired in a closed tank; findings agreed with the electron diffraction results of Robbins and Strand (1970), i.e., the large spherical particles (>0.2 to 1 μm) were predominantly stable alpha-alumina and the irregular submicron particles (highly agglomerated as received) were predominately metastable gamma-alumina.

However, the slower effective particle cooling rate in the exhaust plume of a large SRM may significantly increase the percentage of the alpha form, as observed in recent measurements by Varsi (1976). He reported that Titan III particle samples, collected at high altitude by NASA-Ames and examined by both transmission and reflection electron diffraction at JPL, indicated "...mostly alpha phase for particles in the 0.1 μm size range." Although earlier JPL transmission electron diffraction measurements "...on just a few 0.1 μm particles collected by JPL with an impactor" at

Table V-II Exhaust Products Released into Atmosphere by Space Shuttle SRMs (Partial list: Mission 2)*

Altitude band, km	Δaltitude, km	Time, s	Δtime, s	Average mass flow, 10^3 kg/s	Mass, 10^3 kg	Exhaust products[a] Al_2O_3	HCl	CO	CO_2
						0.302028	0.209315	0.241719	0.0343946
								Exit	Exit
0-0.0095	0.0095	0-2	2	9.444	18.88	5.704	3.953	4.565	0.6495
0.0095-0.039	0.0295	2-4	↑	9.446	18.89	5.704	3.953	4.565	0.6496
0.039-0.087	0.048	4-6	↑	9.446	↑	5.705	3.954	4.566	0.6496
0.087-0.160	0.073	6-8	↑	9.447	↑	5.705	3.954	4.566	0.6497
0.16-0.25	0.090	8-10	2	9.448	18.89	5.706	3.953	4.566	0.6498
0.25-0.50	0.250	10-14	4	9.449	37.79	11.41	7.912	9.134	1.300
			↑						↑
0.50-0.85	0.35	14-18	↑	9.451	37.79	11.41	7.911	9.136	↑
0.85-1.3	0.45	18-22	↑	9.451	37.80	11.42	7.912	9.137	↑
1.3-1.9	0.60	22-26	4	9.454	37.81	11.42	7.914	9.139	1.300
1.9-2.2	0.30	26-28	2	9.445	18.89	5.704	3.953	4.565	0.6496
2.2-2.5	0.30	28-30	2	9.292	18.58	5.612	3.889	4.491	0.6390
2.5-3.3	0.80	30-34	4	8.859	35.43	10.70	7.416	8.564	1.219
			↑						
3.3-4.2	0.90	34-38	↑	8.282	33.12	10.00	6.933	8.006	1.139
4.2-5.1	0.90	38-42	4	7.705	30.81	9.307	6.450	7.448	1.060
5.1-6.0	0.90	42-45.44	3.44	7.123	24.50	7.399	5.128	5.921	0.8426
6-9	3	45.44-56.06	10.62	6.526	69.29	20.93	14.50	16.75	2.383
9-12	↑	56.06-65.52	9.46	6.630	62.70	18.94	13.12	15.16	2.157
12-15	↑	65.52-74.01	8.49	6.925	58.78	17.75	12.30	14.21	2.021
15-18	↑	74.01-81.64	7.63	7.147	54.52	16.47	11.41	13.18	1.875
18-21	↑	81.64-88.70	7.06	7.270	51.32	15.50	10.74	12.40	1.765
21-24	↑	88.70-94.90	6.20	7.320	45.37	13.70	9.497	10.97	1.561
24-27	↑	94.90-100.8	5.90	7.298	43.05	13.00	9.011	10.41	1.481
27-30	↑	100.8 -106.2	5.40	7.227	39.02	11.78	8.167	9.431	1.342
30-33	↑	106.2 -111.2	5.00	7.089	35.44	10.70	7.417	8.565	1.219
33-36	↑	111.2 -116.08	4.88	6.230	30.40	9.180	6.362	7.347	1.045
36-39	3	116.08-120.80	4.72	3.227	15.24	4.602	3.189	3.680	0.5241
39-41.6	2.6	120.80-124.85	4.05	0.8686	3.519	1.063	0.7366	0.8506	0.1210
			TOTAL		915.6	276.5	191.6	221.3	31.49

[a]The mass is indicated below the symbol for each specie.

*NASA JPL Technical Memorandum 33-71

lower altitude, showed the gamma (cubic) structure, Varsi (1976) concluded that "At present it would appear that the evidence is in favor of alpha (hexagonal) structure for the material injected into the stratosphere."

A recent assessment of the interaction of various aluminas with gaseous and aqueous HCl (Cofer and Pellett) indicated that both the metastable (theta, delta, gamma) and stable alpha forms chemisorb gaseous HCl, either dry or moist, to yield significant coverage of the surface by soluble chloride ("saturation" at 12 $\mathring{A}^2$/molecule). In fact, recent studies of anhydrous HCl adsorption (up to 20 torr) at Virginia Polytechnic Institute (NASA-LaRC Grant) have indicated that surface coverage for an alpha sample ($\sim$17 $\mathring{A}^2$/molecule) was about twice that for a Alon-C gamma sample ($\sim$33 $\mathring{A}^2$/molecule).

Summarizing possible Al_2O_3-HCl interactions, while the metastable aluminas tend to be more soluble in the bulk than the alpha (hexagonal) variety, all the known forms of alumina appear to chemisorb HCl and exhibit the potential for attaining relatively high surface coverages of soluble chloride. Thus the probable result of in-cloud chemisorption processes is the production of partially soluble particles which tend to be less effective as ice nucleants; how much less is uncertain.

Since alpha Al_2O_3 is a reasonably active IN source and because of phase and surface-composition uncertainties, we will tentatively assume that as much as 1 to 10% of the total Al_2O_3 is of the stable type. As subsequent estimates will show, the exact percentage is highly important and must be determined accurately.

Thanks to the cooperation of the China Lake Naval Weapons Center and Drs. William Finnegan and Kirk Odencrantz, nucleation tests were run at their facility. They burned an aluminum solid-propellant in their 15 m^3 cold chamber

and determined the temperature activity spectrum of the stable Al_2O_3 so produced. Their results appear below in Table V-III.

Table V-III. Al_2O_3 (Stable) Ice Nuclei Activity

Temp.	Output per gram	(AgI comparison)
-14 to -15°C	1-2 x 10^8 g^{-1}	10^{14} - 10^{15} g^{-1}
-20	~1 x 10^{10} g^{-1}	10^{15} - 3 x 10^{15} g^{-1}

In short the threshold of activation was at -14 to -15°C with the IN concentration reaching ~1 x 10^{10} g^{-1} at -20°C. For reference, the typical effectiveness of the best cloud seeding agent, AgI, is also indicated for various generators (Fletcher, 1962).

The concentration of effective IN in the SGC is at any time (cloud volume) and temperature given simply by:

$$IN = \frac{\text{Mass of } Al_2O_3 \text{ x Activity } (g^{-1})}{\text{Cloud Volume}}$$

For example, at (T + 3) hours the cloud volume is 6 x 10^2 km^3 (6 x 10^{14} ℓ). Assuming the unreasonable case where all the Al_2O_3 is nonchlorided (stable) and T = -14°C, then:

$$IN = \frac{(7 \times 10^7 \text{ g})(10^8 \text{ g}^{-1})}{6 \times 10^{14} \ell} \simeq 10 \ \ell^{-1}$$

Adjusting for the perhaps still conservative values of 1-10% stable Al_2O_3, the concentration of IN at -14°C would be 0.1 - 1 ℓ^{-1}. Continuing in this manner for two cloud temperatures; the 1-10% stable Al_2O_3 assumption; the expanding cloud volume with time and initial Al_2O_3 mass of 150 $\mu g\ m^{-3}$ as given in Chapter III; the IN concentration values of Table V-IV result.

Table V-IV. Ice Nuclei Concentrations from Al_2O_3 (1-10% Active)

(Values versus time and temperature)

Time	Cloud Volume	IN (-14°C)	IN (-20°C)
(T + 3 hrs)	6×10^2 km^3	0.15 - 1.5 ℓ^{-1}	15 - 150 ℓ^{-1}
(T + 1 day)	5×10^3	.02 - 0.2	2 - 20
(T + 3 days)	1.5×10^4	.006 - .06	0.6 - 6

Comparing Table V-IV estimates of potential Al_2O_3 ice nuclei with the natural atmospheric IN background of Fig. V-2, it is evident that the added component is not insignificant. If 10% of the Al_2O_3 is of the stable type, the ice nuclei conceivably produced is roughly 1-2 orders of magnitude above background at (T + 3) hours; and still a factor of 2-5 above background after 1 day. Even for 1% stable Al_2O_3 and (T + 3) hours, note at -20°C that 15 ℓ^{-1} is well above the often quoted natural atmospheric level of 1 ℓ^{-1}. In maritime clouds where ice multiplication may be taking place, the differences between SGC and natural IN concentrations are not so great. After three days natural IN levels generally (but not necessarily always) exceed the values in the expanded rocket cloud volume. Precipitation scavenging, during the rainy season in particular, would likely reduce the residence time and concentration of SGC particulates to insignificant values at ∿3 days and longer. It must be emphasized that this entire rationale hinges on 1-10% of the Al_2O_3 being effective as IN and the rest not at all.

2. Ground Component of Ice Nuclei

An added consideration is the amount of ground soil drawn up into the SGC during rocket launch. If Fig. V-3 (NASA Notes Ref. 14) for a

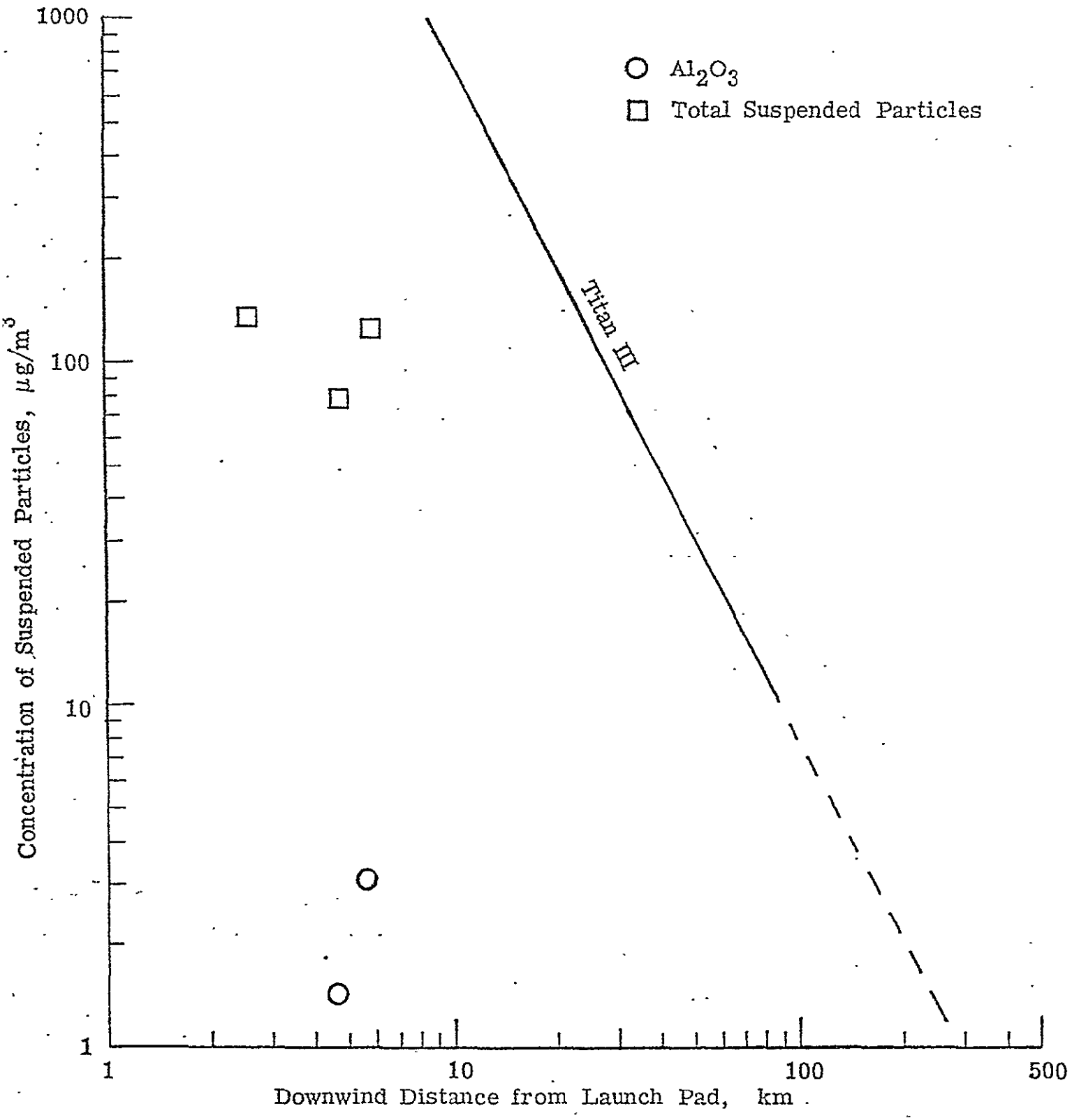

Figure V-3 Particles in Titan III Rocket Cloud Sampled at Ground Level (NASA Notes, Ref. 14)

Titan III launch is representative, then the total suspended material sampled at ground level is some 30-100 times that of the Al_2O_3. Some of this ground material will undoubtedly constitute potential ice nuclei. Most clay-silicates, as shown in Table V-I, will be more effective (warmer nucleation thresholds) than the Al_2O_3, provided no HCl "poisoning" takes place. These active particulates are often found in trace amounts in the earth's crust and may not be abundant at Cape Kennedy; typical sand is not active at temperatures above -18°C (Mason, 1971). Nevertheless, it is inevitable that some ground particles will serve as IN and the concentration may well be significant, as the previous numbers demonstrate. More research and instrumentation on the chemistry of SGC particulates and IN activation spectra are clearly in order.

3. Cloud Seeding Implications

Thus the potential for some cloud seeding exists, particularly within several hours or perhaps a day of launch. The higher values of Table V-IV (15 - 150 ℓ^{-1}) represent substantial seeding concentrations; cloud seeding programs often are designed on comparable values. The NOAA Florida FACE program, aimed at "massive" cloud seeding, attempts to inject 100 AgI nuclei ℓ^{-1} active at -10°C levels. An example of the effectiveness of small pryotechnic seeding rockets (U.S. Navy and Olin Corp.) used on the Florida program is shown in Fig. V-4. While their AgI activity (g^{-1}) at -14 to -20°C is 3-4 orders of magnitude higher than stable Al_2O_3, the great quantity of Al_2O_3 released in shuttle rocket burn results in the relatively high IN concentration of Table V-IV.

Returning to the impact on Florida peninsula clouds in summer, the Al_2O_3 activation threshold of -14°C corresponds to an average 7.2 km

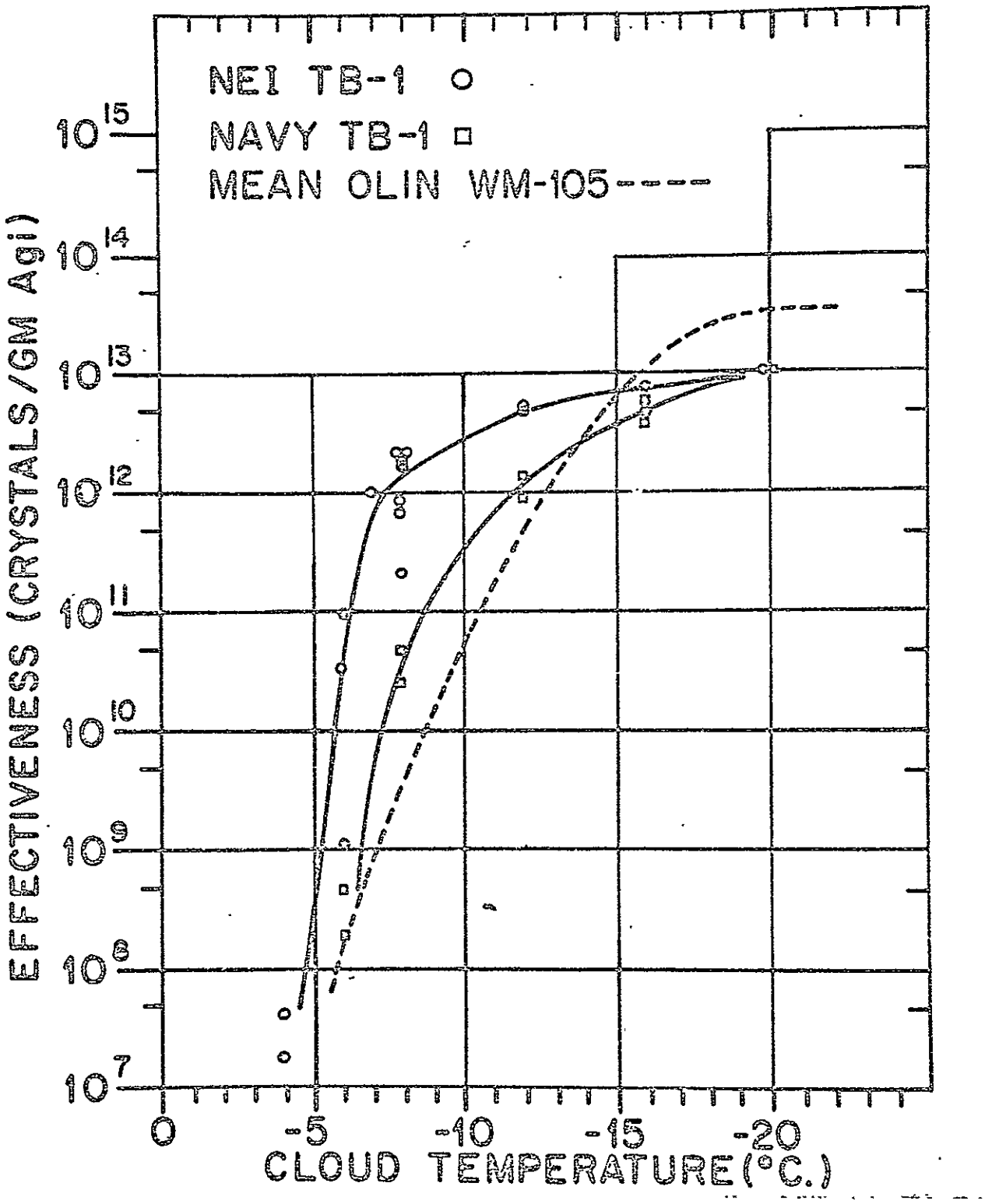

Figure V-4 Nucleating Effectiveness of Seeding Rockets (NOAA FACE Program; Woodley and Sax, 1976)

altitude (Fig. V-1). Note that temperature structure can depart substantially from the standard lapse rate. However, in general it can be stated that clouds with tops below 6-7 km will not be influenced by Al_2O_3 ice nuclei (in winter, 4.5-5.5 km cloud tops appear tolerable).

In deep penetrative convection associated with well developed cumuli and thunderstorms, seeding material most assuredly can reach levels of substantial activation (roughly 7-10 km in summer; 5-9 km in winter). Above these levels (-35°C), generally there are natural IN concentrations far greater than man can produce. In fact at approximately -40°C (10-11 km), spontaneous crystallization of supercooled water drops occurs without the need of any nucleating particles.

The significance of enhanced IN concentrations is far more difficult to assess. Exact cloud seeding effectiveness has been and continues to be a subject of debate. In broad terms, given suitable environmental conditions and substantial supercooled clouds, IN seeding of the order of 10 ℓ^{-1} is believed by some to increase precipitation by perhaps 10-20%. More massive seeding (circa 100 ℓ^{-1}) in thunderstorm airmasses reportedly can diminish damaging hailfall (Sulakvelidze, et al., 1967; Burtsev, et al., 1973; Miller, et al., 1974). These two weather modification effects--potential rainmaking and/or thunderstorm diminution--are most relevant to Florida. Neither are necessarily detrimental, especially the latter. Alternately, seeding at an inopportune time can have the effect of suppressing cloud development and rainfall (Braham, 1966). It has been postulated (Schleusener, 1968) that AgI seeding rates higher than 2 kg hr^{-1} tend to enhance convective activity.

4. Rocket Release Above the SGC

While this analysis is concerned with the low-level SGC, the possible IWM effects at higher levels should not be ignored. It is evident from Table V-II that approximately 8×10^7 g of Al_2O_3 are released at 2-12 km altitudes, a mass equivalent to that in the first two km. Considering that the vertical extent is 5 times as great and that dispersing winds are greater at higher levels, the resultant ice nuclei concentrations of Table V-IV should be down by roughly an order of magnitude at these higher altitudes. Also ground soils, ingested into the SGC, will not immediately reach these levels except by subsequent strong convection. Thus, the possible IWM impact by direct Al_2O_3 release at high levels, while a potential factor in certain circumstances, is proportionately diminished.

5. Summary IWM Implications

In summary, on the assumption that 1-10% of the space shuttle rocket Al_2O_3 (and/or entrained earth material in the SGC) are effective ice nuclei with a threshold of -14°C:

a. The potential for inadvertent weather modification (IWM) exists.

b. The effect could be that of altering precipitation amounts, hail, and severe winds; in the uncontrolled situation involved, the net result could be either an increase or decrease.

c. Concerning rainfall it is more likely that such an effect would lead to an increase of modest amount and be of modest significance (based on non-orographic cloud seeding conducted to date); because of the crucial timing and sizable seeding required to modify hail development, significant alteration appears more improbable, though possible by chance.

d. Seeding effects are more likely in summer when strong convection can carry particulates upward to colder IN activation levels.

e. The levels most conducive to ice nuclei crystallization are approximately 5-10 km, the higher end of the range in summer and the lower levels in winter.

f. Any IWM is more probable at shorter times (T + 3 hours), owing to higher IN concentrations, with the impact diminishing with time. Concentrations may still be somewhat above background after one day in continental type clouds but probably not enough so to perturb weather significantly. At 3 days and beyond, IWM is considered highly improbable.

g. Al_2O_3 (IN) released above the SGC in the 2-12 km altitude range are less concentrated by about an order of magnitude. Some near-term short-range IWM could result if susceptible clouds are present.

h. Because of washout and dilution effects of the SGC with time (particle residence time of a few days in the lower troposphere), no cumulative IWM effect from the projected 40 launches per year is likely. As an added precaution, spacing of rocket launches by several days is recommended.

D. RISK ANALYSIS

1. Evaluation Guides

The previous section (C-5) referred specifically to the weather modification risks associated with shuttle rocket launches. In parallel fashion, one can examine those conditions most favorable to the NOAA FACE seeding program. Their suitable criteria for rain augmentation in Florida are listed in the first column of Table V-V. All "suitable" conditions are relevant risk guides for NASA purposes with the exception of item 7. Here, even isolated (large) cumuli could be substantially stimulated on a local scale.

To this list of most susceptible seeding conditions influencing Florida, one should add the following:

a. short time periods (hours) after launch

b. when thunderstorms or large cyclonic systems are in the vicinity at time of rocket launch

c. when winds are calm or easterly

d. items (c) through (g) of the previous section relating to most conducive season (summer); altitudes (5-10 km); strong convection; and cumulative consequences (only with short-intervals between launches).

Conversely, the second column of Table V-V indicates conditions least favorable for weather modification--planned or inadvertent. Wherever possible, NASA launch schedules should attempt to take advantage of these mesoscale and cloud-microphysical factors. Prevailing westerly winds would also assure that any possible IWM effects take place over the ocean and not over Florida.

Table V-V Florida NOAA FACE Seeding Criteria (Woodley and Sax, 1976)

	Conditions Suitable for "Dynamic" Seeding of Florida Cumuli	Conditions not Suitable for "Dynamic" Seeding of Florida Cumuli	Explanation
1.	unstable lower troposphere, stable middle troposphere and unstable upper troposphere with moisture values not too dry or too wet throughout	stable lower troposphere or unstable troposphere through mid-levels; very dry or very wet through large region of troposphere	For optimum dynamic seeding effects, cumulus clouds need to grow naturally to about -10°C but should be stopped by a capping inversion; heat released by seeding allows cloud to grow beyond inversion into unstable layer above.
2.	hard cauliflower appearance to clouds	fuzzy appearance to clouds	Hard appearance is indicative of young, vigorous cloud with a copious quantity of supercooled water.
3.	tower moving upward through flight altitude	no upward motion to tower	Cloud should be in growing stage of its life cycle for optimum seeding effect.
4.	cloud liquid water content in excess of 1.0 gm^{-3} as measured by Johnson-Williams device	cloud water content less than 0.5 gm^{-3} as measured by Johnson-Williams device	Johnson-Williams instrument measures water content of drops <30μm radius; the presence of supercooled cloud drops is indicative of a youthful tower which has not yet started on the "downhill" part of its life cycle.
5.	ice particle content less than 7.5 per liter	ice particle content greater than 20 per liter	Seeding is pointless if large concentrations of naturally-formed ice already exist in cloud updraft region.
6.	updraft velocity in excess of 7.5 m sec^{-1}	updraft velocity less than 5.0 m sec^{-1}	Strong updraft is indicative of youthful cloud.
7.	convection neither very isolated nor very disturbed	suppressed conditions or disturbed conditions	Seeding effect becomes indistinguishable if all clouds grow to great heights, however, cumulus towers should form in close proximity if seeding is to cause mergers.
8.	weak wind shear conditions	strong wind shear conditions	Cirrus blowoff can decrease surface heating and thus suppress new convection; also natural seeding from cirrus anvils can confuse experimentation.
9.	weak low-level winds	strong low-level winds	Continuity of thermals destroyed by strong low-level winds and convection is suppressed.
10.	continental air mass characteristics	maritime air mass characteristics	It is suspected (though not confirmed) that natural glaciation occurs more readily under maritime air mass conditions.

2. Magnitude of Possible IWM

There is reasonable agreement that the seeding of layered supercooled clouds over orographic terrain can produce precipitation increases of the order of 10-20% (National Academy of Sciences, 1973). The seeding of cumulus clouds brings into play more cloud and environmental variables and less predictable results (Neiburger, 1969). Perhaps the most positive such experiment conducted to date is the Israeli 1961-1966 program in which an average 18% precipitation increase was reported. Simpson and Woodley (1971) reported cases of explosive growth of seeded maritime clouds with perhaps a doubling of precipitation at cloud base level as revealed by radar. (Ground level precipitation enhancement would logically be substantially less, but no corresponding measurements were obtained.) There are numerous other cumulus programs that show little, if any, increase in precipitation and in some cases decreases.

Based on these deductive considerations, the upper limit risk factor for IWM on the NASA Space Shuttle Program could be 20% on a local scale and over short time periods (hours). This is considered a pessimistic view and except for rare situations, the risk factor should be much less. Should the percentage of active Al_2O_3 in the total exhaust be less than 1% and should ground soils in the vicinity of Cape Kennedy be generally devoid of effective clay-silicates, IWM effects via cloud glaciation reduce to the noise level.

Until more information is obtained on the exact chemistry and ice activation spectra of rocket and soil material within the SGC, caution is advised. Launches, whose rocket plumes could interact with existing or predicted large cumuli (or a strong sea breeze regime)

within 1-3 hours, are not recommended.

3. Recommendations

It is advised that further NASA efforts be conducted to provide information vital in validating certain ice phase assumptions necessary in this evaluation. These recommendations are as follows:

a. determine the percentage of stable Al_2O_3 generated in the shuttle exhaust plume

b. perform additional ice nuclei activation spectra of Al_2O_3 (as done by the China Lake Naval Weapons Center for this analysis) and, if possible,
   1. at high temperatures approaching rocket burn and
   2. with the identical SRM propellent mix

c. in future penetrations of the stabilized ground cloud, include membrane filter collections of particulates. These filters can subsequently be processed in the laboratory for perhaps the most definitive indication of ice nuclei active at various temperatures (also fly an automatic IN counter)

d. establish a ground network to evaluate possible downwind changes in precipitation patterns and to collect rain water for chemical analysis (e.g., Al_2O_3, pH).

E. REFERENCES

1. AFCRL (S. Valley, Ed.), 1965: "Handbook of Geophysics and Space Environments", McGraw-Hill (Chap. 2).

2. Bradley, J., 1972: "The Climate of Florida", Climates of the States, Vol. 1, NOAA, U.S. Dept. of Commerce, 45-71.

3. Burtsev, I., I. Gaivoronsky, and A. Kartsivadze, 1973: "Recent advances in studies of the Physical Processes Producing Hail, and Results of Anti-Hail Operations in the USSR", Proc. Intl. Conf. Wea. Mod., Tashkent, WMO, 189-197.

4. Braham, R., 1966: "Project Whitefop: A Convective Cloud Randomization Seeding Project", Dept. Geophys. Sci., Univ. of Chicago.

5. Cofer, W. and G. Pellett, undated: "Chemical Characteristics and Role of Al_2O_3 in SRM Exhaust Clouds", Ref. 13, NASA IWM Working Group, Houston, May 1976.

6. Dobbins, R.A. and L.D. Strand, 1970: "A Comparison of Two Methods of Measuring Particle Size of Al_2O_3 Produced by a Small Rocket Motor", AIAA J., 8, 1544.

7. Fletcher, 1962: "The Physics of Rainclouds", Cambridge Univ. Press, 390 pp.

8. Hallett, J. and S. Mossop, 1974: "Production of Secondary Ice Particles During the Riming Process", Nature, 249, 26-28.

9. Hobbs, P., 1974: "Ice Physics", Oxford Univ. Press, 635 pp.

10. Houghton, H., 1950: "A Preliminary Quantitative Analysis of Precipitation Mechanisms", J. Met., 7, 363.

11. Kuami, M., 1961: "Snow Crystals and the Identification of the Nuclei in the Northern U.S.A.", J. Met., 18, 139.

12. Mason, B., 1971: "The Physics of Clouds", Clarendon Press, 671 pp.

13. Mason, B. and J. Maybank, 1958: "Ice-Nucleating Properties of Some Natural Mineral Dusts", Quart J. Roy. Met. Soc., 84, 235.

14. Miller, J., E. Boyd, and R. Schleusener, 1974: "Hail Suppression Data From Western N. Dakota, 1969-72", Proc. 4th Conf. Wea. Mod., Fort Lauderdale, AMS, 139-143.

15. Mossop, S., 1971: "Ice Multiplication of Ice Crystals in Clouds", Proc. Intl. Conf. Wea. Mod., Australia, AMS, 1-4.

16. NASA Notes, Ref. 14 (HSW, GLG, KHC). NASA IWM Working Group, Houston, May 1976.

17. NASA Staff, 1975: Nozzle Exit Exhaust Products from Space Shuttle Boost Vehicle (Nov. 1973 Design). NASA JPL Tech. Memo. 33-712.

18. National Academy of Sciences, 1973: "Weather and Climate Modification Space Problems and Prospects", Comm. on Atmos. Sciences, Nat. Res. Council, 258 pp.

19. Neiburger, M., 1969: "Artificial Modification of Clouds and Precipitation", WMO Tech. Note 105, 33 pp.

20. Schaefer, V., 1949: "The Formation of Ice Crystals in the Laboratory and the Atmosphere", Chem. Rev., 44, 291.

21. Schleusener, R., 1968: "Hailfall Damage Suppression by Cloud Seeding", Proc. 1st Nat. Conf. Wea. Mod., Albany, NY, AMS, 484-493.

22. Simpson, J. and W. Woodley, 1971: "Seeding Cumulus in Florida: New 1970 Results", Science, 172, 117-126.

23. Sulakveldize, G., N. Bibilashvili, and V. Lapcheva, 1967: "Formation of Precip. and Modification of Hail Processes", Israel Sci. Translations (NSF), 208 pp.

24. Varsi, G., 1976: "Particulate Measurements", presentation at Space Shuttle Environmental Workshop on Stratospheric Effects, March 24-25, 1976.

25. Woodley, W. and R. Sax, 1976: "The Florida Area Cumulus Experiment: Rationale, Design, Procedures, Results, and Future Course", NOAA Tech. Rep. ERL-354-WMPO-6, Boulder, Colo., 204 pp.

Chapter VI

SOLAR ATTENUATION MODEL FOR THE STABILIZED GROUND CLOUD

Outline

Chapter VI

SOLAR ATTENUATION MODEL FOR THE STABILIZED GROUND CLOUD

The effects of aerosols on the atmospheric transmission of solar energy have been debated since early in this century. Humphreys (1913) concluded that volcanic dust caused a cooling in the average surface temperature of the earth. The effect of the increasing haziness around cities, which is attributed to increased air pollution, has been studied by numerous authors. Bryson (1968) has concluded the steady decline in average temperature of the earth over the past decade is a result of increasing global pollution levels. Mitchell (1971), also working on the problem, showed that increasing pollution may lead to a warming or a cooling of the earth depending on the aerosols' radiative properties. On a smaller scale, the effects of increasing air pollution in urban areas have been summed up by Landsberg (1962) and Peterson (1969). Their findings indicate that urban areas receive an average of 15 to 20% less solar radiation than rural regions. The reports quoted here indicate the uncertainty in ascertaining the direct effects of air pollution on solar energy.

The model was designed for rapid operation by reducing computational demand wherever possible. In addition, the model was designed to require only easily accessible input data. This criteria served the final goal of maintaining generality and versatility in the models when possible.

The transmission of solar radiation through the atmosphere is computed using an iterative technique to solve the radiative transfer equation (Dave and Gazday). This technique first approximates the total intensity as that due to first-order scattering only. Successive approximations include the next highest order or scattering until the

desired accuracy is obtained. Thus, the final calculated intensity includes multiple-scattering effects to the order of accuracy desired.

The transmission of sunlight through the atmosphere is a complex phenomenon. Rough estimates of the loss of radiation from a direct beam of sunlight can be obtained quite easily using single-scattering techniques (Van De Hulst, 1957). However, since we are interested in determining a heat budget at the ground, we are required to use more complex techniques referred to as multiple-scattering approximations. Single-scattering techniques yield the amount of solar energy lost from the direct beam of sunlight (direct radiation); the multiple scattering method, however, yields the single-scattering result with the addition of all the light (diffuse radiation) scattered in the downward direction. Since the earth's surface collects all sunlight directed downward, the multiple-scattering result is significantly more accurate for our purposes (Hammond, 1973).

Multiple-scattering calculations are considerably more complex because they require the solving of an integro-differential equation called the radiative transfer equation (R.T.E.). The equation has historically been used largely in the fields of astronomy and physics. However, with the realization that anthropogenic air pollution may effect the global radiation balance, and hence the climate of this planet (Charlson and Pilet, 1969), the R.T.E. recently has been used to calculate the effects of pollution of the atmospheric radiation balance of the earth.

In principle we know how to solve the R.T.E. using one of the various numerical techniques. The most widely used methods include the doubling method (Hansen, 1971), discrete ordinate method (Chandrasekhar, 1960),

spherical harmonic method (Bergstrom and Viskanta, 1972), and the iterative method (Braslau and Dave, 1972). The computational demand of the discrete ordinate method is quite large, thus this method was not utilized for the model. Of the remaining three techniques, the iterative method was chosen for this model because program modifications are easily performed using this method.

The primary difficulty encountered in applying these techniques is the calculation of the scattering and absorption properties of the medium. Scattering and absorption of electromagnetic radiation (light) by particles or droplets are described by Mie scattering theory. Mie scattering theory is the classical solution describing the interaction of electromagnetic waves with spherical bodies. Scattering theory uses the refractive index of the particle, the size of the particle and the wavelength of the interacting light to calculate the scattering and absorption properties of the particle.

The effects of cloud droplets and aerosol particles on the incoming solar radiation can be calculated by using the Mie scattering theory. Since aerosol particles occupy a whole range of sizes, the overall optical characteristics of an aerosol are obtained by integrating the optical properties of each size interval over the whole range of particle sizes. The effects of clouds on solar radiation require a complete knowledge of the droplet size distribution and concentration within the cloud (Twomey, et al., 1970). Since this data is generally not available, we must resort to average cloud conditions. Therefore, we assume that the cloud is homogeneous (all particles are the same size) and that the concentration of cloud droplets present is directly related to

the amount of cloud cover reported. Using these approximations, the effects of clouds can be calculated by using the Mie scattering properties of a single sized water droplet in varying concentrations. This technique provides a method of including the effects of aerosols and cloud droplets on the atmospheric transmission of sunlight.

The effects of cloud droplets, aerosol particles and the gases present in the atmosphere are combined to produce the overall transmission properties of the atmosphere. The model developed for this purpose is a modified version of a model developed by Braslau and Dave in 1972. The model divides the atmosphere into a number of layers. The optical properties are considered constant throughout each layer, but may change from layer to layer. The model computes the diffuse radiation at each level in the atmosphere. The total amount of sunlight transmitted throughout the atmosphere to the ground level is then calculated by adding the amount of diffuse radiation in the downward direction to the attenuated amount of direct radiation. This result provides the amount of sunlight which strikes the earth's surface.

Transmission of atmospheric radiation is calculated using the plane-parallel form of the radiative transfer equation. This equation calculates the transfer of monocromatic light through a non-homogeneous atmosphere and may be written:

$$\mu \frac{dI(\tau;\mu,\phi)}{d\tau} = I(\tau;\mu,\phi) - W(\tau) J(\tau;\mu,\phi) \qquad (3)$$

$\mu \equiv |\cos \theta|$ where θ is the angular deviation between the angle of propagation and the local zenith μ is defined as upward, while $-\mu$ is downward

ϕ - azimuth angle from the horizon

J - is called the source function, it provides the amount of radiation added to a specific direction (μ, ϕ) due to scattering from all other angles

τ - normal optical depth, it is the sum of optical depth due to scattering and absorption by molecules and particles

$\tau(S, M)$ - optical depth due to Mie scattering (particles)

$\tau(S, R)$ - optical depth due to Rayleigh scattering (molecules)

$\tau(C, M)$ - optical depth due to Mie absorption (particles)

W - albedo of single scattering, defined as the ratio of optical depth due to all types of scattering divided by total optical depth

I - intensity of radiation at optical depth τ in the atmosphere, propagating in the direction (μ, ϕ)

The source function includes all scattering and absorption properties of the medium. Essentially it represents the amount of direct radiation which is converted to diffuse radiation by interaction with the medium. The source function can be represented by an equation of the form:

$$J(\tau;\mu,\phi) = \tfrac{1}{4}\cdot e^{-\frac{\tau}{\mu_o}}\cdot P(\tau;\mu,\phi:-\mu\ ,\phi\ )\cdot F + \tfrac{1}{4}\cdot\pi\cdot\int_{-1}^{+1}\int_{0}^{2\pi} P(\tau;\mu,\phi;\mu',\phi')\cdot I(\tau;\mu',\phi')\cdot d\mu'\cdot d\phi' \qquad (4)$$

F - Flux at top of atmosphere

τ, μ, ϕ - have same meaning as before .

μ_o, ϕ_o - represent the direction of incoming diffuse radiation

P - the phase function

The phase function represents the angular distribution of the scattered radiation. The normalized scattering function is defined by:

$$P(\tau,\mu,\phi;\mu',\phi') = T(\tau)\cdot M(\mu,\phi;\mu',\phi') + [1 - T(\tau)]\cdot R(\mu,\phi;\mu',\phi') \qquad (5)$$

$T(\tau)$ - turbidity factor and is defined as

$$T(\tau) = \Delta\tau(S,M)/[\Delta\tau(S,M) + \Delta\tau(S,R)]$$

M - the normalized Mie scattering phase function

R - the normalized Rayleigh scattering phase function

The treatment of the Mie and Rayleigh phase functions is determined by the numerical technique chosen. For use in the iterative technique, the functions are expanded in a Fourier series whose argument is the difference between the azimuth angles of the incident and scattered radiation. When this technique is employed it is advantageous to express the intensity and source functions in the form of Fourier series also. Since the azimuth integration performed in equation 4 can be carried out analytically, this reduces the computational

demand to that of a single integration (Braslau & Dave, 1972). Finally the computational demand is reduced even further since only the first term of the Fourier series for intensity is needed for the calculation of total radiation flux. Thus, the Mie and Rayleigh phase functions may be expressed as:

$$R(\text{Cos}\theta) = \sum_{k=1}^{k} A_k^{(r)} \cdot P_{k-1}(\text{Cos}\theta)$$

$$M(\text{Cos}\theta) = \sum_{k=1}^{k} A_k^{(m)} \cdot P_{k-1}(\text{Cos}\theta) \qquad (6)$$

$A_k(R)$ - Rayleigh legendre coefficients given by:

$A_1 = 1,\ A_2 = 0,\ A_3 = 1/2$

P - ordinary legendre polynomials

θ - scattering angle between incident and scattered radiation

$A_k(M)$ - legendre coefficients for Mie phase function

The legendre coefficients for the Mie phase function depend only on the size distribution concentration and optical properties of the aerosol particles. The coefficients are given by:

$$A_k^{(m)} = \frac{\lambda^2}{\pi B(s,m)} \cdot \int_{r_1}^{r_2} L_k(\alpha, m) \cdot n(r) \cdot dr \qquad (7)$$

λ - wavelength of incident radiation

$n(r)$ - size distribution of aerosols

L_k - unnormalized legendre coefficients of the series representing the scattering phase function of a single particle

α - size parameter defined as $X = 2\pi r/\lambda$

M - complex refractive index

B(s,m) - volume scattering coefficient for the medium

The volume scattering coefficient can be calculated using the efficiency factor for scattering and is given by:

$$B(s,m) = \pi \cdot \int_{r_1}^{r_2} Q_s(\alpha, m) \cdot n(r) \cdot r^2 \cdot dr \qquad (8)$$

Q_s - efficiency factor for scattering

The unnormalized legendre coefficients used arise from the expansion of the complex Mie amplitudes by the repeated use of recurrent relationships between the derivatives and the products of legendre functions (Deirmendjian 1969). The method was suggested by Hartel (1970) and first carried out by Sekera (1952). The power of this technique lies in the fact that these unnormalized coefficients are independent of direction, thus they can be computed for the aerosol or cloud particles in advance. We have used a modified version of a calculational procedure developed by Dave (1970) to compute these coefficients. This calculation is performed before the actual radiation model is operated and are read as input data by the radiation model. This technique saved considerable computer time. (See Appendix B-1 for program listing.)

Therefore, the final expressions for the Mie and Rayleigh phase functions may be written using the addition theorem of spherical harmonies to express θ in terms of μ and ϕ as:

$$M(\mu,\phi;\mu^1,\phi^1) = \sum_{n=1}^{N} F_n^{(m)}(\mu,\mu^1)\cdot\mathrm{Cos}(n-1)\cdot(\phi^1-\phi)$$

$$R(\mu,\phi;\mu^1,\phi^1) = \sum_{n=1}^{3} F_n^{(r)}(\mu,\mu^1)\cdot\mathrm{Cos}(n-1)\cdot(\phi^1-\phi) \qquad (9)$$

The only remaining step needed to render the radiative transfer equation solvable is the addition of two boundary conditions. These conditions are defined by assuming that there is no incident diffuse radiation striking the top of the atmosphere and similarly that there is no radiation reflected upward at the base of the atmosphere. These conditions are expressed as:

$$I_m(o,-\mu) \equiv o;\ I_m(\tau_b,+\mu) \equiv o \qquad (10)$$

The effect of ground reflection is included by using a technique developed by Chandrasekhar (1960). The intensity calculated by solving the previous equations is increased by an amount $I_*(\tau, \mu)$. The radiation reflected by the ground is assumed to be isotropic. The procedure used involves solving the radiative transfer equation for the reflected ground radiation. The R.T.E. has the form:

$$\mu\frac{dI_*^c(\tau,\mu)}{d\tau} = I_*^c(\tau,\mu) - W(\tau)\cdot J_*^c(\tau,\mu)$$

$$J_*^c(\tau,\mu) = \tfrac{1}{2}\cdot\int_0^1 P^{(1)}(\tau;\mu,\mu_1)\cdot e^{-(\tau_b-\tau)/\mu_1}\cdot d\mu_1 + \qquad (11)$$

$$\tfrac{1}{2}\cdot\int_{-1}^{+1} P^{(1)}(\tau;\mu,\mu^1)\cdot I_*^c(\tau;\mu^1)\cdot d\mu^1$$

with boundary conditions given by

$$I_*^c(o;-\mu) \equiv o$$

and (12)

$$I_*^c(\tau_b;+\mu) \equiv 1$$

This set of equations applies for the case of Lambertian illumination ($Ig(-\mu o) = 1$). Finally, we have:

$$I_*^{(1)}(\tau_1;\ \pm\mu) \equiv Ig(-\mu o)\cdot I_*^c(\tau_1;\ \pm\mu) \tag{13}$$

The reflectivity R is defined as the ratio of the upward flux given by:

$$Ig(-\mu o)\cdot\int_o^1\int_o^{2\pi} \mu\cdot d\mu\cdot d\phi = \pi\cdot Ig(-\mu o) \tag{14}$$

to the total downward flux. The downward flux has contributions from:

direct solar radiation $\pi\cdot\mu o\cdot F\cdot\exp(-\tau_b/\mu o)$ (15)

downward flux due to diffuse radiation

$$\int_o^1\int_o^{2\pi} I(\tau_b;-\mu,\phi)\cdot d\mu\cdot d\phi \equiv \pi_g(\tau_b;-\mu o) \tag{16}$$

downward flux due to scattered ground radiation

$$2\cdot\pi\cdot Ig(-\mu o)\cdot\int_o^1 I_*^c(\tau_b;-\mu)\cdot\mu\cdot d\mu = \pi\cdot Ig(-\mu o)\cdot\bar{S}(\tau_b) \tag{17}$$

Rearranging the terms in the reflectivity equation we have:

$$Ig(-o) = \frac{R\cdot[\mu o\cdot F\cdot e^{-\tau_b/\mu o} + g(\tau_b;-\mu o)]}{1 - R\cdot\bar{S}(\tau_b)} \tag{18}$$

The equations presented form a complete set which can be solved to yield the flux of solar radiation at any level in the atmosphere. It only remains to define the properties of the atmosphere for use in the radiation model.

Before these equations can actually be used in a practical model, some simplifying assumptions should be made to reduce the computational demand of the model. The effects of including polarization on the total net flux calculations has been shown to be insignificant (Adams & Kattawar). Thus, polarization has not been included so the scalar form of the R.T.E. can be used. Aerosol particles present in the stabilized ground cloud have refractive indexes which vary considerably with the particle's composition. We have assumed an average value of 1.5 for the real part of the refractive index. We have also assumed for this part of our calculation that the particles are low absorbing, the imaginary part of the refractive index is 0.03. Although it is known that aerosol particles in general do absorb solar radiation, Braslau and Dave have compared the results of their model for the cases of absorbing and non-absorbing aerosols, and their results show that only a minor change occurs in the net flux calculations when aerosol absorption of less than 0.05 is included (Braslau and Dave, 1972).

The radiative transfer equation presented previously is valid for a single frequency only. Since most solar energy is emitted between 4000 and 6000 Angstroms, we have chosen 5000 Angstroms as the wavelength used in this model. More accuracy could be obtained, with a drastic increase in computational demand, by calculating the ground flux in each wavelength and then integrating the result over the entire solar spectrum.

The significant changes in the model required for this calculation are the inclusion of the absorption bands for water vapor, atmospheric gases and pollutants (See Figure 1). Techniques are available to approximate these absorption bands (Bergstrom and Viskanta, 1972). There is no reason why the model could not be operated over the entire range, except that the computer time required is excessive. One final simplification was utilized, the model is used three times a day at 9:00 a.m., 12:00 noon and 3:00 p.m. local time. The results from these three runs are combined to estimate the total radiation received during a particular day. These simplifications in the model significantly reduce the computational demand of the model.

The atmosphere is divided into thirty layers; the top five layers are five kilometers in depth, while the lower twenty-five layers are only one kilometer in depth. The stabilized ground cloud is assumed to be homogeneous after T + 3 hours, from the mixing height level down to the ground level. The calculation proceeds from the top of the atmosphere downward, with the effects of ground reflection added separately.

A standard atmosphere is used to specify the Rayleigh attenuation coefficients and also the Mie attenuation coefficients down to the mixing height level. The Rayleightcoefficients B(s, r) and the Mie coefficients B(s, m) are given by McClatchey (1972) for the standard mid-latitude atmosphere. These coefficients are used to compute the normal optical depth and the turbidity for each layer.

$$\tau_i = B(s,r)_i + B(s,m)_i \qquad (19)$$

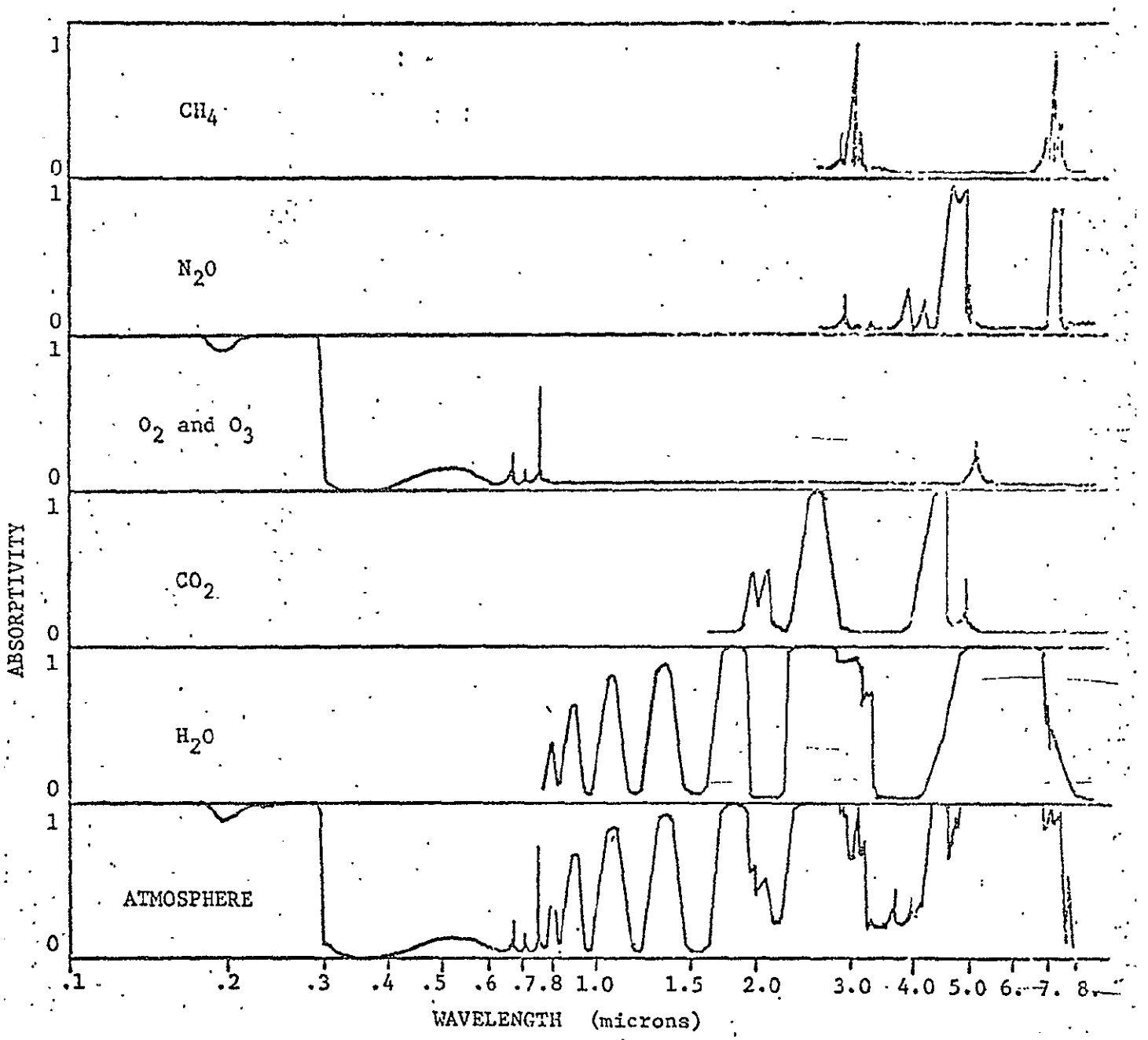

FIGURE 1

Absorption spectra for H_2O, CO_2, O_3, N_2O and the atmosphere.

$$T_{i\ldots}(\tau) = \Delta\tau_i(s,m)/[\Delta\tau_i(s,m) + \Delta\tau_i(s,r)] \qquad (19)$$

The legendre coefficients for each layer are calculated using equation 7, where the size distribution is assumed to be constant after T + 3 hours. Thus, the optical properties of all thirty layers are completely determined for the standard atmosphere. A value of .3 was used for the albedo. This value is read into the model as data so that it can be changed quickly if desired.

If clouds are present during the calculation period, their effects are included at the three kilometer level and below. The cloud droplets are all assumed to be average sized stratus cloud droplets (4 microns in radius)(Mason 1971). The concentration of droplets is determined by converting local climatological cloud cover data to tenths of sky cover. The cloud ceiling reported by local weather stations is used to determine the thickness of the cloud layer. Since the scattering efficiency factor for 4 micron sized water droplets was previously calculated (Appendix B-1), the attenuation coefficient for cloud layers B(s,c) can be computed using equation 8. Therefore, the total attenuation coefficient for the layers is just the sum of B(s,m) and B(s,c). Finally, the legendre coefficients for the layer are simply the standard coefficients plus the coefficients computed for the cloud layer using equation 7. This determines all the optical properties of the cloud layer needed for the flux calculation.

The mixing depth determines the height in the atmosphere penetrated by the stabilized ground cloud. The aerosol mass concentration of the stabilized ground cloud is determined by the assumed dispersion. The mass concentration is converted to a number concentration of particles between the reported size interval. The total number of particles in each .1 micron size interval is computed. The results of this computation are used in equation 8 to determine the new attenuation coefficient for the layers. This procedure is similar to the procedure used to determine the attenuation coefficient for layers of cloud droplets. Finally, the legendre coefficients are computed using equation 7. The new values for the legendre coefficients and the attenuation coefficients replace the standard coefficients for all levels below the mixing height.

Recalling equation 4, it is seen that the first term of the source function is the contribution due to scattering of direct solar radiation to the source function. This is the primary scattering term. The iterative technique approximates each successive order of scattering by using the previous result to obtain each higher order scattering term. Thus, the primary scattering is approximated by:

$$J_1^{(1)}(\tau i;\pm\mu) = \tfrac{1}{4}\cdot F\cdot \exp(-\tau i/\mu o)\cdot P_1(\tau_i;\pm\mu,-\mu o) \qquad (20)$$

where P is given by equation 5.

The successive approximation of the intensity function is then given by:

$$Im^{(1)}(\tau_i;-\mu) = Im^{(1)}(\tau_{i-1};-\mu)\cdot\exp(-\Delta\tau_i/\mu) + W(\tau_i)\cdot\overline{Jm}^{(1)}(\tau_i;-\mu)\cdot [1 - \exp(-\Delta\tau_i/\mu)] \qquad (21)$$

for the upward intensity and similarly for the downward intensity. Successive orders of scattering are included in the source function by approximating equation 4 as:

$$Jm^{(1)}(\tau_i;\pm\mu) = J_1^{(1)}(\tau_i;\pm\mu) + \tfrac{1}{2}\cdot\int_0^1 P_1(\tau_i;\pm\mu,-\mu^1)\cdot Im^{(1)}(\tau_i;-\mu^1)\cdot d\mu^1 + \tfrac{1}{2}\cdot\int_0^1 P_1(\tau_i;\pm\mu,\mu^1)\cdot Im^{(1)}_{-1}(\tau_i;\mu^1)\cdot d\mu^1 \qquad (22)$$

Jm is calculated using a sub-program called SOURCE for listing see Appendix B-3. This approximation is substituted in equation 21 to obtain the intensity function which includes the next order of scattering. This new intensity is then inserted into equation 22 to calculate the new source function which now includes scattering of the next order. The procedure is continued until the desired agreement between Im and Im+1 is achieved. The criteria used for this model terminates the procedure when:

$$(Im+1 - Im) \leq .001*Im \qquad (23)$$

The effects of ground reflection are included using a procedure entirely analagous to that presented above. The only significant difference being that calls to SOURCE are replaced with calls to sub-program GROUND. (For listing see Appendix B-4.) The procedure is applied only once for the ground reflected radiation since it is assumed to be reflected isotropically at the ground.

The model finally integrates the intensity function, which now includes all effects due to ground level reflection, through all downward angles to obtain the net downward flux. This is accomplished using the flux equation given by:

$$F_d(\tau) = 2\cdot\pi\cdot\int_0^1 I^{(1)}(\tau;-\mu)\cdot\mu\cdot d\mu \qquad (24)$$

This flux value represents the total amount of diffuse radiation reaching the ground level. The directly transmitted radiation is computed and added to the diffused using:

$$\text{Flux} = \text{Flux} + I_o\cdot\exp(-\tau_b/\mu o) \qquad (25)$$

As mentioned previously the model is used three times a day to obtain the final value which gives the total flux for the entire day. A listing of the main program is provided in Appendix B-2.

The model was tested at the city of Albany since measured values of solar radiation are also available. The results of the week-long model validation run are presented in Figure VI-2. A second plot of the measured values of solar insolation for the same period is also included in the graph to facilitate the comparison. In Figure VI-3, we have plotted the amount of clouds present and also the cloud ceiling for the same time period. From a study of the graphs, it is seen that the calculated values and the measured values of solar insolation agree quite closely for the period.

The model was then used to demonstrate the effect of the stabilized ground cloud on solar energy transmission for the Florida latitude. Cloud cover was set equal to zero for these calculations.

Figure 4 shows the overall results of percent decrease of ground level solar radiation versus aerosol mass concentration within the stabilized ground cloud. We have carried out the complete radiation transfer calculation in an atmosphere clear of water clouds. The limit of vertical mixing was assumed to be 850 meters and 1550 m. Below the mixing height, the stabilized ground cloud is homogeneously mixed in the vertical direction. Figure 4 constitutes the basis for our impact assessment with respect to the radiation flux received at ground level.

RESULTS

1. Any effects resulting from the absorption of solar radiation by the stabilized ground cloud (deposition of heat energy in the atmosphere) are negligible, if the absorption coefficient of the particles within the S.G.C. is less than 0.03.

2. The scattering of solar radiation by the stabilized ground cloud resulting in a decrease of solar energy received at the ground amounts to maximal 15%.

Under those high scattering conditions, the S.G.C. would have to be dispersed homogeneously between ground and 1550 m with an average mass concentration of 150 $\mu g/m^3$ which could occur at times up to T + 3 hrs. For times greater T + 3 hrs., we anticipate the decrease of solar radiation at ground to be less than 15% under all meteorological conditions. This change of heat energy deposition at the ground is not sufficient to cause significant changes in the vertical mixing of air causing such effects as cumulus cloud formation, etc. We, therefore, conclude that there will be no detectable impact on "weather" resulting from the interaction of the stabilized ground cloud with solar radiation. However, we anticipate a reduction in "visibility". Since there will soon be a secondary air quality standard with respect to "visibility", some attention should be devoted to the radiation-interaction problem.

RESEARCH RECOMMENDATIONS

For more precise calculations, the real and imaginary part of the extinction coefficient of the S.G.C. aerosol must be known. If the aerosol absorption coefficient exceeds 0.05, then the problem must be reassessed.

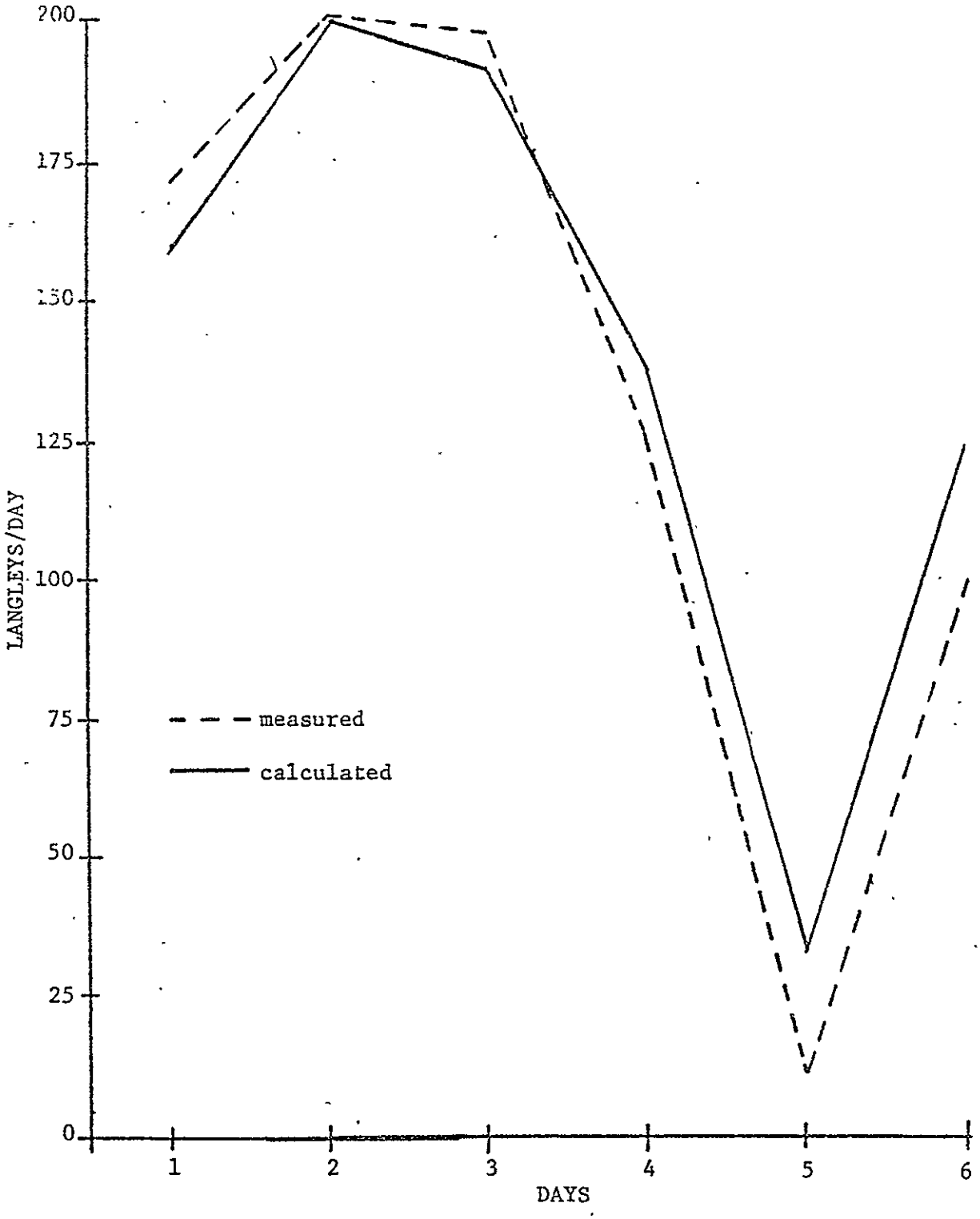

FIGURE VI-1

Comparison of measured and calculated values of solar insolation for a six-day period.

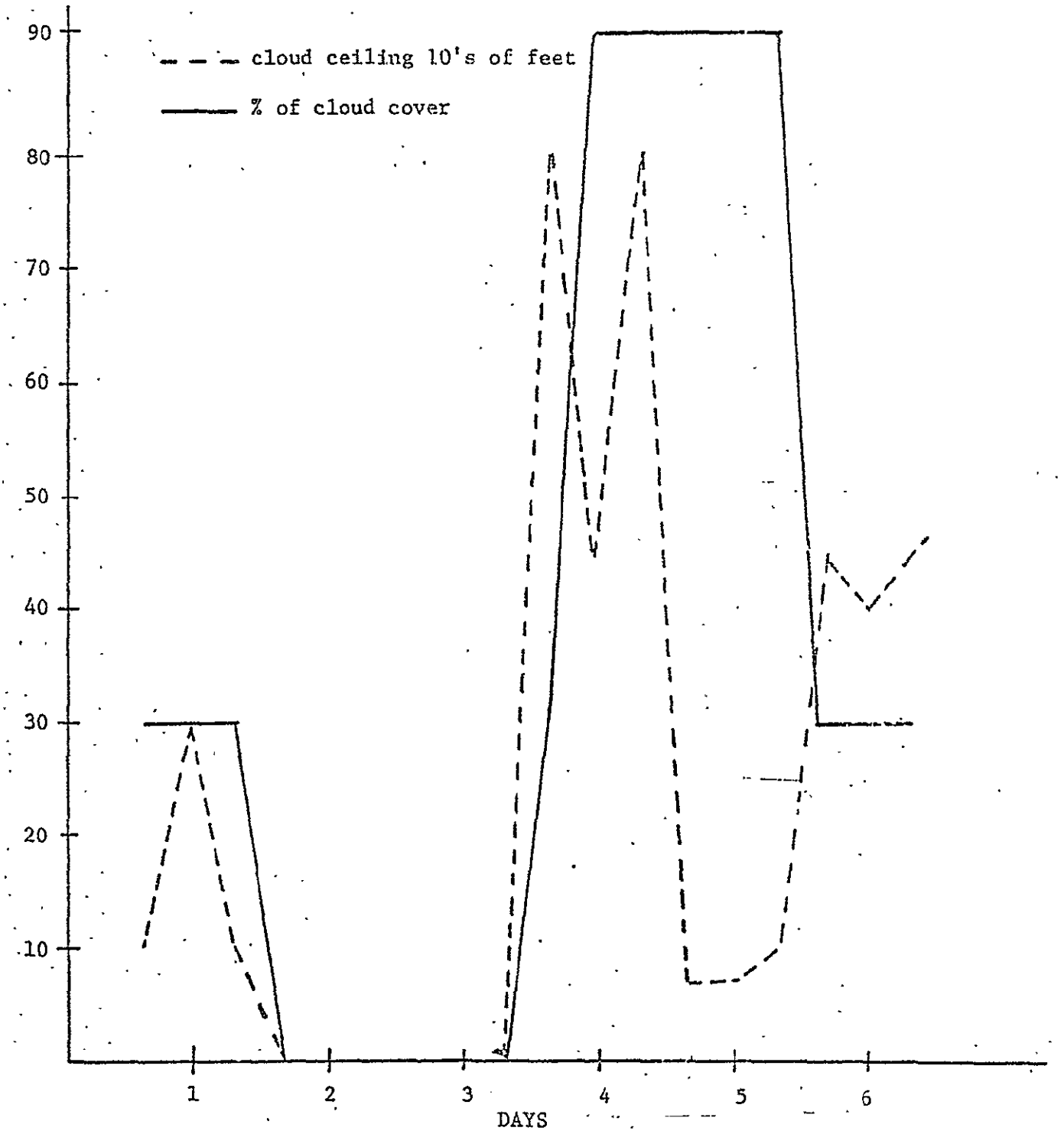

FIGURE VI-2

Cloud cover and cloud ceiling height for the six-day modeling period.

PERCENT LOSS OF SOLAR RADIATION
DUE TO STABILIZED GROUND CLOUD
15
10
5
0
MIXING HEIGHT
1550 m.
MIXING HEIGHT
850 meters
0
20
40
60
80
100
120
140
S.G.C. MASS CONCENTRATION
μg/m³

Figure VI-3

REFERENCES

1. Adams, C.N. and G.W. Kattawar: "Solution of the Equations of Radiative Transfer by an Invariant Imbedding Approach", J. of Quantum Spectroscopy and Radiative Transfer, 10:341.

2. Bergstrom, R.W. Jr. and R. Viskanta, 1972: "Theoretical Study of the Thermal Structure and Dispersion in Polluted Urban Atmospheres", Lafayette, Ind.: Purdue University (Aug. 1972) p. 53.

3. Bergstrom, R.W. Jr. and R. Viskanta, 1972: "Theoretical Study of the Thermal Structure and Dispersion in Polluted Urban Atmospheres", Lafayette, Ind.: Purdue University (Aug. 1972) p. 172.

4. Braslau, N. and J.V. Dave, 1972: "Effect of Aerosols on the Transfer of Solar Energy Through Realistic Model Atmospheres: Part I - Non-Absorbing Aerosols", Palo Alto, CA: IMB Research Report #RC-4114 (Nov. 1972).

5. Braslau, N. and J.V. Dave, 1972: "Effect of Aerosols on the Transfer of Solar Energy Through Realistic Model Atmospheres: Part I - Non-Absorbing Aerosols", Palo Alta, CA: IMB Research Report #RC-4114 (Nov. 1972) p. 11.

6. Braslau, N. and J.V. Dave, 1972: "Effect of Aerosols on the Transfer of Solar Energy Through Realistic Model Atmospheres: Part II - Absorbing Aerosols", Palo Alto, CA: IMB Research Report #RC-4152 (Dec. 1972).

7. Bryson, R.A., 1968: "All Other Factors Being Constant...", Weatherwise, 21:56.

8. Chandrasekhar, S., 1960: "Radiative Transfer", New York: Dover Publications, Inc., p. 54.

9. Chandrasekhar, S., 1960: "Radiative Transfer", New York: Dover Publications, Inc., p. 279.

10. Charlson, R.J. and M.J. Pilat, 1969: "Climate - The Influence of Aerosols", J. of Appl. Meteor., 8:1001 (Dec. 1969).

11. Dave, J.V. and J. Gasdag: "A Modified Fourier Transform Method for Multiple Scattering Calculations in a Plane Parallel Atmosphere", Applied Optics, 9:1457.

12. Dave. J.V., 1970: "Coefficients of the Legendre and Fourier Series for the Scattering Functions of Spherical Particles", Applied Optics, 9-8:1888 (Aug. 1970).

13. Dave. J.V., 1970: "Coefficients of the Legendre and Fourier Series for the Scattering Functions of Spherical Particles"; Applied Optics, 9-8:1889 (Aug. 1970).

14. Deirmendjian, D., 1969: "Electromagnetic Scattering of Spherical Polydispersions", New York: American Elsevier Publishing Co., Inc., p. 16.

15. Hammond, A.L., 1973: "Solar Energy: Proposal for a Mjaor Research Program", Science, 180:1116 (Dec. 1973).

16. Hansen, J.E., 1971: "Multiple Scattering of Polarized Light in Planetary Atmospheres: Part I - The Doubling Method"; J. of Atmospheric Science, 28:120 (Jan. 1971).

17. Humphreys, W.J., 1913: "Cooling of the Earth by Atmospheric Particles", Bulletin of Monthly Weather Observations, 6:1.

18. Landsberg, H.E., 1962: "City Air - Better or Worse", Sumposium: Air Over Cities, U.S. Public Health Service, Taft Sanitary Engineernig Center, Technical Report A62-5, Cincinnati, Ohio.

19. Mason, B.J., 1971: "The Physics of Clouds", Oxford: Clarendon Press p. 112.

20. McClathchey, R.A. and others, 1972: "Optical Properties of the Atmosphere", Bedford, MA: Air Force Cambridge Research Lab., Report #AFCRL-72-0497, Env. Res. Paper #411 (Aug. 1972).

21. Mitchell, J.M., 1971: "The Effect of Atmospheric Aerosols on Climate with Special Reference to Temperature Near the Earth's Surface"; Journal of Applied Meteorology, 10:703.

22. Peterson, J.T., 1969: "The Climate of Cities: A Survey of Recent Literature", U.S. Public Health Service, National Air Pollution Control Administration Publ. AP-59.

23. Sekera, Z., 1952: "Legendre Series of the Scattering Functions for Spherical Particles", Report #5, Contract AF19 (122) 239, ASTIA AD-3870.

24. Twomey, S., H. Jacobowitz and H.B. Howell, 1970: "Light Scattering by Cloud Layers", J. Atmos. Sci., 24:70 (Jan. 1970).

25. Van De Hulst, H.C., 1957: "Light Scattering by Small Particles", New York: John Wiley & Sons, Inc., p. 5.

UNNORMALIZED LEGENDRE CO-EFFICIENTS PROGRAM LISTING

```
      INTEGER P,Q
      REAL TA(4),TB(2),TC(2),T(4),COEF(100)
      REAL NOC,NOB,KOC,KOB
      COMPLEX BCAP(500),ADOD(500)
      COMPLEX RF,RRF,RRFX,WM1,FNA,FNB,TC1,TC2,WFN(2),ACAP(500)
      COMMONP,Q,K,ADOD,ACAP,CKR
      EQUIVALENCE (WFN(1),TA(1)),(FNA,TB(1)),(FNB,TC(1))
      READ(5,5)RFR,RFI,X
    5 FORMAT(3F10.2)
      DO 300 LIN=1,6
      X=.1*LIN
    2 RFR=1.5
    3 X=2.*3.1416*X/.5145
      RF=CMPLX(RFR,-RFI)
      RX=1./X
      RRF=1./RF
      RRFX=RRF*RX
      T(1)=2*X+10.
      NMX1=1.10*T(1)
      NMX2=T(1)
      IF(NMX1.GT.150) GO TO 22
      NMX1=150
      NMX2=135
   22 ACAP(NMX1+1)=(0.,0.)
C      THE FIRST LOOP COMPUTES THE MIE FUNCTIONA AND B USING A
C      DOWNWARD RECURSION TECHNIQUE
      DO 23 N=1,NMX1
      NN=NMX1-N+1
      ACAP(NN)=(NN+1)*RRFX-1.0/((NN+1)*RRFX+ACAP(NN+1))
   23 CONTINUE
      T(1)=COS(X)
      T(2)=SIN(X)
      WM1=CMPLX(T(1),-T(2))
      WFN(1)=CMPLX(T(2),T(1))
      WFN(2)=RX*WFN(1)-WM1
      TC1=ACAP(1)*RRF+RX
      TC2=ACAP(1)*RF+RX
      ACAP(1)=(TC1*TA(3)-TA(1))/(TC1*WFN(2)-WFN(1))
      BCAP(1)=(TC2*TA(3)-TA(1))/(TC2*WFN(2)-WFN(1))
      FNA=ACAP(1)
      FNB=BCAP(1)
      T(1)=3.0
      QEXT=(TB(1)+TC(1))*T(1)
      QSCAT=(TB(1)**2+TB(2)**2+TC(1)**2+TC(2)**2)*T(1)
      N=2
   65 T(1)=2*N-1
```

```
      T(2)=N-1
      T(3)=2*N+1
      WM1=WFN(1)
      WFN(1)=WFN(2)
      WFN(2)=T(1)*RX*WFN(1)-WM1
      TC1=ACAP(N)*RRF+N*RX
      TC2=ACAP(N)*RF+N*RX
      ACAP(N)=(TC1*TA(3)-TA(1))/(TC1*WFN(2)-WFN(1))
      BCAP(N)=(TC2*TA(3)-TA(1))/(TC2*WFN(2)-WFN(1))
      FNA=ACAP(N)
      FNB=BCAP(N)
      T(4)=TB(1)**2+TB(2)**2+TC(1)**2+TC(2)**2
      QEXT=QEXT+(T(3)*TB(1)+TC(1))
      QSCAT=QSCAT+T(3)*T(4)
      N=N+1
      IF(N.LE.NMX2)GO TO 65.
      WRITE(6,50) T(4)
   50 FORMAT(@ TO BAD@,E20.8)
  100 T(1)=2.0*RX**2
      NUMT=N
      QEXT=QEXT*T(1)
      QSCAT=QSCAT*T(1)
      WRITE(6,6)QEXT,QSCAT
    6 FORMAT(2E20.8)
      N=N/2*2
      N=N+2
      K=N+1
C      THE ODD AND EVEN SUMS OF A AND B ARE COMPUTED FOR LATER USI
      ADOD(N)=0.0
      ADOD(K)=0.0
  110 N=N-2
      K=N-1
      NOC=1./N+(1./(N+1))
      KOC=1./K+(1./(K+1))
      KOB=1./(K+1)+(1./(K+2))
      NOB=1./(N+1)+(1./(N+2))
      ADOD(N)=BCAP(N)*NOC-NOB*ACAP(N+1)+ADOD(N+2)
      ADOD(K)=BCAP(K)*KOC-KOB*ACAP(K+1)+ADOD(K+2)
      IF(N.NE.2) GO TO 110
      DO 104 K=1,12
      I=K*10
      WRITE(6,102) ACAP(I),BCAP(I),ADOD(I)
  102 FORMAT(6E20.8)
  104 CONTINUE
      K=0
C      THE MAIN PROGRAM CALCULATES AN SERIES APPROXIMATION
C      TO THE UNNORMALIZED LEGRENDRE COEFFICIENTS NEEDED IN
C      THE RTE MODEL
      KTOT=NUMT-2
      TMO=.0
      BKT=0.0
  105 K=K+1
      TMO=0.0
```

```
      BKT=0.0
      KC=(K+1)/2*2
      IF(KC.EQ.K) GO TO 175
      KPRIM=(K-1)/2
      M=KPRIM
      IF(K.GT.1) GO TO 115
      A10=2.
      A11=A10
      B10=1.
      P=M+1
      Q=P
      CALL LSUM
      BKT=B10*CKR
      GO TO 160
  115 I=0
      A10=4*(K-1)*(K-2)*A10/((2*K-1)*(2*K-3))
      A11=A10
      B10=(K-2)**2*B10/(K-1)**2
      B11=B10
      Q=M+I+1
      P=M-I+1
      CALL LSUM
      BKT=B11*CKR+BKT
      IF(I.EQ.KPRIM) GO TO160
      GO TO 150
  140 M=M+1
      I=0
      A11=(2*M-K)*(2*M-1+K)*A11/((2*M+K)*(2*M-K+1))
      P=M+1
      Q=P
      CALL LSUM
      BKT=B10*CKR+BKT
      B11=B10
      IF(I.EQ.KPRIM) GO TO160
  150 I=I+1
      B11=(K-2*I+1)*(K+2*I-2)*B11/((K-2*I)*(K+2*I-1))
      P=M-I+1
      Q=M+I+1
      CALL LSUM
      BKT=B11*2*CKR+BKT
      IF(I.LT.KPRIM) GO TO150
  160 TMO=A11*BKT+TMO
      IF(M.LT.KTOT) GO TO140
      COEF(K)=(K-.5)*TMO
      COEF(K)=ABS(COEF(K))
      IF(K.LT.NUMT) GO TO 105
      GO TO 220
  175 KPRIM=(K-2)/2
      M=KPRIM
      IF(K.GT.2)GO TO 185
      AD10=4./3.
      AD11=AD10
      BD10=1.0/2.0
```

```
      BD11=BD10
      P=M+1
      Q=P+1
      CALL LSUM
      BKT=BD10*CKR*2
      GO TO 200
  185 I=0
      AD10=4*(K-1)*(K-2)*AD10/((2*K-1)*(2*K-3))
      AD11=AD10
      BD10=(K-1)*(K-3)*BD10/(K*(K-2))
      BD11=BD10
      P=M+1
      Q=P+1
      BKT=BD11*CKR*2+BKT
      CALL LSUM
      IF(I.EQ.KPRIM) GO TO 200
      GO TO 195
  180 M=M+1
      I=0
      AD11=(2*M-K+1)*(2*M+K)*AD11/((2*M+K+1)*(2*M-K+2))
      P=M-I+1
      Q=M+I+2
      CALL LSUM
      BKT=BD10*CKR*2+BKT
      BD11=BD10
      IF(I.EQ.KPRIM) GO TO 200
  195 I=I+1
      BD11=(2*I+K-1)*(2*I-K)*BD11/((2*I-K+1)*(2*I+K))
      P=M-I+1
      Q=M+I+2
      CALL LSUM
      BKT=BD11*2*CKR+BKT
      IF(I.LT.KPRIM) GO TO195
  200 TMO=AD11*BKT+TMO
      IF(M.LT.KTOT) GO TO180
      COEF(K)=(K-.5)*TMO
      COEF(K)=ABS(COEF(K))
      IF(K.LT.NUMT) GO TO 105
  220 WRITE(6,230)(COEF(K),K=1,NUMT)
  230 FORMAT(5E14.4)
  240 WRITE(7,250)(COEF(K),K=1,NUMT)
  250 FORMAT(8E10.4)
  300 JINA=JINA+1
      END


      SUBROUTINE LSUM
C      LSUM COMPUTES THE INNER MOST SERIES OF THE APPROXIMATION
C      FO USE IN THE MAIN PROGRAM
      INTEGER P,Q
```

```
      COMPLEX ADOD(500),ACAP(500)
      COMPLEX A,A1,D,E
      COMMONP,Q,K,ADOD,ACAP,CKR                                    28
      IF(P.EQ.1) GO TO 10
      A=ACAP(P-1)
      A1=ACAP(Q-1)
    5 D=(2*P-1)*(P-1)*A/P+(2*P-1)*ADOD(P)
      E=(2*Q-1)*(Q-1)*A1/Q+(2*Q-1)*ADOD(Q)
      E=CONJG(E)
      CKR=REAL(D*E)
      RETURN
   10 IF(P.EQ.Q) A1=CMPLX(0.0,0.0)
      A=CMPLX(0.0,0.0)
      GO TO 5
      END
@END
@ELT,DIL D.D
1.33341   0.0        4.5
@END
@FIN
```

000232

APPENDIX B-2

RADIATIVE TRANSFER MODEL -- MAIN PROGRAM LISTING

```
      COMPILER(DIAG=3)
      REAL INT(30,20),INTO
      DIMENSION CLOU(3),CLOUC(3),CCOEF(34),BETA(10),BETR(10),
     X  BTA(10),QSCAT(7),COEF(6,34),ACO(11,34),VAL(10),
     X TURB(10),TAU(31),CONC(3),AER(10),FAC(6),
     X PHASE(30,20,11),GNT(30,20),SOUR(30,20),OSOUR(30,20),HMXT(3)
     X,FA(6),BTR(10),CA(6)
      COMMONPHASE,INT,GNT,LI,JI,DELT,I,OSOUR,SOUR
      DATA /FA/.1984,.2218,.1462,.1091,.0932,.0725/
      READ(5,26)BETA
      READ(5,26)BETR
   26 FORMAT(5F15.10)
      READ(5,39)AER
   39 FORMAT(5E10.4)
      READ(5,28)QSCAT
   28 FORMAT(7F10.8)
      READ(5,22)CCOEF
   22 FORMAT(8E10.4)
      DO 30 I=1,6
   30 READ(5,22)(COEF(I,K),K=1,34)
      BET0=1.25E-6
      BET1=1.64E-5
      TAU(31)=0.
      AMDA=.5145
      FLUX=295.
      CR=4.
      NUM=34
      ELEV=.247
      CORR=1.-ELEV
      PI=3.1416
      NUMT=0
      CBET=0.
      DO 46 J=1,20
      IF(J.LE.10)GNT(1,J)=0.
   46 IF(J.GT.10)GNT(30,J)=1.
      READ(5,17)ALBED
   17 FORMAT(F10.2)
      DAS=160.
      C=0.
      DR=.1
      CO=0
      DO 47 I=1,100
      R=.1*I
      C=DR/R**4+C
      IF(I.LT.50)CO=DR/R+CO
      IF(I.LE.6)FAC(I)=DR/R**4
```

```
   47 IF(I.LE.6)FA(I)=DR/R
      C=1./C
      CO=1./CO
      READ(5,53)C1,C2,C3
   50 DAS=DAS+1
      JIN=0
   53 FORMAT(3F10.2)
      JINO=0
   51 IF(JINO.EQ.1)GO TO 55
      READ(5,20)CLOU
      DO 52 I=1,3
      IF(CLOU(I).LT..2)CLOU(I)=CLOU(I)*C1
      IF(CLOU(I).GT..2)CLOU(I)=CLOU(I)*C2
   52 IF(CLOU(I).GT..8)CLOU(I)=CLOU(I)*C3
   20 FORMAT(3F10.2)
      READ(5,20)CLOUC
      READ(5,20)HMXT
      READ(5,20)CONC
   55 JIN=JIN+1
      NUMT=NUMT+1
      CLOUC(JIN)=CLOUC(JIN)/3280.8+ELEV
      ICEIL=CLOUC(JIN)+.5
      IHMXT=HMXT(JIN)+.75
      IF(CLOU(JIN).LT..01) GO TO 200
      CBET=2.E-11*CLOU(JIN)
      CBET=PI*QSCAT(7)*CR**2*CBET
C       ATTENUATION COEFFICIENTS DUE TO THE PRESENCE OF CLOUDS
C       ARE COMPUTED USING THE SCATTERIN PROPERTIES OF 4 MICRON DR
      DO 180 K=1,NUM
      ACO(11,K)=AMDA**2*CCOEF(K)*2.E-10*CLOU(JIN)/(PI*CBET)
  180 CONTINUE
      CBET=CBET*1.E9
C       SCATTERIN COEFFICIENTS DUE TO AEROSOLS ARE COMPUTED IN
C       THIS LOOP.
  200 DO 250 L=1,10
      IF(CLOU(JIN).LT..01)CBET=0.0
      BET=BETA(L)
      BER=BETR(L)
      IF(L.GT.4)BET=BET-BETA(L-1)
      IF(L.GT.4)BER=BER-BETR(L-1)
      BTA(L)=BET
      BTR(L)=BER
      IF((10-IHMXT).GE.L) GO TO 235
      DO 215 I=1,6
      R=.1*I
      CON=CONC(JIN)*FA(I)*CO*3.E-12/(4.*PI*R**3)
      IF((10-ICEIL).LT.L.AND.ICEIL.NE.0) GO TO 214
      IF(CLOU(JIN).GT.0.)CON=CON-.1*CON*CLOU(JIN)
  214 VAL(I)=QSCAT(I)*CON*R**2*PI
  215 CA(I)=CON
      BET=.5/18.*(VAL(1)+4*VAL(2)+2*VAL(3)+4*VAL(4)
     X +2*VAL(5)+VAL(6))
      DO 230 K=1,NUM
```

```
      DO 220 I=1,6
      R=.1*I
  220 VAL(I)=COEF(I,K)*CA(I)
      ACO(L,K)=AMDA**2*.5/(PI*BET*18.)*
     X (VAL(1)+4*VAL(2)+2*VAL(3)+4*VAL(4)+2*VAL(5)+VAL(6))
      IF((10-ICEIL).GE.L)ACO(L,K)=ACO(L,K)+ACO(11,K)
  230 CONTINUE
      GO TO 246
  235 BET=BET*1.E-9
      DO 245 K=1,NUM
      DO 240 I=1,6
      R=.1*I
      CON=AER(L)*FAC(I)*C
      IF((10-ICEIL).GE.L.OR.L.LE.6)GO TO 240
      IF(CLOU(JIN).GT.0.)CON=CON-.1*CON*CLOU(JIN)
  240 VAL(I)=COEF(I,K)*CON
      ACO(L,K)=AMDA**2*.5/(PI*BET*18.)
     X*(VAL(1)+4*VAL(2)+2*VAL(3)+4*VAL(4)+2*VAL(5)+VAL(6))
      IF((10-ICEIL).GE.L.OR.L.LE.6) GO TO 245
      ACO(L,K)=ACO(L,K)+ACO(11,K)
  245 CONTINUE
  246 CONTINUE
      BET=BET*1.E9
      BTA(L)=BET
      TURB(L)=(BET+CBET)/(BET+CBET+BER)
      IF((10-ICEIL).LT.L.OR.L.LE.6)TURB(L)=BET/(BET+BER)
  250 CONTINUE
   40 FORMAT(5E10.4)
C       THE AZIMUTHAL ANGLE OF THE SN IS COMPUTED USING THE NUMBER
C       OF DAYS SINCE THE SUMMER SOLSTICE
      RND=2.*PI/360.
      AT=43.*RND
      DEC=DAS*360./365.2563*RND
      DEC=23.48*RND*COS(DEC)
      H=ABS(45.*RND*(NUMT-2))
      PMUO=(SIN(AT)*SIN(DEC)+COS(AT)*COS(DEC)*COS(H))
      PMUO=-1.*ABS(PMUO)
      WRITE(6,41)PMUO
   41 FORMAT(E10.4,@ ANGLE@)
      IF(DAS.LT.162..AND.JIN.EQ.1)HUX=FLUX
      FLUX=HUX*.225
      IF(JIN.EQ.2)FLUX=HUX*.55
      WRITE(6,191)FLUX
  191 FORMAT(@ FLUX  =  @,F4.0)
      T=0.
C      THE LOOP COMPUTESTHE SCATTERIN PHASE FUNCTION FOR USE
C       IN LATER CALCULATIONS
      DO 350 L=1,30
      IF(L.GT.24) GO TO 270
      IF(L.GT.5) GO TO 256
      N=1
      BET=L*BTA(N)+BETO
      BER=L*BTR(N)+BET1
```

```
      TAU(L)=(BET+BER)+T
      T=TAU(L)
      BET2=BET
      BET3=BER
      GO TO 265
  256 IF(L.GT.11) GO TO 258
      N=2
      BET=BTA(N)+BET2
      BER=BTR(N)+BET3
      BET2=BET
      BET3=BER
      GO TO 265
  258 IF(L.GT.16) GO TO 260
      N=3
      BET=BTA(N)+BET2
      BER=BTR(N)+BET3
      BET3=BER
      BET2=BET
      GO TO 265
  260 N=4
      BET=BTA(N)+BET2
      BER=BTR(N)+BET3
      BET2=BET
      BET3=BER
  265 TAU(L)=BET+BER+T
      T=TAU(L)
      GO TO 300
  270 N=L-20
      TAU(L)=BTA(N)+BTR(N)+CBET+T
      IF(N.LE.6)TAU(L)=TAU(L)-CBET
      IF(L.EQ.30)TAU(L)=BTA(N)*CORR+BTR(N)*CORR+CBET*CORR+T
      IF((30-L).GE.ICEIL) GO TO 290
      IF(L.EQ.30)CBET=CBET*CORR
      TAU(L)=TAU(L)-CBET
  290 T=TAU(L)
  300 CONTINUE
      DO 350 J=1,11
      PMUP=-J*.1
      IF(J.EQ.11)PMUP=-PMU0
  278 DO 350 I=1,20
      PMU=-I*.1
      IF(I.GT.10) PMU=(I-10)*.1
      PMU2=1.
      PPMU2=1.
      FONEM=ACO(N,1)*PMU2*PPMU2
      PPMU3=PMUP
      PMU3=PMU
      DO 320 K=2,NUM
      FONEM=ACO(N,K)*PMU3*PPMU3+FONEM
      PPMU1=PPMU2
      PMU1=PMU2
      PPMU2=PPMU3
      PMU2=PMU3
```

```
      PMU3=2.*PMU*PMU2-PMU1-(PMU*PMU2-PMU1)/(K+1)
      PPMU3=2.*PMUP*PPMU2-PPMU1-(PMUP*PPMU2-PPMU1)/(K+1)
  320 CONTINUE
      FONER=3.*(3.-PMU**2-PMUP**2+3*PMU**2*PMUP**2)/8.
      PHASE(L,I,J)=TURB(N)*FONEM+(1.-TURB(N))*FONER
  350 PHASE(L,I,J)=ABS(PHASE(L,I,J))
      CP=0
      CPO=0.
      DO 352 L=1,30
      DO 351 J=1,20
      DO 351 N=1,10
  351 CP=CP+PHASE(L,J,N)
      CP=1./CP
      DO 352 J=1,20
      DO 352 N=1,10
  352 PHASE(L,J,N)=PHASE(L,J,N)*CP
      DO 354 L=1,30
      DO 353 J=1,20
  353 CPO=CPO+PHASE(L,J,11)
      CPO=1./CPO
      DO 354 J=1,20
  354 PHASE(L,J,11)=PHASE(L,J,11)*CPO
   45 FORMAT(5E10.4,@TATATATA@)
      WRITE(6,45)(TAU(L),L=25,30)
C      THE FIRST APPROXIMATION TO THE INTENSITY FUNCTION IS
C      CALCULATED INCLUDING ONLY FIRST ORDER SCATTERING
      DO 380 L=1,30
      DO 380 J=1,10
      DO 380 I=1,2
      DTA=TAU(L)
      LB=-1
      JI=J
      LI=L
      D=J
      PMU=-.1*D
      V=-1.*ABS(DTA/PMU)
      V=EXP(V)
      IF(I.EQ.1)GO TO 356
      LI=31-L
      LB=1
      JI=J+10
      PMU=-PMU
      DTA=-1.*(ABS(TAU(LI)-TAU(LI+LB)))
      V=-1.*ABS(DTA/PMU)
      V=EXP(V)
  356 IF(L.NE.1)GO TO 370
      INT(LI,JI)=0.
      GO TO 380
  370 DTA=-1.*ABS(TAU(LI)-TAU(LI+LB))
      V=-1.*ABS(DTA/PMU)
      V=EXP(V)
      DELT=TAU(30)-TAU(LI)
      W=-1*ABS(TAU(LI+1)/PMU0)
```

```
      OSOUR(LI,JI)=FLUX*EXP(W)
     X *PHASE(LI,JI,11)
      INT(LI,JI)=INT(LI+LB,JI)*V+OSOUR(LI,JI)*(1.-V)
      CALL GROUND
      GNT(LI,JI)=GNT(LI+LB,JI)*V+SOUR(LI,JI)*(1.-V)
  380 CONTINUE
  400 DO 500 J=1,10
C      SUCCESSIVE ORDERS OF SCATTERING ARE INCLUDED IN THE
C      INTENSITY CALCULATION  UNTIL COMPARISON CRITERIA IS MET
      DO 500 I=1,2
      DO 480 L=1,30
      DTA=TAU(L)
      LB=-1
      JI=J
      LI=L
      PMU=-J*.1
      IF(I.EQ.1)GO TO 450
      LI=31-L
      LB=1
      JI=J+10
      PMU=-PMU
  450 IF(L.NE.1) GO TO 475
      GO TO 480
  475 CALL SOURCE
      DTA=-1.*(ABS(TAU(LI)-TAU(LI+LB)))
      V=-1.*ABS(DTA/PMU)
      V=EXP(V)
      IF(JI.EQ.10)INTO=INT(LI,JI)
      INT(LI,JI)=SOUR(LI,JI)*(1.-V)+INT(LI+LB,JI)*V
  480 CONTINUE
  500 CONTINUE
      WRITE(6,482)INTO,INT(30,10)
  482 FORMAT(2E10.4,@INTOINTO@)
      IF(ABS(INT(30,10)-INTO).LE..001*INTO)GO TO 510
      GO TO 400
C      THE EFFECTS OF GROUND REFLECTION ARE INCLUDED IN THE FINAL
C      CALCULATION OF THE DIFFUSE COMPONENT OF THE GROUND LEVEL I
  510 DO 550 J=1,10
      PMU=-.1*J
      VAL(I)=INT(30,J)*-PMU
  550 SOUR(2,J)=GNT(30,J)*-PMU
      I=1
  540 TEGRAL=.9/30.*(VAL(1)+4*VAL(2)+2*VAL(3)+4*VAL(4)+2*VAL(5)
     X +4*VAL(6)+2*VAL(7)+4*VAL(8)+2*VAL(9)+VAL(10))
  555 SOUR(I,1)=2.*TEGRAL
      I=I+1
      IF(I.EQ.3)GO TO 561
      DO 560 J=1,10
  560 VAL(J)=SOUR(2,J)
  561 CONTINUE
      IF(I.EQ.2) GO TO 540
      REFL=   ALBED*(PMU0*FLUX*EXP( TAU(30)/PMU0)+SOUR(2,1))
     X /(1-ALBED*SOUR(1,1))
```

```
      DO 580 J=1,10
      GNT(30,J)=REFL*GNT(30,J)
      INT(30,J)=INT(30,J)+GNT(30,J)
  580 VAL(J)=INT(30,J)*.1*J
      TEGRAL=.9/30.*(VAL(1)+4*VAL(2)+2*VAL(3)+4*VAL(4)+2*VAL(5)
     X +4*VAL(6)+2*VAL(7)+4*VAL(8)+2*VAL(9)+VAL(10))
      INT(30,1)=TEGRAL*2.*PI
      FLU=-1*ABS(TAU(30)/PMU0)
      INT(30,1)=INT(30,1)+FLUX*EXP(FLU)
      WRITE(6,80) INT(30,1)
   80 FORMAT(1E14.5)
      TIN =INT(30,1)+TIN
      IF(JIN.NE.3) GO TO 55
      WRITE(6,585)TIN
  585 FORMAT(@ SOLAR FLUX@,3X,F6.2)
      TIN =0
      NUMT=0
      JIN=0
      IF(DAS.LT.166)GO TO 50
      END
```

000338

APPENDIX B-3

RADIATIVE TRANSFER MODEL -- SUB-PROGRAM SOURCE LISTING

```
      SUBROUTINE SOURCE
C      SOURCE COMPUTES SUCCESSIVE APPROXIMATIONS TO THE SOURC.
C      FUNCTIONWHICH INCLUDE HIGHER ORDER SCATTERING
      REAL INT(30,20)
      DIMENSION VAL(10),OSOUR(30,20)
     X,PHASE(30,20,11),GNT(30,20),SOUR(30,20)
      COMMONPHASE,INT,GNT,L,K,DELT,II,OSOUR,SOUR
      PI=3.1416
      SOUR(L,K)=0
      JO=1
      JI=JO+9
      KI=K
      DO 15 I=1,2
    5 DO 10 J=JO,JI
   10 VAL(J-JO+1)=PHASE(L,KI,J-JO+1)*INT(L,J)
      TEGRAL=.45/30.*(VAL(1)+4*VAL(2)+2*VAL(3)+4*VAL(4)
     X +2*VAL(5)+4*VAL(6)+2*VAL(7)+4*VAL(8)+2*VAL(9)+VAL(10))
      JO=11
      JI=JO+9
      IF(II.EQ.2)KI=K-10
      IF(II.EQ.1)KI=K+10
   15 SOUR(L,K)=OSOUR(L,K)+TEGRAL+SOUR(L,K)
      RETURN
      END
```

000035

APPENDIX B-4

RADIATIVE TRANSFER MODEL -- SUB-PROGRAM GROUND LISTING

```
      SUBROUTINE GROUND
C      SUBROUTINE COMPUTES THE SOURCE FUNCTION NEEDED TO
C     . INCLUDE THE EFFECTS OF GROUND LEVEL REFLECTION IN THE
C      INTENSITY CALCULATION
      REAL INT(30,20)
      DIMENSION VAL(20),OSOUR(30,20)
     X,PHASE(30,20,11),GNT(30,20),SOUR(30,20)
      COMMONPHASE,INT,GNT,L,K,DELT,II,OSOUR,SOUR
      LI=L
      LB=-1
      IF(II.EQ.2)LB=1
      SOUR(L,K)=0
      TEGRAL=0
      DO 10 J=1,20
      JI=J
      KI=K
      IF(J.LE.10) GO TO 8
      IF(K.LT.10)KI=K+10
      IF(K.GT.10)KI=K-10
      JI=J-10
    8 CONTINUE
      VAL(J)=PHASE(L,KI,JI)*GNT(LI+LB,J)
   10 CONTINUE
      TEGRAL=.45/60.*(VAL(1)+4*VAL(2)+2*VAL(3)+4*VAL(4)+2*VAL(5)+
     X 4*VAL(L)+2*VAL(7)+4*VAL(8)+2*VAL(9)+4*VAL(10)+2*VAL(11)+
     X4*VAL(12)+2*VAL(13)+4*VAL(14)+2*VAL(15)+4*VAL(16)+2*VAL(17)
     X +4*VAL(18)+2*VAL(19)+VAL(20))
      DO 13 J=1,10
      PI=J*.1
    9 VAL(J)=PHASE(L,K,J)*EXP(-DELT/PI)
   13 CONTINUE
   11 TEGRAL=.45/30.*(VAL(1)+4*VAL(2)+2*VAL(3)+4*VAL(4)
     X +2*VAL(5)+4*VAL(6)+2*VAL(7)+4*VAL(8)+2*VAL(9)+VAL(10))
     X +TEGRAL
      SOUR(L,K)=SOUR(L,K)+TEGRAL
      RETURN
      END
@END
```

Chapter VII

FLORIDA SYNOPTIC CLIMATOLOGY

Outline

Chapter VII

FLORIDA SYNOPTIC CLIMATOLOGY

A. OVERVIEW

The following description of the Climate of Florida has been synthesized from many different published data sources. Special tabulations of unpublished data have also been constructed to supplement the published sets. In particular, extensive use has been made of the tabulated climatic summaries from Bradley (1972), Newell et al., (1972), Baldwin (1974), Court (1974), various NOAA publications, Air Weather Service Climatic Briefs, U.S. Navy Station Climatic Summaries and selected NASA Technical Memorandums and Notes.

B. SURFACE SYNOPTIC CLIMATOLOGY

1. Temperature

The normal average daily temperature for January and July is shown in Fig. VII-1 and Fig. VII-2 as taken from Court (1974). Note the elimination of significant north-south temperature contrast from January to July across Florida. The normal mean daily range of temperature varies from 12°C to 10°C north to south across the peninsula in January and from 10.5°C to 7.5°C in July.

Figure VII-3 (Court, 1974) shows the mean interdiurnal variability of minimum and maximum temperatures in January and July. In general the variability decreases from winter to summer and from north to south as continental effects lessen.

2. Dew Point Temperature

January and July mean dew point temperatures (Court, 1974) are shown in Fig. VII-4 and Fig. VII-5 respectively. Seasonal variations parallel those of temperature quite closely. A mean dew point temperature of 23°C is quite representative of the Florida peninsula in July.

3. Relative Humidity

Analysis of relative humidity for 1200 and 1800 GMT are presented in Fig. VII-6 thru Fig. VII-9 for January and July. These times approximate the time of highest and lowest relative humidity respectively. The data were gleaned from selected NOAA and military climatic summaries with variable record periods of at least 10 years. Little difference in the 1200 GMT values between January and July is noted. A relative inland minimum is noted during the early afternoon with slightly drier conditions prevailing in January. Figure VII-10 taken from Baldwin (1974)

shows the hourly relative humidity variation for selected stations based upon data for the 1954-1968 period.

4. Fog

Days of heavy fog as defined by the occurrence of a visibility less than or equal to 0.4 km are shown in Fig. VII-11 and Fig. VII-12 for the May-October and November-April periods. The data source is the same as used for the fog frequency maps. Fog is rarely observed along the middle and lower east coast and is a maximum in the northwestern part of the state in winter. The gradient between coastal and inland locations along the peninsula is larger than the figures suggest as fog is quite rare along the immediate coastal strip.

5. Visibility

Figure VII-13 and Fig. VII-14 taken from Eldridge (1966) show visibility frequencies over the coterminus U.S. by season. The data are based upon the 1948-1958 period with only Miami, Tampa and Jacksonville data used to construct the Florida analyses. The results, however, are compatible with synoptic experiences in that the best visibilities are found along the Florida lower east coast and with the highest values found in summer.

6. Cloud Cover

Mean cloud cover from sunrise to sunset for the May-October and November-April periods is shown in Fig. VII-15 and Fig. VII-16. These six month periods comprise the approximate wet and dry seasons across the Florida peninsula. The data source is the same as previously indicated with more attention here devoted to small scale variations.

A warm season maximum is located along the sea breeze convergence region just inland from the lower east coast with a relative minimum in the Lake Okeechobee area. During the cool or relatively dry season a relative cloud minimum is found in the southwestern part of the peninsula. Daytime cloudiness is a maximum along most of the east coast and in the extreme northwest.

7. Precipitation

Rainfall maps were constructed from all available civilian and military data for the months of March, June, September and December with the results shown in Fig. VII-17 thru Fig. VII-20. December rainfall is relatively sparse with a gradual decrease from northwest to southeast. An exception is the relative maximum along the lower east coast. March is the wettest month during the dry season everywhere except along the lower east and southwest coasts and the Keys. A relative rainfall maximum is noted from just north of Tampa across the peninsula to Cape Canaveral.

By June the rainy season is well underway with the maximum rainfall totals now found inland in the lower part of the peninsula. A rather large rainfall gradient is noted along the entire east coast (and to some extent the west coast) with a relative minimum in the Lake Okeechobee region. Convective rainfall is enhanced in the sea breeze convergence region approximately 10-20 km inland. The relatively cool waters of Lake Okeechobee act to suppress convection. September marks the culmination of the rainy season in the southern and western regions of the peninsula whereas elsewhere things begin to dry out somewhat. The central and lower east coast inland rainfall maximum is still evident as it persists throughout the summer.

The number of days of measureable rainfall ($\geq$ 0.25 mm) is shown in Fig. VII-21 and Fig. VII-22 for the May-October and November-April periods. Approximately 50% of the days record measureable rain during the summer along the lower east coast sea breeze convergence zone. This number decreases rapidly right along the immediate coast with a value of 36% in the Cape Canaveral area. During the cool season the inland maximum is replaced by a coastal and panhandle maximum. Finally, on an annual basis the standard deviation of the number of days with measureable rain increases from 12 to 16 north to south across the peninsula.

The mean annual number of days with precipitation $\geq$ 12.7 mm and the mean annual precipitation from days with 12.7 mm or more as a percent of the total rainfall (Court, 1974) are shown in Fig. VII-23 and Fig. VII-24. Comparison of Fig. VII-21 thru Fig. VII-24 suggests that rainfalls reach the 12.7 mm category on 25-30% of all rain days and account for 70-80% of the annual rainfall total across the peninsula.

Table VII-I taken from Wallace (1975) shows the diurnal frequency of precipitation by amount and category by season. The data source was "Climatography of the United States", No. 82, "Decennial Census of the United States Climate" for the years 1951-1960; published by the U.S. Weather Bureau, 1962-1963 in addition to Part A of the Uniform Summary of Surface Weather Observations, on file at the U.S. Air Force, Environmental Technical Applications Center. The data were harmonically analyzed to obtain amplitudes and phases of the diurnal and semidiurnal cycles. Amplitudes were normalized by dividing them by the 24 hour mean of the parameter in question.

Approximately 10-12% of the summer hours are associated with precipitation versus 7-10% in the winter. Trace amounts occur 4-6% of the time whereas heavier amounts (>2.5 mm h^{-1}) occur 2% and 1% of the time in summer and winter. The time of maximum occurrence is generally mid-afternoon with the exception of Jacksonville in winter. The normalized amplitudes suggest that the afternoon maximum is much more pronounced in summer. Normalized amplitudes in excess of unity can occur, e.g., if the precipitation frequency was near zero during the night and high during the daytime, with symmetry about a noontime peak.

8. Thunderstorm Frequency

The mean Florida thunderstorm frequency for the May-October and November-March periods is shown in Fig. VII-25 and Fig. VII-26. Civilian and military data sources were used to construct the analyses. Additional details with special emphasis on Cape Canaveral can be found in reports by Neumann (1968, 1970). The analyses suggest that during the warm season thunderstorms are suppressed along the immediate coast and in the Lake Okeechobee area, consistent with monthly rainfall statistics. Winter frequencies are considerably reduced with the maximum shifting to the panhandle area.

Table VII-II gives the diurnal cycle in the thunderstorm frequency by season for a number of Florida stations based upon data derived from Wallace (1975). The percentage of summer hours with audible thunder ranges from 3 to 6% with a maximum across central Florida. A very strong late afternoon peak is noted for all stations. Winter frequencies are considerably reduced across the peninsula (several stations have been combined to achieve a reasonable sample size) with a much weaker early

evening maximum. A weak morning maximum is noted across the panhandle region in winter. Caution must be used in interpreting this data as Wallace notes due to variable record lengths and differing decibel levels required for thunder to be heard at the various stations.

9. Winds

Prevailing wind directions and mean wind speeds for all available civilian and military locations in the state of Florida are shown in Fig. VII-27 thru Fig. VII-30 for the months of March, June, September and December. Wind speeds average 4 ms^{-1} except near 5 ms^{-1} along portions of the lower east coast in March. Directional consistency is weak. By June the mean wind speeds are reduced to 3-4 ms^{-1} with easterly flow south of 28°N and a tendency for southwesterly flow further to the north, suggesting an east-west surface ridge line oriented across the mid peninsula. By September surface winds are easterly everywhere with average speeds of 4 ms^{-1}. Northerly components giving way to northeasterly components from north to south prevail in December with mean speeds in the 4-5 ms^{-1} range. Note, the listed wind directions refer to <u>prevailing</u> wind directions. Little information is available on surface wind variability for most of the stations listed in the figures. Along the east coast wind speeds increase by about 1 ms^{-1} with easterly flow and decrease by nearly the same amount with southwesterly flow. For reference surface wind roses taken from Baldwin (1974) for January and July are presented in Fig. VII-31 and Fig. VII-32.

10. Fronts

Figure VII-33 thru Fig. VII-38 show the frequency of cold, warm and stationary fronts, in days per 10 years, for the conterminus

United States based upon tabulations from the 1200 GMT Daily Weather Map for the 1951-1970 period. The data were presented by Morgan et al., (1975). A north-south gradient of cold frontal passage is quite evident with the exception of December. Warm frontal passages across the peninsula are comparatively rare. Bosart and Korty (1976)* have provided a tentative hypothesis for this observation in terms of the Carolina coastal baroclinic zone. Stationary front frequencies suggest a maximum across central Florida in all seasons except late spring and summer. This is related to the well known tendency for cold fronts to stagnate across central Florida.

11. Stagnating Anticyclones

Korshover (1976) has presented a climatology of stagnating anticyclones for the 1936-1975 period based upon tabulations from the Daily Weather Map published by NOAA. Figures VII-39 thru Fig. VII-42 show the number of cases of atmospheric stagnation (four days or more) for this 40 year period by season. Stagnation is defined for those anticyclonic regions where surface geostrophic winds are under 7 ms^{-1} and hence actual winds are considerably less. The highest frequencies are found in autumn across the southeastern states. Some stagnation cases are found across northern Florida in all seasons with a pronounced spring maximum across east central Florida.

12. Cape Canaveral Climatological Data

Figure VII-43 shows the Air Weather Service Climatic Brief for Cape Canaveral for the 1950-1968 period. This is provided as a reference for more detailed information.

*Published in preprint volume of the Conference on Coastal Meteorology, September 1976, Virginia Beach, sponsored by the American Meteorological Society.

C. UPPER AIR CLIMATOLOGY - FLORIDA

1. Temperature

Newell et al., (1972) have published the only information which gives upper air conditions across Florida in which all six radiosonde stations are used. The period of record is 1957-1964 and is based mainly on the 0000 GMT observations.

Table VII-III gives the 850 mb, 700 mb and 500 mb temperatures by winter and summer season across Florida. The summer uniformity is rather remarkable such that detailed Cape Canaveral data should be representative of the entire peninsula. As would be expected from synoptic considerations the coldest winter temperatures are found across the northwestern panhandle at Eglin AFB (Valparaiso) with a modest thermal gradient across the peninsula at all levels.

Upper air summaries prepared by the National Climatic Center (NOAA) for a few of these stations suggest the following standard deviations of temperature north to south across the peninsula: (a) 850 mb: 4.5 to 3.0°C in winter and 1.3 to 0.9°C in summer, (b) 700 mb: 3.6 to 2.6°C in winter and 1.3 to 0.9°C in summer, (c) 500 mb: 3.0 to 2.0°C in winter and about 1.0°C in summer.

2. Moisture

Moisture data is not as definitive or as widely published as temperature data. Tabulated summaries (0000 GMT data) available from the National Climatic Center suggest the following patterns: (a) 850 mb: 60-75% across most of the Florida peninsula and 40-50% across the northwest panhandle in winter, 70-75% and rather uniform in summer, (b) 700 mb: 25-35% from north to south in winter and a fairly uniform 55-65% in

summer, (c) 500 mb: uniform 20-30% in winter and 40-50% in summer. Specifics for Cape Canaveral will be presented in a later section.

3. Winds

Table VII-IV gives the u and v wind components (ms^{-1}) at the surface, 850 mb, 700 mb and 500 mb for the six Florida radiosonde stations based upon the Newell et al., (1972) data. In addition, standard deviations of the u and v components are given at 850 mb and 500 mb. The basic winter west-southwest flow increasing with height is evident above the surface with a strong gradient across the Florida peninsula. At the surface the picture is more confused but a winter westerly flow across the western panhandle giving way to a northerly flow along the upper east coast and a east-northeasterly along the lower east coast is suggested.

The summer surface picture is probably confused by sea breeze effects with an easterly and westerly flow along the east and west coasts respectively and a southerly flow along the panhandle area. Aloft an east-southeast flow across the lower peninsula gives way to a westerly flow across northern Florida. Clearly an east-west oriented ridge line sits across central Florida in the mean data in summer. This ridge line can oscillate north and south as judged by the greater variability of the u as opposed to v components in summer at the selected levels. Note also the southward slope with height of the boundary between the summer easterlies and westerlies.

4. Morning and Afternoon Mixing Heights

Holzworth (1972) compiled data on seasonal and annual mixing heights (morning and afternoon) for selected coterminus United States stations for the 1960-1964 period. Table VII-X shows the summarized

data for Tampa, Miami and Jacksonville. No data is readily available for the other Florida stations. A general increase in mixing height is noted from winter to summer with reduced wind speeds as convective heating becomes more dominant. Inland locations would probably have lower morning mixing heights and somewhat higher afternoon values.

Table VII-XI summarizes the episode-days of high meteorological air pollution potential for episodes lasting at least two days for these stations. For example, both Tampa and Jacksonville have 29 episode-days in winter of mixing heights under 1000 m and winds under 6 ms^{-1}, or about 6.5% of the winter days. The results suggest that the upper and lower Florida peninsula is most sensitive to air stagnation in winter and summer respectively.

D. UPPER AIR CLIMATOLOGY - CAPE CANAVERAL

1. Temperature, Moisture and Winds

Table VII-V gives a 20 year summary of temperature, standard deviation of temperature and relative humidity for selected lower tropospheric pressure levels for the indicated months. Likewise, Table VII-VI summarizes the data by height levels but only for a 10 year period and for different months. As an approximate conversion factor, note that the 850 mb and 700 mb levels closely approximate 1.5 km and 3.1 km respectively at the latitude of Florida. Reasonable consistency for the Cape Canaveral data is seen amoung Table VII-III, Table VII-V, and Table VII-VI despite the varying record lengths. Note especially the very moist conditions in the late summer and early fall. This is typical of the east coast of Florida at that time.

Table VII-VII summarizes Cape Canaveral wind statistics by level in more detail based upon a 50% cumulative frequency of u and v components. Considerable seasonal variation is evident in the lower troposphere. Note especially the deep mean easterly flow of September in terms of the potential for the shuttle exhaust cloud to remain over land.

2. Diurnal Variations

In an effort to assess the possible significance of diurnal variations, ten years of 0000 GMT and 1200 GMT Cape Canaveral data were assembled on WBAN-33 forms provided by the National Climatic Center. Table VII-VIII shows the results for the lower troposphere. The 1200 GMT sounding is uniformly cooler and has a higher relative humidity through 900 mb with the differences becoming indistinct by the 850 mb level. Little difference in the height field is noted.

Diurnal wind frequencies by quadrant for June and December are shown in Table VII-IX for the 850 mb surface. The results are rather interesting and warrant future investigation. Differences between onshore and offshore wind components are apparently rather negligible by time or by season. However, the 1200 GMT observations feature enhanced southerly flow in comparison to the 0000 GMT observation, especially in summer. More months and data for the 0600 GMT and 1800 GMT radiosonde release times need to be investigated to either support or refute this finding. A possible explanation might be based on differential heating whereby the peninsula cools more than the adjacent water at night and heats up more during the daytime. This would lead to relatively higher and lower 850 mb heights over the inland peninsula by late afternoon and daybreak respectively and thus favoring enhanced southerly flow along the east coast in the early morning. If this explanation has any merit, then Tampa, located along the west coast, should have a greater relative northerly flow at the 1200 GMT observation time.

E. SEA BREEZE AND RELATED EFFECTS

During most of the warm season the Florida peninsula is relatively unaffected by large-scale organized synoptic scale disturbances. Weather during this period is then determined by differential heating between land and sea and the attendant interaction with the synoptic scale flow. This means that the sea breeze, an almost daily occurrence, will play a major role in determining the local weather patterns. Climatological information on the strength, duration, inland and vertical extent of the sea breeze circulation is lacking. However, the many observational and theoretical papers in the literature on the subject suggest that the average inland extent of the sea breeze is 10-15 km with the vertical circulation confined to the lowest 500-1000 m.

The picture in Florida is complicated by the existence of a double sea-breeze superimposed on small but significant variations in the prevailing synoptic flow. Frank et al., (1967), Frank and Smith (1968) and Pielke (1973) have shown that preferred shower locations over central and south Florida depend strongly on the location of the sea breeze convergence zone. Recall the inland precipitation maximum along the entire east coast during the warm season that was discussed previously. On an annual basis Miami International Airport and Miami Beach receive 143 and 109 cm of rain respectively, although the distance between the stations is only 10 km. The observed difference is almost entirely accounted for by warm season precipitation.

In general on a typical summer day lines of showers form along the windward and leeward coasts of south and central Florida. The windward shower line tends to move toward the lee coast during the day and has a

tendency to merge with the leeward line in the late afternoon. This process is particularly evident on days with moderate easterly synoptic scale flow such that extensive precipitation occurs along the west coast sea breeze convergence. Immediate east coastal locations do not have much rain in such situations. Under light wind conditions, the shower lines show little movement during the day, a not too pleasant a prospect for those individuals living along the sea breeze convergence zone. With a westerly or southwesterly synoptic scale flow the sea breeze convergence zone is closer to the east coast so that rainfall probabilities along the immediate shoreline are enhanced compared to further inland. These factors are taken into account in Cape Canaveral thunderstorm forecasting and are important to consider when assessing the probability of the space shuttle exhaust cloud encountering an active thunderstorm cell.

Neumann (1968, 1970) has carried out the most definitive study of frequency and duration of Cape Canaveral thunderstorms. For reference purposes Fig. VII-44 shows a map of the Cape Canaveral area. A similar summer precipitation gradient prevails between Titusville and the ocean front, although somewhat weaker, as compared to Miami Airport and Miami Beach.

Figure VII-45 and Fig. VII-46 show the prominent daily summer thunderstorm peak reaching 50% in July and August in the vicinity of the Kennedy Space Center. The strongly diurnal nature of the percent of days with a thunderstorm is quite evident. The data in these figures is based upon 13 years: 1951-1952 and 1957-1967. It is also instructive that Neumann finds that 11% of the thunderstorm occurences at

Cape Canaveral take place entirely between regular hourly surface reports. This implies a significant underestimation of thunderstorm frequencies in the published climatological summaries (e.g., Wallace [1975]) which are based entirely on hourly observations.

Figure VII-47 shows that the beginning and end of the Cape Canaveral thunderstorm season is associated with a strengthening and weakening of the 1200 GMT 1000 m resultant wind, consistent with the ideas expressed previously. More details are provided in Fig. VII-48 on the annual variation in the 1200 GMT 1000 m vector and scalar winds under conditions with and without afternoon thunderstorms. Afternoon thunderstorms are clearly favored by westerly wind components and suppressed by easterly components during the summer. Afternoon thunderstorms during the cool season are especially prevalent in the strong southwesterly flow ahead of the more potent migrating troughs at that time of the year.

The data is summarized in Fig. VII-49 which shows the probability of afternoon thunderstorms over the entire May-September thunderstorm season as a function of the 1200 GMT 1000 m wind speed and direction. The contrast between northeasterly and southwesterly flow is remarkable. Southwesterly flow days are associated with a sea breeze convergence zone very close to the coast and the developing thunderstorm cells then can drift towards the ocean during the afternoon. Finally, Fig. VII-50 shows a forecast monogram for the peak of the thunderstorm season around 1 August. With a wind of 250 degrees between 5 and 9 ms^{-1} the afternoon thunderstorm probability reaches 90%.

F. CONCLUSIONS

The data presented in the previous sections can be used for many individual purposes. In terms of the space shuttle program it becomes important to worry about possible inadvertent weather modification by the stabilized ground cloud. Clearly, the risk is greatest when the exhaust cloud remains over or near land, especially populated areas. These risks would be enhanced under the following synoptic conditions:

1. Surface sea breeze regime and weak westerly flow at 1000 and 2000 m in summer
2. Pre cold front squall lines that occasionally occur in the winter and early spring
3. Post cold frontal (weak with easterly surface flow giving way to weak westerly flow aloft
4. Pre warm front passage in winter with low land onshore flow veering to offshore flow aloft
5. Weak stationary front located south of Cape Kennedy with surface onshore flow veering to offshore flow aloft
6. Stagnating anticyclonic conditions
7. General easterly flow of late summer and early fall across the Florida peninsula
8. Thunderstorm events
9. Tropical storm situations

Items (1) through (3) above are in particular quite difficult to evaluate without further research. The surface wind field on sea breeze days is relatively well known. Unfortunately, the lower tropospheric wind field is not at all well documented in terms of diurnal and seasonal variations as a function of the prevailing synoptic patterns. Consequently, accurate mesoscale three-dimentional trajectories are rather difficult to compute.

Pre cold front squall lines may occasionally move across northern and central Florida in the winter and early spring. These squall lines are usually oriented from northeast to southwest and may propagate southeastward at speeds up to 40 knots. The frequency of occurrence may reach two to four times per month at the height of the cool season. Such squall lines usually die out before they reach south Florida. Strong low level southerly flow ahead of the squall lines carries the potential risk of incorporating particulate matter from the space shuttle exhaust into the active cumulonimbus clouds of these systems. The risk would be greatest within the first 24-hours after launch.

The results from Morgan et al., (1975) suggest possibly two warm front episode days per winter month across central and northern Florida. Assuming a 12-hour frontal passage this would work out to be about a maximum warm front influence of 3% during a mid-winter month. Convective activity often accompanies warm frontal passage especially in northern Florida. Pre frontal veering winds can carry the exhaust cloud northward into the region of favorable convection.

Stationary fronts are more ambiguous because the lower tropospheric wind field can be considerably different depending upon such factors as frontal intensity and distance from the station. An upper bound of 4 days per winter month gives an upper bound of a 13% influence and this will be an overestimate of the true risk.

The results from Korshover (1976) and Holzworth suggest that relatively stagnant conditions are possible in winter and early spring across central and northern Florida from 3 to 6% of the time, ranging down to 1 to 2% in summer. Normally such situations are associated with

stable air but occasional air mass thunderstorms during the warm season pose some risk for vertical mixing.

The deep easterly flow regime of late summer and early fall becomes a special problem if the exhaust cloud encounters active precipitation cells after launch. This risk is difficult to assess with the data currently in hand. Overall, the thunderstorm problem is perhaps potentially most serious because of uncertainties in precise prediction. Neumann (1968, 1970) has compiled a very valuable data set which obviously is heavily used in thunderstorm prediction at Cape Canaveral. His data suggest that 1200 GMT 1000 m level winds of 1 ms^{-1} or less can be encountered 4.5% of the time during the May-September period. This number increases to 15.1% for a 2 ms^{-1} or less cut off point. This suggests in turn that the exhaust cloud can still be within 10 km of Cape Canaveral more than an hour after launch, assuming relatively light surface winds, on a substantial number of summer mornings. How this simple calculation would change based upon the 0000 GMT data is unknown now and is worthy of further research.

Finally, tropical storm situations carry potential risk because of the active cumulonimbus clouds associated with such systems and potential for inadvertent weather data. Historical data (Court, 1974) suggest that from 10-15% of the June-October Florida rainfall is associated with tropical disturbances.

G. RECOMMENDATIONS FOR FURTHER RESEARCH

The most pressing need is to establish typical and atypical three-dimensional air trajectories in the lower troposphere as a function of the time of the year and prevailing synoptic situation over the Florida peninsula. Likewise, temporal and spatial variations of various meteorological parameters on scales of several hours and several tens of kilometers needs to be better documented. In particular, the following is suggested.

1. Diurnal and seasonal variations of the lower tropospheric wind field across Florida using the 0000, 0600, 1200 and 1800 GMT winds aloft observations. Published studies rarely refer to winds other than at the 0000 GMT observation time.

2. Diurnal and seasonal variations of various meteorological surface parameters along a line perpendicular to the east coast to better understand the complex mesoscale air motions. Existing stations in the Jacksonville area offer such an opportunity for research. The present upper air network does not permit such a study above the surface layer, however.

3. Establish hail frequencies across Florida on a county by county basis to better assess the risk of inadvertent weather modification during convective situations.

4. Better establish precipitation frequency, intensity and duration as a function of the time of day and season from the existing hourly precipitation network across Florida.

H. REFERENCES

1. Baldwin, J.L., 1974: "Climates of the United States", U.S. Dept. of Commerce, 113 pp.

2. Bradley, J.T., 1972: "The Climate of Florida", Climates of the States, Vol. I, NOAA, U.S. Dept. of Commerce, 45-71.

3. Court, A., 1974: "The Climate of the Coterminus United States", in World Survey of Climatology, Vol. II, Climates of North America, edited by R. Bryson and F.K. Hare.

4. Eldridge, R.G., 1966: "Climatic Visibilities of the United States", J. Appl. Meteor., Vol. 5, #3, 277-282.

5. Frank, N.L. and D.L. Smith, 1968: "On Correlations of Radar Echoes over Florida with Various Meteorological Parameters", J. Appl. Meteor., Vol. 7, #4, 712-714.

6. Frank, N.L., P.L. Moore and G.E. Fisher, 1967: "Summer Shower Distribution over Florida Peninsula as Deduced from Digitized Radar Data", J. Appl. Meteor., Vol. 6, #3, 309-316.

7. Holzworth, G.E., 1972: "Mixing Heights, Wind Speeds and Potential for Urban Air Pollution throughout the Contiguous United States", Envir. Prot. Agency, Office of Air Programs, Publ. # AP-101, 118 pp.

8. Korshover, J., 1976: "Climatology of Stagnating Anticyclones East of the Rocky Mountains, 1936-1975", NOAA Tech. Memo. ERL-ARL-55, 26 pp.

9. Morgan, G.M., D.G. Brunkow and R.C. Beebe, 1975: "Climatology of Surface Fronts", Illinois State Water Survey, ISWS-75-CIR-122, 46 pp.

10. Neumann, C.J., 1968: "Frequency and Duration of Thunderstorms at Cape Kennedy, Part I", ESSA Tech. Memo., WBTM-SOS-2.

11. Neumann, C.J., 1970: "Frequency and Duration of Thunderstorms at Cape Kennedy, Part II", ESSA Tech. Memo., WBTM-SOS-6.

12. Newell, R.E., J.W. Kidson, D.G. Vincent and G.J. Boer, 1972: "The General Circulation of the Tropical Atmosphere and Interactions with Extratropical Latitudes, Vol. I", MIT Press, Cambridge, Mass., 258 pp.

13. Pielke, R., 1973: "An Observational Study of Cumulus Convection Patterns in Relation to the Sea Breeze over South Florida", MOAA Tech. Memo. ERL-OD-16, 81 pp.

14. Wallace, J.M., 1975: "Diurnal Variations in Precipitation and Thunderstorm Frequency over the Caterminus United States", Mon. Wee. Rev., 103, #5, 406-419.

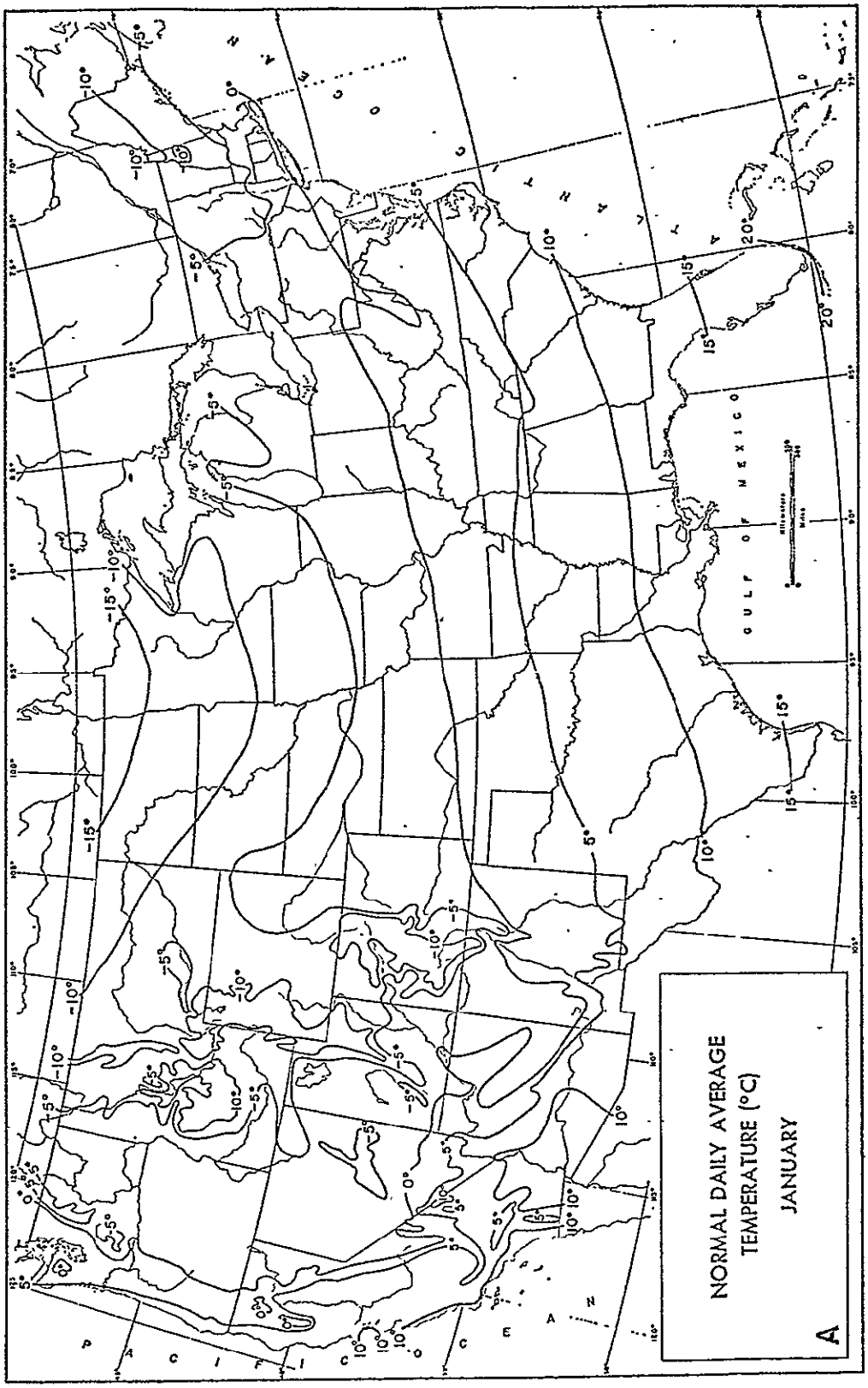

Figure VII-1: January Mean Temperature

After Court (1974)

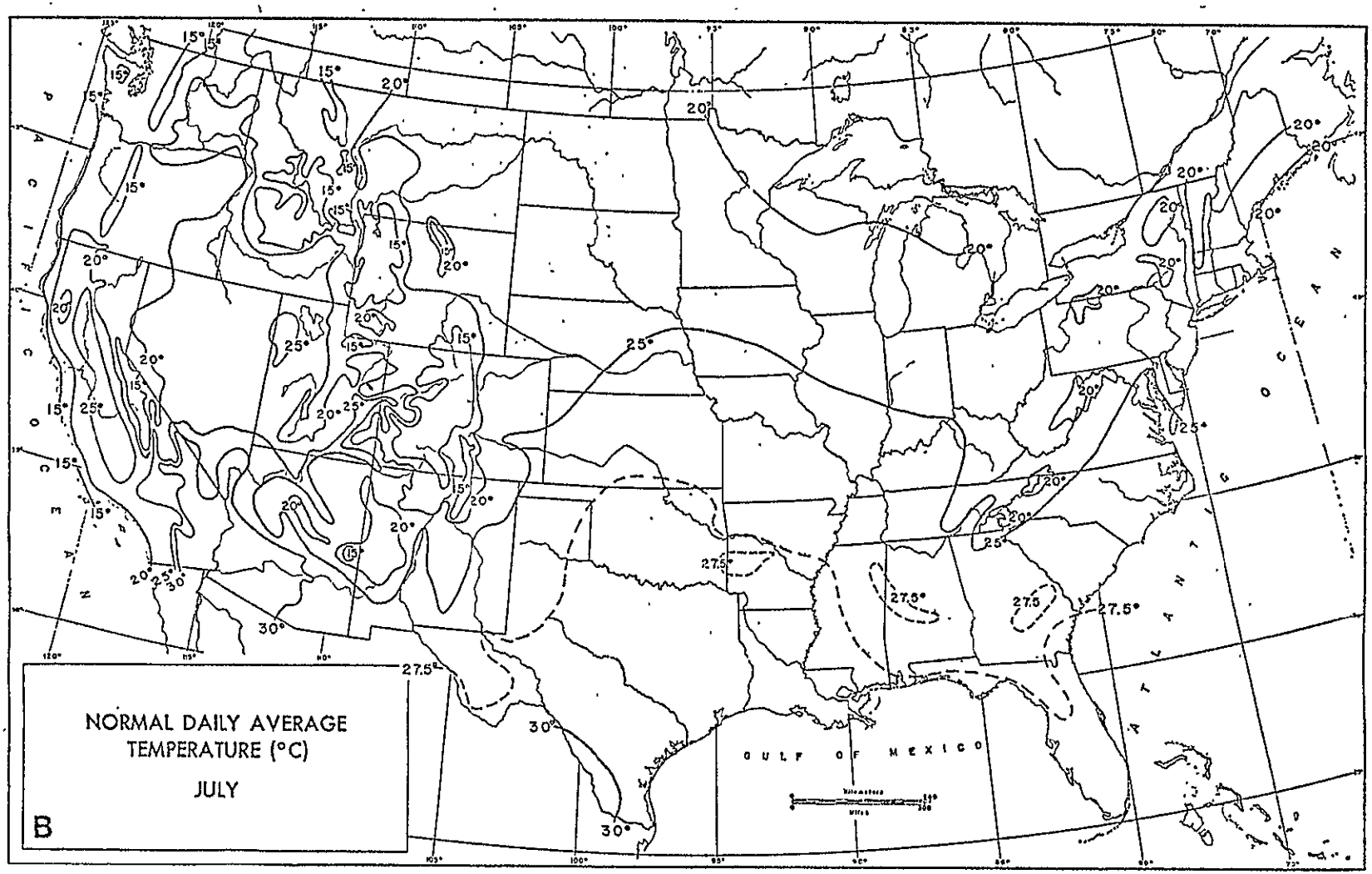

Fig.36. Mean monthly temperatures, 1931–1960, in January (A) and July (B), interpolated from U.S. Weather Bureau National Atlas map.

Figure VII-2: July Mean Temperature

After Court (1974)

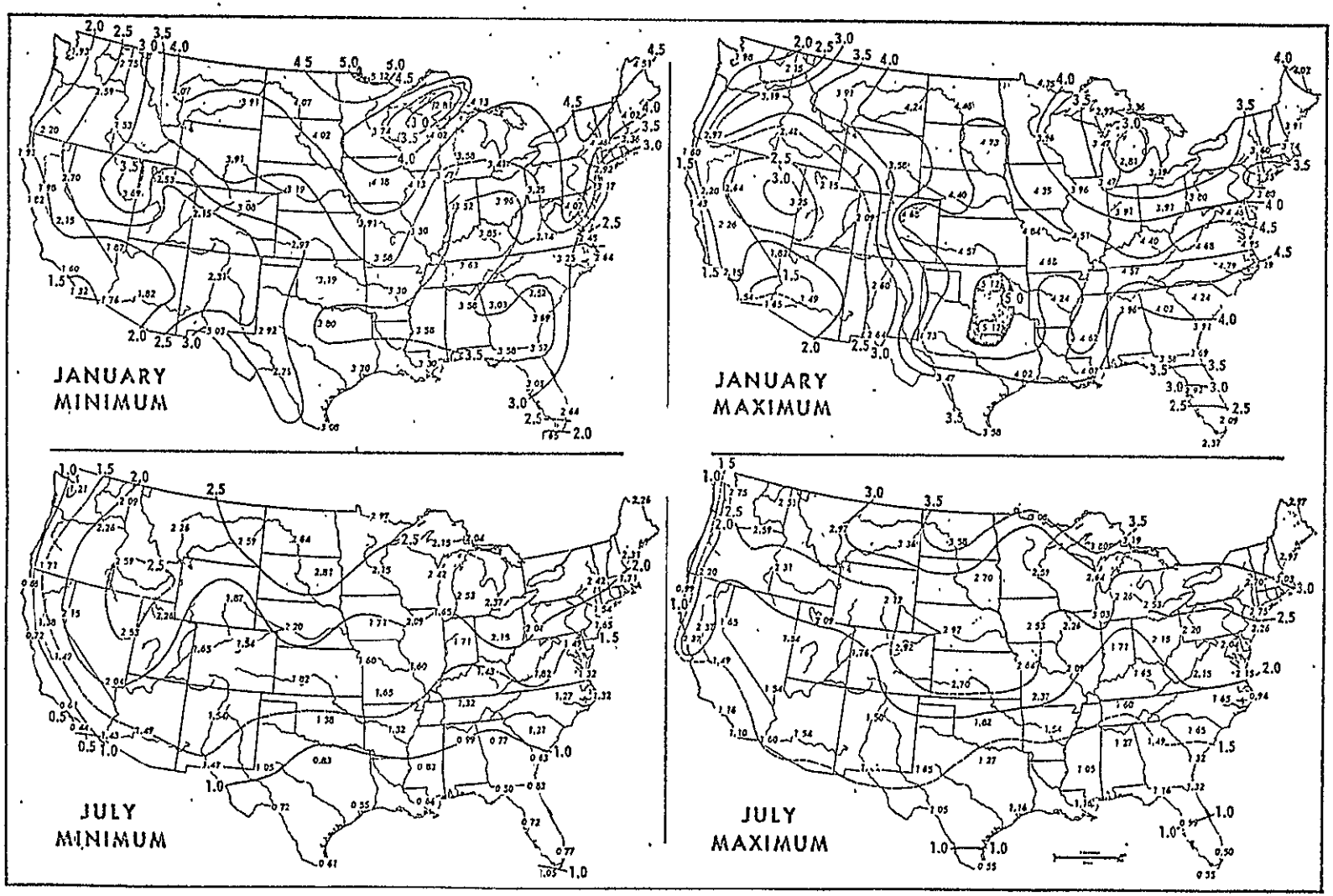

Fig.37. Mean interdiurnal variability of minimum and maximum temperatures (°C) in January and July, based on data at 75 stations, 1957–1961. (Prepared by Stanley Marsh from data of LANDSBERG, 1966.)

Figure VII-3: Mean Interdiurnal Variability of Minimum and Maximum Temperatures (°C)

After Court (1974)

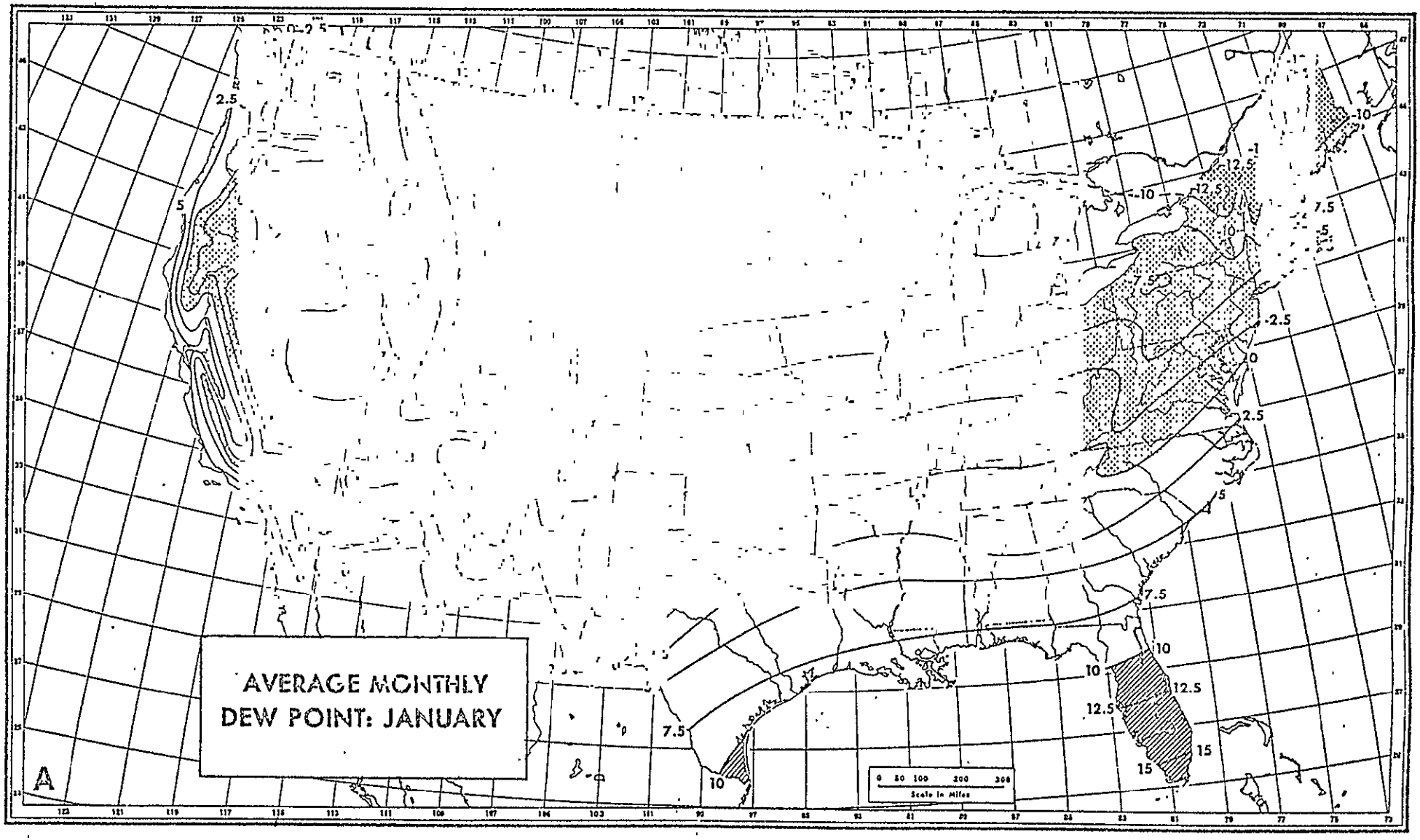

Figure VII-4: Mean January Dew Point

After Court (1974)

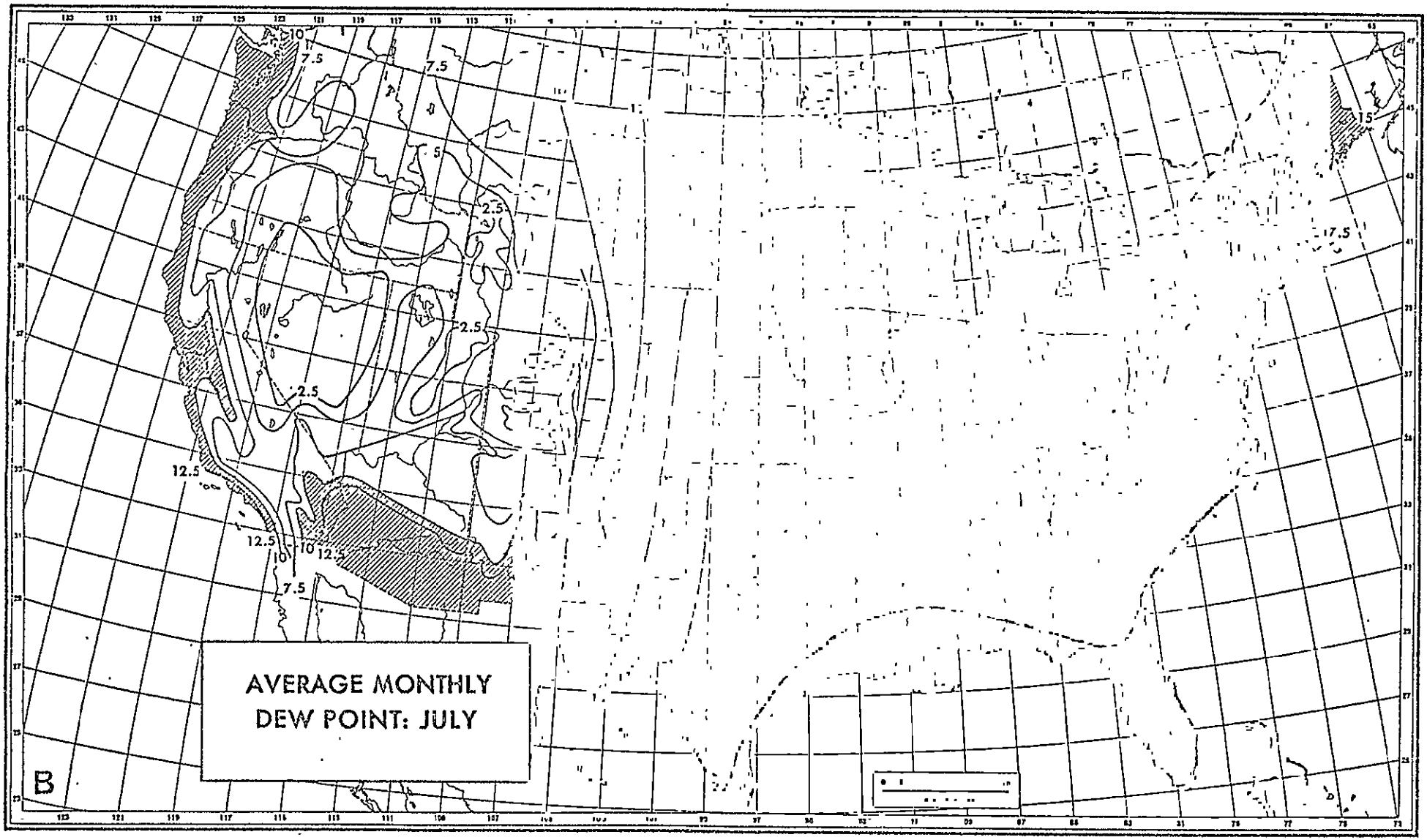

Fig.10. Mean monthly dew point (°C) in January (A) and July (B), based on observations every three hours at 200 stations during 10 years ending in 1959 or 1960. (Especially prepared by Dr. Arthur V. Dodd from data used for Dodd, 1965.)

Figure VII-5: Mean July Dew Point

After Court (1974)

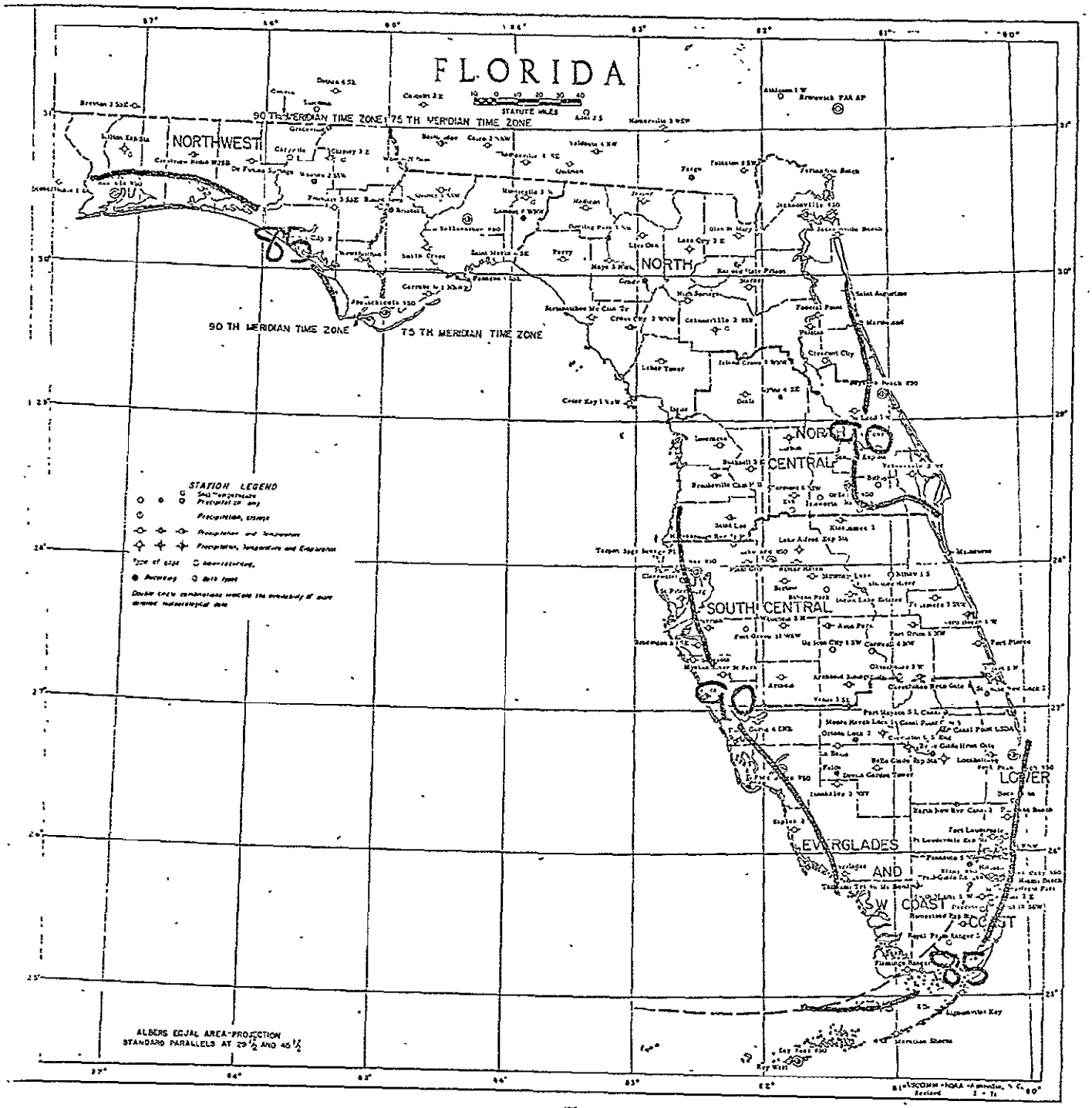

Figure VII-6: Surface Mean % Relative Humidity
January 1200 GMT

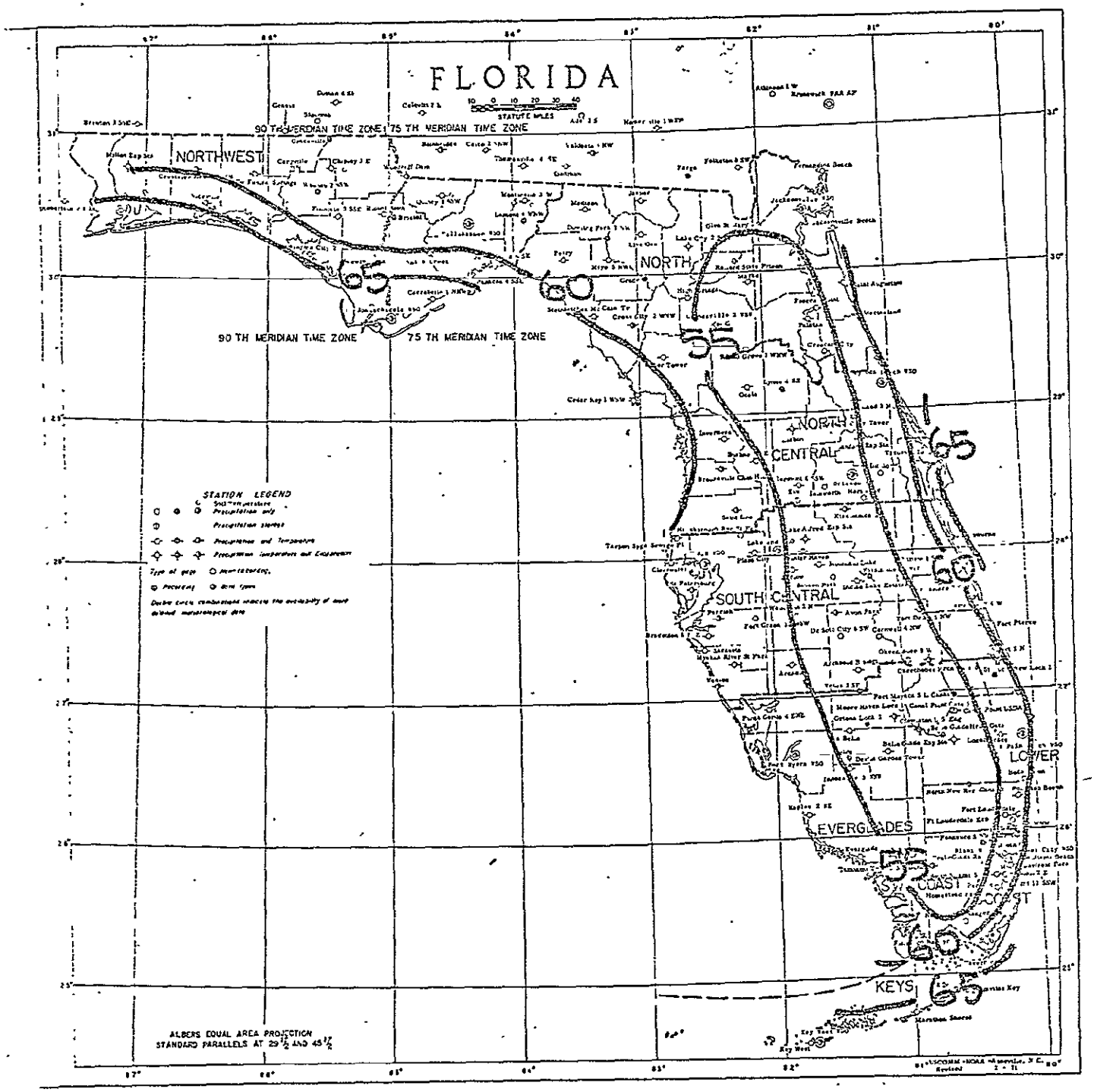

Figure VII-7: Surface Mean % Relative Humidity
January 1800 GMT

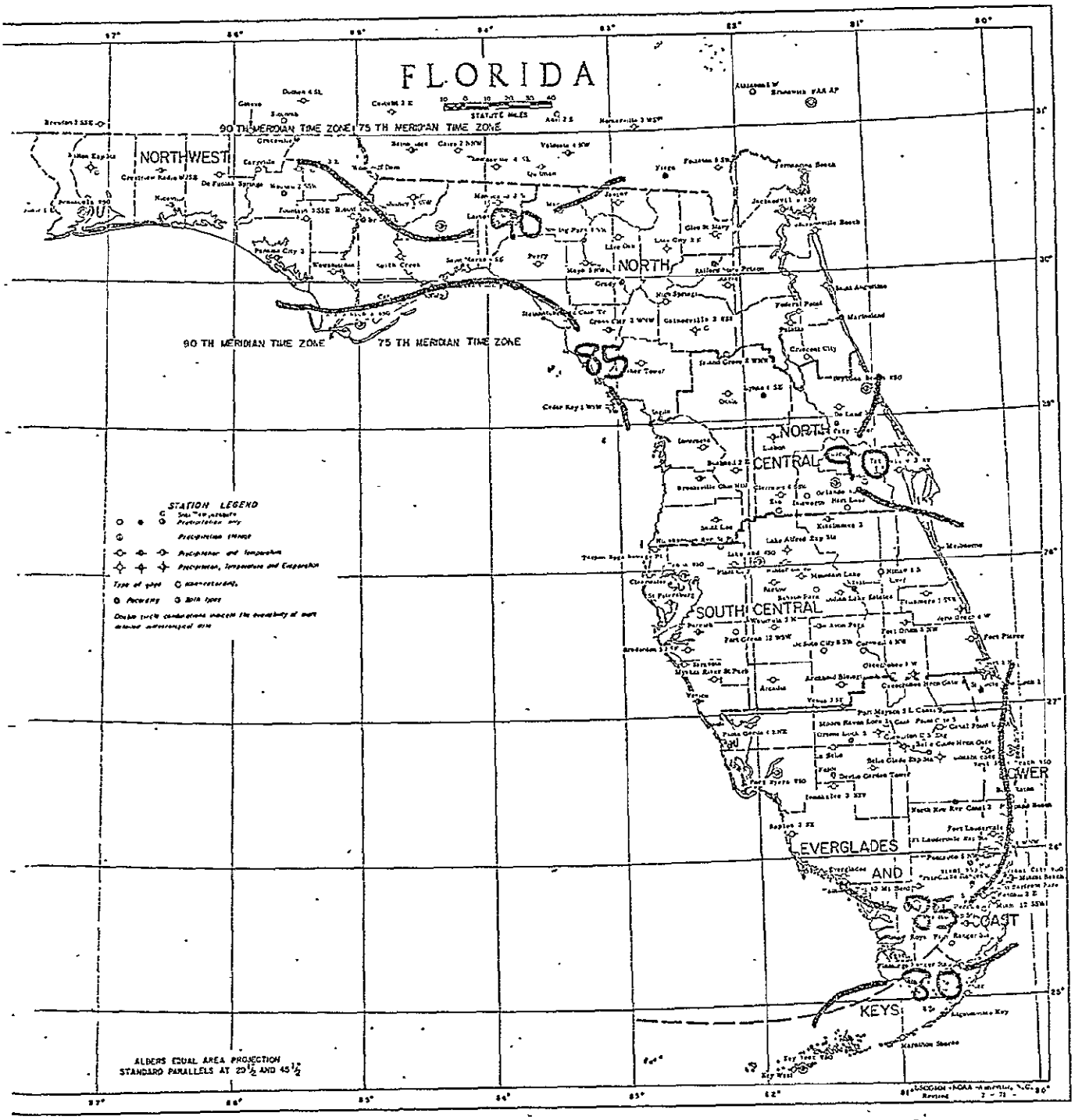

Figure VII-8: Surface Mean % Relative Humidity
July 1200 GMT

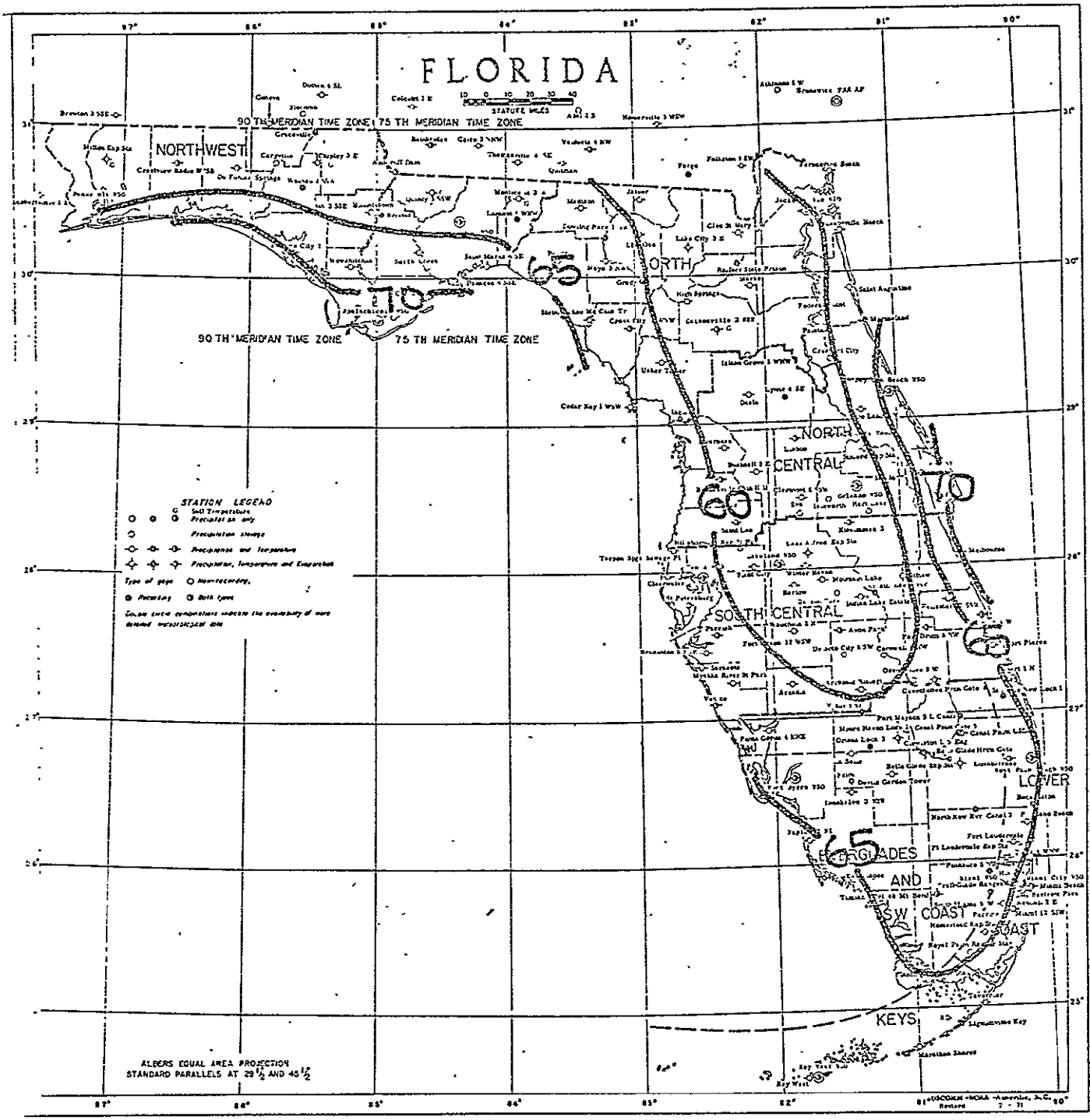

Figure VII-9: Surface Mean % Relative Humidity
July 1800 GMT

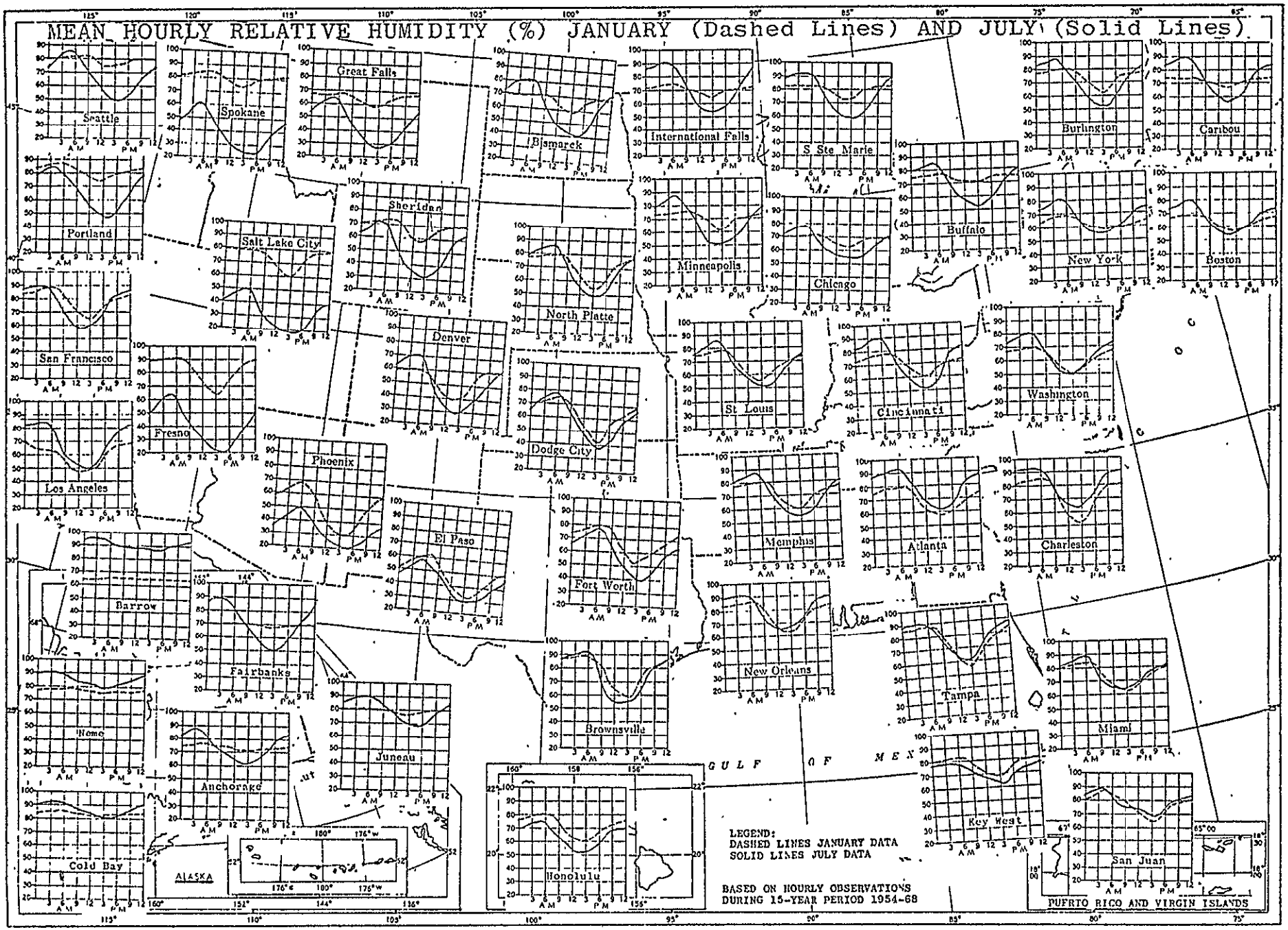

REPRODUCIBILITY OF THE ORIGINAL PAGE IS POOR

Figure VII-10: Mean Hourly % Relative Humidity: Jan. (dashed) July (solid) After Baldwin (1974)

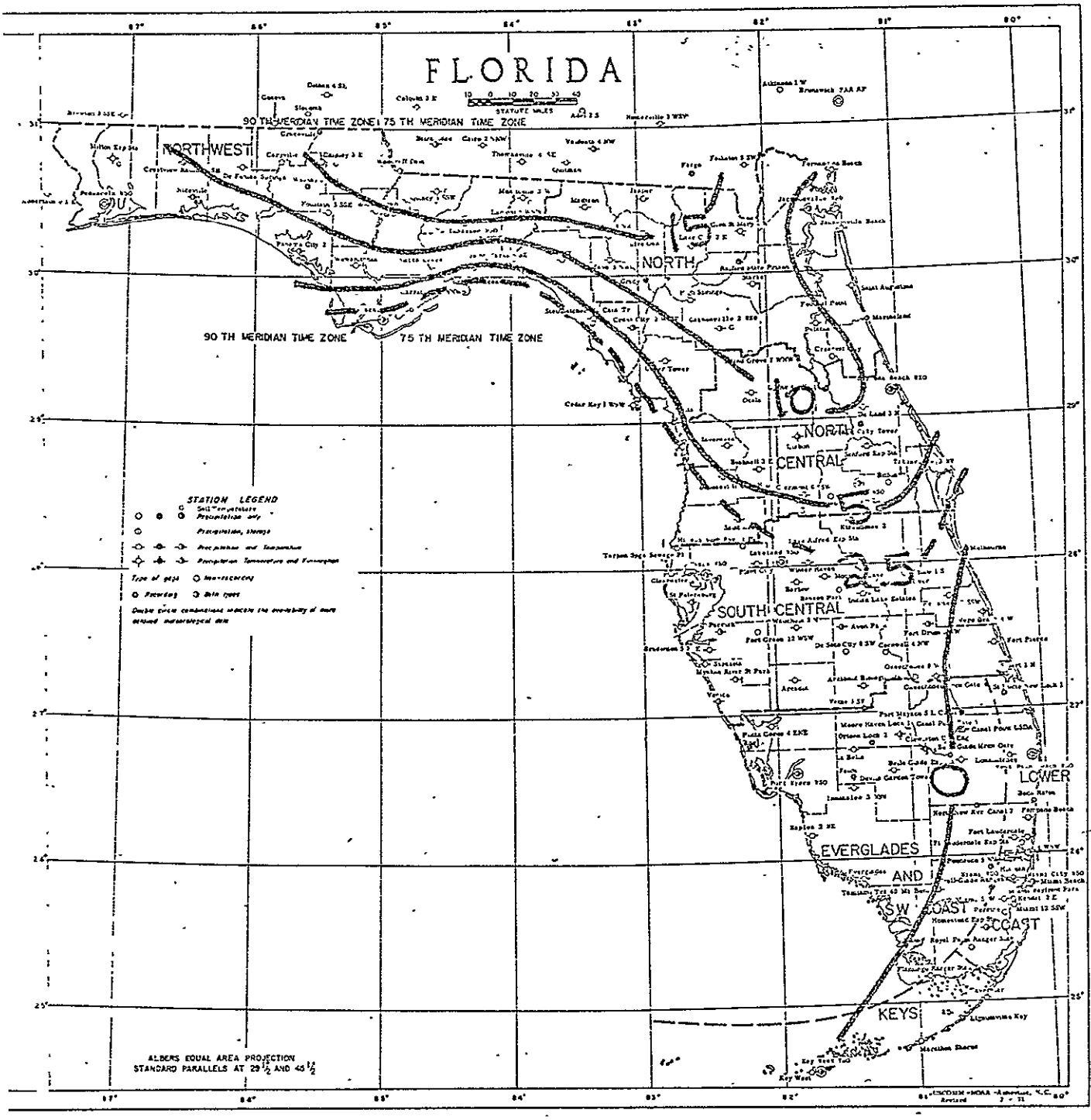

Figure VII-11: Days of Heavy Fog: Visibility $\leq$ 0.4 km
May-October

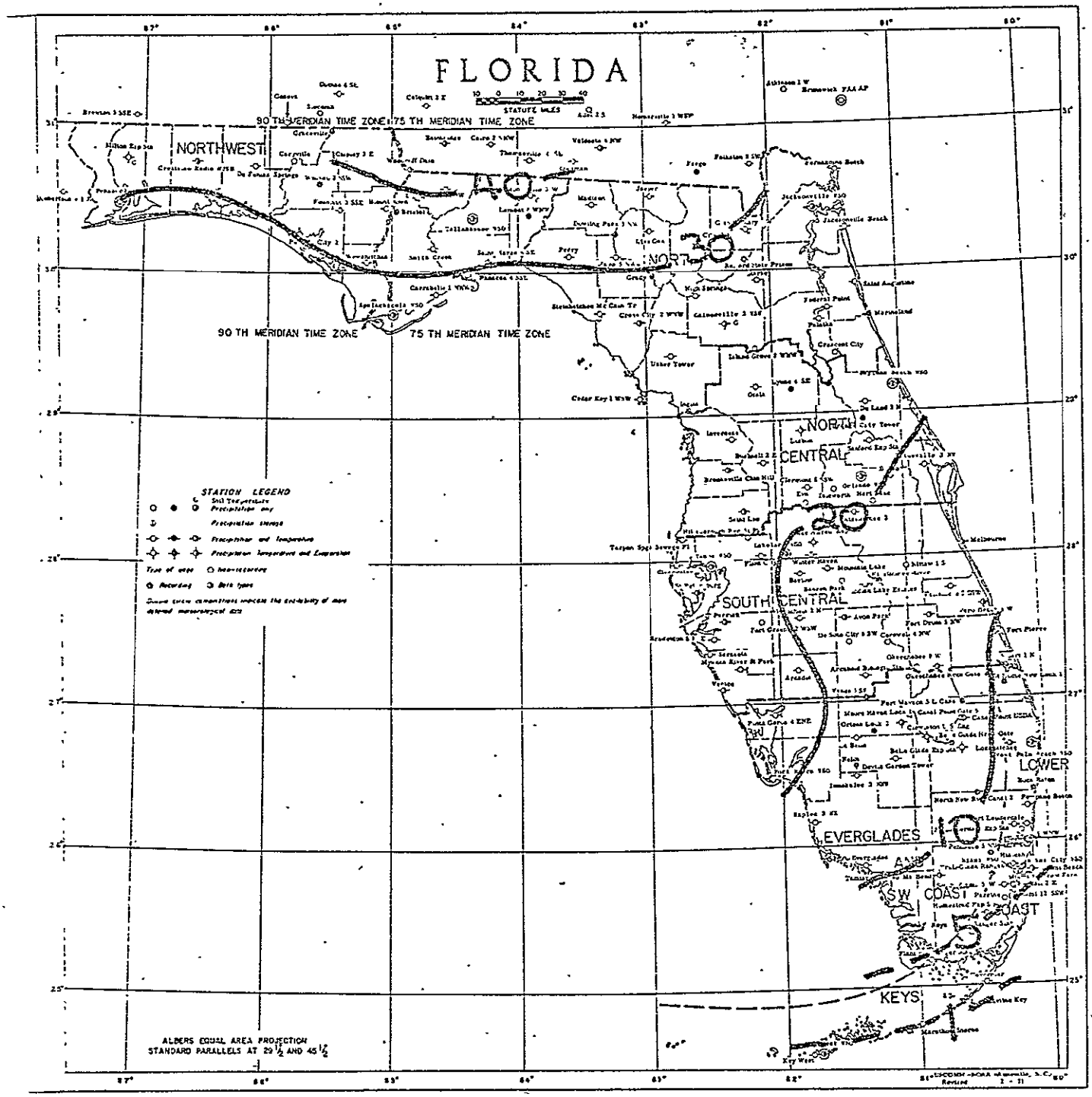

Figure VII-12: Days of Heavy Fog: Visibility ≤ 0.4 km
November-April

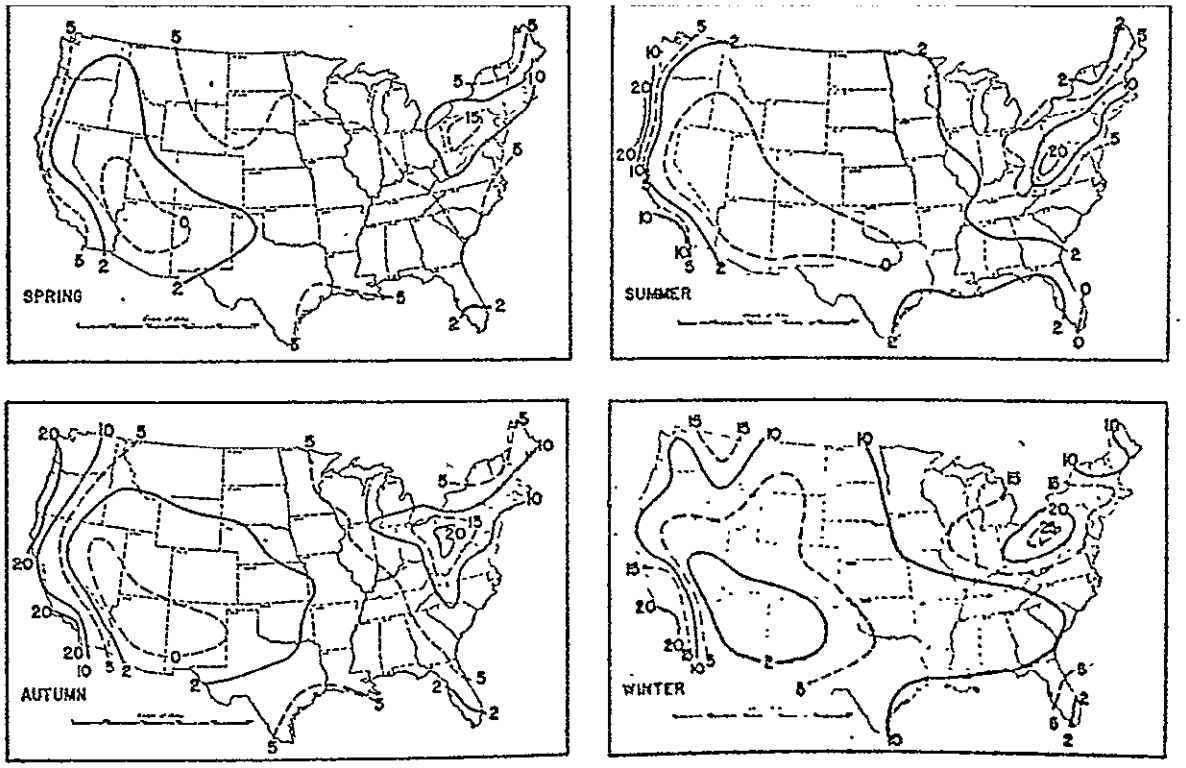

FIG. 2. Percentage of time by seasons the visibility is less than 2.5 km.

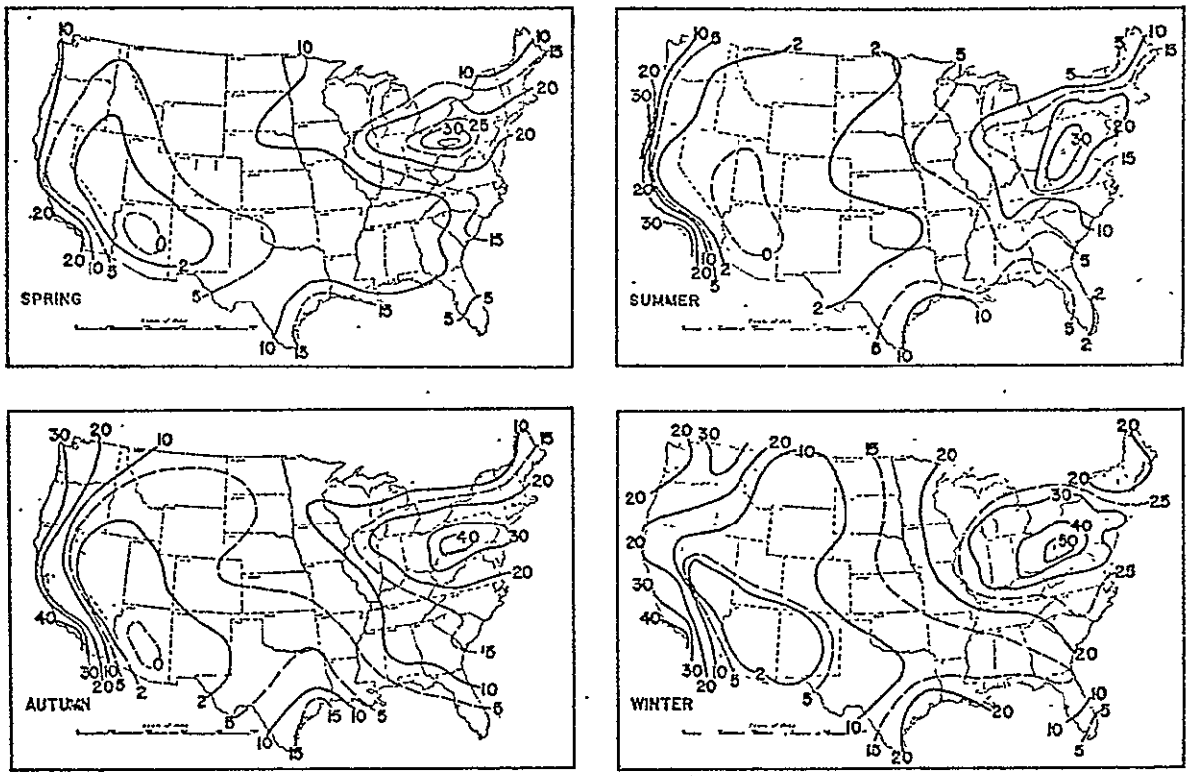

FIG. 3. Percentage of time by seasons the visibility is less than 5.0 km.

Figure VII-13: Surface Visibility

After Eldridge (1966)

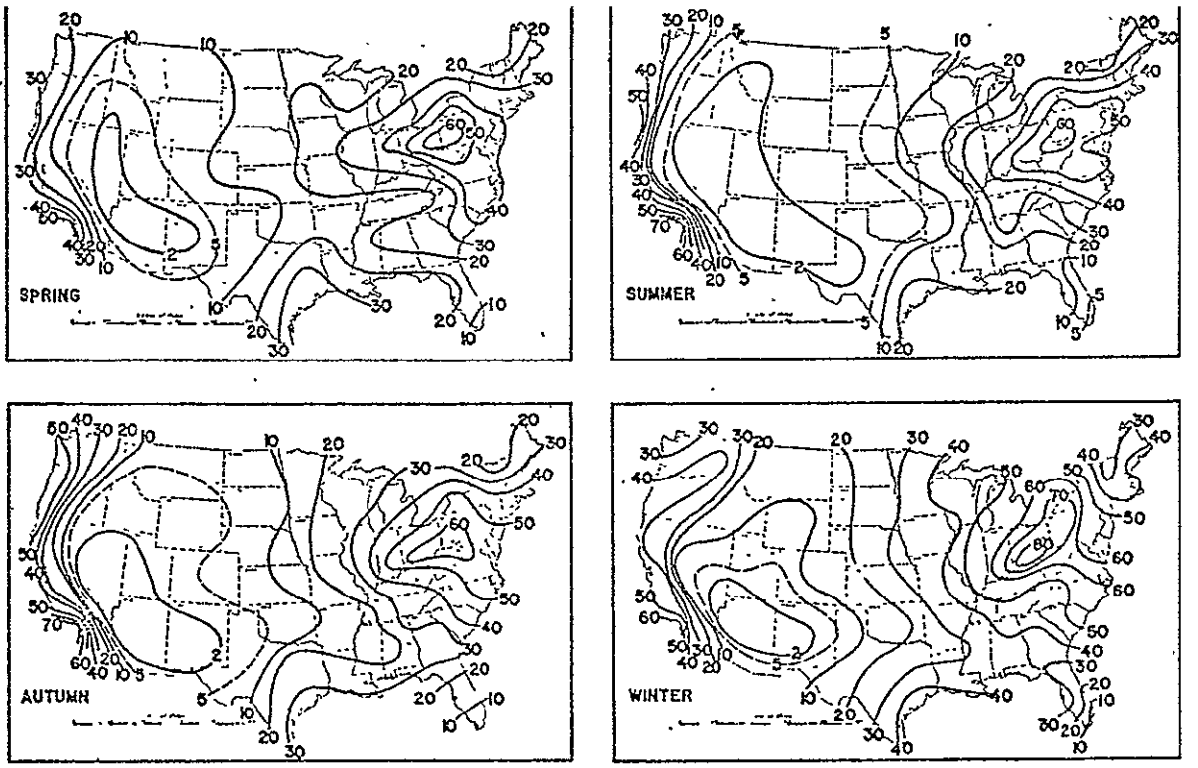

FIG. 4. Percentage of time by seasons the visibility is less than 10 km.

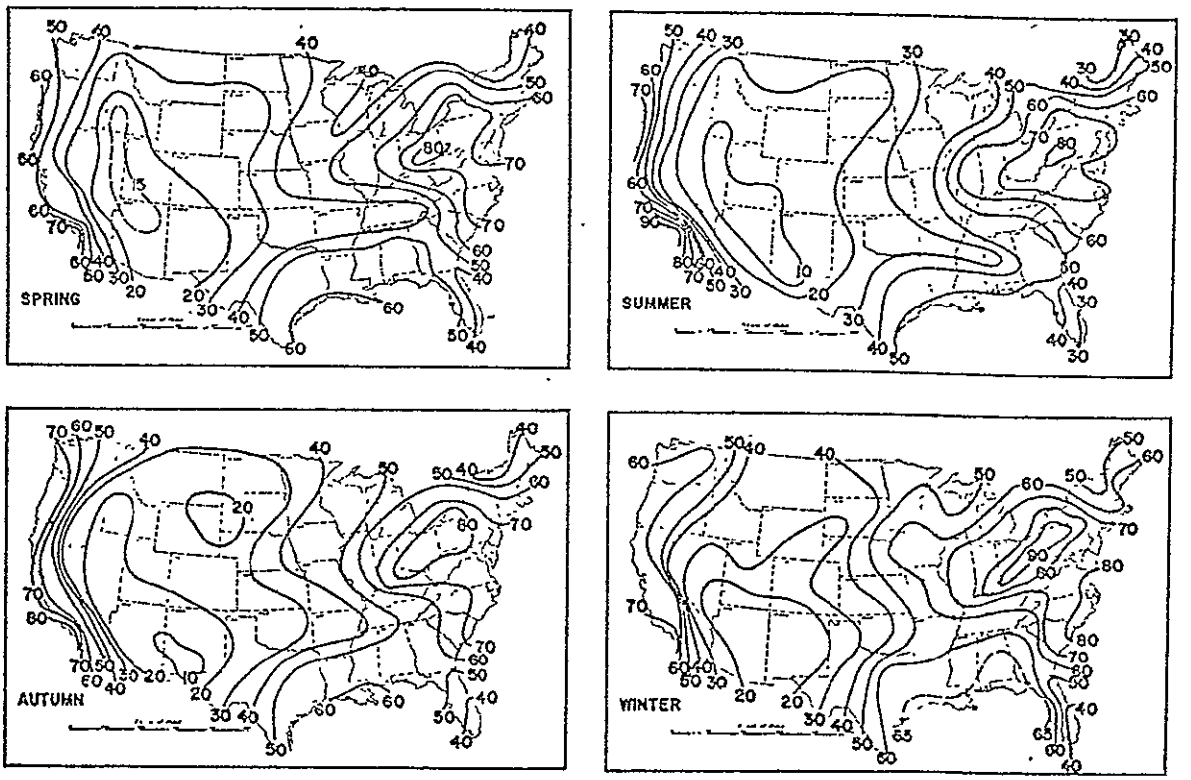

FIG. 5. Percentage of time by seasons the visibility is less than 20 km.

Figure VII-14: Surface Visibility

After Eldridge (1966)

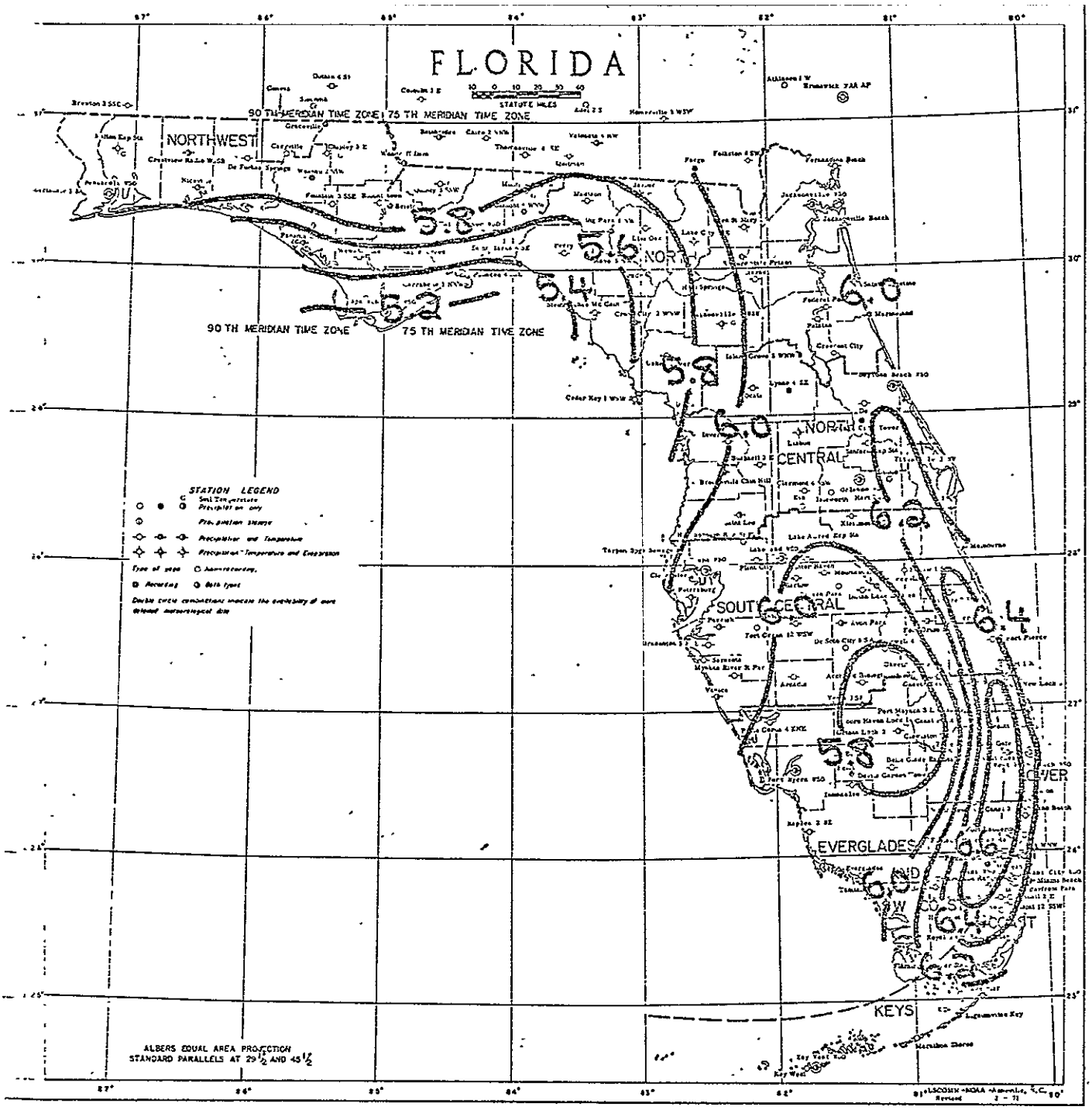

Figure VII-15: Mean Cloud Cover (Tenths) Sunrise-Sunset May-October

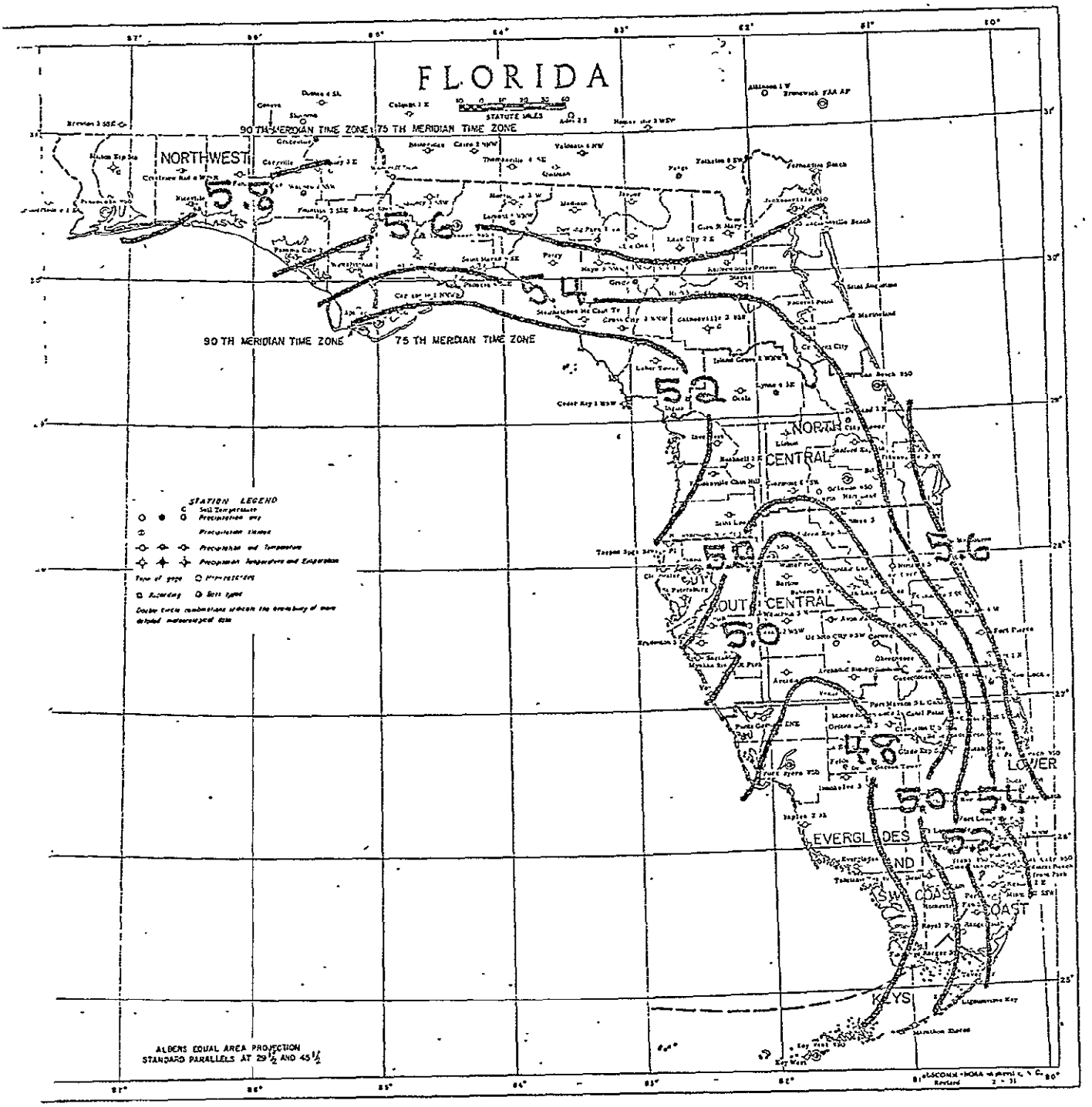

Figure VII-16: Mean Cloud Cover (Tenths) Sunrise-Sunset
November-April

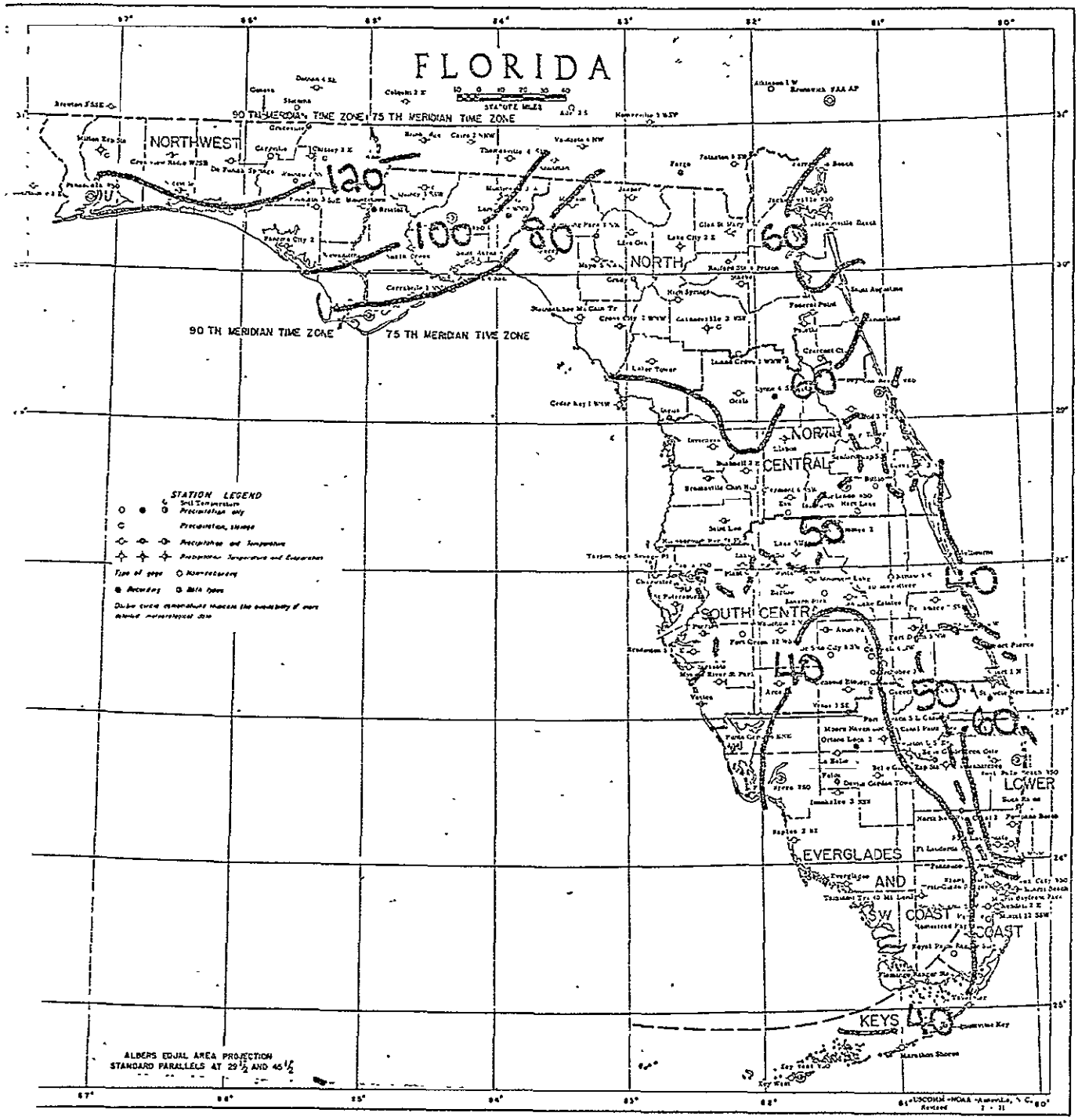

Figure VII-17: Mean Monthly Precipitation (mm)
December

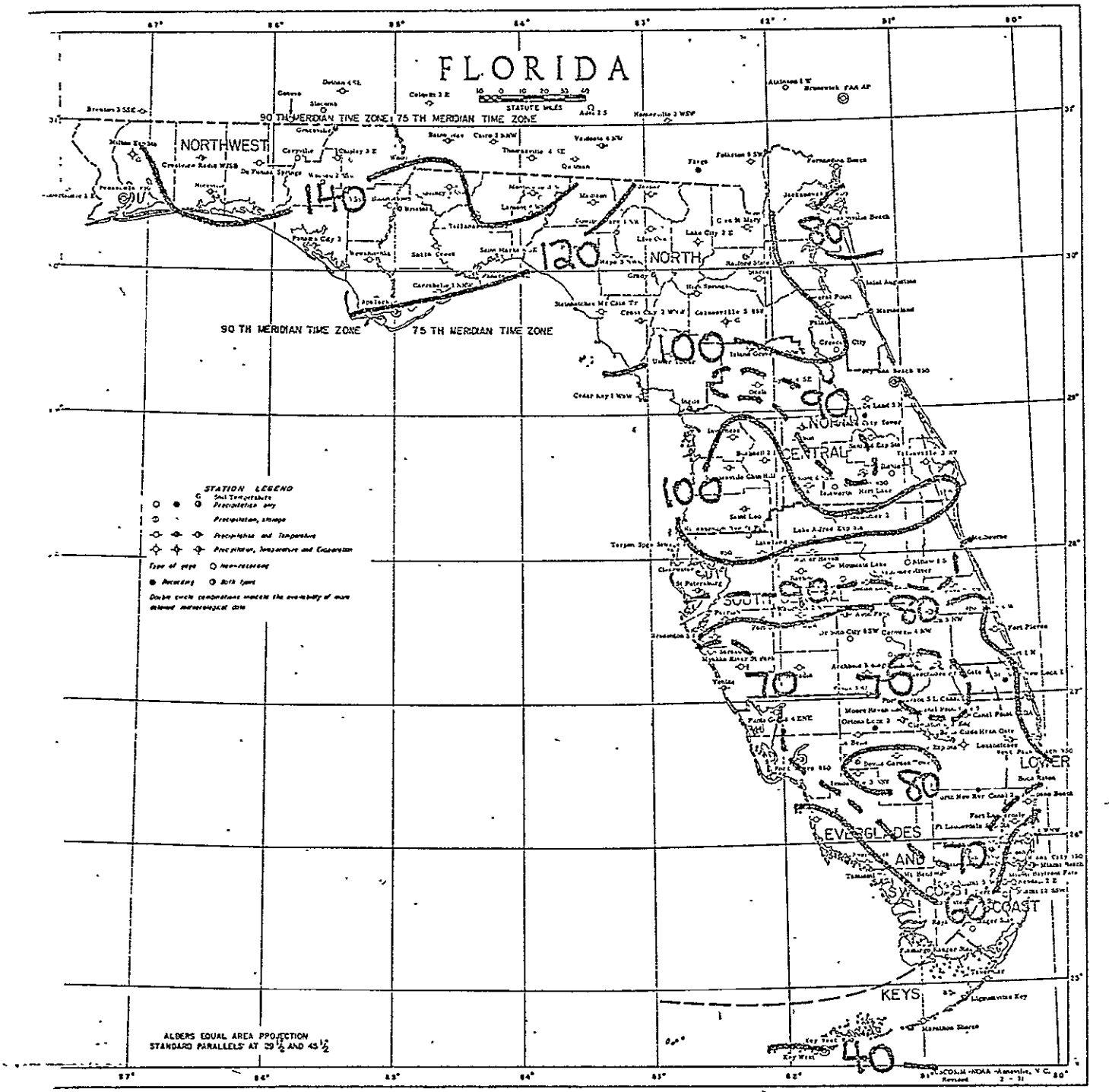

Figure VII-18: Mean Monthly Precipitation (mm)
March

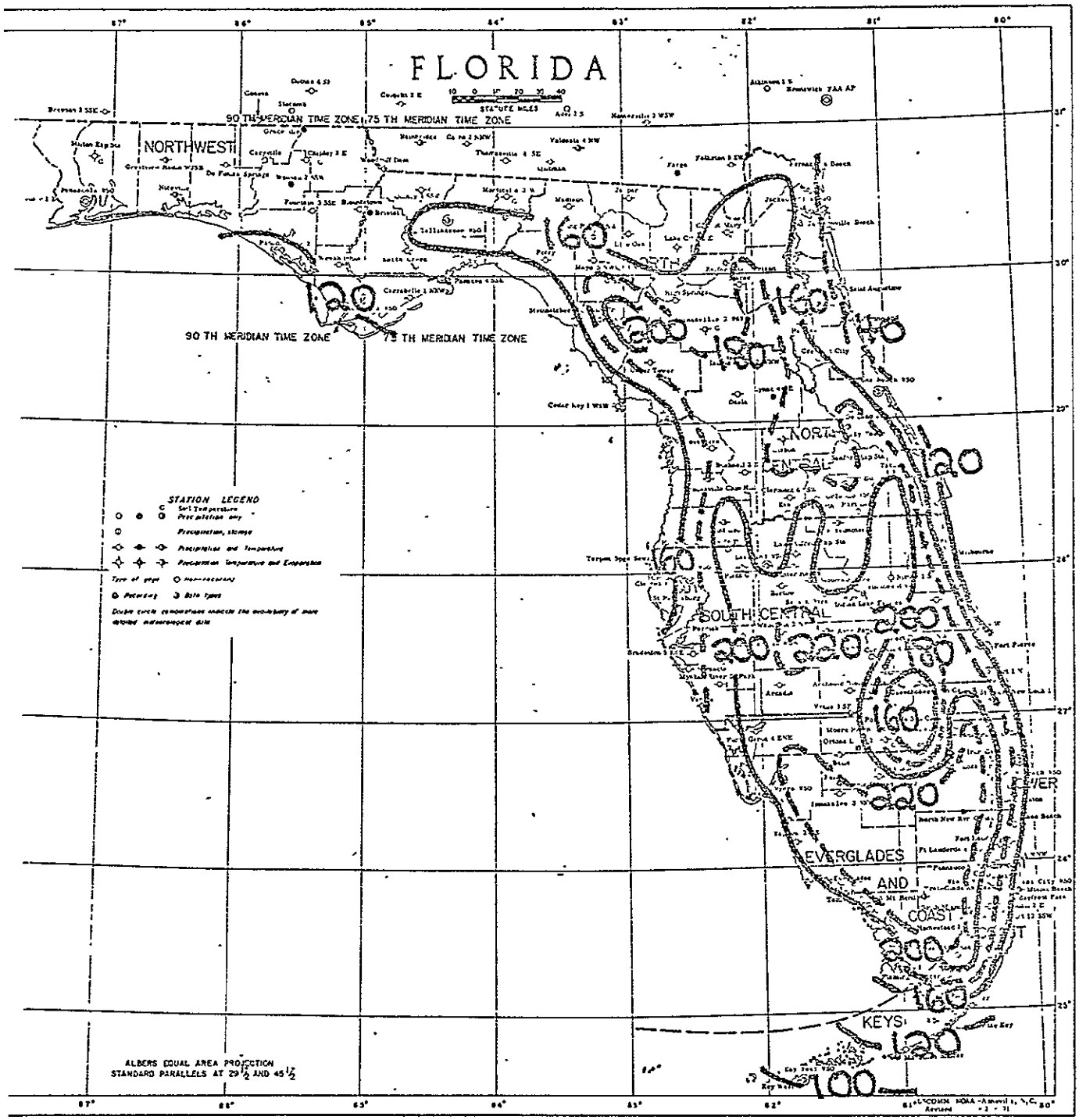

Figure VII-19: Mean Monthly Precipitation (mm)
June

Figure VII-20: Mean Monthly Precipitation (mm)
September

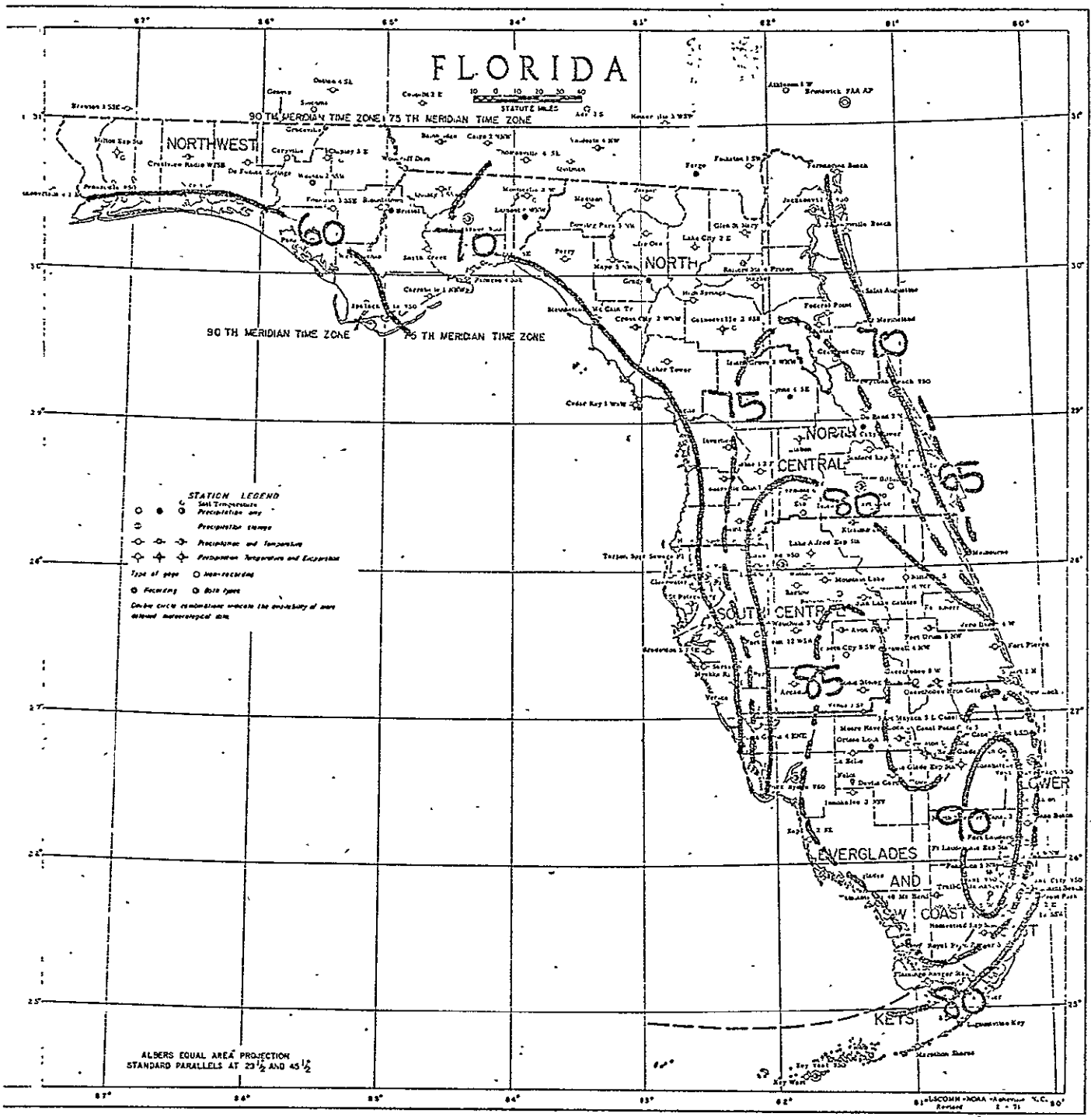

Figure VII-21: Mean Number of Days Precipitation ≥ 0.25 mm
May-October

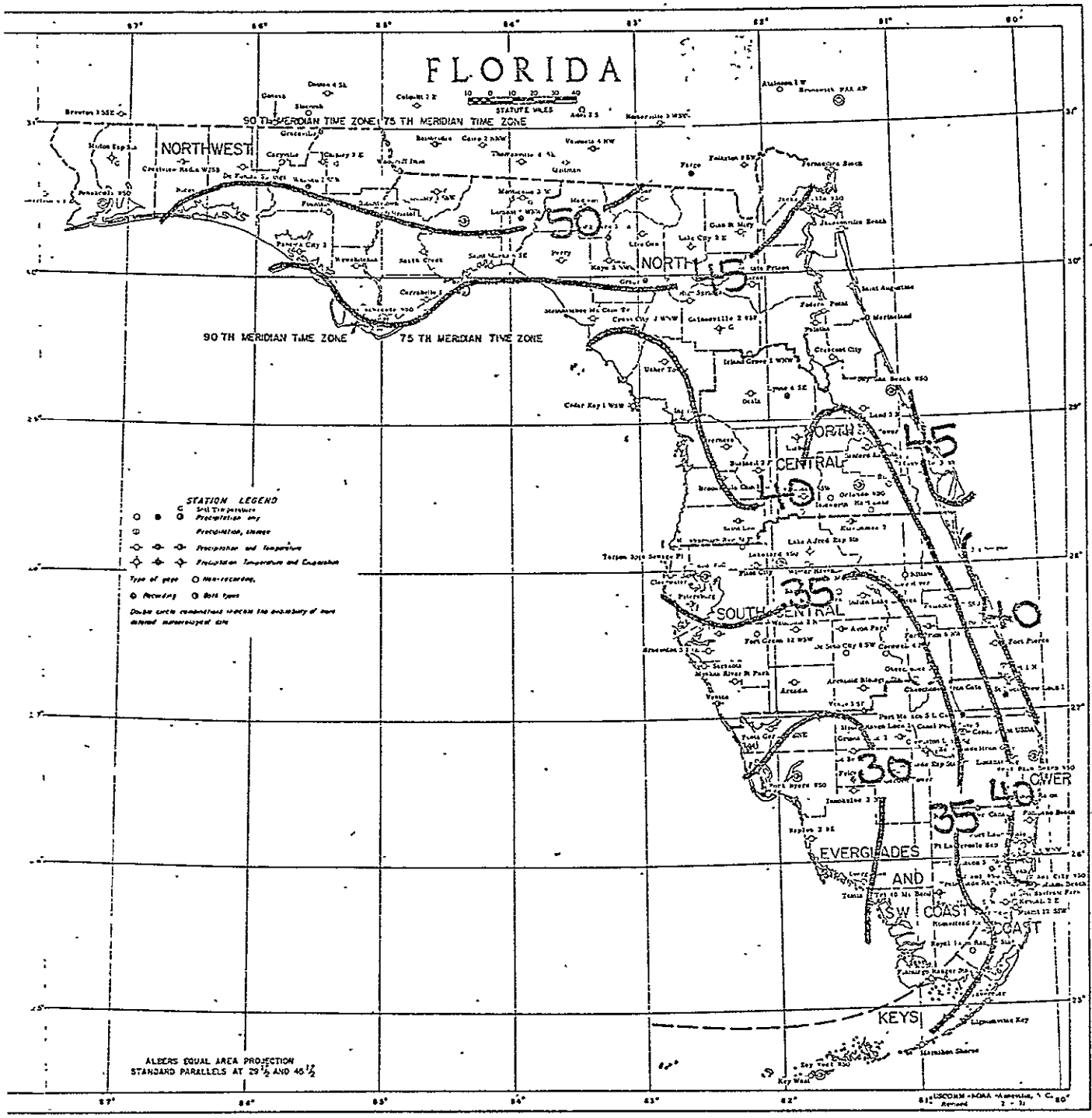

Figure VII-22: Mean Number of Days Precipitation ≥ 0.25 mm
November-April

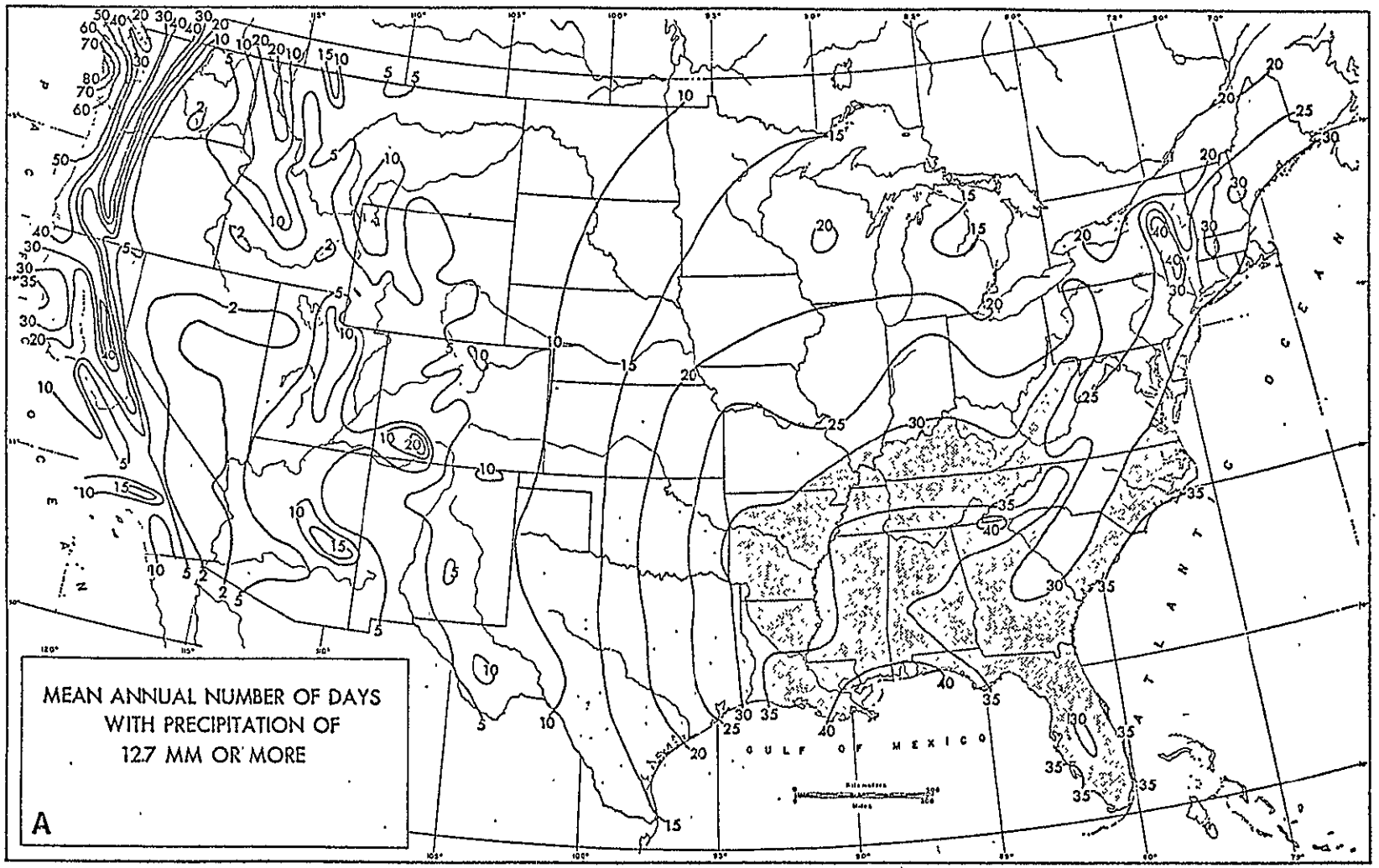

Figure VII-23: Mean Annual Number of Days with Precipitation of 12.7 mm or more

After Court (1974)

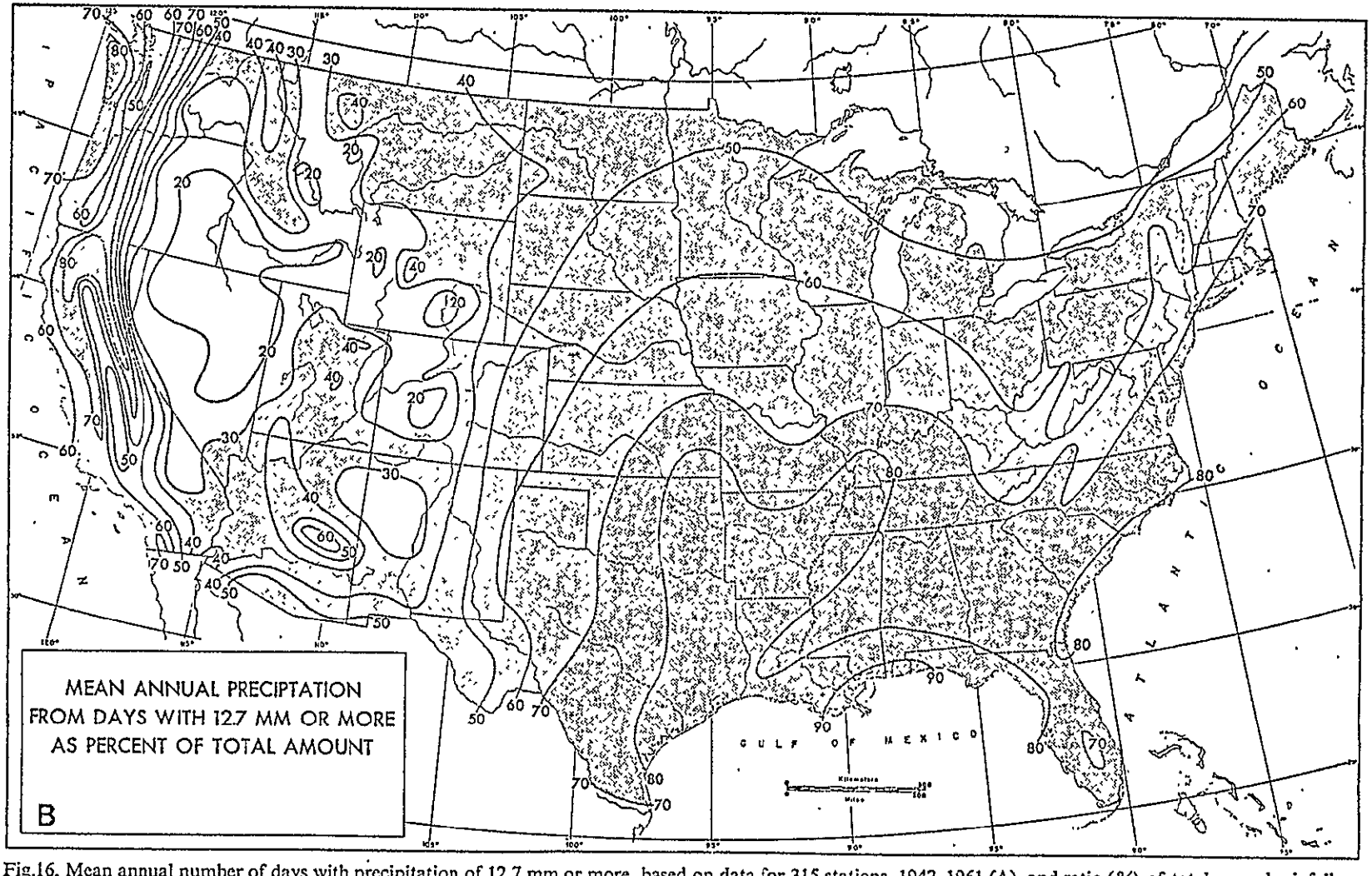

Fig.16. Mean annual number of days with precipitation of 12.7 mm or more, based on data for 315 stations, 1942–1961 (A), and ratio (%) of total annual rainfall on such days to total from all days (B) based on data for 315 stations, 1942–1961. (From PAULHUS and MILLER, 1964.)

Figure VII-24: Mean Annual Precipitation from Days with 12.7 mm or more as percent of Total Amount

After Court (1974)

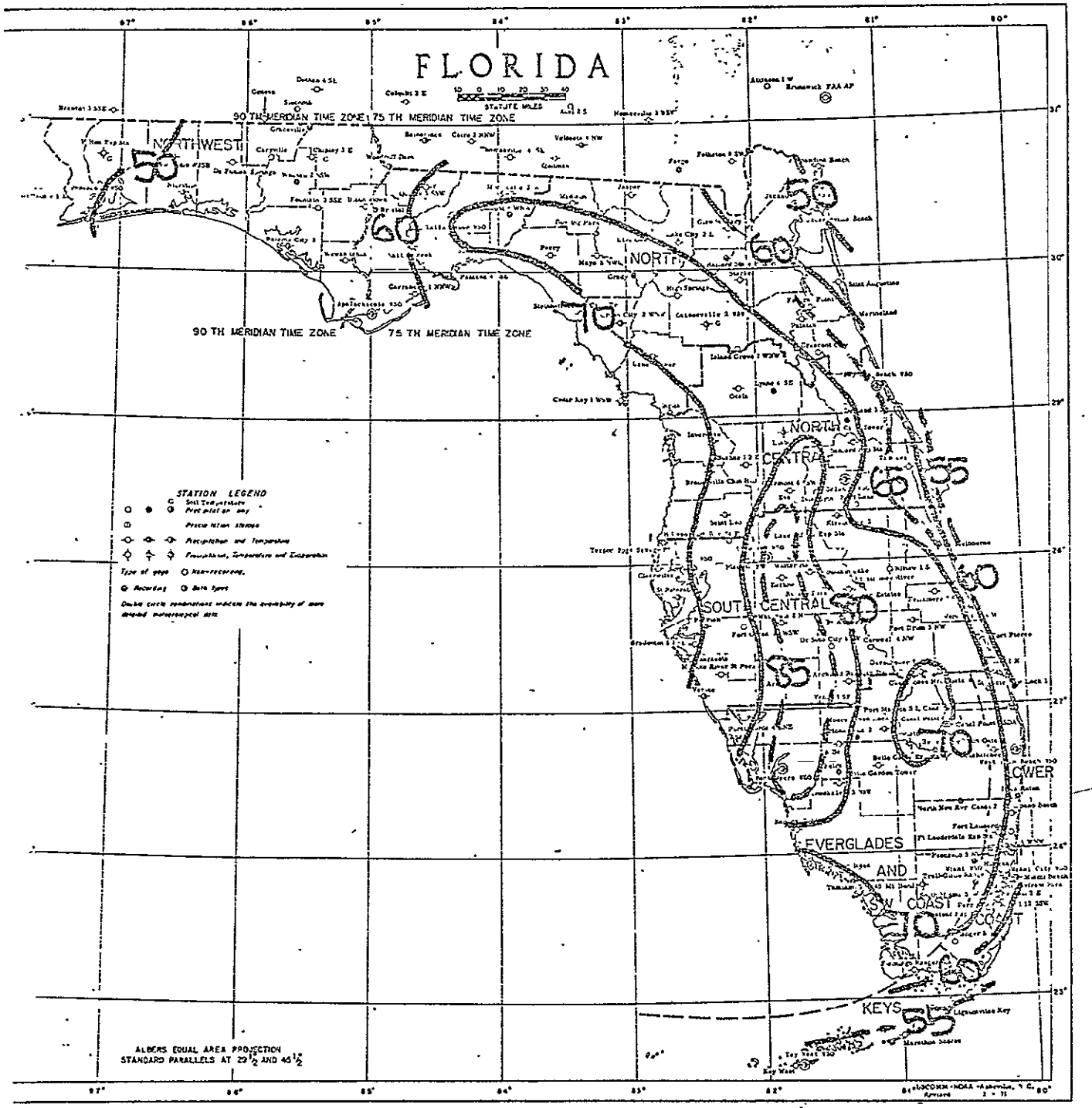

Figure VII-25: Number of Thunderstorm Days
May-October

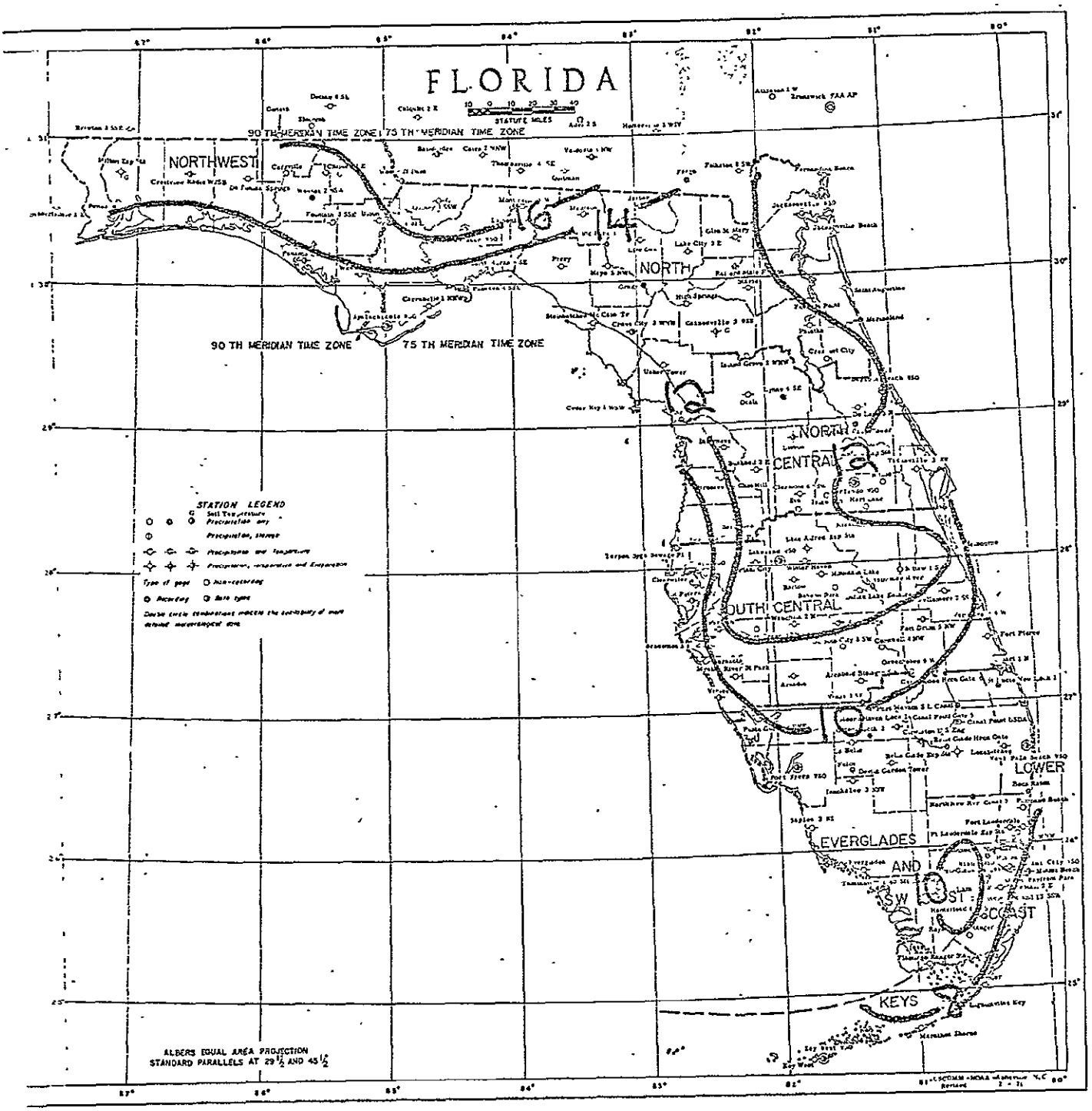

Figure VII-26: Number of Thunderstorm Days
November-April

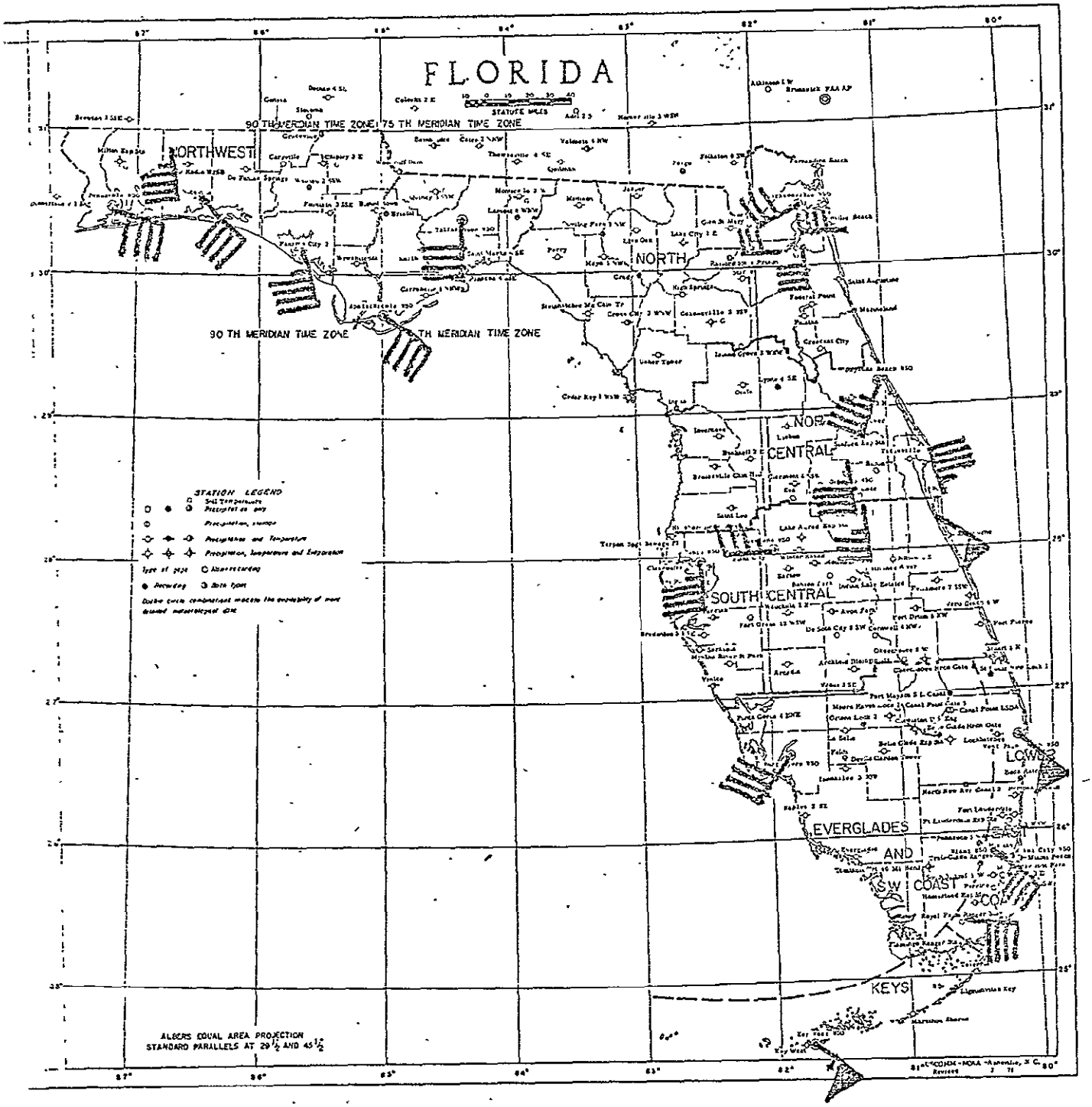

Figure VII-27: Prevailing Surface Wind Direction and Speed (ms^{-1})
March

Pennant = 5 ms^{-1}
Full Barb = 1 ms^{-1}
Half Barb = 0.5 ms^{-1}

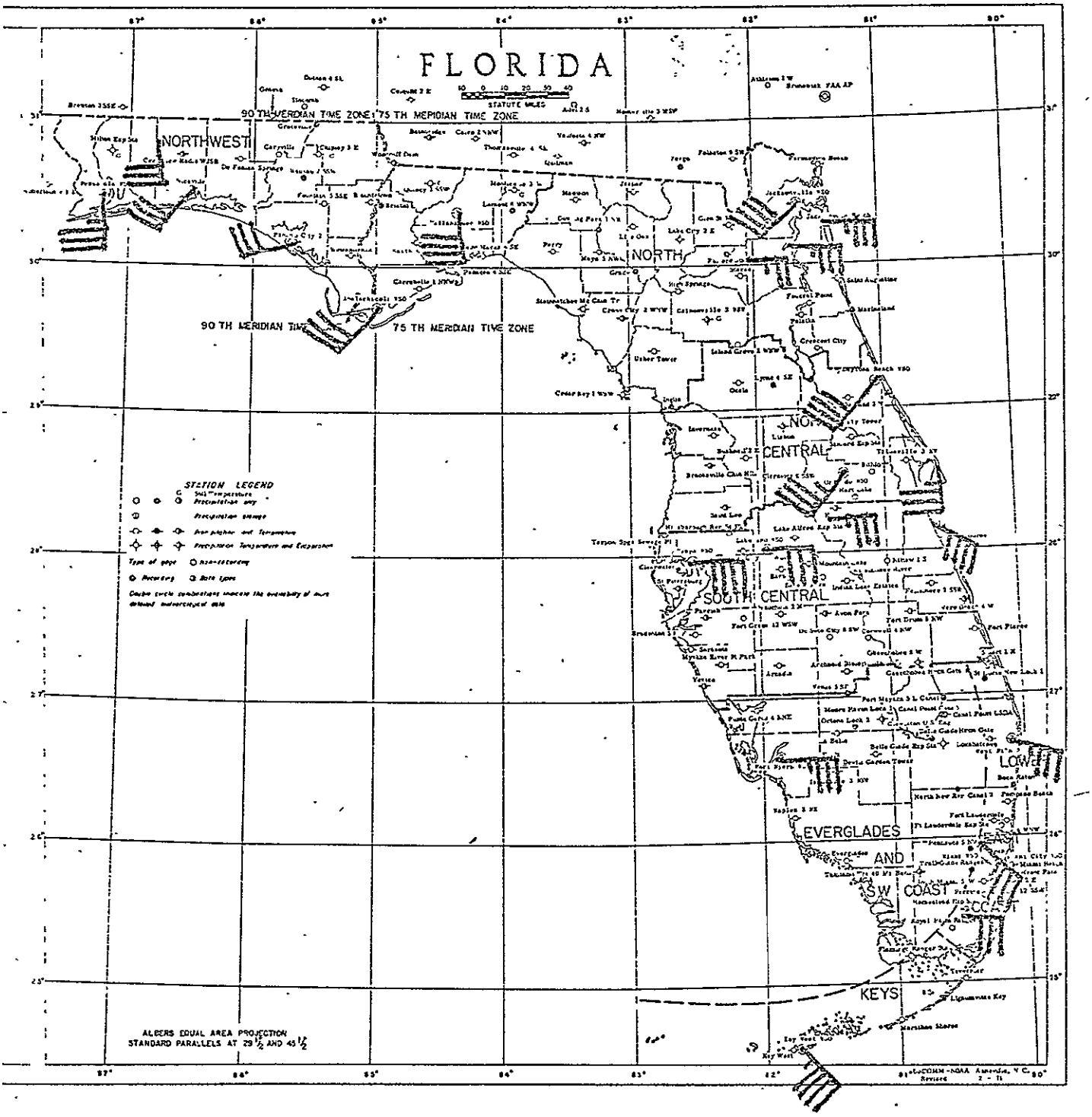

Figure VII-28: Prevailing Surface Wind Direction and Speed (ms^{-1})
June

Pennant = 5 ms^{-1}
Full Barb = 1 ms^{-1}
Half Barb = 0.5 ms^{-1}

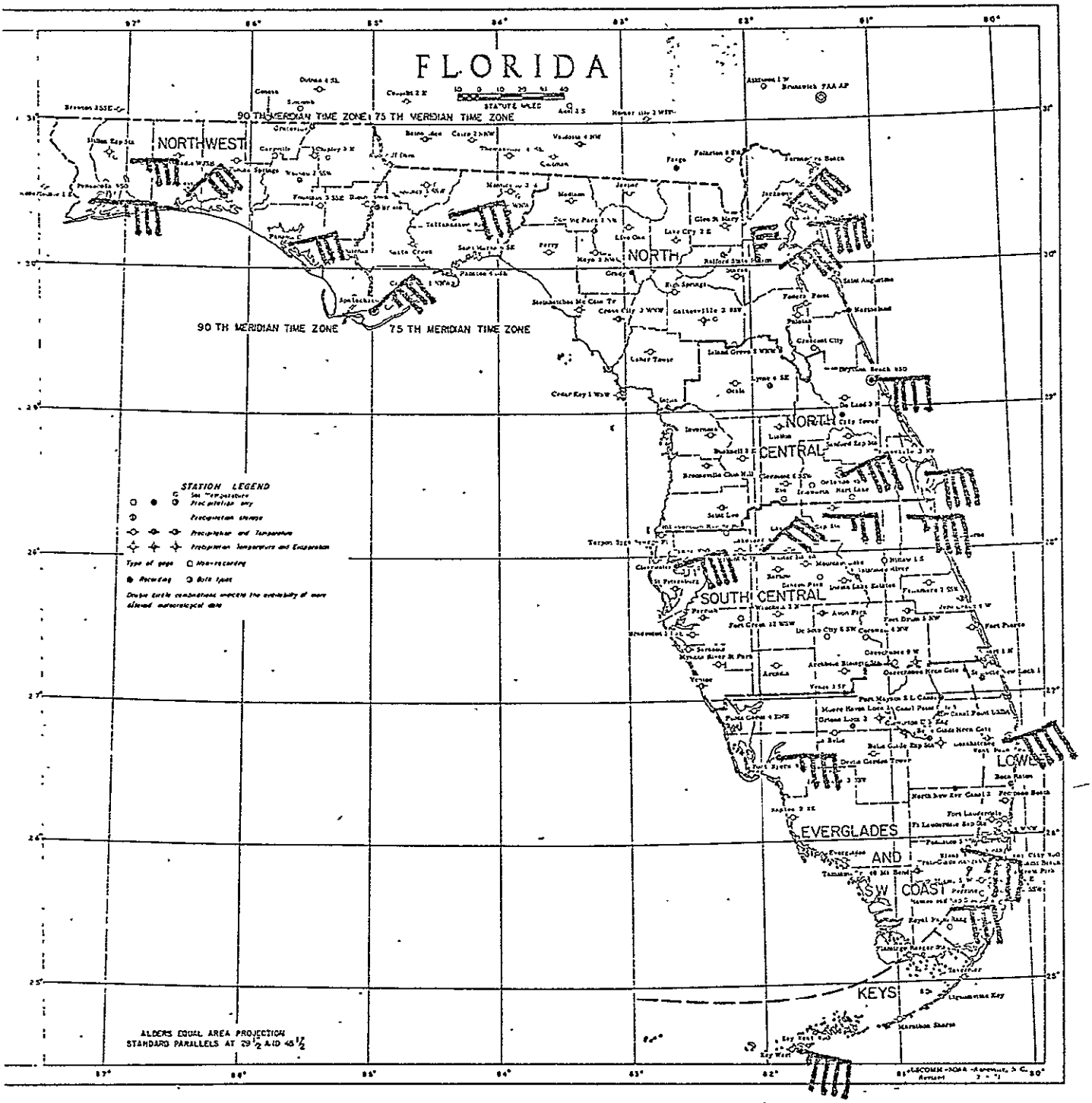

Figure VII-29: Prevailing Surface Wind Direction and Speed (ms^{-1}) September

Pennant = 5 ms^{-1}
Full Barb = 1 ms^{-1}
Half Barb = 0.5 ms^{-1}

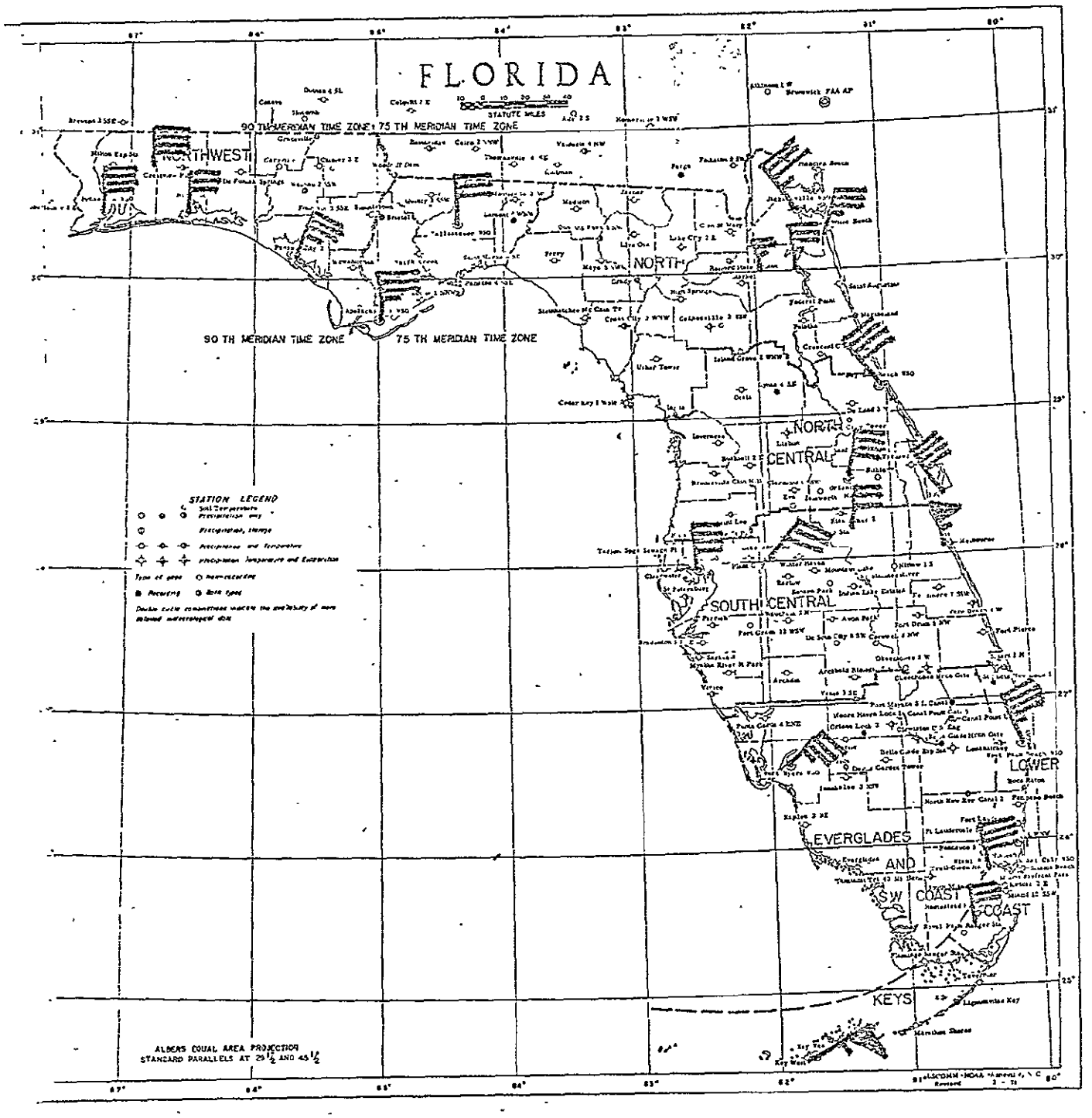

Figure VII-30: Prevailing Surface Wind Direction and Speed (ms^{-1})
December

Pennant = 5 ms^{-1}
Full Barb = 1 ms^{-1}
Half Barb = 0.5 ms^{-1}

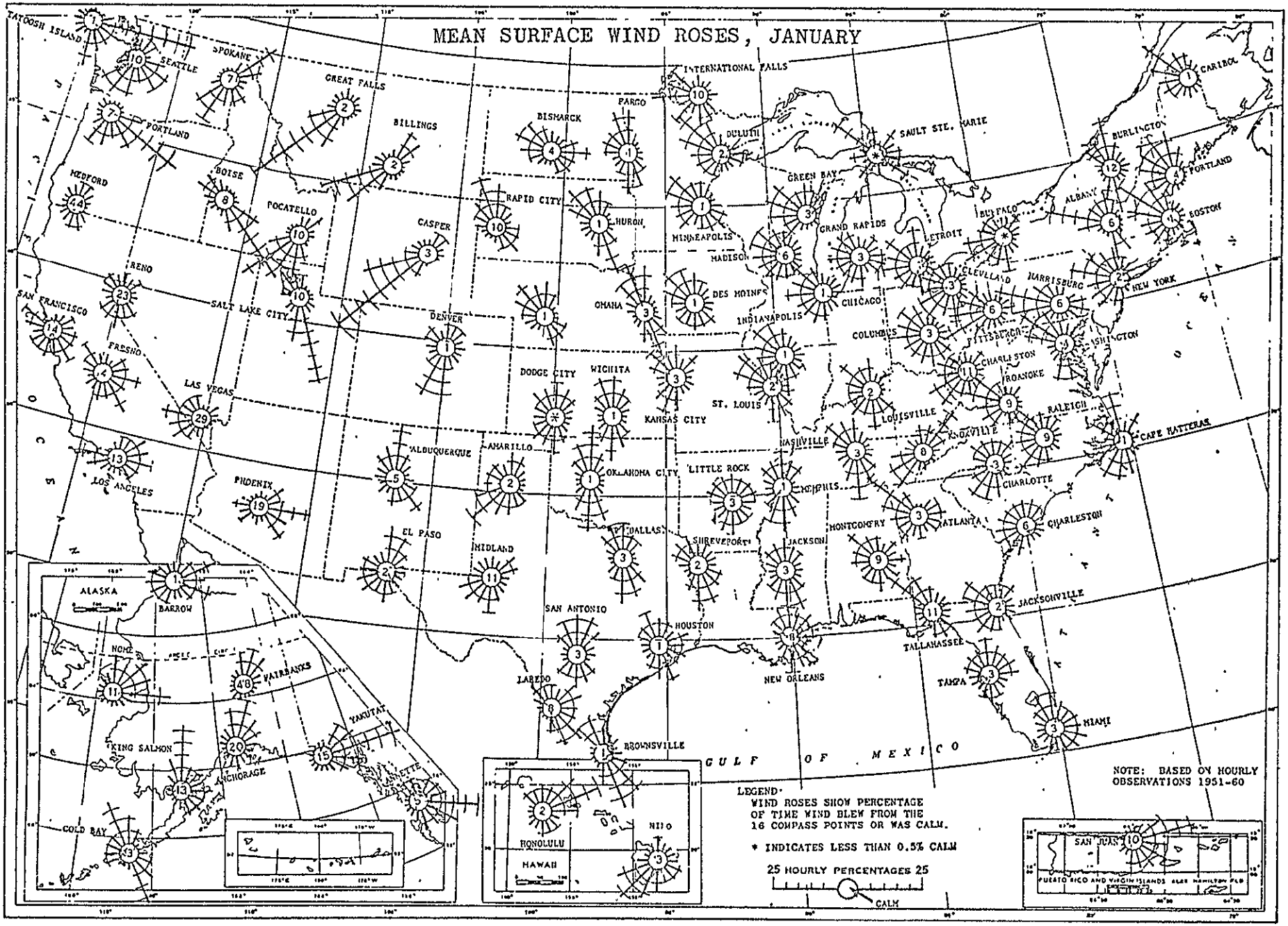

Figure VII-31: Mean Surface Wind Roses: January

After Baldwin (1974)

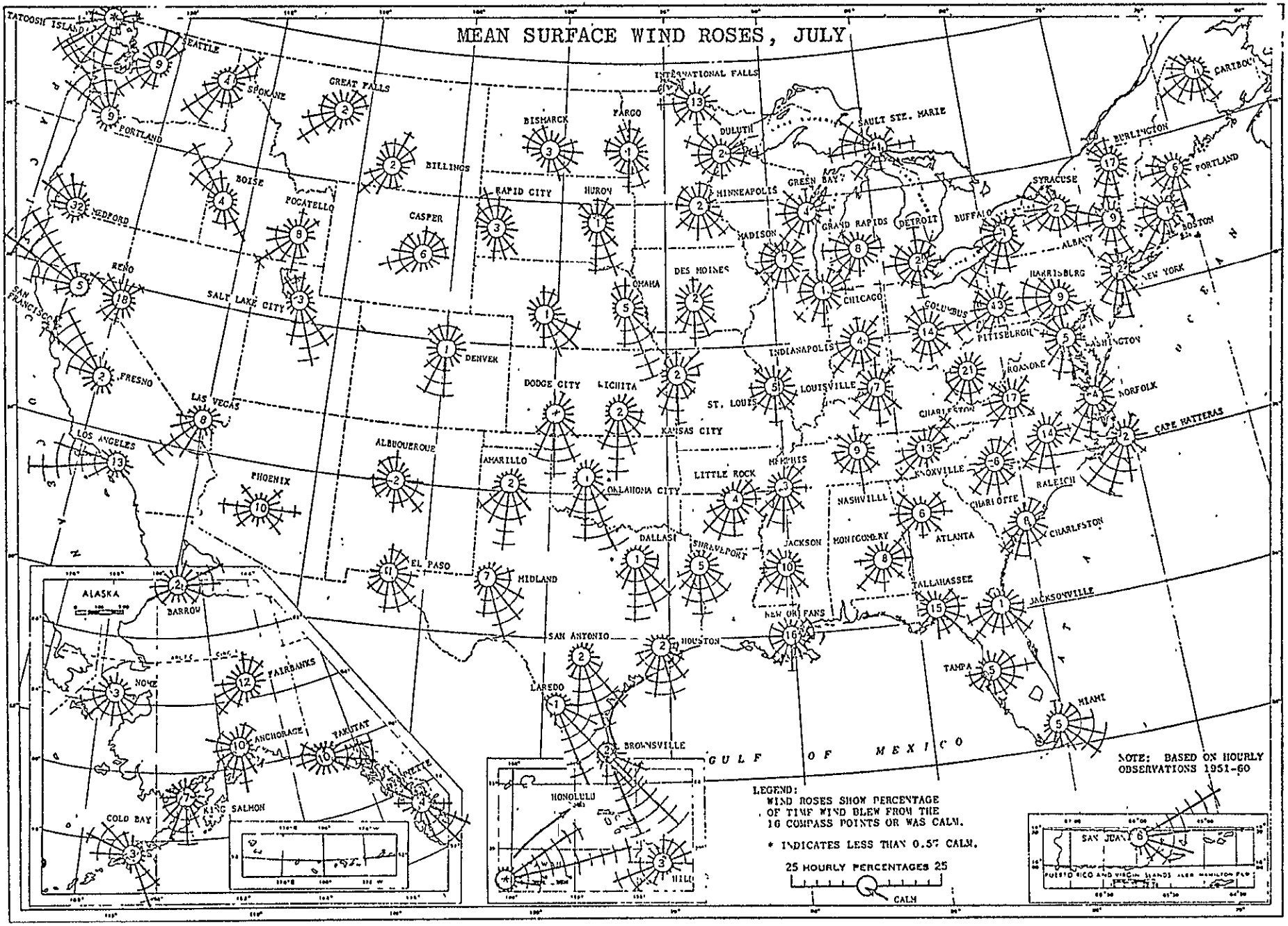

Figure VII-32: Mean Surface Wind Roses: July

After Baldwin (1974)

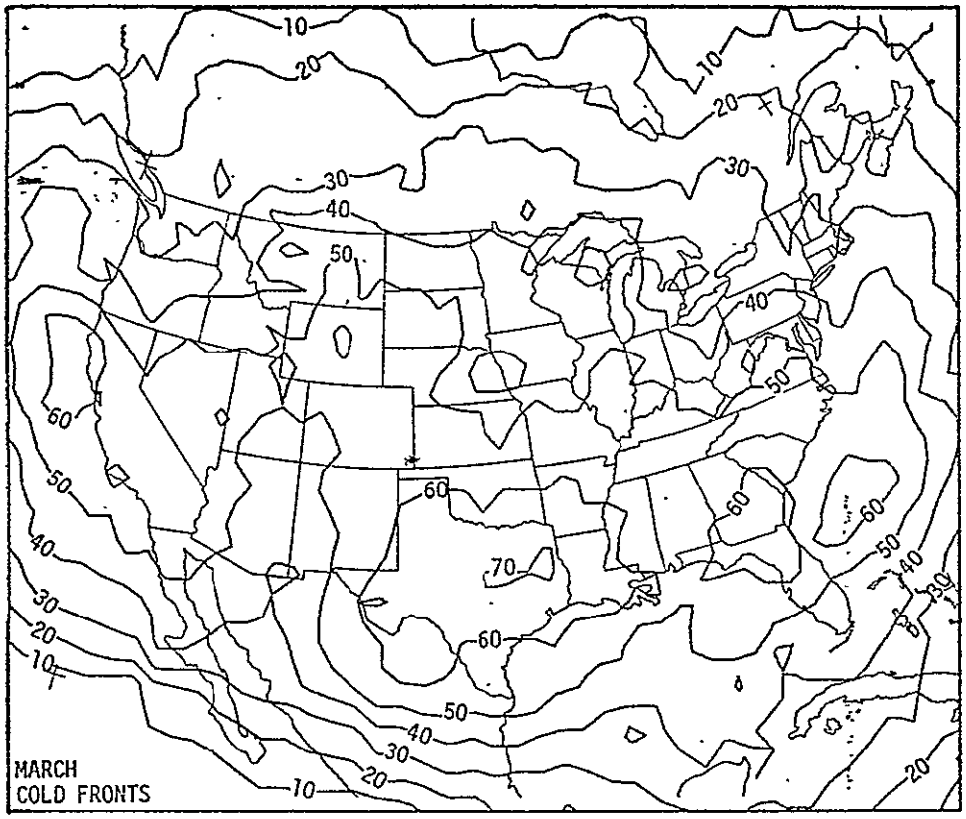

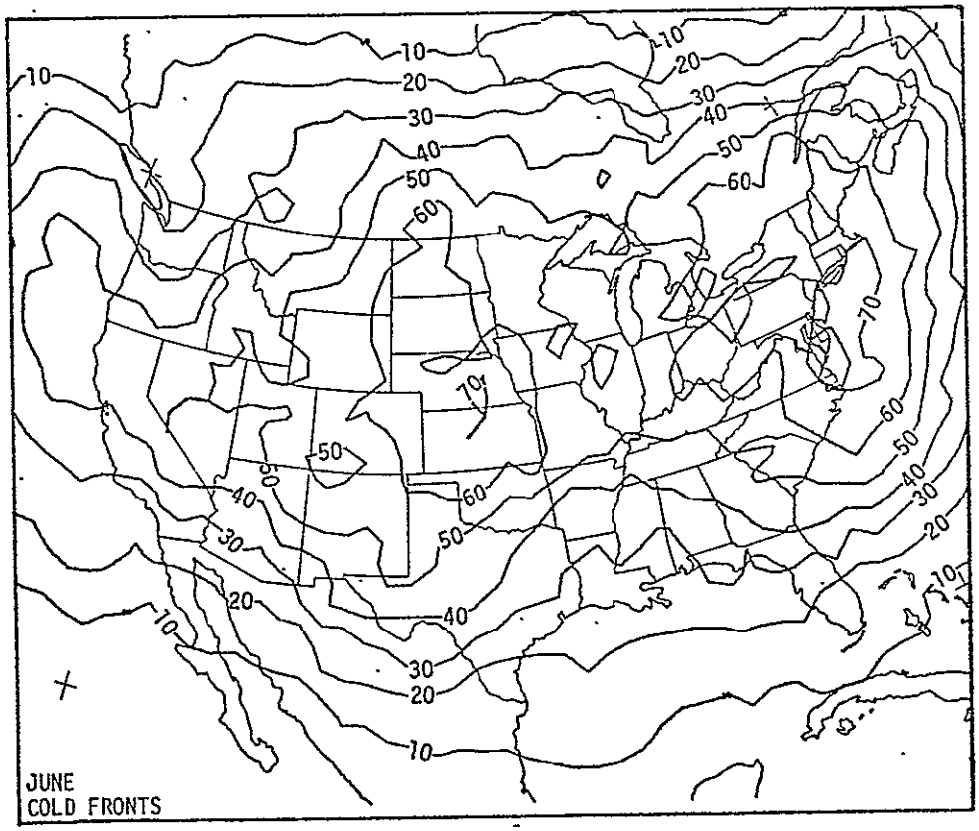

Figure VII-33: Cold Front Climatology
March, June

After Morgan et al. (1975)

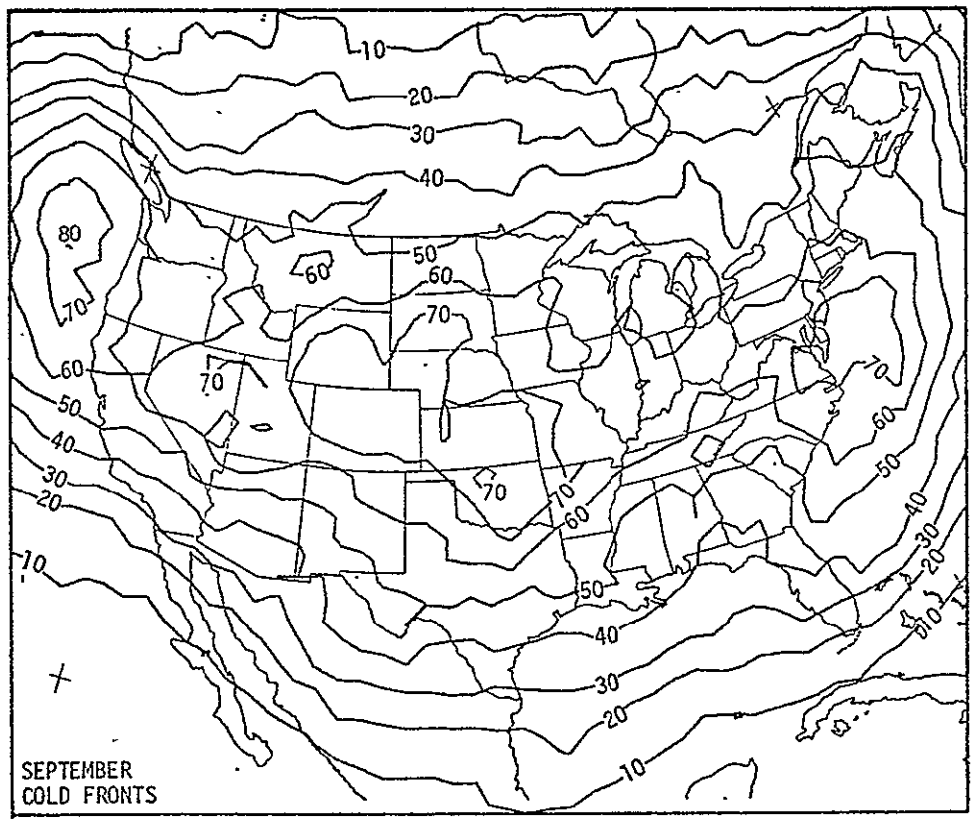

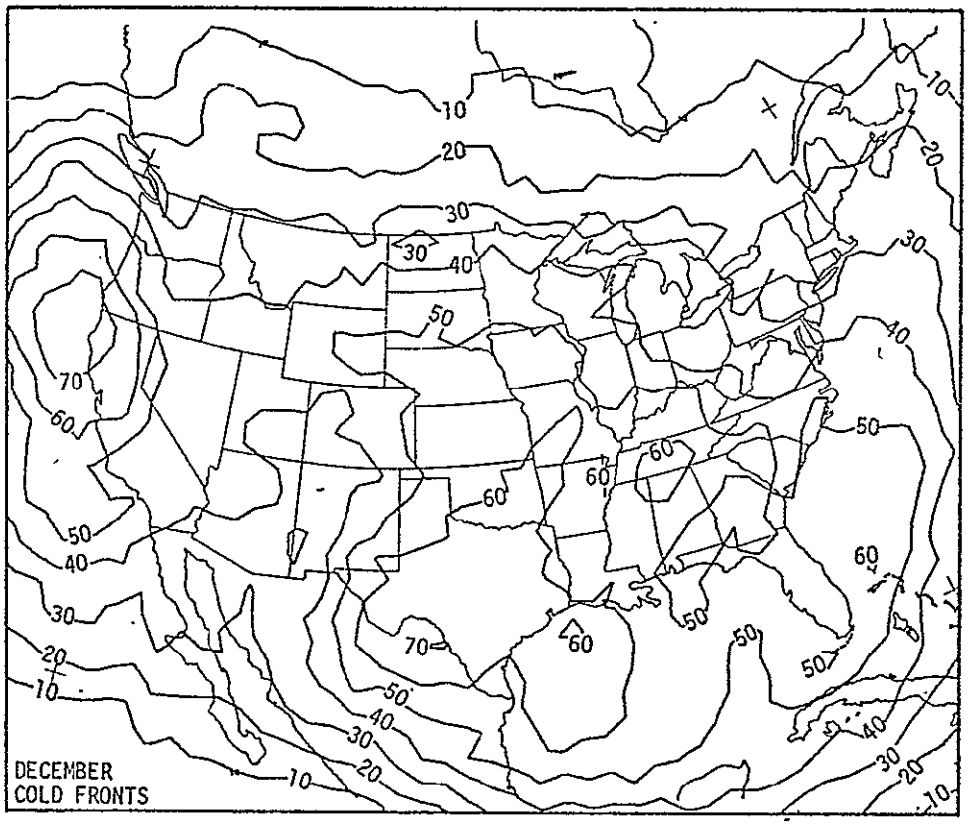

Figure VII-34: Cold Front Climatology
September & December

After Morgan et al. (1975)

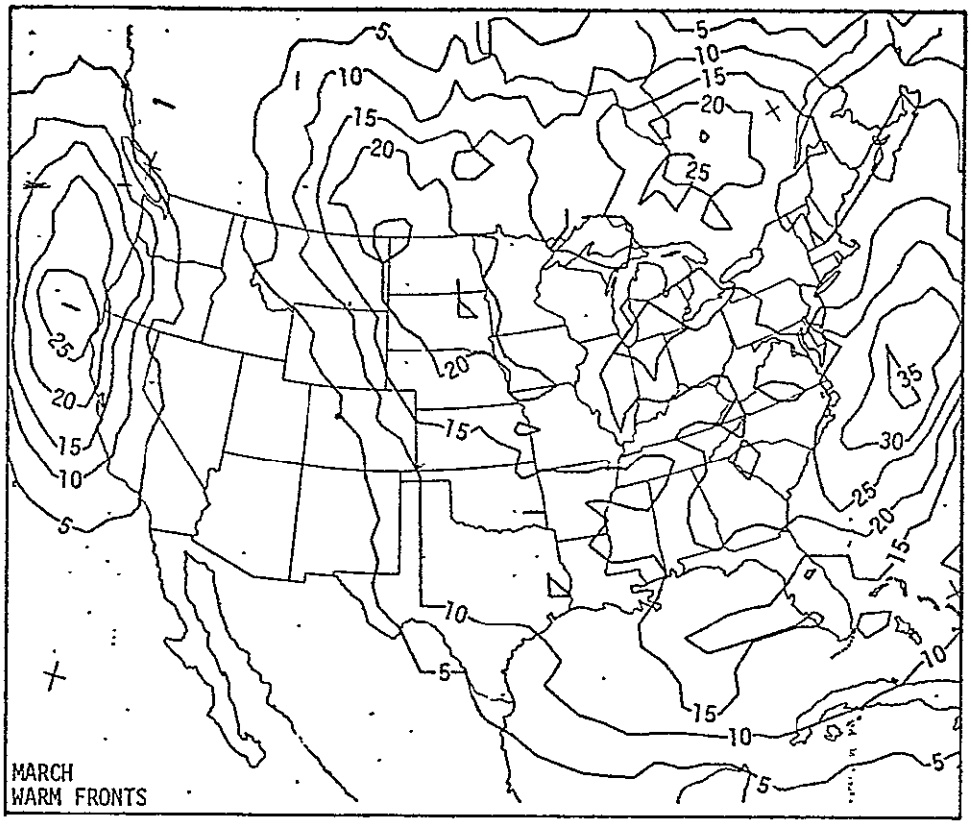

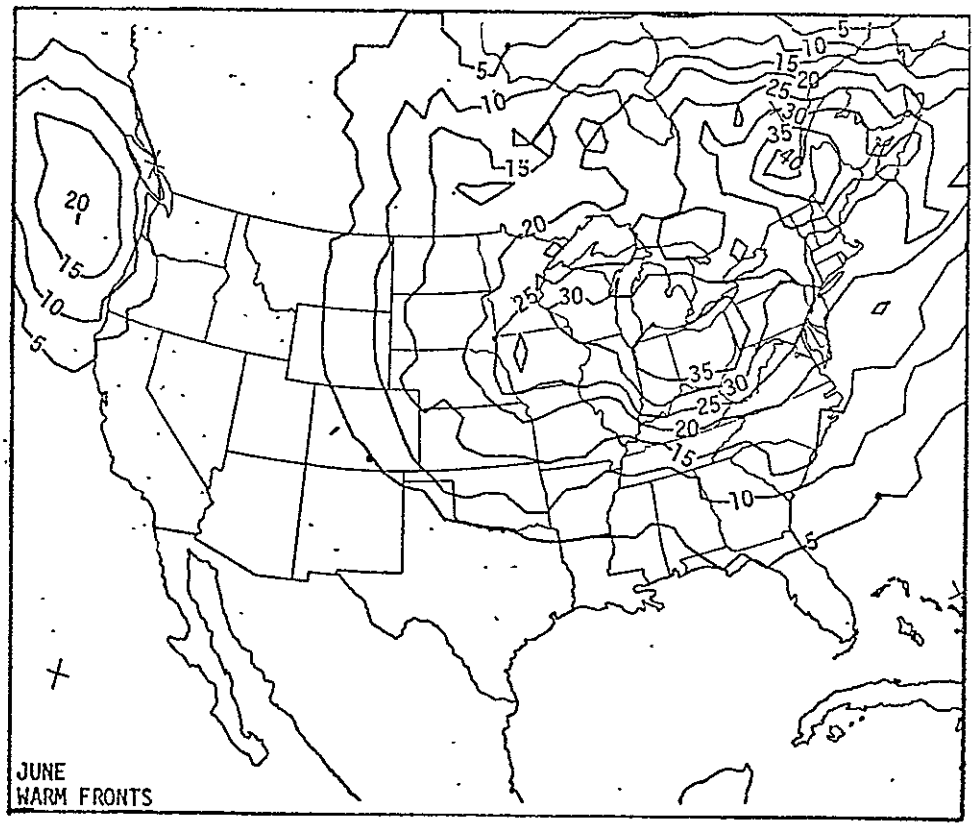

Figure VII-35: Warm Front Climatology
March & June

After Morgan et al. (1975)

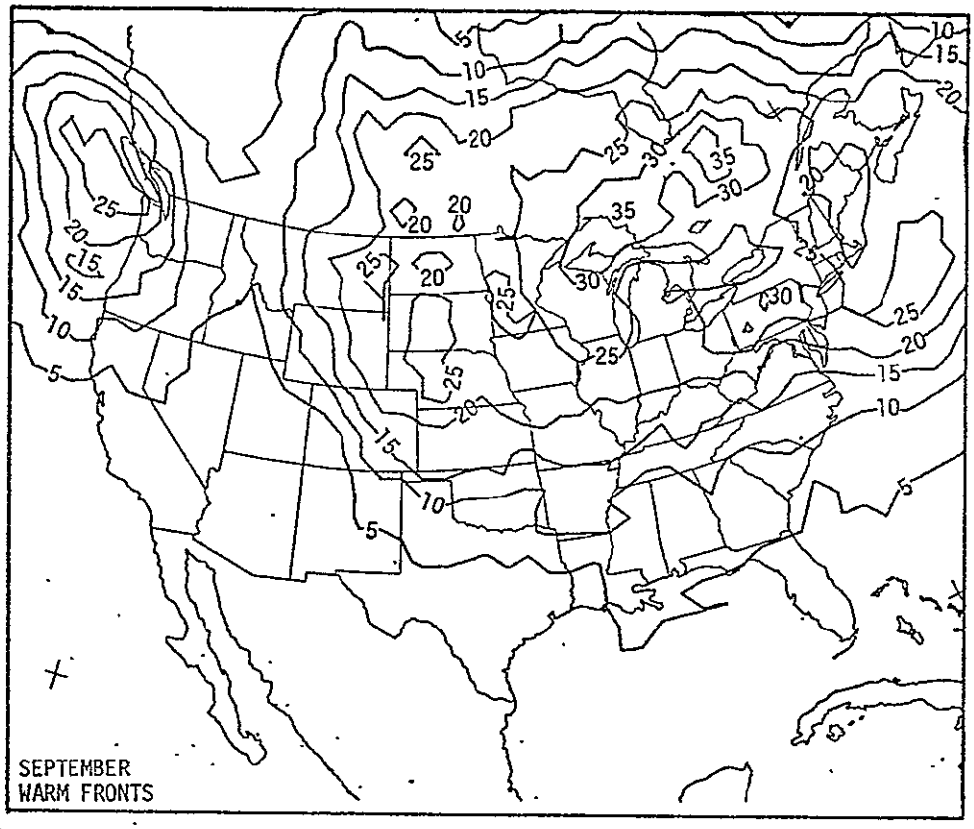

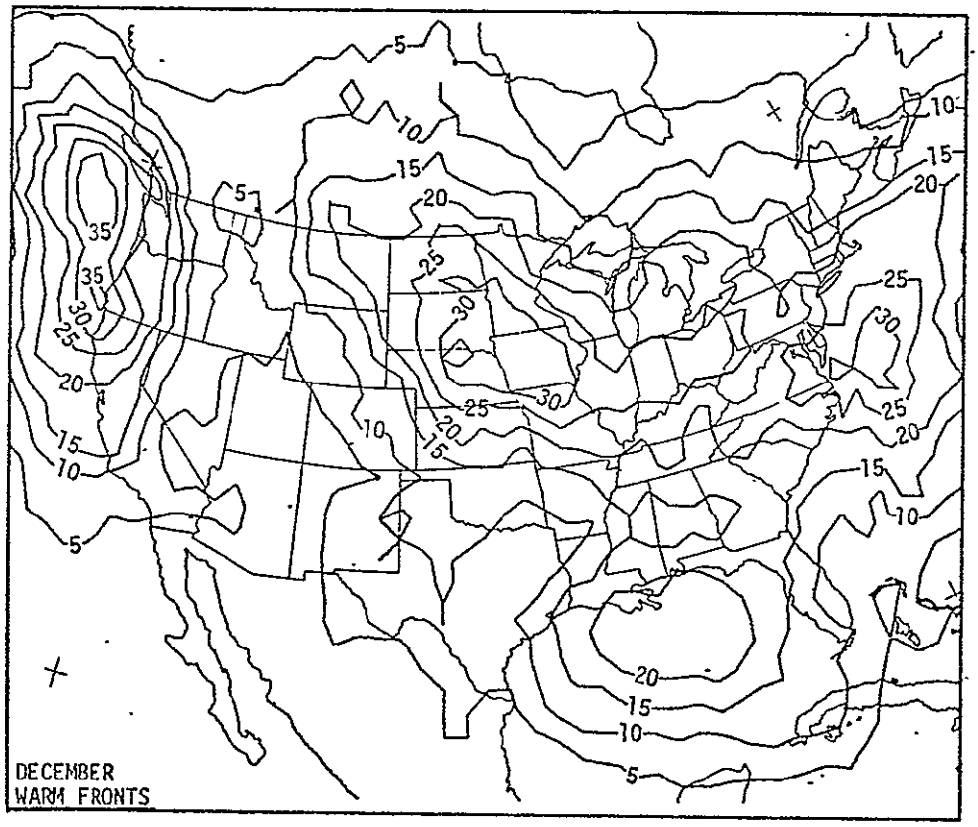

Figure VII-36: Warm Front Climatology
September & December

After Morgan et al. (1975)

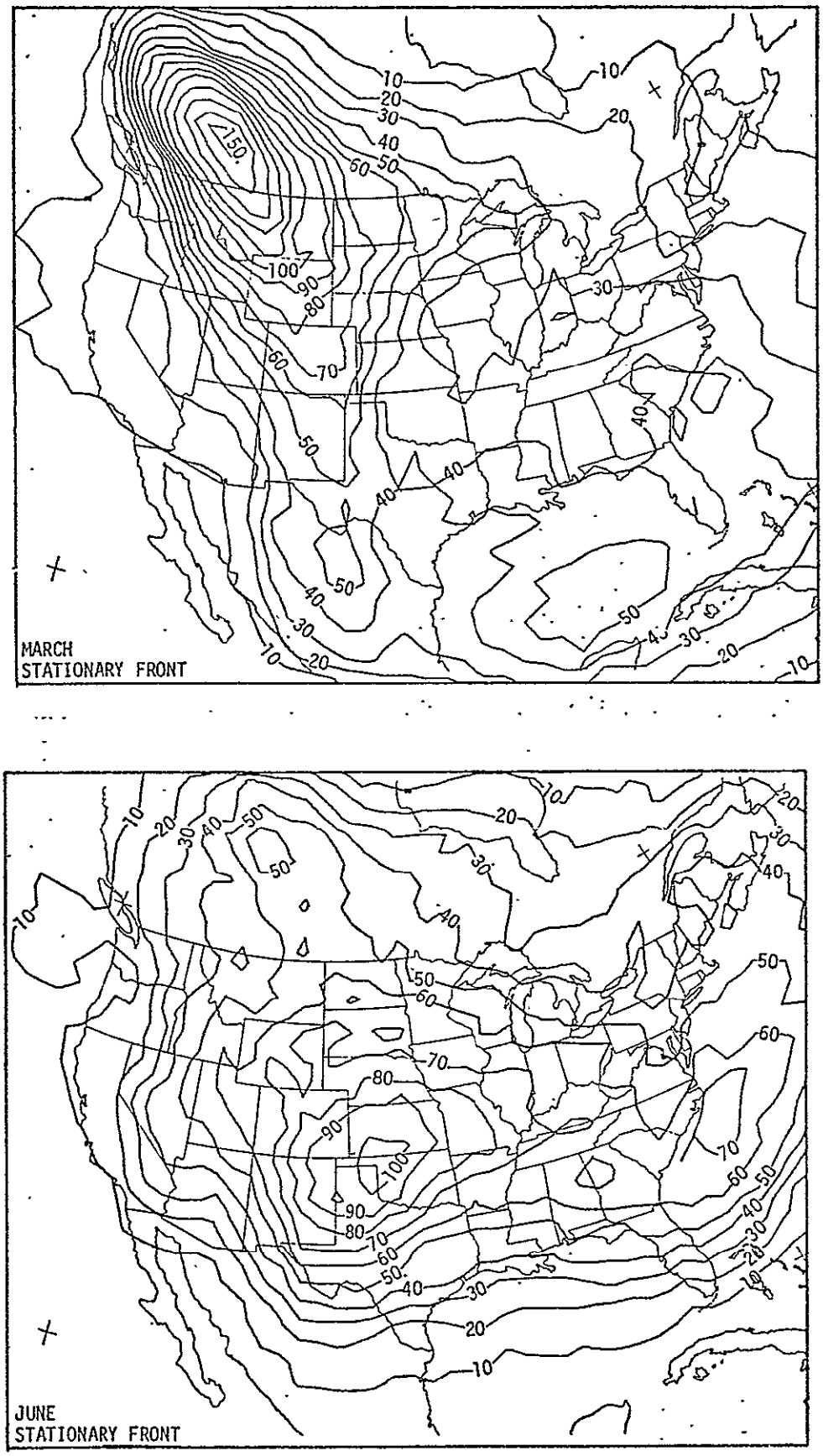

Figure VII-37: Stationary Front Climatology

After Morgan et al. (1975)

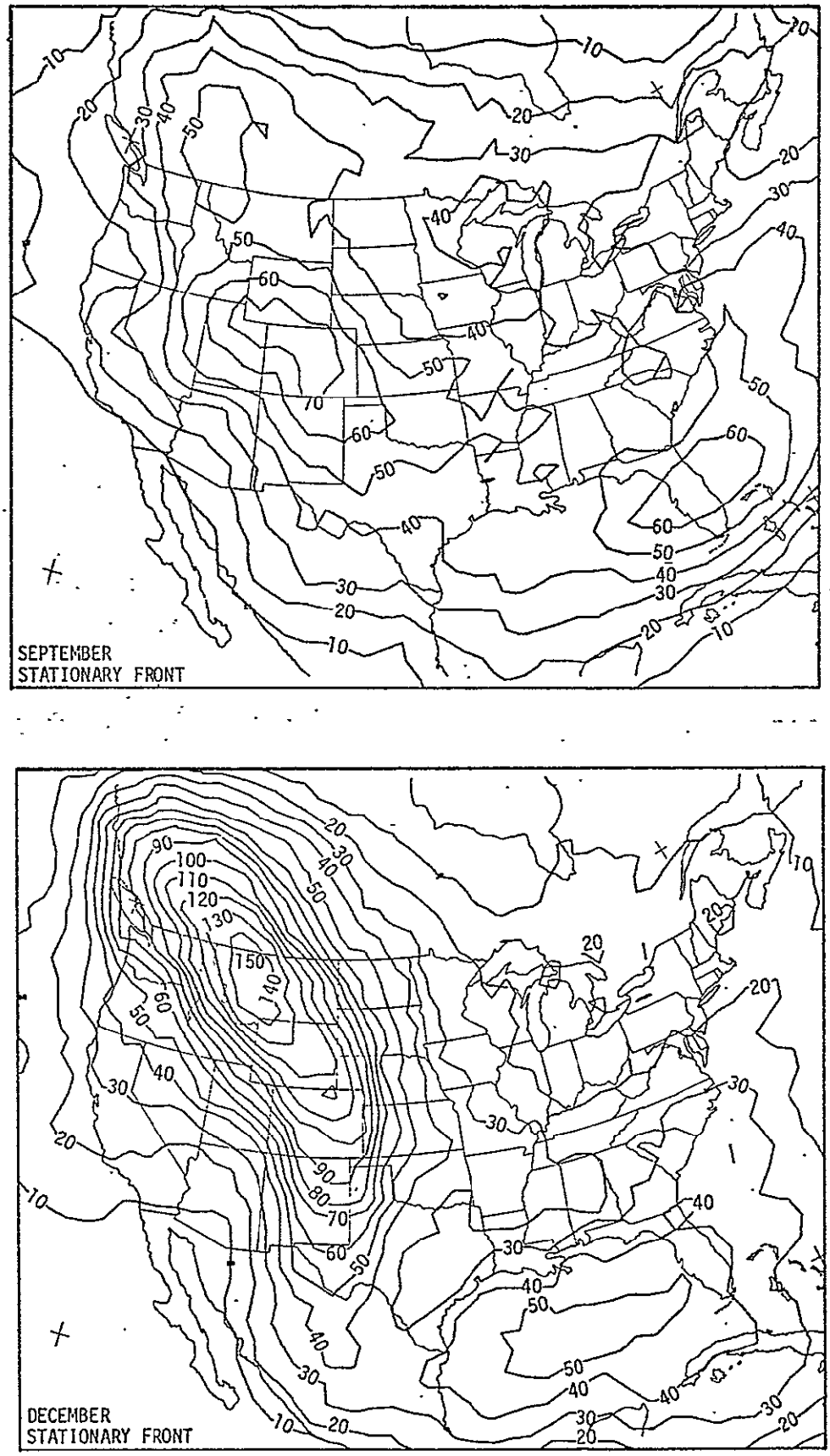

Figure VII-38: Stationary Front Climatology
September & December

After Morgan et al. (1975)

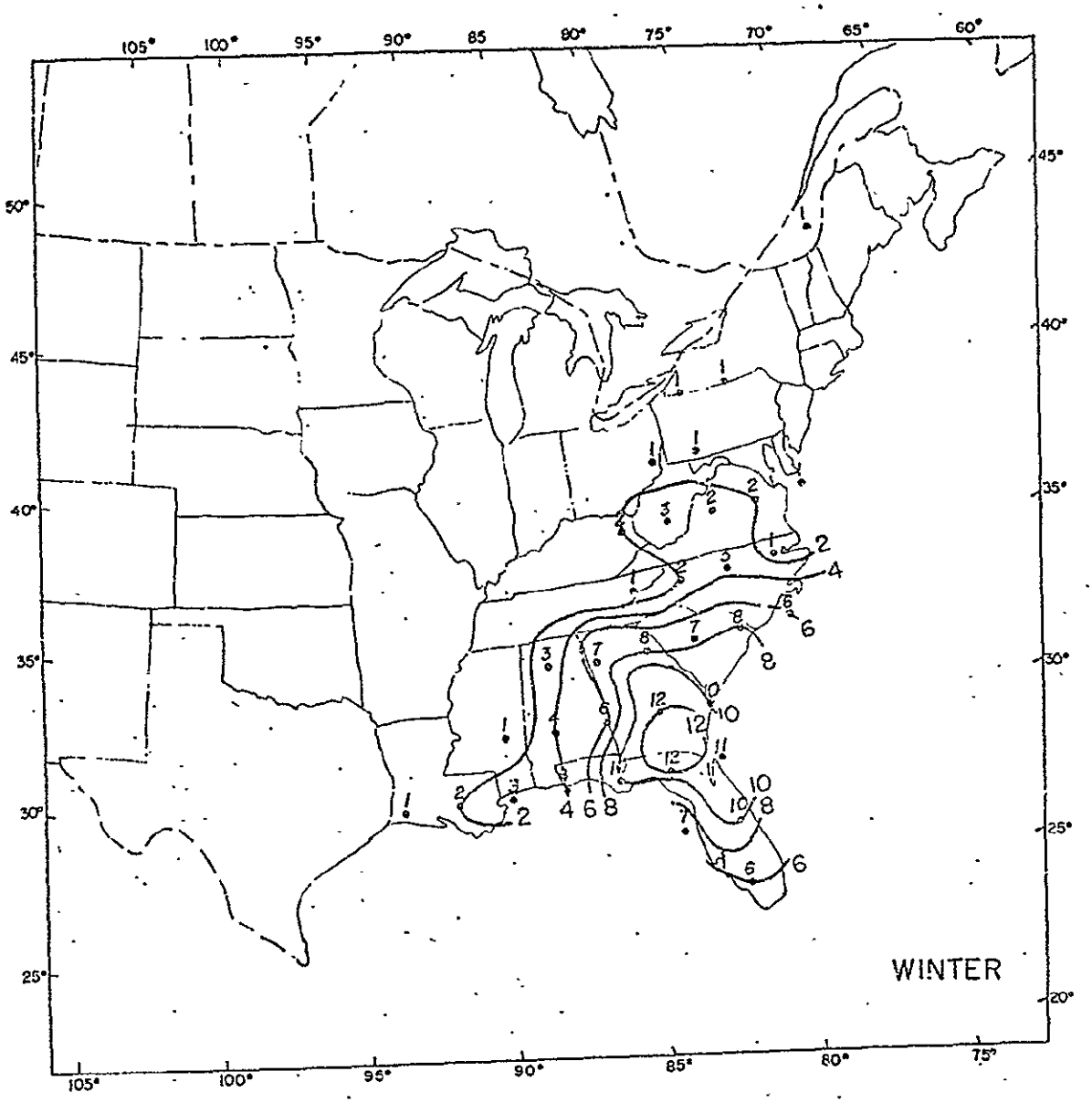

Winter - December, January, February

Figure 7. Seasonal distribution of atmospheric stagnation (four days or more), 1936-1975.

Figure VII-39: Winter Atmospheric Stagnation

After Korshover (1976)

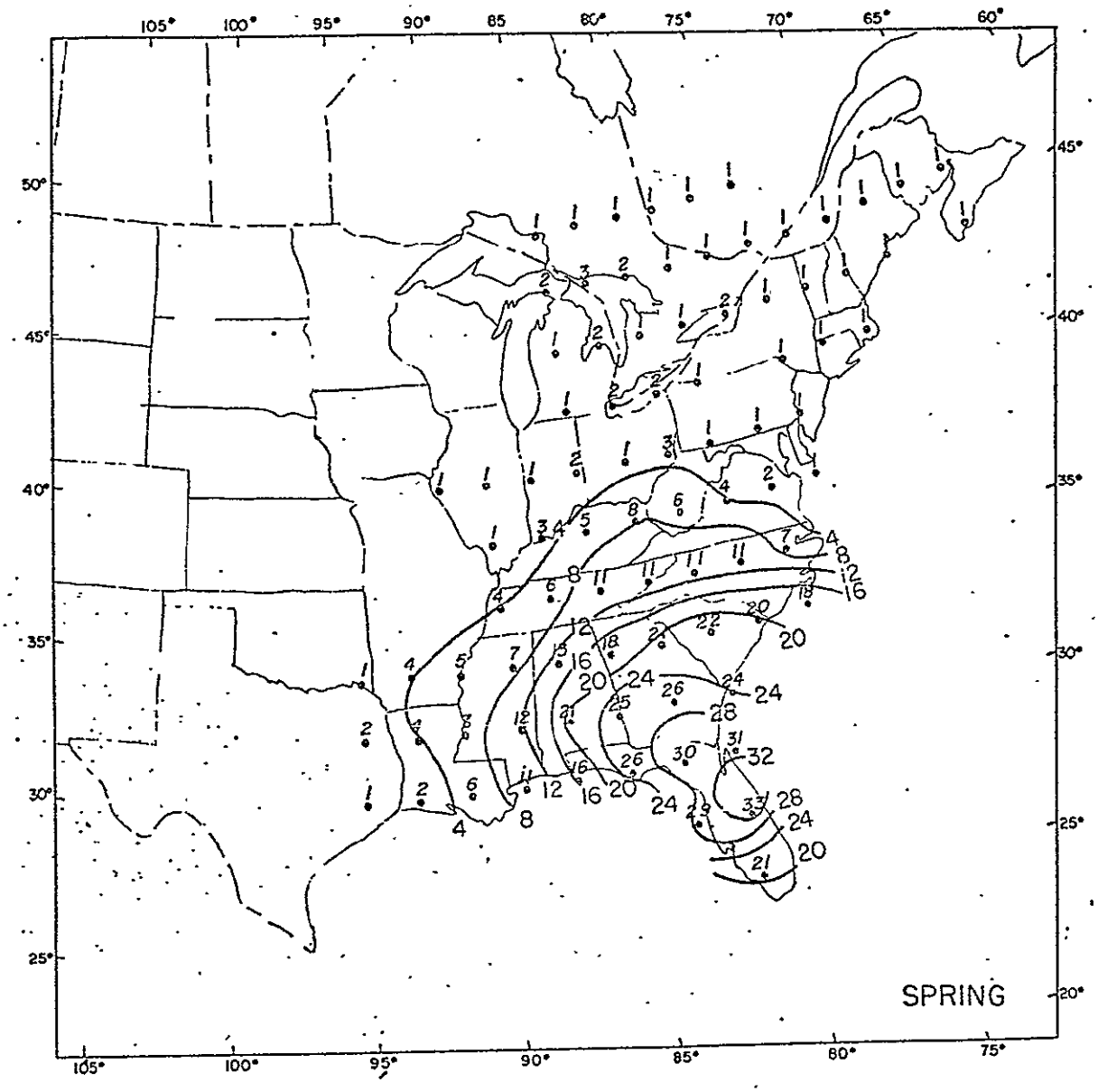

Spring - March, April, May

Figure 7. (Continued)

Figure VII-40: Sprint Atmospheric Stagnation

After Korshover (1976)

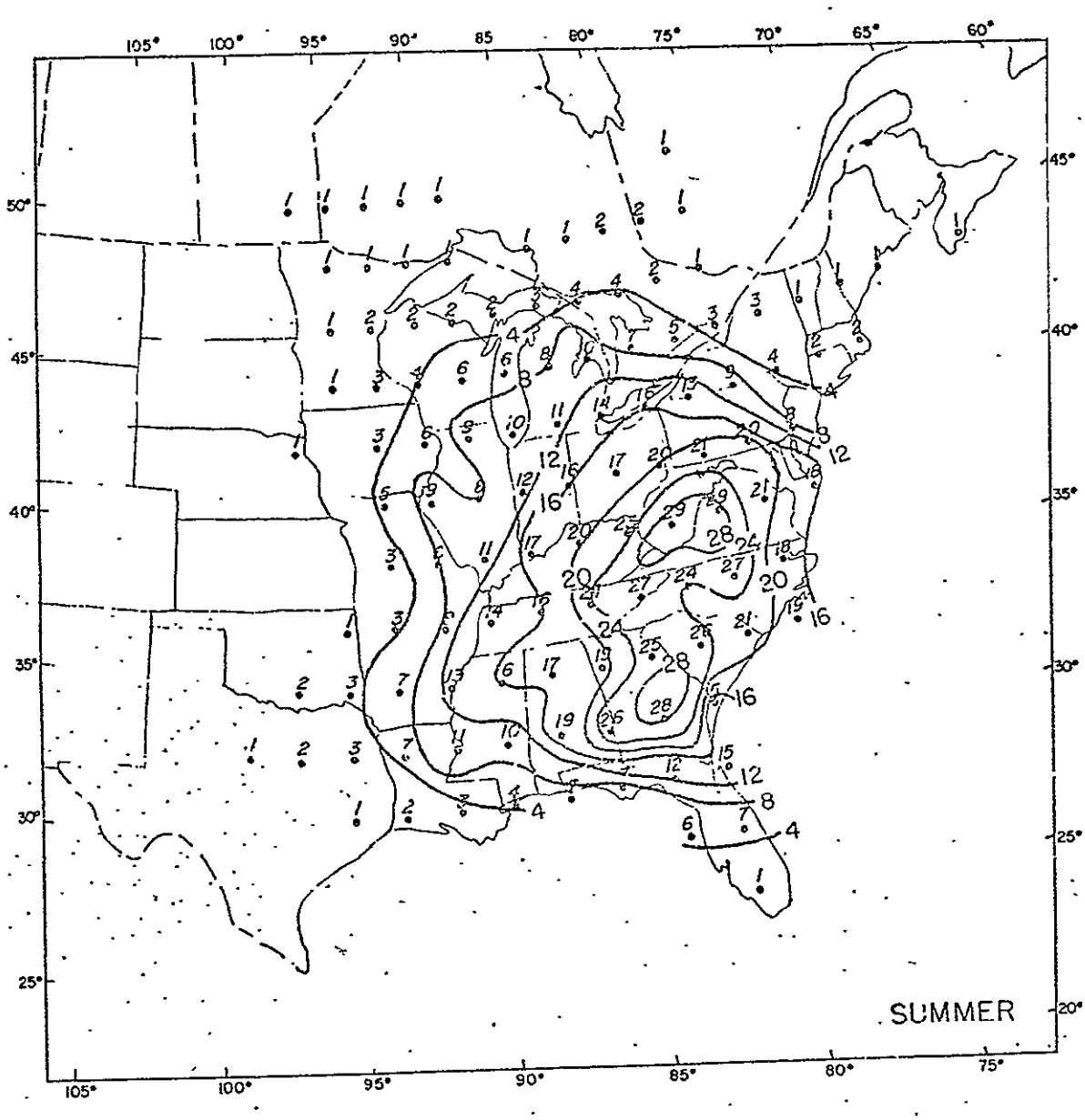

Summer - June, July, August

Figure 7. (Continued)

Figure VII-41: Summer Atmospheric Stagnation

After Korshover (1976)

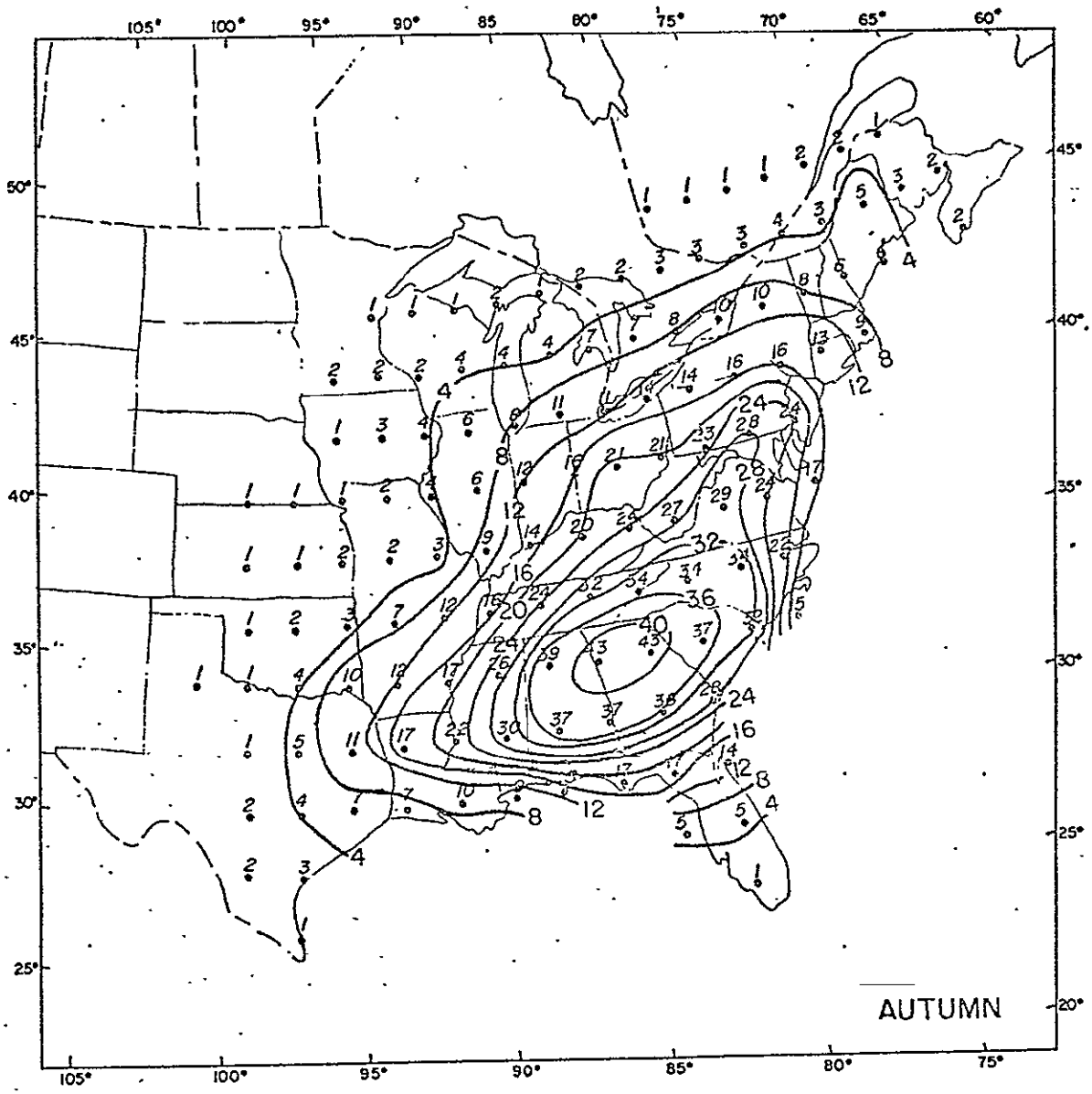

Autumn - September, October, November

Figure 7. (Continued)

Figure VII-42: Autumn Atmospheric Stagnation

After Korshover (1976)

AWS CLIMATIC BRIEF

CAPE KENNEDY AFS, FLORIDA — PERIOD 1950-65 — WBAN # 12000 — WMO # 74794

Prepared by ETAC (FEB 1970) — N 28 29 W 80 33 — ELEVATION: 19 ft — STN LTRS: XMR

MONTH	TEMPERATURE (°F)				PRECIPITATION (in)				WIND (KT)			MEAN					MEAN NUMBER OF DAYS										MEAN CLDS (TENTHS)
	EXTREME MAXIMUM	MEAN DAILY MAXIMUM	MEAN DAILY MINIMUM	EXTREME MINIMUM	MEAN TOTAL	MAXIMUM IN 24 HOURS	MEAN SNOWFALL	MAX SNOWFALL IN 24 HOURS	PREVAILING DIRECTION	MEAN SPEED	EXTREME (PEAK) SPEED (GUSTS)	RELATIVE HUMIDITY 0400	RELATIVE HUMIDITY 1300	DEW POINT (°F)	VAPOR PRESSURE (in Hg)	PRESSURE ALTITUDE (Feet) 99.95%	PRECIP ≥ 0.01 in	PRECIP ≥ 0.5 in	SNOWFALL ≥ 0.1 in	SNOWFALL ≥ 1.5 in	THUNDERSTORMS	FOG (< 7 miles)	TEMPERATURE (°F) MAXIMUM ≥ 90	TEMPERATURE (°F) MAXIMUM ≥ 80	TEMPERATURE (°F) MINIMUM ≤ 32	TEMPERATURE (°F) MINIMUM ≤ 0	
JAN	82	69	52	29	3.0	3.0	0	0	NW	8	46	89	65	53	.40	350	7	2	0	0	1	11	0	1	1	0	5
FEB	86	70	53	28	3.4	2.1	0	0	N	9	43	89	67	55	.43	350	8	2	0	0	1	8	0	3	#	0	5
MAR	88	73	57	34	4.1	5.6	0	0	N	9	46	83	64	57	.47	350	9	3	0	0	3	7	0	5	0	0	5
APR	89	77	62	44	2.0	2.6	0	0	ESE	9	53	86	62	61	.54	350	6	1	0	0	4	3	0	10	0	0	5
MAY	94	82	67	47	1.8	1.4	0	0	E	8	37	90	64	67	.66	250	7	1	0	0	7	3	1	25	0	0	5
JUN	98	86	72	61	4.2	2.7	0	0	S	7	43	93	69	72	.78	200	10	3	0	0	13	2	4	30	0	0	5
JUL	95	88	74	67	5.7	3.6	0	0	S	6	41	94	70	74	.84	150	11	4	0	0	13	1	6	31	0	0	5
AUG	94	88	74	67	6.0	5.8	0	0	E	6	60	95	71	74	.84	200	11	4	0	0	16	2	6	31	0	0	6
SEP	94	86	74	62	8.9	6.9	0	0	E	8	68	90	72	73	.81	250	14	5	0	0	9	1	1	29	0	0	6
OCT	91	81	70	50	5.1	6.4	0	0	N	8	38	87	68	67	.66	350	12	3	0	0	4	3	#	21	0	0	5
NOV	86	75	60	31	3.5	5.9	0	0	NW	8	37	87	66	61	.54	300	8	2	0	0	1	7	0	7	#	0	5
DEC	85	70	53	25	1.6	1.4	0	0	NW	8	37	87	65	54	.42	250	7	1	0	0	1	8	0	1	1	0	5
ANN	98	79	64	25	49.2	6.9	0	0	E	8	69	90	65	64	.60	300	110	31	0	0	73	56	18	194	2	0	5
EYR	11	11	11	11	11	11	11	11	14	14	7	14	14	14	14	10	11	11	11	11	13	13	11	11	11	11	14

REMARKS

RUSSWO:
POR: Hourly Obsns: Jun 50-Dec 53, Apr 56-Apr 66.
Daily Obsns : Jun 50-Dec 53, Apr 56-May 65.

NOTE; *DATA NOT AVAILABLE. #LESS THAN 0.5 DAY, 0.5 OR 0.05 INCH, OR 0.5 PERCENT (%) AS APPLICABLE.

FLYING WEATHER (%FREQ)	HOURS (LST)	JAN	FEB	MAR	APR	MAY	JUN	JUL	AUG	SEP	OCT	NOV	DEC	ANN	EYR
CIG less than 3000 feet and/or VSBY less than 3 miles	00-02	14	15	7	4	4	4	1	2	8	9	11	12	7	
	03-05	19	18	9	7	5	5	1	4	8	11	12	12	9	
	06-08	21	21	13	8	5	6	2	5	8	9	13	15	10	
	09-11	12	14	13	7	4	7	4	7	9	10	11	11	9	
	12-14	10	11	11	5	3	8	7	9	12	12	11	9	9	
	15-17	7	10	8	4	4	8	8	8	12	12	8	7	8	
	18-20	8	9	7	4	5	4	4	5	11	10	7	8	7	
	21-23	10	11	7	3	4	4	1	3	9	9	7	10	7	
	ALL HOURS	12	14	9	5	4	6	4	5	9	10	10	11	8	14
CIG less than 1500 feet and/or VSBY less than 3 miles	00-02	8	9	4	1	1	1	#	#	1	2	5	6	3	
	03-05	13	12	6	4	2	2	#	2	1	3	7	7	5	
	06-08	15	14	10	4	2	3	1	2	2	4	7	10	6	
	09-11	8	8	7	2	1	1	1	1	2	3	4	6	4	
	12-14	4	5	4	1	#	1	1	1	2	2	3	4	2	
	15-17	2	5	3	2	1	1	1	1	3	2	3	3	2	
	18-20	4	4	3	1	1	#	1	1	3	2	3	2	2	
	21-23	5	5	4	1	#	1	#	1	1	1	3	3	2	
	ALL HOURS	7	8	5	2	1	1	1	1	2	2	4	5	3	14
CIG less than 1000 feet and/or VSBY less than 2 miles	00-02	5	6	2	1	1	1	#	#	#	1	3	4	2	
	03-05	10	9	5	3	1	1	#	1	1	2	5	5	4	
	06-08	12	11	6	3	2	2	1	2	2	3	5	8	5	
	09-11	6	6	4	1	1	1	#	#	1	1	3	4	2	
	12-14	2	3	1	1	#	1	1	#	1	1	1	2	1	
	15-17	1	3	2	1	#	1	1	#	1	1	2	2	1	
	18-20	2	3	2	#	#	0	#	#	1	1	2	2	1	
	21-23	3	3	2	#	#	0	#	#	#	#	2	3	1	
	ALL HOURS	5	5	3	1	1	1	#	1	1	1	3	4	2	14
CIG less than 200 feet and/or VSBY less than ½ mile	00-02	2	1	0	#	0	#	0	0	0	1	#	2	#	
	03-05	4	2	1	1	#	#	0	#	#	#	#	2	1	
	06-08	5	4	1	#	0	0	0	#	1	#	1	3	1	
	09-11	1	1	#	0	0	0	0	0	#	#	#	1	#	
	12-14	0	#	0	0	0	0	#	0	#	#	0	0	#	
	15-17	0	#	#	0	#	#	0	#	0	#	0	#	#	
	18-20	#	#	0	0	0	0	#	0	0	0	0	0	#	
	21-23	1	#	0	0	0	0	0	#	0	0	#	1	#	
	ALL HOURS	2	1	#	#	#	#	#	#	#	#	#	1	#	14

Figure VII-43: Cape Canaveral Climatic Summary

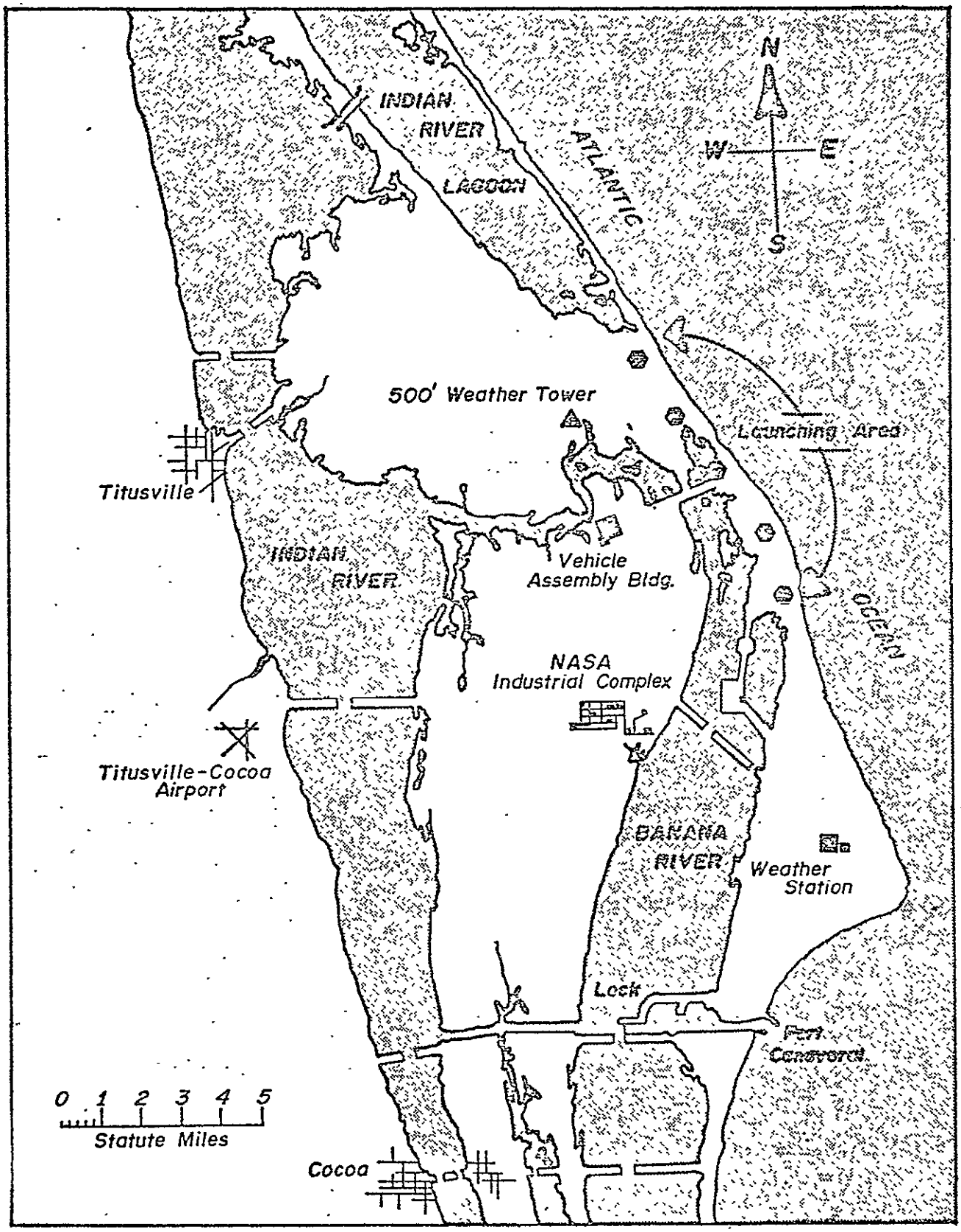

After Neumann (1970)

Figure 13. Map of Cape Kennedy area.

Figure VII-44: Cape Canaveral Area Map

Figure 1a. Probability (%) of at least one thunderstorm on August 1 (EST) between time T_o and time $T_o + \Delta T$. (data derived from Part I).

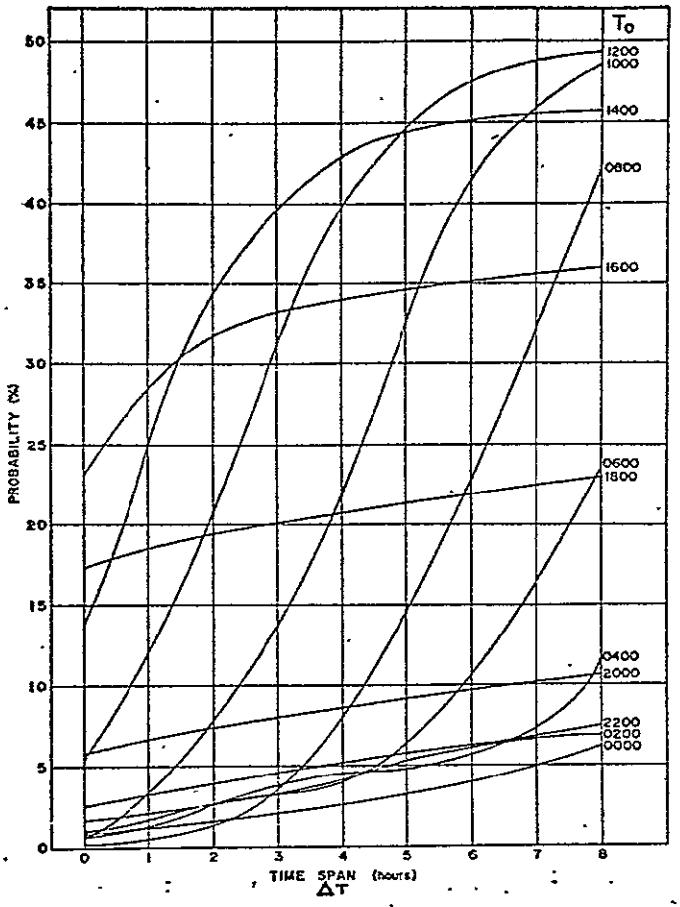

Figure 1b. Daily thunderstorm frequencies (top panel) smoothed over periods of 5, 15, and 31 days (data derived from Part I).

After Neumann (1970)

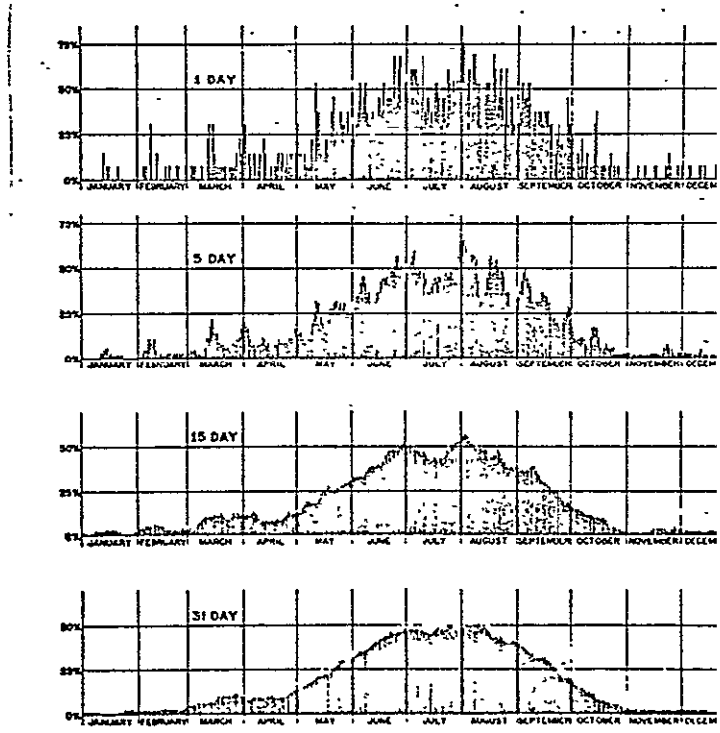

Figure VII-45: Smoothed Cape Canaveral Daily Thunderstorm Frequencies (lower Panel)

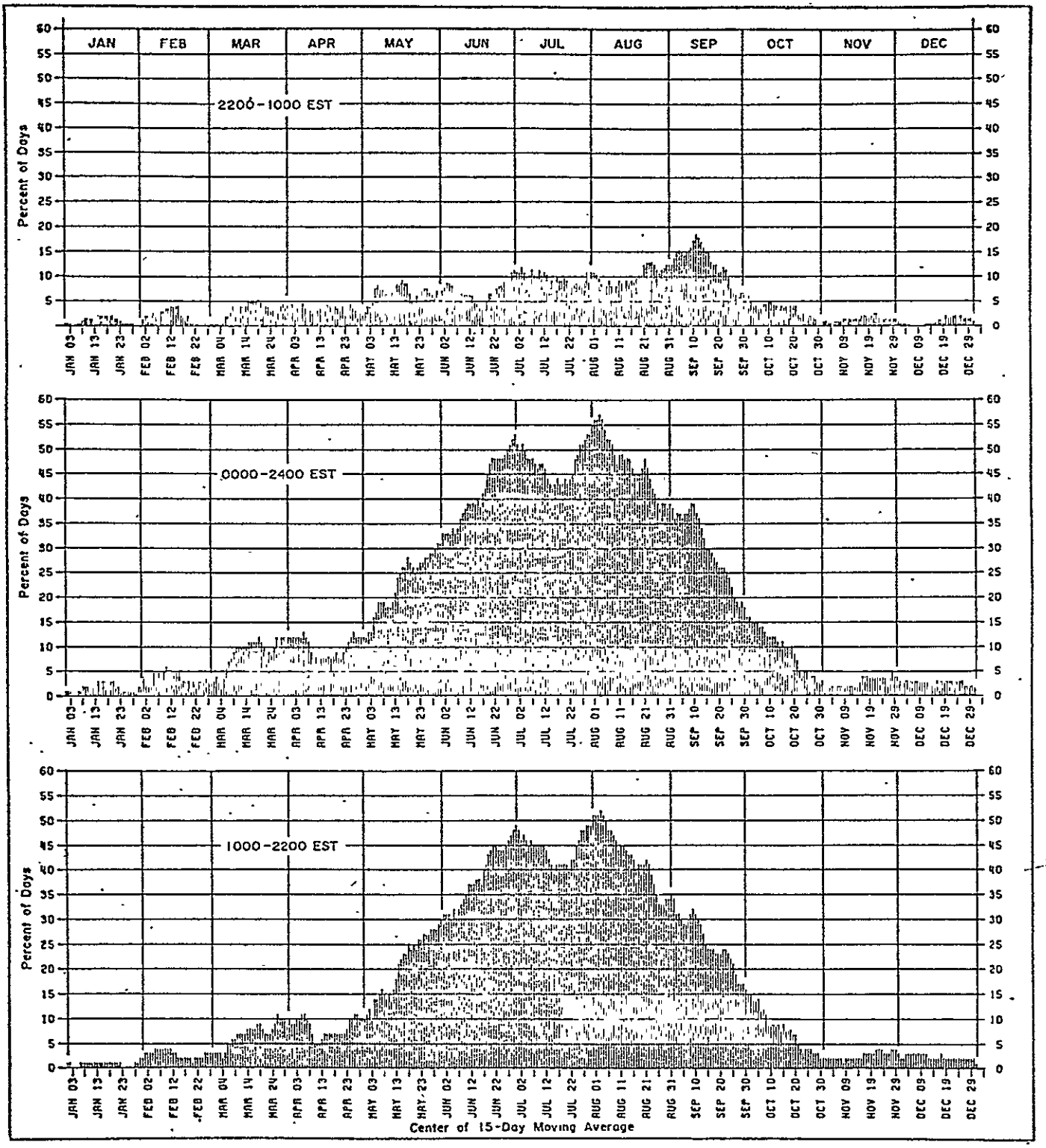

After Neumann (1970)

Figure 2. Probability of thunderstorms at or in the immediate vicinity of the Kennedy Space Center over specified time intervals (data derived from Part I).

Figure VII-46: Thunderstorm Probability at Cape Canaveral as a Function of Time

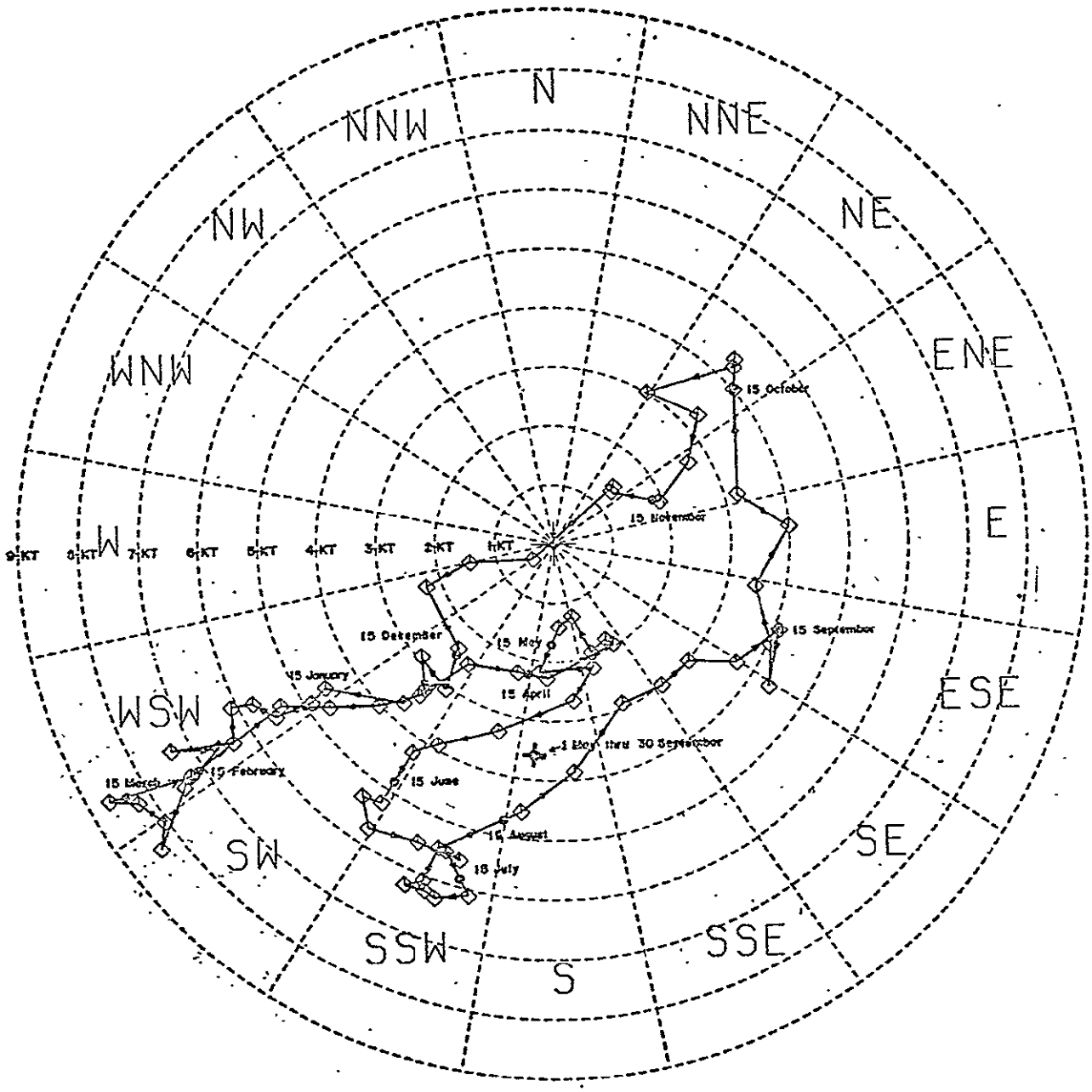

After Neumann (1970)

Figure 4. Location (◈) of the 1200 GMT 3000-foot resultant wind at the Kennedy Space Center for each of the 73 dates referred to in figure 3. The location (⊛) of the resultant wind for the 15th day of each month is interpolated from the location of the adjacent 5-day positions. The location (✣) of the resultant wind for the entire thunderstorm season is 187 degrees at 3.6 knots.

Figure VII-47: Cape Canaveral 1200 GMT 1000 meter Resultant Winds during the Thunderstorm Season

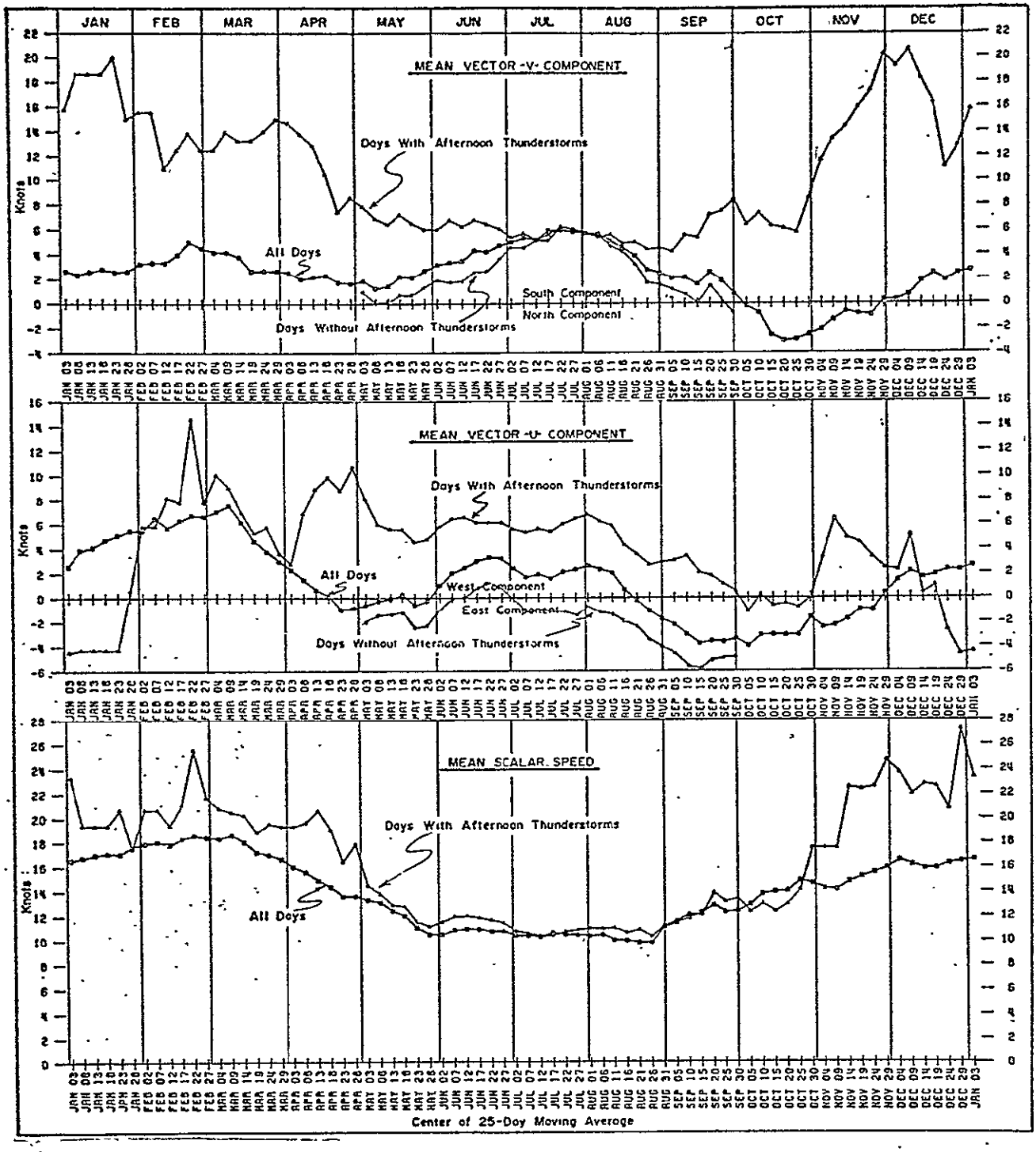

After Neumann (1970)

Figure 6. Annual variation in the 1200 GMT 3000-foot vector and scalar winds under conditions with and conditions with and without afternoon thunderstorms. The vector locations of the wind components under conditions without afternoon thunderstorms are given for the period May through September only.

Figure VII-48: Cape Canaveral 1200 GMT 1000-m Vector and Scalar Wind Variations During the Summer Season.

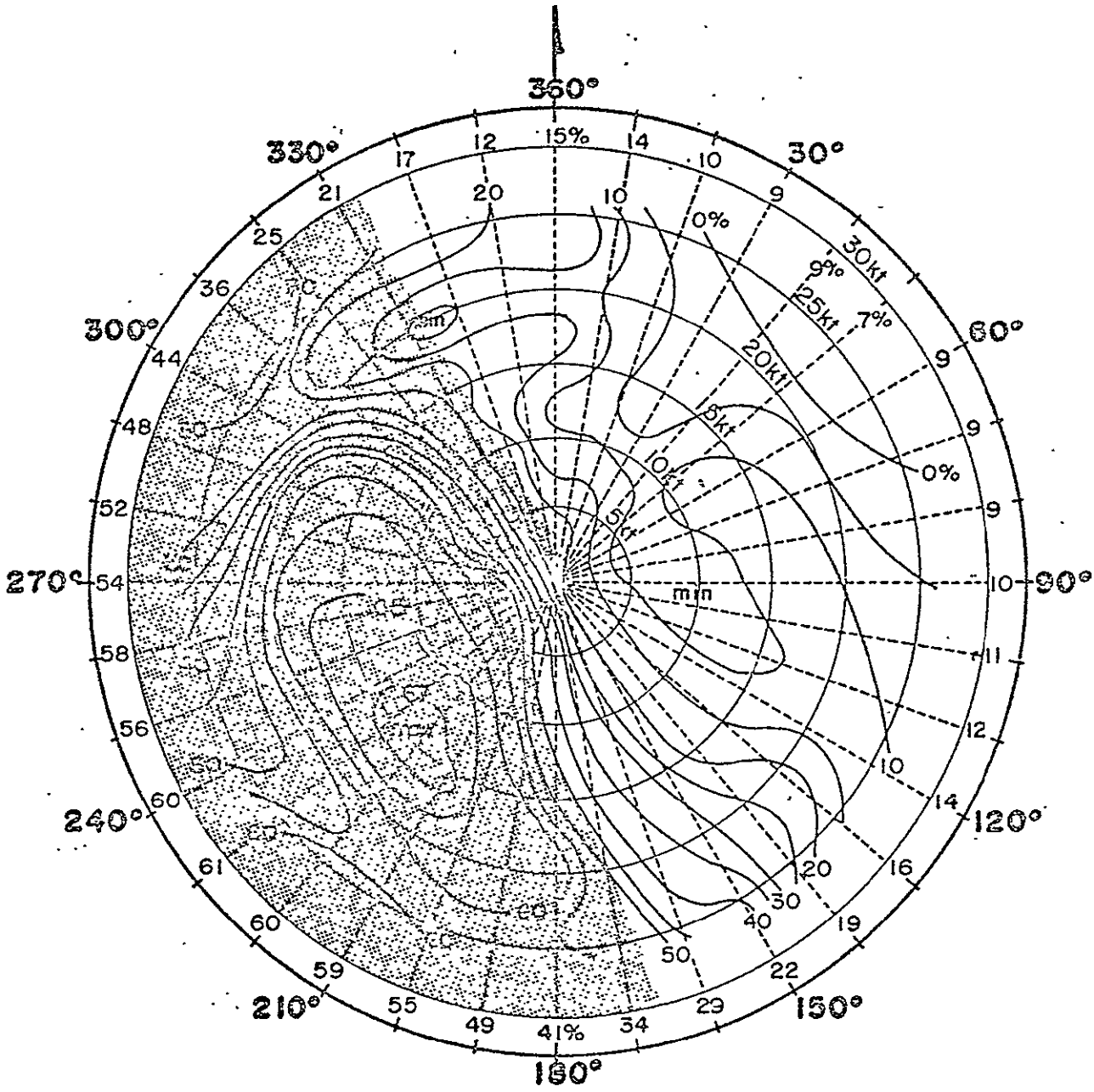

After Neumann (1970)

Figure 9. Probability of afternoon thunderstorms over the entire May through September thunderstorm season as a function of the 1200 GMT 3000-foot wind speed and direction. Values entered perimetrically in outer circle are the probabilities (%) for this direction without regard to the speed. This chart not to be used operationally since it applies to the season as a whole. Shading shows relative location of the Florida eastern coast.

gure VII-49: Cape Canaveral Thunderstorm (DM) Probability over May-September Period Based on 1200 GMT 1000-m Wind Speed and Direction

PERCENT PROBABILITY OF ONE OR MORE AFTERNOON(1000-2200EST) THUNDERSTORMS AT OR IN IMMEDIATE VICINITY OF CAPE KENNEDY AS A FUNCTION OF THE 3000 FT 1200GMT WIND SPEED AND DIPECTION(DDD). LETTER PRECEEDING DIRECTION IS A PROBABILITY CONFIDENCE FACTOR RASED ON NUMBER OF OBSERVATIONS WHERE -A- REPRESENTS MAXIMUM AND -D- REPRESENTS MINIMUM CONFIDENCE. SEE TEXT FOR FURTHER EXPLANATION.

1200GMT 3000 FT WIND SPEED(KTS)

	DDD	01	02	03	04	05	06	07	08	09	10	11	12	13	14	15	16	17	18	19	20	21	22	23	24	25
	(NOTE...DOUBLE ASTERISK INDICATES PROBABILITY LESS THAN 10 PERCENT.)																									
D	010	33	34	34	33	31	30	28	26	25	24	21	22	22	22	23	23	24	23	23	23	23	24	25	24	23
D	020	31	31	31	30	29	28	26	24	22	21	19	17	16	16	16	16	17	18	18	18	18	17	16	16	15
D	030	27	27	26	25	24	23	21	20	18	17	15	13	12	11	11	11	11	11	10	10	**	**	**	**	**
D	040	20	18	17	16	14	14	13	12	10	**	**	**	**	**	**	**	**	**	**	**	**	**	**	**	**
D	050	16	15	12	10	**	**	**	**	**	**	**	10	**	**	**	**	**	**	**	**	**	**	**	**	**
D	060	15	13	10	**	**	**	**	**	**	**	**	10	**	**	**	**	**	**	**	**	**	**	**	**	**
D	070	17	15	12	**	**	**	**	**	**	**	**	10	11	11	11	10	**	**	**	**	**	**	**	**	**
C	080	18	16	13	11	**	**	**	**	**	**	**	10	11	11	12	11	11	10	**	**	**	**	**	**	**
C	090	18	16	14	12	10	**	**	**	**	**	**	10	11	12	12	12	11	10	**	**	**	**	**	**	**
C	100	16	15	12	11	**	**	**	**	**	**	**	**	**	**	**	**	10	10	**	**	**	**	**	**	**
C	110	15	14	12	11	10	**	**	**	**	**	**	**	**	**	**	**	**	**	**	**	**	**	**	**	**
B	120	15	14	13	12	11	11	**	**	**	**	**	**	**	**	**	**	**	10	10	11	11	10	**	**	**
A	130	16	15	14	14	13	12	12	12	12	12	12	12	13	13	14	15	16	16	17	18	18	18	17	14	13
A	140	15	15	15	15	14	13	14	14	14	14	14	14	13	14	15	16	18	19	20	22	23	23	23	22	22
A	150	17	17	17	17	16	17	18	18	19	19	19	20	21	22	24	26	27	28	29	30	31	32	34	36	37
A	160	18	18	18	19	19	20	22	23	23	25	25	26	28	29	29	30	31	32	33	34	35	36	37	39	40
A	170	21	22	24	25	27	28	29	31	32	34	35	36	37	37	38	40	42	44	46	48	49	49	51	52	52
A	180	22	29	30	31	34	35	36	38	39	40	42	43	45	47	48	52	55	58	60	60	59	58	54	54	55
A	190	21	29	31	36	38	38	41	42	44	45	47	49	52	54	57	57	58	58	58	58	57	57	55	53	53
A	200	25	34	38	41	44	47	50	52	54	56	58	59	60	62	63	63	62	62	62	61	60	59	58	55	56
A	210	32	39	47	50	54	56	59	62	65	67	69	70	71	71	71	71	70	69	66	63	63	62	60	62	64
A	220	39	46	54	59	61	61	68	71	73	74	75	76	79	79	78	77	74	70	66	64	65	64	64	65	71
A	230	42	50	59	63	65	68	72	74	76	78	79	80	81	81	80	79	77	73	69	68	66	65	66	66	68
A	240	49	56	65	70	72	75	78	79	81	83	83	84	85	85	85	84	83	80	77	74	72	68	67	67	68
A	250	56	62	73	77	79	80	84	86	87	89	90	91	91	91	91	91	91	90	87	84	80	77	73	73	72
A	260	52	58	69	73	75	78	80	82	83	85	86	88	88	88	88	88	88	87	85	82	77	73	68	66	64
A	270	53	61	70	74	77	79	81	83	85	86	87	88	89	89	89	89	88	87	86	85	82	70	66	64	61
A	280	52	60	66	71	74	78	78	80	82	85	86	87	87	87	86	86	86	85	82	80	73	67	61	57	53
C	290	51	57	62	68	71	72	73	76	79	80	80	83	84	85	83	81	81	81	79	74	66	59	53	52	51
D	300	47	52	56	60	64	65	66	66	70	71	75	75	75	75	74	74	75	72	73	63	52	46	42	52	55
D	310	39	42	45	48	50	52	49	50	57	58	58	59	57	55	55	52	50	51	51	39	35	34	33	40	45
D	320	32	34	35	37	39	39	40	35	41	40	39	39	39	38	38	35	34	36	28	22	25	26	26	29	34
D	330	26	28	28	29	29	29	29	29	29	29	28	27	27	27	27	21	26	23	18	12	14	19	21	25	29
D	340	24	26	26	27	25	25	24	23	24	28	23	20	20	20	22	18	22	18	17	14	14	18	20	24	25
D	350	26	26	28	28	26	25	24	20	20	19	18	18	18	20	22	19	23	21	20	18	18	20	22	24	24
D	360	31	32	33	32	31	30	26	25	24	22	21	21	21	22	23	24	27	27	26	25	25	27	28	28	28

PROBABILITY WITH 3000 FT WINDS CALM IS 29 PERCENT. TO ESTIMATE THE PROBABILITIES FOR PERIODS OTHER THAN 1000-2200EST, MULTIPLY TABULAR VALUES BY FOLLOWING FACTORS-

PERIOD	MULTIPLICATION FACTOR	PERIOD	MULTIPLICATION FACTOR
1000-1100EST	.06	1000-1500EST	.65
1000-1200EST	.15	1000-1600EST	.82
1000-1300EST	.29	1000-1700EST	.90
1000-1400EST	.42	1000-1800EST	.96

THESE DATA VALID FOR 5-DAY PERIOD CENTERED ON AUG 01. UNCONDITIONAL PROBABILITY OF ONE OR MORE THUNDERSTORMS ON THIS DATE IS 51 PERCENT.

ELLIPSES BELOW SHOW THE DISTRIBUTION OF THE 1200GMT 3000 FT WINDS ASSUMING A BIVARIATE NORMAL DISTRIBUTION OF THE U AND V COMPONENTS. INNER AND OUTER ELLIPSES ENCLOSE 50 AND 90 PERCENT OF THE CASES. EACH SCALE MARK ON AXES IS WORTH FOUR KNOTS.

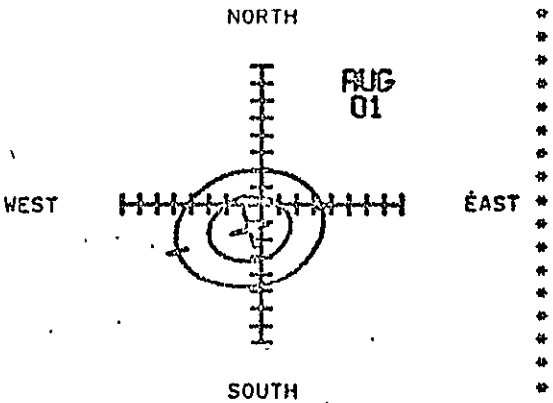

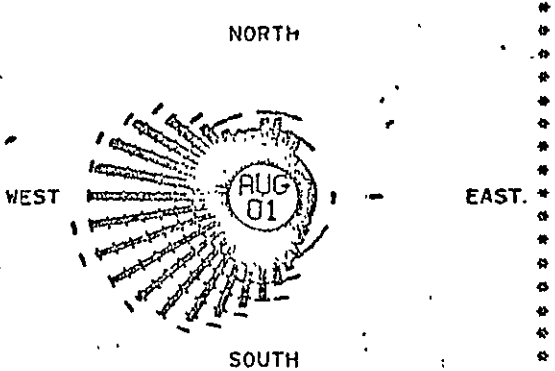

DIAGRAM ABOVE SHOWS THE AFTERNOON THUNDERSTORM PROBABILITY ON THIS DATE FOR EACH 1200GMT 3000 FT WIND DIRECTION, REGARDLESS OF SPEED. EACH CONCENTRIC ARC IS WORTH 10 PERCENT.

SEE TEXT FOR FURTHER EXPLANATION OF THESE DIAGRAMS.

Figure VII-50: Sampel Cape Canaveral Thunderstorm Forecasting Monogram

TABLE VII-I (Wallace - 1975)

Diurnal Frequency of Precipitation by Amount and Category by Season

Station	Percentage of hours with Precipitation (Trace or More)		Phase of Diurnal Cycle (Time of Maximum--GMT)		Normalized Amplitude	
	Jun-Aug	Nov-Mar	Jun-Aug	Nov-Mar	Jun-Aug	Nov-Mar
Jacksonville	10	10	2100	1300	.90	.10
Orlando	12	9	2100	2000	1.10	.15
West Palm Beach	11	9	1800	2000	.65	.20
Miami	10	7	1900	1800	.40	.10
	Percentage of Hours with Precip > 2.5 mmh^{-1}		"		"	
	Jun-Aug	Nov-Mar	Jun-Aug	Nov-Mar	Jun-Aug	Nov-Mar
Jacksonville	1.8	1.1	2100	1400	1.05	.20
Orlando	2.2	1.1	2100	2300	1.15	.40
West Palm Beach	2.1	1.1	1900	2100	.70	.35
Miami	2.0	0.9	2100	2000	.60	.25
	Percentage of Hours with a Trace		"		"	
	Jun-Aug	Nov-Mar	Jun-Aug	Nov-Mar	Jun-Aug	Nov-Mar
Jacksonville	5	5	2100	1300	.60	.05
Orlando	6	4	2100	2100	.55	.20
West Palm Beach	5	5	1800	2000	.50	.15
Miami	5	4	1900	1800	.35	.20

TABLE VII-II (Wallace - 1975)

Diurnal Cycle in the Thunderstorm Frequency by Season

Station	Percentage of Hours of Audible Thunder		Phase of Diurnal Cycle (Time of Max-GMT)		Normalized Amplitude	
	Jun-Aug	Nov-Mar	Jun-Aug	Nov-Mar	Jun-Aug	Nov-Mar
Eglin AFB	4.5	5.5	2000	0300	.65	.20
Panama City	3.2	4.8	2000	1000	.70	.45
Tallahassee	4.8	7.6	2100	1600	1.30	.30
Jacksonville	2.8	1.7	2100	2300	1.40	.40
Daytona Beach	4.9	3.2	2100	2300	1.50	.65
Orlando	3.8		2200		1.60	
Tampa	4.4	2.2	2200	0000	1.55	.35
Vero Beach	5.6		2100		1.40	
Fort Myers	4.4		2200		1.60	
West Palm Beach	3.2	2.0	2100	0000	1.10	.30
Miami	3.7		2100		1.10	

TABLE VII-III

Mandatory Level Temperatures Across Florida

After Newell, et al. (1972)

Station	850 mb		700 mb		500 mb	
	Dec-Feb	Jun-Aug	Dec-Feb	Jun-Aug	Dec-Feb	Jun-Aug
Eglin AFB	7.6	17.5	1.5	8.1	-14.2	-7.1
Jacksonville	8.0	17.5	1.8	8.4	-13.9	-7.2
Cape Canaveral	10.0	17.7	3.8	8.1	-12.3	-7.4
Tampa	9.6	17.8	3.6	7.9	-12.0	-7.3
Miami	11.3	17.4	5.1	8.2	-10.4	-7.4
Key West	12.2	17.8	5.7	8.4	- 8.7	-7.1

Units (°C)

TABLE VII-IV

Mandatory Level Winds Across Florida After Newell et al. (1972)

December-February

Station	Surface		850 mb				700 mb		500 mb			
	u	v	u	σ(u)	v	σ(v)	u	v	u	σ(u)	v	σ(v)
Eglin AFB	0.2	-0.0	5.2	6.9	0.4	7.8	13.0	1.5	23.3	10.8	3.5	10.9
Jacksonville	0.1	-0.7	6.3	6.6	1.4	6.9	12.8	1.5	22.9	10.9	2.1	9.7
Cape Canaveral	0.5	-0.8	8.1	6.1	2.2	8.7	10.1	1.7	29.4	6.1	5.1	14.5
Tampa	1.0	-1.2	3.7	6.7	1.1	5.8	15.7	2.8	18.1	8.2	3.6	7.8
Miami	-0.8	-0.2	2.2	6.9	0.6	4.9	7.2	1.6	15.5	8.6	5.0	7.0
Key West	-1.1	-1.7	1.5	6.5	0.3	5.1	6.1	1.0	17.0	8.3	1.7	6.2

June-August

	u	v		σ(u)	v	σ(v)	u	v	u	σ(u)	v	σ(v)
Eglin AFB	0.9	1.8	0.4	4.6	0.2	4.1	1.3	0.0	2.7	5.9	0.1	5.0
Jacksonville	-1.9	1.4	1.2	4.6	0.5	4.1	1.6	0.3	2.5	5.6	0.2	4.7
Cape Canaveral	-1.8	0.4	-1.0	6.6	1.7	5.0	1.3	1.4	2.0	8.4	0.6	6.0
Tampa	0.5	-0.3	-0.7	4.4	1.1	3.5	1.0	0.8	1.0	5.4	0.6	4.3
Miami	-1.9	0.9	-1.6	4.3	0.6	3.2	- 0.7	0.9	- 0.4	5.2	1.1	4.0
Key West	-2.0	0.6	-2.3	4.1	0.7	3.1	- 1.0	0.9	- 0.9	4.8	0.5	3.5

UNITS: ms^{-1}

TABLE VII-V

Cape Canaveral: Selected Upper Air Data by Pressure

		Jan	Apr	Jul	Oct
1000 mb	T(°C)	15.7	20.5	25.6	23.2
	(T)	4.8	2.9	1.7	2.7
	%RH	73	70	80	75
850 mb	T(°C)	9.3	12.5	17.3	14.3
	(T)	3.7	3.1	1.2	2.5
	%RH	56	56	71	69
700 mb	T(°C)	3.1	5.0	7.9	6.7
	(T)	3.1	2.4	1.2	2.1
	%RH	33	34	59	46

Data Source: Patrick AFB 1950-1956
Cape Canaveral 1956-1970 0000 GMT Only

TABLE VII-VI

Cape Canaveral: Selected Upper Air Data by Height

	March		June		September		December	
	T(°C)	%RH	T(°C)	%RH	T(°C)	%RH	T(°C)	%RH
Surface	20.7	81	27.5	79	27.9	80	18.5	85
500 m	17.5	74	23.2	80	23.7	83	16.1	78
1000 m	14.7	75	20.0	72	19.7	79	13.2	78
1500 m	12.4	75	17.2	73	17.2	78	10.8	75
2000 m	10.1	63	13.9	69	14.7	74	9.4	57
3000 m	5.0	41	8.5	65	9.4	70	5.1	25
4000 m	- 0.6	33	2.9	42	3.9	64	- 0.3	--
5000 m	- 6.9	33	- 2.8	42	- 1.8	57	- 6.3	--

Data Source: NASA - Cape Canaveral (1950-1960)
0000 GMT Data Only

TABLE VII-VII

Cape Canaveral: 50% Cumulative Frequency Winds by Height

	March					June				
	u	v	θ	V_r	$\|\bar{V}\|$	u	v	θ	V_r	$\|\bar{V}\|$
Surface	- 0.4	-0.4	045	0.6	3.7	- 0.9	-0.0	090	0.9	2.8
1000 m	2.6	0.8	253	2.7	7.4	- 0.3	0.7	156	0.8	4.6
2000 m	6.0	0.6	264	6.0	8.4	0.5	0.0	270	0.5	4.6
3000 m	9.4	0.4	268	9.4	11.7	1.0	-0.2	281	1.0	4.5
4000 m	13.5	-0.3	271	13.5	15.5	1.2	-0.4	288	1.3	4.6
5000 m	17.2	-0.3	271	17.2	19.2	1.3	-0.4	287	1.4	4.8

	September					December				
	u	v	θ	V_r	$\|\bar{V}\|$	u	v	θ	V_r	$\|\bar{V}\|$
Surface	- 2.8	-0.6	078	2.9	3.0	- 0.0	-1.4	360	1.4	3.1
1000 m	- 3.7	-0.4	084	3.7	5.5	- 0.6	-0.7	041	0.9	7.1
2000 m	- 2.6	-0.4	081	2.6	5.2	1.7	-0.2	083	1.7	6.3
3000 m	- 1.3	-0.3	077	1.3	4.8	5.0	-0.0	270	5.0	8.1
4000 m	- 1.8	-0.2	084	1.8	4.8	9.1	0.2	269	9.1	11.4
5000 m	- 0.7	-0.4	060	0.8	4.9	11.8	0.4	268	11.8	14.3

UNITS: ms^{-1}
θ = resultant wind direction
V_r = resultant wind speed
$|\bar{V}|$ = scalar mean wind speed

Data Source: 1950-1960 - NASA
0000 GMT Only

TABLE VII-VIII

Cape Canaveral: Diurnal Variation of Height
Temperature and Relative Humidity

Time GMT	Surface			950 mb			900 mb			850 mb		
	PRES(mb)	T(°C)	%RH	HT(m)	T(°C)	%RH	HT(m)	T(°C)	%RH	HT(m)	T(°C)	%RH
March												
0000	1017.0	18.4	73	587	16.1	65	1045	13.1	66	1524	10.3	63
1200	1017.7	14.8	85	588	14.6	71	1045	12.1	67	1522	10.0	60
June												
0000	1014.6	25.9	78	583	22.3	74	1052	19.6	71	1542	16.6	70
1200	1015.2	23.3	89	585	21.4	79	1058	18.9	72	1542	16.2	70
September												
0000	1013.7	26.1	80	577	22.5	79	1046	19.7	77	1536	16.8	76
1200	1014.0	23.7	89	577	22.0	83	1046	19.2	79	1536	16.5	76
December												
0000	1018.6	15.9	79	596	14.5	67	1052	12.0	64	1529	9.7	59
1200	1019.1	12.9	85	595	13.6	72	1049	11.6	66	1528	9.7	58

DATA SOURCE: WBAN 33 Forms 1960-1969
National Climatic Center

TABLE VII-IX

Cape Canaveral: 850 mb Diurnal Wind Frequencies (%)

Time (GMT)		Direction Frequency (%)				Onshore	Offshore	Northerly	Southerly
		001-090	091-180	181-270	271-360	← (%) →			
June	0000	23	24	29	24	47	53	53	47
	1200	19	26	44	11	45	55	30	70
Dec.	0000	14	15	35	36	29	71	50	50
	1200	12	17	40	31	29	71	43	57

DATE SOURCE: WBAN 33 Forms 1960-1969
National Climatic Center

TABLE VII-X

Florida Mean Seasonal and Annual Morning and Afternoon

Mixing Heights (H) and Wind Speeds (u) for NOP[1] and ALL[2] Cases After Holzworth (1972)

Station	Time	Winter					Spring					Summer					Autumn					Annual				
		H, m			U, m sec^{-1}		H, m			U, m sec^{-1}		H, m			U, m sec^{-1}		H, m			U, m sec^{-1}		H, m			U, m sec^{-1}	
		NOP	All	% NOP	NOP	All	NOP	All	% NOP	NOP	All	NOP	All	% NOP	NOP	All	NOP	All	% NOP	NOP	All	NOP	All	% NOP	NOP	All
Jacksonville, Florida	M	345	403	79.4	5.2	5.9	447	477	90.4	5.3	5.6	567	583	91.1	4.3	4 4	418	458	85.9	4.7	5 0	444	480	86.7	4.9	5.2
	A	1058	1104	80.1	6.7	7.0	1639	1667	86.1	7.1	7.2	1681	1712	68.0	5.6	5 8	1321	1342	80.4	6.5	6 5	1424	1456	78.6	6.5	6.7
Tampa, Florida	M	394	436	85.8	5.8	6.1	503	526	91.7	5.6	5.8	656	674	91.1	4.2	4.3	419	439	89.2	5.4	5.6	493	519	89.4	5.3	5 4
	A	1052	1079	81.4	6 4	6.6	1523	1544	87.8	6.7	6.8	1460	1526	68.9	5.0	5.3	1401	1429	84.4	6.4	6.8	1359	1394	80.6	6.2	6 4
Miami, Florida	M	654	707	87.2	5.4	5.7	947	980	91.1	5.7	5.9	1041	1071	88.3	4.3	4.5	872	933	82.4	5.0	5 3	878	923	87.2	5.1	5.3
	A	1208	1221	89.2	6.4	6.5	1440	1459	87.4	6 8	6.9	1360	1383	73 7	5.3	5.5	1315	1341	78.7	6.6	6 9	1330	1351	82.2	6.3	6 5

DATA SOURCE: 1960-1964

[1]NOP: Omitting Cold Advection and Precipitation Cases

[2]ALL: Includes all Available Data

TABLE VII-XI

Episode-Days of High Meteorological Air Pollution Potential

(After Holzworth [1972])

Station	Wind Speed (ms^{-1})	Mixing Heights (M) 500	10000	1500	2000
Jacksonville	2	0(0)	0 (0)	0 (0)	0 (0)
	4	0(0)	2 (5) Win.	12 (28) Win.	23 (50) Win.
	6	1(3) Win.	12(29) Win.	43(116) Win.	105(314) Aut.
Tampa	2	0(0)	0 (0)	0 (0)	0 (0)
	4	0(0)	1 (2) Spr.	9 (23) Win.	15 (38) Sum.
	6	1(2) Win.	14(29) Win.	79(234) Win.	127(406) Sum.
Miami	2	0(0)	0 (0)	0 (0)	0 (0)
	4	0(0)	0 (0)	17 (38) Sum-Aut.	25 (60) Sum.
	6	0(0)	3(11) Win.	79(207) Sum.	128(406) Sum.

DATE SOURCE: 1960-1964

First figure is the number of episodes; the number of episode-days is given in parentheses. Seasonal Peaks as Indicated.

Chapter VIII

SYNTHESIS

The following risk situations for inadvertent weather modification due to the space shuttle exhaust are now summarized

1. Exhaust cloud encountering active convective precipitation cells with consequent vertical transport to the upper troposphere and potential for acid rain

(a) sea breeze convergence during the warm season with attendent afternoon thunderstorms. Effects include possible localized hail and brief wind gusts in excess of 20 ms^{-1}. Affected area is less than 100 km^2 with a time scale of less than T + 1 day.

(b) frontal and prefrontal activity including squall lines with attendent thunderstorms. Effects include possible localized hail, wind gusts in excess of 30 ms^{-1} and tornadoes. Affected area is 100-500 km^2 with a time scale of less than T + 2 days.

(c) general air mass thunderstorms not associated with (a) and (b) above but responding to different summer synoptic flow patterns. Effects include possible localized hail and brief wind gusts in excess of 20 ms^{-1}. Affected area is less than 100 km^2 with a time scale of less than T + 1 day.

(d) tropical storms in the vicinity of the Florida peninsula within 24 hours of launch time. Potential effect of shuttle exhaust cloud caught up in the circulation of a tropical storm is unknown in terms of inadvertent weather modification. A subsequent change of direction of such a storm might be interpreted as <u>not</u> an "act of God" by some people with possible social and legal problem from communities in the landfall region.

NOTE: Approximately 10-12% of the summer hours are associated with precipitation versus 7-10% in winter across Florida. Trace amounts occur 4-6% of the hours whereas heavier amounts (> 2.5 mmh^{-1}) occur 2% and 1% of the time respectively in Florida. The time of maximum occurrence is generally midafternoon with the exception of northern Florida in winter. The percentage of summer hours with audible thunder ranges from 3 to 6% with a maximum across central Florida. A very strong late afternoon peak is noted for all stations. Winter frequencies are considerably reduced with a much weaker early evening maximum. Overall, these numbers should provide an overall upper bound of the percentage chance of encountering an active cumulonimbus cloud at any random time.

2. In the months November-April, when advective and radiative fogs maximize, very significant worsening of visibility conditions in foggy situations could occur within the area affected by the dissipating S.G.C. up

to T + 1 day (area affected up to 10^4 km^2) and particularly under wind flow conditions from the S-E quadrant.

3. Minor risk associated with easterly flow in lower troposphere (unless tropical disturbances are present) particularly in those situations where atmosphere is stable under those conditions, clouds do not reach the level where ice phase processes are operative. However, overseeding of warm clouds with CCN could result in a very significant reduction of precipitation over the entire area affected by the dispersing cloud. Effect diminishes after T + 1 day. (Criteria: shallow warm cloud system and no ice phase.)

4. Stagnating anticyclonic conditions with reduced dispersion of S.G.C. Little cloudiness is normally associated with conditions of this type. The impact is therefore restricted only in the area of visibility detoriation and solar energy reduction. This constitutes therefore a nuisance and conceivably might violate EPA standards. On rare occasions air mass thunderstorms may develop, particularly along the sea breeze convergence zone, under stagnant anticyclonic conditions during the warm season. The risk would then be equivalent to 1(c) above.

5. Possible modification of a major hurricane located east of Florida peninsula at time of launch. Air from launch site would participate in the storm circulation and might indeed cause some modification effects producing unknown results. Any subsequent veering of such a storm would undoubtedly cause serious social and legal problems.

6. Cumulative effects: for the projected 40 launches per year assuming several days spacing between launches is considered negligible.

7. Minimal risk and impact: strong westerly winds system extending through the lower troposphere.

REASSESSMENT CRITERIA

A reassessment is required if:

(a) the volume of the stabilized ground cloud differs by more than 50% of the value assumed here

(b) the number of giant particles in the stabilized ground cloud with radius larger than 20 μ exceeds 1 particle per 1000 cm^3

(c) the number density of ice nuclei in the stabilized ground cloud exceeds 5% of the total number of particles present in the S.G.C. (irrespective of particle size)

(d) the launch area is moved out of the Florida area (our assessments relies heavily upon the climatology of the launch area).